AUSTRALIAN ACOUSTICAL SOCIETY CONFERENCE

ACOUSTICS TODAY

H. Vivian Taylor Memorial Conference

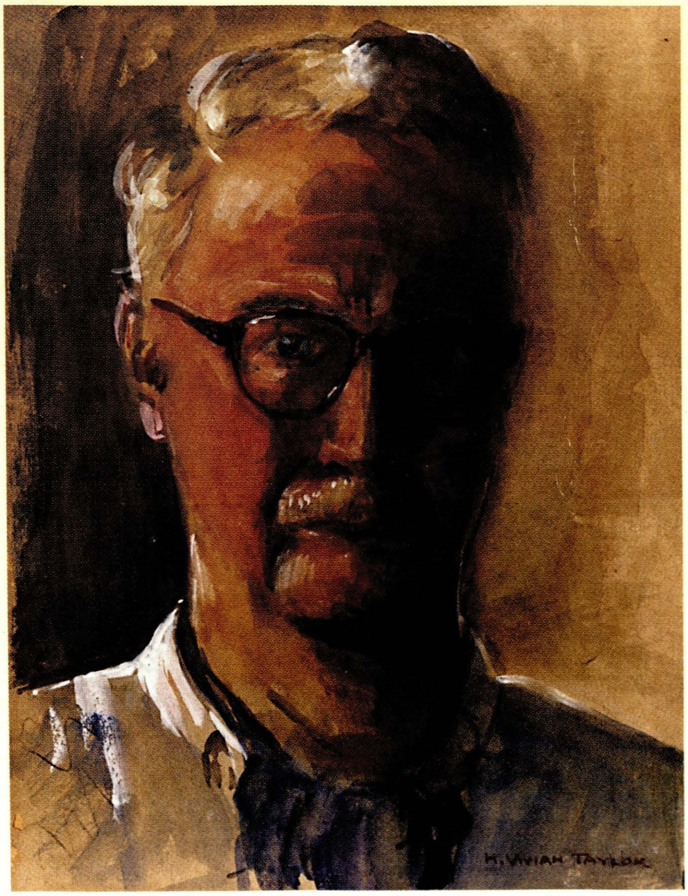

Hosted by the Victoria Division

Wednesday 24 to Friday 26, November 1999 at the Hilton Hotel MELBOURNE

W Williams

PROCEEDINGS

of

ACOUSTICS TODAY

AUSTRALIAN ACOUSTICAL SOCIETY CONFERENCE

Wednesday 24 to Friday 26
November 1999

at the Hilton Hotel
Melbourne

The above logo is from early editions (1979 – 81) of The Bulletin of the Australian Acoustical Society

All papers printed in this Proceedings were selected after a review of submitted abstracts by a sub-committee of the Victoria Division of the AAS. The opinions and conclusions expressed in the papers are those of the Authors, not necessarily the Society.

C.G.Don, (Editor)

Printed for the Australian Acoustical Society
by Llenlees Printers,
6 Clarice Rd, Box Hill, Victoria 3128.

AUSTRALIAN ACOUSTICAL SOCIETY CONFERENCE

ACOUSTICS TODAY

Melbourne, 24 – 26 November, 1999.

WELCOME

The acoustics of today is based on the acoustics of yesterday just as the acoustics of tomorrow will grow from the knowledge and skills of today. With these thoughts in mind, the Committee charged with creating a conference called **Acoustics Today** felt it would be enriching to spend some moments glancing back to the start of the Society and surveying the changes which have taken place during the intervening years. Thus each day's proceedings will start with an invited paper from foundation members of the Society: – Gerald Riley and Anita Lawrence. Further, the Committee decided to honour the first President of the Society, and a very well respected acoustic consultant in both Victoria and New South Wales, H.Vivian Taylor, by dedicating this Conference to his memory. We look forward to hearing something of his life and times from his son, Hugh Taylor, who has agreed to speak during the Conference Dinner in the Dandenongs. Finally, we trust that a display of memorabilia will bring back memories among our senior members and rouse the curiosity of the younger members.

Acoustics Today is not just about the past. The wide range of papers included in these proceedings is evidence of the current dynamic nature of acoustics. It is ideas such as these that will lead acoustics into the next century and millennium.

Enjoy the conference now, learn of the past, and step with us into the future.

1999 Conference Committee

Geoff Barnes
Mark Debevc
Charles Don
Louis Fouvy
Elizabeth Lindqvist
Ian McLeod
Keith Porter

AUSTRALIAN ACOUSTICAL SOCIETY CONFERENCE

ACOUSTICS TODAY

Melbourne, 24 – 26 November, 1999.

PROGRAMME

Wednesday 24th November:

4.00pm	Registration Desk opens
6.30 – 8.30pm	*Welcome reception*

Thursday 25th November:

8.00am Registration Desk opens

9.00 – 9.10am *Opening and welcome*

9.10 – 9 30 *Opening address*

9.30 – 10.00 *Invited Paper:*
A forerunner of Australian acoustics,
Gerald Riley.

Morning tea break

10.20 – 10.45 Acoustical rating of windows, doors and facades, ***J L Davy.*** p 1

10.45 – 11.10 Facade glazing noise reduction performance, ***N Broner and B Johnson.*** p 9

11.35 – 12.00 An investigation of noise from stairs bonded to an apartment bedroom, ***Graeme E Harding.*** p 15

12.00 – 12.25 Sensing a buried object acoustically, ***Charles Don and David Lawrence.*** p 23

1:50 RmB

Lunch

Thursday 25th November:

1.25 – 1.50 pm

ROOM A A new initiative in international metrology:- acoustics, ultrasonics, vibration, sonar, p 31
Suszanne Thwaites.

ROOM B Contoured foam absorbers, p 39
J P Parkinson, M D Latimer and J R Pearse.

1.50 – 2.15

ROOM A "PsySound"; A computer program for psychoacoustical analysis, p 47
D Cabrera.

ROOM B Advances in the control and calibration of transducer installations, p 55
Poul Svensgaard and Bernard Ginn.

Chas Don.

2.15 – 2.40

ROOM A Low frequency noise loudness vs annoyance, p 61
N Broner and R Hellman.

ROOM B The development of a high performance absorptive roadside noise barrier, p 67
J F Upton.

2.40 – 3.05

ROOM A Occupational noise management – educating the workforce, p 71
N Koolik, D Eager and R Tonin.

ROOM B Traffic Noise Revisited, p 79
C L Fouvy.

Afternoon tea break

3.20 – 3.45 Evaluating the American FHWA traffic noise model in Melbourne, p 97
Neil Huybregts and Stephen Samuels.

3.45 – 4.10 In-situ determination of insertion loss of roadside noise barriers in urban environment, p 105
Edwin C K Chui, Maurice Yeung and K M Li.

4.10 – 4.35 Turbulence effects, p 111
I D McLeod and C G Don.

4.35 – 5.15 *Workshop: Memorabilia of Acoustics.*

CONFERENCE DINNER, INCLUDING AGM

6.15pm departure from Hilton, return about midnight.

Friday 26th November

9.00 – 9 30am	*Invited Paper:* Australian Acoustical Society from the beginning to the end of the 20th Century. (A personal (NSW) view of its history), ***Anita Lawrence.***	
9.30 – 9.55	Concert hall design: Variations on a theme of Beranek, ***Fergus Fricke.***	p 119
9.55 – 10 20	Vibrato frequency and phase lock on operatic duet quality, ***Melanie Duncan, Carol Williams and Gordon Troup.***	p.131

Morning tea break

10.40 – 11.05	Active control of large electrical transformer noise using near-field error sensing, ***Xun Li, Xiaojun Qiu, Rongrong Gu, Robert Koehler and Colin H Hansen.***	p 141
11.05 – 11.30	Noise control at gas-fired compressor stations, ***Tim Marks.***	p 149
11.30 – 11.55	Sampling the reverberant sound pressure field for sound power and transmission loss measurements in the laboratory, ***E A Lindqvist, P Carrozza, J L Watson and P E Dale.***	p 157
11.55 – 12.20	Flow resistivity as a measure of sound absorption with applications, ***J P Parkinson, M D Latimer and J R Pearse.***	p 165

Lunch

1.20 – 1.45	Accelerometer calibration with imperfect exciters (shakers), ***L P Dickinson and N H Clark.***	p 173
1.45 – 2.10	On acoustic lagging of pipes, ***S Kanapathipillai and K P Byrne.***	p 181
2.10 – 2.35	Attenuating noise in pipes, ***J P Parkinson, M D Latimer and J R Pearse.***	p 195
2.35 – 3.00	*Closing ceremony – presentation of prizes.*	

AUSTRALIAN ACOUSTICAL SOCIETY CONFERENCE

ACOUSTICS TODAY

Melbourne, 24 – 26 November, 1999.

This conference has been dedicated to

HUGH VIVIAN TAYLOR

Founding President of the Society

"Throughout Vivian Taylor's life, his drive, enthusiasm and capacity for thought enabled him to become an unparalleled success in his Professional fields of Architecture and Acoustics."

The above quote from an obituary in The Bulletin of the Australian Acoustical Society, following his death on 15th March 1981, summarises the high respect held for one of the pioneering figures in Australian acoustics.

Born on 19th December, 1894, he was educated at Scotch College and undertook architectural studies at the Working Men's College (now R.M.I.T.) and at Swinburne Technical College, in Melbourne.

While serving in the A.I.F. and then the R.A.F., his main areas of deployment were in submarine minefield work at the entrance to Port Phillip Bay and in communication networks. After the war he became an assistant to a firm of Melbourne architects and was registered as an Architect in Victoria during 1923. Late that year he commenced private practice: initially on commercial and domestic architecture. About this time, acoustics began to seriously interest Vivian and he started working professionally in acoustics in 1928. Early commissions included some 55 churches and a number of public halls, generally involving both architectural and acoustic design.

The arrival of "talking pictures" in Australia in 1929 required acceptable acoustic conditions to ensure the satisfactory reproduction of the sound. From 1930 to 1941 his office acted as consultants for at least 434 theatres and public halls, many receiving acoustic treatment while others were new developments where Vivian was both architect and acoustician.

In 1931, Vivian established a reverberation chamber in Melbourne for acoustic testing to obtain absorption coefficients of imported and locally made acoustic materials and furnishings, using the 1925 recalibration method suggested by Sabine. Later he followed the 1927 method, using electronic loud speakers instead of organ pipes.

Between 1935 and 1940, he was consultant architect and acoustic adviser to the South Australian Government during the completion of the Houses of Parliament in Adelaide. When a pin is dropped on the Speaker's desk it is clearly audible in all parts of the Chamber and Galleries. During 1940 to 1956 he was consultant to the ABC, designing and overseeing construction of facilities in all states and in Port Moresby. He acted as consultant to NSW Department of Railways for the construction of the Circular Quay Railway in Sydney and was responsible for the Princess Gate Project over the railway yards in Melbourne. Other projects included noise reduction at quarries, wool sales rooms and bowling centres, shielding transformer noise and town planning and zoning.

He was granted Membership of the fledgling Acoustical Society of America in 1931. From 1964 Vivian attended the meetings that led to the formation of the Victorian Acoustical Society, which eventually fused with those in other states to form the Australian Acoustical Society. He was elected as founding President in 1971. He was created a Member of the Most Excellent Order of the British Empire by her Majesty, Queen Elizabeth II, in June, 1968, for Services to Acoustics. In 1971, he became a Life Fellow of the Royal Australian Institute of Architects and was elected as the first Fellow of the AAS in September, 1972.

AUSTRALIAN ACOUSTICAL SOCIETY CONFERENCE

ACOUSTICS TODAY
Melbourne, 24 – 26 November, 1999.

An invited paper:

A FORERUNNER OF AUSTRALIAN ACOUSTICS

Gerald Riley

This paper will review the acoustic achievements of H.Vivian Taylor as viewed by one of his contemporaries, Gerald Riley.

This photograph, with the caption "DO YOU REMEMBER . . .?" appeared in The Bulletin of the Australian Acoustical Society, December 1979, and shows Gerald Riley speaking to Vivian Taylor.

AUSTRALIAN ACOUSTICAL SOCIETY CONFERENCE

ACOUSTICS TODAY

Melbourne, 24 – 26 November, 1999.

An invited paper:

AUSTRALIAN ACOUSTICAL SOCIETY FROM THE BEGINNING TO THE END OF THE 20th CENTURY (A personal (NSW) view of its history)

Anita Lawrence, FAAS

I remember receiving a telephone call from Peter Knowland, then employed by an engineering consultancy, Norman & Addicoat of Sydney. At the time I was a lecturer in Architectural Science in the Faculty of Architecture of the University of New South Wales, and I was responsible for much of the acoustics teaching for the undergraduate architecture students. Peter suggested that it was time to organise a meeting to "Discuss the possible formation of an acoustical society in Australia. I agreed, and the first meeting was held in his offices on August 5th, 1964.

Unfortunately, I don't have a list of attendees, but the following were recorded in the minutes as having expressed opinions. Vivian Taylor, who had acoustical consultancy offices in both Sydney and Melbourne, explained that the formation of an Australia-wide acoustical organisation was currently under discussion in Victoria. Jack Rose, of (what was then) the National Acoustics Laboratory supported the formation of a society. I supported the idea and I thought it should be organised to include as many interested people as possible, but in order to attain a reasonably acceptable professional level it would be necessary to introduce different grades of membership. Howard Pollard, a lecturer in physics at the University of New South Wales was also supportive, and pointed out that there are many branches of acoustics - architectural, music and physical.

John Irvine, then working for CSR, which at that time was developing materials for acoustical uses, welcomed the idea, as did Warwick Mehaffey of the ABC. Ted Weston, of the then Building Research laboratory and working in building acoustics, thought that there may be commercial interests which might support the society, but they should not have voting rights. Horrie Weston, an officer with the Department of Hẻalth said that the main purpose would be the dissemination of information. Ernie Benson and Mark Eiseler also contributed to the discussion.

Finally, Peter Knowland summed up and said that the community was becoming more aware of acoustics and that there was an increased use of acoustic consultants. The proposed society's aims would include promoting the teaching of acoustics in universities and schools, agreement on methods of test and standards, and improving the community's understanding of acoustics.

The first motion was passed: "We would be a group-in-formation and the first aim should be to obtain information about the draft constitution of any other proposed acoustical society and we were in favour of an Australia-wide acoustical group".

A committee was elected to consider the formation of an Australia-wide group, to prepare a draft constitution including conditions of membership, to suggest activities and consider the organisation of a symposium and to call another general meeting in a few months time. The four committee members were Peter Knowland, Warwick Mehaffey, John Irvine and myself. Finally, those present donated 10 shillings per head (about a dollar) for preliminary expenses.

Much work then ensured, and the NSW and Victorian committees battled with drafting an acceptable constitution, one of the most difficult areas was deciding on the requirements for admission to the various proposed grades of membership. As there were few, if any people with direct academic qualifications in "acoustics" it was difficult to define who should be eligible for the professional grade of "Member". Eligibility for admission was considered to be someone eligible for membership of a profession recognised as a professional by the Commonwealth Public Service. At that time there were a number of well-respected acousticians without academic qualifications, so a "grandfather" clause was included to allow those who had been working at a professional level in acoustics for a number of years to also be admitted to corporate membership. (In hindsight, this particular method of entry should have been restricted to the first few years of the Society's life).

By 1964 Victoria and NSW had unincorporated societies but it was not until 1971 that the incorporation of the Australian Acoustical Society (in NSW) was achieved, - on April 1st. The seven grades of membership, which now exist, were established and annual fees ranged from $10 for corporate membership to $6 for Affiliates, Subscribers and Students. There were two divisions, NSW and Victoria, and each had an elected committee of ten, two of whom could be members of, and elected by the non-corporate members. Each Division appointed five federal Councillors who had the overall responsibility for the Society.

The first meeting of the Council of the AAS was held on 18th April, 1971, at my home in Sydney. Jack Rose (NSW) was in the Chair, and Councillors present were Ron Barden, Jim Bryant, Gerald Riley, Vivian Taylor and Graeme Harding from Victoria and Louis Challis, Peter Knowland, John Irvine and myself representing NSW. Vivian

Taylor was elected as the first President and Peter Knowland Vice-President. Jim Bryant took on the arduous task of General Secretary and John Irvine that of Treasurer.

At the first Annual General Meeting of the NSW Division in June 1971, when the first Divisional Committee was elected, Jack Rose mentioned the idea of the AAS applying to hold an International Congress on Acoustics meeting (ICA) in Australia. The University of New South Wales had been approached regarding providing a venue and members were asked to investigate the possibility of sponsorship from government and industry. It was hoped to hold the 1987 ICA in Sydney, but the decision was made to hold it in a Spanish-speaking country, and Madrid was selected. A number of us attended the Madrid meeting and called on the Australian Ambassador to host a party for ICA VIP's. It turned out that the "Australian" delegation only included one true Aussie - Carolyn, Cliff Winter's (of Bruel & Kjaer) wife. The 10th ICA finally took place in Sydney in 1980.

The 10th ICA was very successful - although unfortunately the UNSW venue, on the lower campus, was rather scattered. One unintended "Highlight" was the Congress Dinner, in the Roundhouse of the UNSW Union. The whole waiting staff staged a strike in support of better conditions, and the delegates and their guests had to wait many hours before being served! Even rather staid European delegates succumbed to throwing paper darts (I presume that somehow liquid refreshments had been obtained).

Before this, in Western Australia, impatience had arisen at the rather slow progress towards incorporation of the AAS and a WA Acoustical Society had been formed. Eventually they were persuaded to join NSW and Victoria in the AAS and they were formally admitted in 1972. Later, Queensland and SA formed Divisions and now there are five State Divisions, each contributing two Councillors.

NSW held annual conferences, and the one in 1972 was held at Terrigal, a coastal town north of Sydney. "Noise Legislation and Regulation" was the topic - as several society members were engaged as advisors to the NSW government on the development of noise control acts, etc. There were some quite interesting episodes involving senior legal contributors, around the hotel pool !

Not content with hosting the ICA in 1980, Council decided to apply to host an Inter-Noise, the annual international conference of the International Institute of Noise Control Engineering. I-INCE normally rotates its meeting locations between North America, Europe and Asia-Pacific. We hoped to hold the 1990 meeting in Sydney, but Sweden was the choice instead. We were successful in 1991, and hopefully many of those here today were able to participate. I was the General Chairman and the location was again the UNSW - but on the upper campus this time - the conference was opened by the Governor of NSW, Gordon Samuels, who was also the Chancellor of the university at the time.

Another area in which AAS members have been prominent, is in the preparation of Australian Standards on acoustics and vibration. There are very many of these now, some of which are quite unique - such as the series on aircraft and road traffic noise intrusion - building siting and construction (a third in the series, dealing with rail traffic noise and vibration is in preparation). As well, several are involved in International Standards preparation. As it is now the policy of Standards Australia to adopt ISO and IEC Standards, unless there are substantial local reasons why they can't be adopted, it is very important that we have as much input at the Working Group stage as possible. Anyone who has been involved with ISO or IEC knows, this means physical presence. AAS has recently applied to become a member of the reconstituted Standards Australia. When approved by the Standards Council in November this will enable the AAS to appoint a Councillor.

It seems to me that currently, noise, as one of the more obvious aspects of acoustics as far as the community is concerned, has lost some of the prominence it was previously accorded. Of course, in Sydney the "Second Sydney Airport" erupts as front page news every now and again (as it has for the last decade or so). But noise, which is after all, rather a localised problem, tends to get rather overshadowed by the other environmental problems of global warming, air and water pollution. However, to those directly affected, noise has the ability to markedly degrade the quality of life. Room acoustics still continues to defy exact scientific analysis and design - but then of course, the results are subjective. Poor Sydney, it is most unlikely to ever be given the chance to build an acoustically good Opera House !

From small beginnings, and as a result of the early enthusiasm of a few Victorian and NSW acousticians, the AAS was formed and has continued to exist for 28 years. Let us hope that it will celebrate its centenary in 2000.

Reproduced from The Bulletin, December 1981, the year Anita became President of the Society.

AUSTRALIAN ACOUSTICAL SOCIETY CONFERENCE

ACOUSTICS TODAY

Melbourne, 24 – 26 November, 1999.

ACOUSTICAL RATING OF WINDOWS, DOORS AND FACADES

J. L. Davy

CSIRO Building, Construction and Engineering

ABSTRACT

Sound Transmission Class (STC) is used as a single rating for sound insulation in Australia. STC is appropriate for rating the sound insulation of an internal wall against the human voice. STC is not appropriate for rating the sound insulation of an external building facade against road, rail and aircraft noise. This paper discusses the relative merits of a number of possible alternative single number ratings. These are the Outdoor Indoor Transmission Class (OITC) from ASTM standard E 1332-90 (Reapproved 1994), the Aircraft Noise Attenuation of a building component (ANA_c) from Australian Standard AS 2021-1994, and $R_w + C_{tr}$ from International Standard ISO 717-1:1996(E). Standards Australia has proposed replacing the Australian STC Standard AS 1276-1979 with ISO 717-1:1996. This means that Australia will probably switch from STC to R_w for internal walls. The efforts of the Australian Window Association to develop an appropriate acoustical rating scheme for the sound insulation of windows and doors will be reported. The rating scheme adopted will affect the relative ranking of single and double glazed windows. Examples of the different rating schemes on a range of windows will be presented.

INTRODUCTION

Sound insulation is measured using 18 or more third octave frequency bands of random noise, including those with standard band centre frequencies in the range from 100 Hz to 5 kHz. The measurement is usually made with a diffusely incident sound field so that an average is obtained over all possible angles of incidence. Because the sound insulation for a discrete frequency tone varies rapidly as a function of frequency and angle of incidence, there is normally no point in using smaller measurement bandwidths or reduced ranges of angles of incidence.

To compare the sound insulation of different constructions, it is useful to have a single number rating which is derived from the 18 or more values measured at different band centre frequencies. In Australia, Sound Transmission Class (STC) has been used to rate the sound insulation of internal walls. STC is defined in Australian standard AS 1276-1979 [1], which is based on the North American standard ASTM E 413-87 (1994) [2]. Standards Australia [3] has proposed replacing AS 1276-1979 with the international standard ISO 717-1:1996 [4]. This means that Australia is likely to switch from STC to the weighted sound reduction index (R_W) for the single number rating of internal walls. STC will continue to be available through the current version of ASTM E 413, and is explained in appendix ZA of the draft Australian standard [3].

Normally, R_W is the same as, or differs by 1 dB from STC. However larger differences can occasionally occur. R_W differs from STC in three ways. It is evaluated using the frequency range from 100 Hz to 3.15 kHz, rather than 125 Hz to 4 kHz used by STC. The sound insulation values used to calculate it are rounded to 0.1 dB, rather than the 1 dB used for STC. R_W does not apply the maximum unfavourable deviation of 8 dB that is used by STC.

The preface to AS 1276-1979 [1] states that, "The classification system described in this standard applies to the derivation of a single number to denote the sound attenuation properties of walls, floors and ceilings used to divide spaces within commercial or domestic buildings. An order of rank is required for these partitions to correlate with subjective impressions of the reduction of many household and commercial sounds which have most of their energy in the mid-frequency range and relatively less in the higher and lower frequencies. The classification system described in this standard does not apply to conditions in which the sound spectra differ markedly from those of household and commercial sounds, especially in cases where low and/or high frequency components predominate. These include the sounds produced by motor vehicles, most forms of industrial machinery, and power transformers."

Unfortunately, because there has been no other single number rating available for rating sound insulation, STC has been used in Australia to rate the sound insulation of facades, windows and doors. In particular, the Sydney Aircraft Noise Insulation Project (SANIP) has used STC when specifying the sound insulation of windows. Dunn [5] compared the dB(A) reductions for aircraft and traffic noise with the STC rating for 104 different building elements. He "found, on average, that aircraft noise and traffic noise is attenuated by 4.6 and 6.0 dB respectively, less than the numerical value of the appropriate STC rating." Dunn's average values of 5 and 6 dB respectively (rounded to the nearest 1 dB) were used as corrections to tables of STC values in the Australian Standards AS 2021-1994 [6] and AS 3671-1989 [7]. These differences are only correct on average. They have large variations, which make STC unsuitable for ranking the sound insulation of facades.

1. ACOUSTICAL RANKING OF FACADES

Existing international schemes which are suitable for ranking the sound insulation of facades use dB(A) reduction. They differ in the frequency range and spectrum shape used. The French use a range from 100 Hz to 5kHz with a spectrum given by Auzou [8]. The Scandinavians use a range from 100 Hz to 3.15 kHz with a spectrum given in Nordtest Method NT ACOU 061 [9]. However NT ACOU 061 does allow the use of different frequency ranges and spectra. It gives the standard spectrum and six other spectra over the frequency range from 50 Hz to 5 kHz. The North Americans use the

Outdoor-Indoor Transmission Class (OITC), whose spectrum is defined in ASTM E 1332-90 [10]. OITC, which uses a frequency range from 80 Hz to 4 kHz, was developed by Walker [11]. It has been adopted by the North Americans [12,13], for the acoustical rating of exterior windows, doors and glazed wall sections.

The Germans still use R_W for the acoustical rating of windows. This explains the strange form of ISO 717:1-1996. It is a compromise between the French dB(A) reduction method and the German R_W method. ISO 717:1-1996 introduces two spectral correction terms C and C_{tr}. $R_W + C_{tr}$ is the dB(A) reduction for the standard Scandinavian traffic noise spectrum [9] over the frequency range from 100 Hz to 3.15 kHz. The Scandinavian spectrum was used instead of the French spectrum because it was available in the extended frequency range from 50 Hz to 5 kHz. R_W + C is the dB(A) reduction for pink noise in the range from 100 Hz to 3.15 kHz. ISO 717:1-1996 allows the frequency range to be extended down to 50 Hz and/or up to 5 kHz Most acoustical experts would have preferred to replace R_W with a single value equal to R_W + C, and the introduction of a new single number rating equal to $R_W + C_{tr}$. Unfortunately, the Germans insisted on the retention of R_W, both on its own and as part of the dB(A) reductions. This, coupled with the different frequency ranges, makes ISO 717-1:1996 confusing.

According to ISO 717-1:1996 [4], the spectrum used to calculate R_W + C is appropriate for living activities (talking, music, radio, tv), children playing, railway traffic at medium and high speed, highway road traffic at greater than 80 km/h, jet aircraft at short distance, and factories emitting mainly medium and high frequencies. The spectrum used to calculate $R_W + C_{tr}$ is appropriate for urban road traffic, railway traffic at low speeds, propeller driven aircraft, jet aircraft at large distance, disco music, and factories emitting mainly low and medium frequency noise.

Australian Standard AS 2021-1994 defines the aircraft noise attenuation of a component (ANA_C) as a dB(A) reduction, and gives an average jet aircraft noise spectrum from 100 Hz to 5 kHz.

2. AWA ACOUSTIC CERTIFICATION SCHEME

In January 1997, the author was commissioned by the Australian Window Association (AWA), formerly the Residential Window Association (RWA), to develop an acoustic certification scheme for windows and glass doors. While writing the first and second drafts, the author was not aware that the second edition of ISO 717 [4] had just been published on the 15 December 1996. The first edition of ISO 717 did not contain spectral correction terms, so it could not be considered for use. Because he did not want to adopt yet another different spectrum, the author considered using ANA_C and OITC. He decided on OITC because it agreed moderately well with the average traffic noise spectrum used by Dunn [5]. Also the aircraft take off noise spectra measured by Robert Bullen (private communication) suggested that the ANA_C spectrum should be extended to a lower frequency and have its low frequency values increased. While writing the third draft [14], the author considered changing to $R_W + C_{tr}$, but reject the idea because of the better agreement of OITC's spectrum shape with Dunn's [5] average of locally measured traffic spectra.

Later, under pressure from international colleagues, the author looked again at the OITC spectrum shape. The OITC spectrum (Walker [11]) is the average of aircraft take off, freeway and railway spectra. The author was surprised to discover that its aircraft take off spectrum had more low frequency content than its freeway spectrum. It also has more low frequency content than the aircraft noise spectrum in AS 2021-1994. The author has been told by members of Standards Australia's EV/11 committee, which is responsible for AS 2021-1994, that the current wisdom is that the aircraft noise spectrum in AS 2021-1994 is "about right". This has been confirmed by his colleague Narang (personal communication), who is the main acoustical consultant to the Sydney Aircraft Noise Insulation Project (SANIP). The reference for Walker's aircraft noise spectra is Raney and Cawthorn [15]. The only spectral information in [15] that looks at all similar to the aircraft spectrum used by Walker is the bottom graph of Fig. 34.6 in [15] which pertains to the time 10 seconds after the aircraft is overhead. This time was probably chosen because it is close to the middle of the over all sound pressure time history. This spectrum was measured "during take off for a commercial jet aircraft powered by four low-bypass-ratio turbofan engines, measured at a location 5500 m (18,000 ft) from brake release (the start of ground roll) with the aircraft at an altitude of approximately 350 m (1100 ft)." Given the change in aircraft noise spectra, this spectrum is probably no longer relevant. Walker's aircraft noise spectrum appears to be a smoothed version of this spectrum given by Raney and Cawthorn.

The reference for Walker's road traffic noise spectrum is Scholes *et al.* [16]. Surprisingly the spectral information in this paper is octave band data. It is not clear how Walker extrapolated the octave band data to third octave band data. The other surprise is that it is United Kingdom rather than North American data.

The railway spectrum is from unpublished United States Gypsum Corporation test data. It is fairly irregular in shape. Thus there is probably not much averaging involved with this spectrum. All this new information casts some doubt on the current validity of the OITC spectrum.

The author then made more inquiries about the Australian road traffic noise spectra in Dunn's paper [5]. Subjectively, the Canberra measurements were effected by low frequency rumble from distant traffic crossing a busy bridge across Lake Burley Griffin. The Australian Academy of Sciences, where the Canberra measurements were made, sits on relatively high ground overlooking Lake Burley Griffin. The new freeway, which was the reason for the measurements, passes through a tunnel in this high ground. The Rohans Road measurements in Melbourne were made on a secondary road, and may have been affected by low frequency noise from more distant major roads.

The Australian road traffic spectra were then compared to a number of international road traffic spectra [8, 9, 16-24]. None of the international road traffic noise spectra had as much low frequency energy as the Australian road traffic spectra. This cast further doubt on the Australian road traffic spectra which had been used to support the OITC spectrum shape.

The author was also concerned about the greater uncertainity in sound insulation measurements at low frequencies. Also a lot of existing sound insulation data is only available down to 100 Hz. After considering all the above information, the author has recommended that the AWA draft acoustic certification scheme change from using OITC to $R_W + C_{tr}$.

3. DOES THE SINGLE NUMBER RATING MATTER?

Because of the different sound insulation frequency spectrum shapes, the single number rating scheme can have a marked effect on the relative ranking of different types of construction. This is particularly noticeable when comparing single and double leaf constructions.

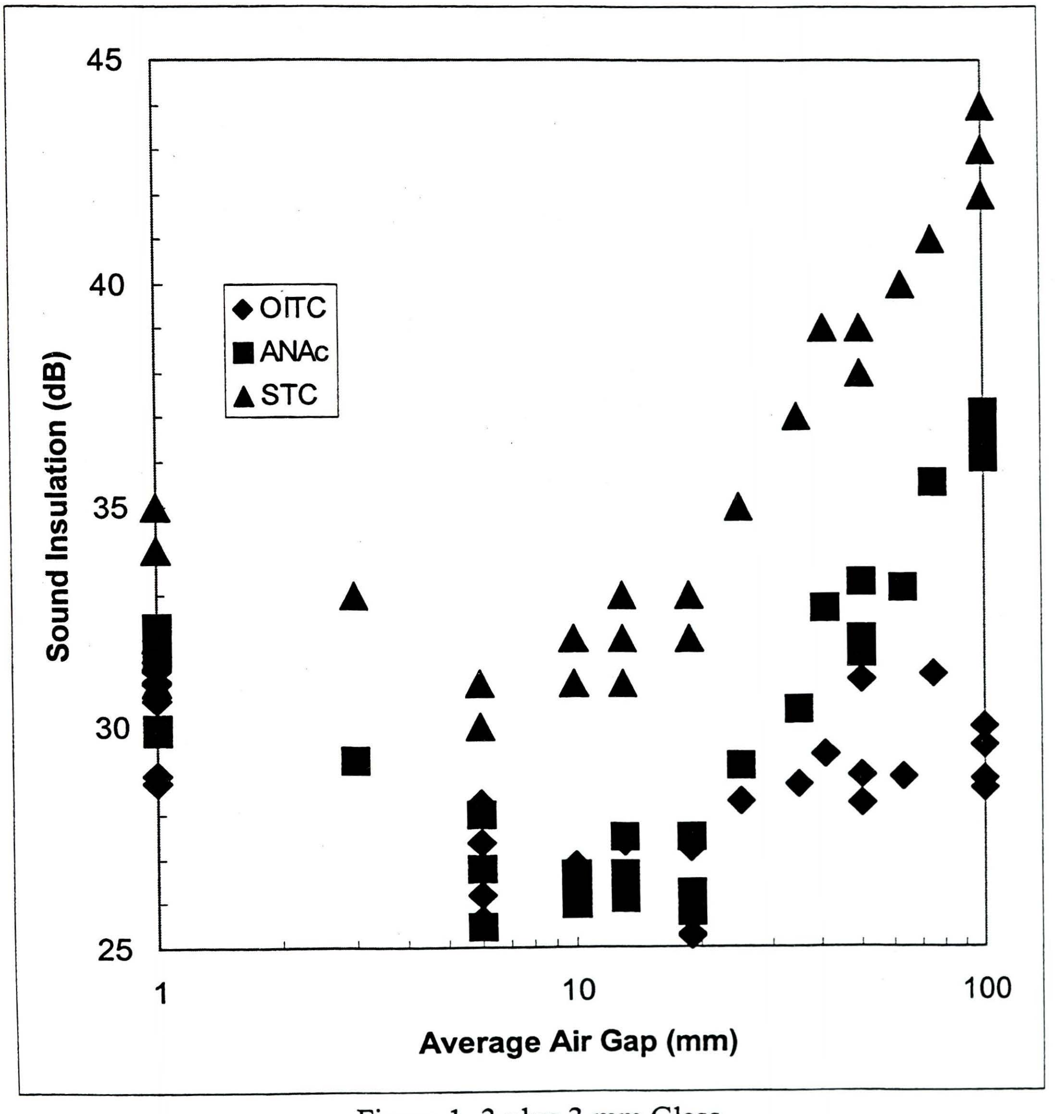

Figure 1. 3 plus 3 mm Glass

Fig. 1 shows the OITC, ANA_C and STC values for a range of average air gap values. The 1 mm spacing is a nominal value used to show glass with a zero air gap. This includes 2 cases of monolithic 6mm glass, 5 cases of 6 mm laminated glass and two cases of two 3 mm glass panes touching each other. The STC values show a minimum value at 6 mm and then a rise to significantly above the no air gap values for large air gaps. The ANA_C and OITC values show minimum values in the 10 to 20 mm range. The ANA_C values rise slightly above the no air gap values for large air gaps. The

OITC values never rise significantly above the zero air gap values. It should be noted that the R_w + C_{tr} values would be similar to the ANA_c values. All but one of the non-laminated glass values in Fig. 1 are derived from measurements made by Quirt [25]. The reason for the low OITC values with large air gaps is due to very low measured values at 80 Hz. While some of these low values will be due to the mass-air-mass resonance, this does not appear to have always been the case.

Similar results can be seen for 6 plus 6 mm glass in Fig. 2 and for 3 plus 6 mm glass in Fig. 3. Thus the choice of single number rating will determine whether it is worthwhile using double glazing for sound insulation because it changes the relative ranking of the different glass constructions.

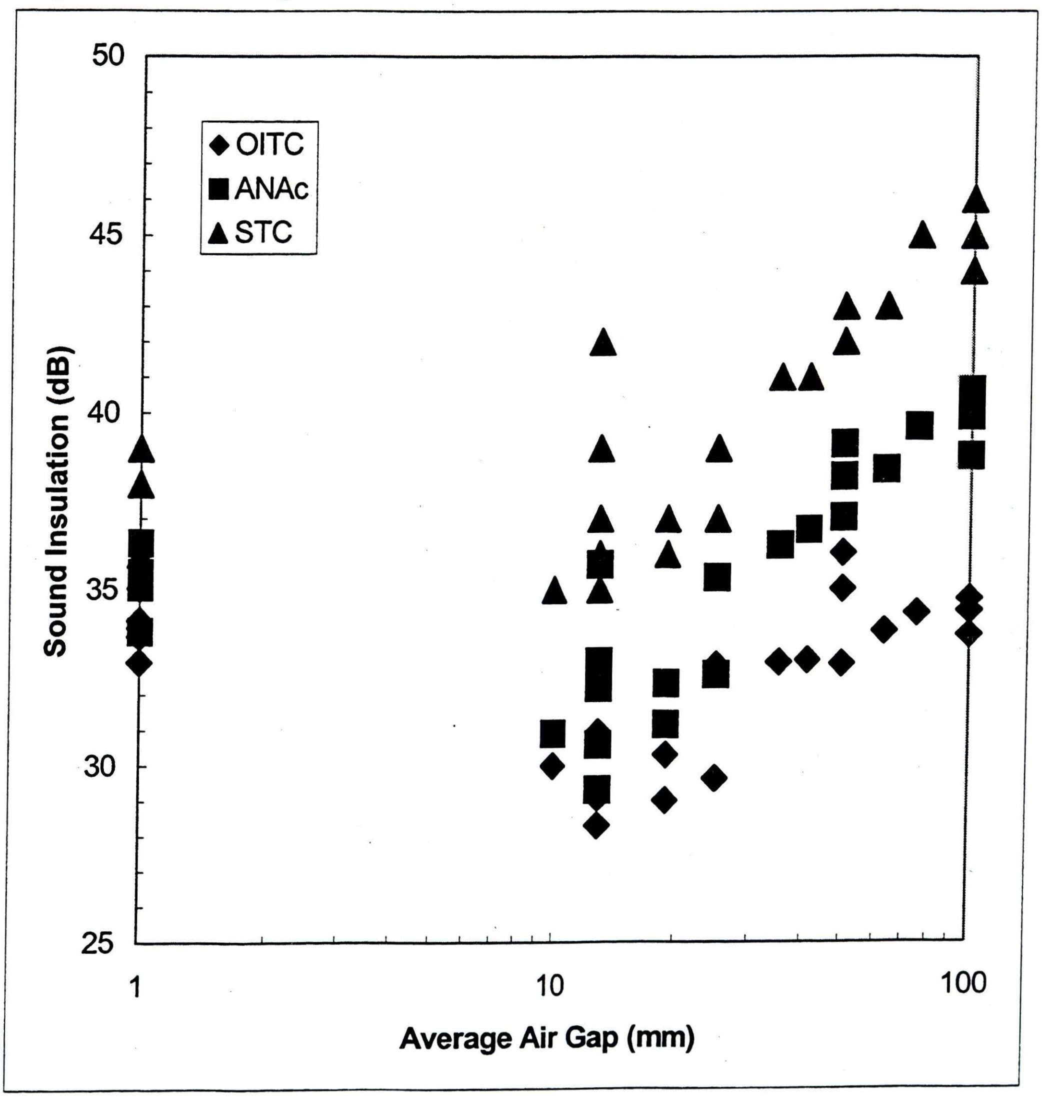

Figure 2. 6 plus 6 mm Glass

4. CONCLUSIONS

STC and R_w are unsatisfactory for rating the sound insulation of external windows, doors and facades. R_w + C_{tr}, ANA_c or OITC should be used instead. R_w + Ctr appears to be the best choice because it is an international standard and can be extended down to 50 Hz, if needed in the future.

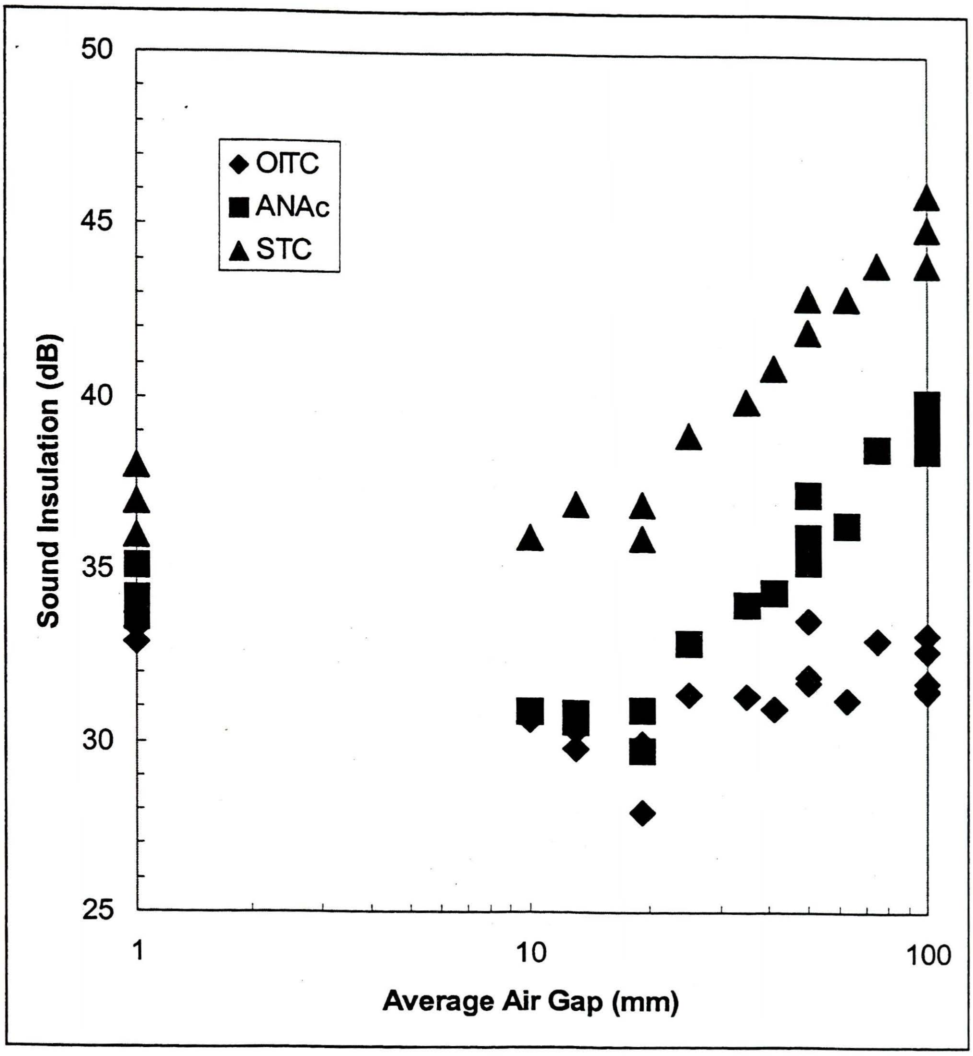

Figure 3. 3 plus 6 mm Glass

REFERENCES

[1] Australian Standard AS 1276-1979, Methods for determination of sound transmission class and noise isolation class of building partitions, Standards Australia, 1979.

[2] ASTM Standard ASTM E 413-87 (Reapproved 1994), Standard classification for rating sound insulation, American Society for Testing and Materials, 1994.

[3] Draft Australian Standard DR 99085 CP, Acoustics - Rating of sound insulation in buildings and of building elements - Part 1: Airborne sound insulation (Revision of AS 1276-1979) (To be AS 1276.1), Standards Australia, 1999.

[4] International Standard ISO 717-1:1996, Acoustics - Rating of sound insulation in buildings and of building elements - Part 1: Airborne sound insulation, International Organisation for Standardisation, 1996.

[5] I P Dunn, 'Comparison of STC rating to dB(A) reduction for aircraft and traffic noise', Acoustics Australia, 17/1, Apr 1989, p 11-13.

[6] Australian Standard AS 2021-1994, Acoustics - Aircraft noise intrusion - Building siting and construction, Standards Australia, 1994.

[7] Australian Standard AS 13671-1989, Acoustics – Road traffic noise intrusion - Building siting and construction, Standards Australia, 1989.

[8] S Auzou, 'Étude des caracteréristiques acoustiques de matériaux et d'équipements', Cahiers du CSTB, 173, Oct 1976, p 1-140.
[9] Nordtest Method NT ACOU 061, Windows: Traffic Noise Reduction Indices, Nordtest, 1987.
[10] ASTM Standard ASTM E 1332-90 (Reapproved 1994), Standard classification for determination of outdoor-indoor transmission class, American Society for Testing and Materials, 1994.
[11] K W Walker, 'Single number rating for sound transmission loss', Sound and Vibration, 22, Jul 1988, p 20-26.
[12] AAMA Publication No. AAMA 1801-95, Voluntary specification for the acoustical rating of residential, commercial, heavy commercial and architectural windows, doors and glazed wall sections, American Architectural Manufacturers Association, 1995.
[13] ASTM Standard ASTM E 1425-91, Standard practice for determining the acoustical performance of exterior windows and doors, American Society for Testing and Materials, 1991.
[14] J L Davy, 'The Residential Window Association acoustic certification scheme', Third Draft, DBCE DOC. 97/54(M), CSIRO, May 1997.
[15] J P Raney and J M Cawthorn, 'Aircraft Noise', Chapter 34, Handbook of noise control, second edition, edited by C M Harris, McGraw-Hill Book Company, 1979.
[16] W E Scholes, A C Salvidge and J W Sargent, 'Barriers and traffic noise peaks', Applied Acoustics, 5/3, 1972, p 205-222.
[17] P Hammarfors and A Kajland, 'Sound-pressure analyses of noise from motor vehicles, Acustica, 18, 1963, p 258-269.
[18] N Olsen, 'Statistical study of traffic noise', APS-476, Division of Physics, National Research Council of Canada, 1970.
[19] N Olsen, 'Survey of motor vehicle noise', Journal of the Acoustical Society of America, 52/5, 1972, p 1291-1306.
[20] E J Rathé, F Casula, H Hartwig and H Mallet, 'Survey of the exterior noise of some passenger cars', Journal of Sound and Vibration, 29/4, 1973, p 483-499.
[21] A Alexandre, J-Ph Barde, C. Lamure and F J Langdon, 'Road Traffic Noise', Applied Science Publishers, 1975.
[22] G Kårfalk, 'Generalized traffic noise spectra', Report 78-16, Chalmers University, 1978.
[23] J D Quirt, 'Acoustic insulation factor: a rating for the insulation of buildings against outdoor noise', Building Research Note No. 148, Division of Building Research, National Research Council of Canada, Revised June 1980.
[24] J S Bradley, 'Insulating buildings against aircraft noise: a review', IRC IR-760, Institute for Research in Construction, National Research Council of Canada, 1998.
[25] J D Quirt, Measurements of the sound transmission loss of windows, Building Research Note No 172, National Research Council of Canada, 1981.

AUSTRALIAN ACOUSTICAL SOCIETY CONFERENCE

ACOUSTICS TODAY
Melbourne, 24 – 26 November, 1999.

FACADE GLAZING NOISE REDUCTION PERFORMANCE

N. Broner and B. Johnson

Vipac Engineers And Scientists Ltd., Private Bag 16,
Port Melbourne, Melbourne, Australia 3207

ABSTRACT

Traffic noise exposure has been shown to be a widely experienced acoustic stressor. Many times, the approach is to upgrade the glazing in a building facade with the hope that the internally experienced traffic noise level will be reduced accordingly. We will report the results of an investigation to document the real benefit that can be achieved, in practice, as a result of various single glazing alternatives that were considered in a recent building project. The existing glazing was initially tested for noise reduction and then the facade glazing performance was progressively upgraded. Two separate contractors worked on two different units simultaneously so as to ascertain the potential difference due to workmanship. The initial upgrades were with the existing glazing in place but with upgraded seals around the windows. Further upgrades included the use of thicker single panes and the use of a single laminated glazing. The results show that the initial glazing did not perform well with an STC of the order of only STC15 but that with care and an appropriate glazing, the STC could be increased to the order of STC 30 and above.

1. INTRODUCTION

Traffic noise exposure has been shown to be a widely experienced acoustic stressor. Many times, the approach is to upgrade the glazing in a building facade with the hope that the internally experienced traffic noise level will be reduced accordingly. In order to determine the real-world improvements obtainable from such an approach, Vipac conducted acoustic tests on a building facade where the acoustic improvement could be documented as various window treatments were implemented. Below, we report on the results of the testing and discuss the real world implications.

2. METHODOLOGY

The simplest method of assessing the performance of various window configurations was to perform a sound transmission loss test across each of the desired constructions and then to compare the relative performances. Given that there was expected to be a slight difference in performance between single and double width windows (due to the differences in both glazing area and perimeter length), one of each type was tested. Furthermore, two different contractors were engaged to separately install each of the selected window configurations to see what variations resulted from nominally similar upgrades.

Two apartments having similar dimensions and interior surface finishes were chosen for the testing.

In order to correctly simulate traffic pass by noise, actual traffic noise was recorded prior to the testing. The noise was recorded at a distance of roughly seventy meters from the side of the Tullamarine Freeway. A five-minute traffic noise sample was then selected and used as our transmission loss test source noise. This allowed the transmission loss and STC of each window configuration to be determined and compared. for an identical traffic noise exposure. The testing was conducted in general accordance with AS2253 and AS1276.

The pre-recorded traffic noise recording was played through a loudspeaker, which was located on the outside of the building, at a distance of 1 meter away from the window being tested. Sound pressure levels were recorded on both sides of the window by traversing the microphone along the window while maintaining an average distance of 0.5 meters from it on the source side and 2 meters from it on the receiver side. Each room's reverberation time and ambient background sound levels were measured as well. The measured levels were then used to calculate the facade sound transmission loss and an overall STC rating.

3. WINDOW TEST CONFIGURATIONS

A total of 7 different window configurations were chosen for testing. The seven configurations are listed below.

- **Current Window** - existing 3 mm openable sash windows were tested before modifications were performed.

- **Low Level Refurbishment Upgrade** - existing windows were treated as follows:

1. Existing vents blanked off at the top of the window.
2. Q-lon seals in a PVC retro carrier face fixed to the head of the top sash.

Aquamatic seals in a PVC retro carrier fixed to the top of the head of the inner sash to seal the meeting rails.

• **High Level Refurbishment Upgrade** - existing windows were treated as follows:
1. Existing vents blanked off at the top of the window.
2. Q-lon seals in a PVC retro carrier face fixed to the head of the top sash.
3. Aquamatic seals in a PVC retro carrier fixed to the top of the head of the inner sash to seal the meeting rails.
4. Side seals on bottom sashes replaced with Q-lon seals.
5. Seals in top sashes at meeting rail replaced with Q-lon seals.

• **5mm Window** - new 5mm thick monolithic glass windows were tested.

• **6mm Window** - new 6mm thick monolithic glass windows were tested.

• **6.38mm Lam Window** - new 6.38mm thick laminated glass windows were tested.

• **6.76mm Lam Window** - new 6.76mm thick laminated glass windows were tested.

4. MEASUREMENT RESULTS

As expected, results varied slightly from contractor to contractor and from single to double type windows. Generally, the results were good and slightly better than predicted in our earlier reports. Table 1 below shows a summary of the results.

Table 1. Facade STC Performance for various window types and upgrades

Window Type	**Contractor #1**		**Contractor #2**	
Glass Type	**Single**	**Double**	**Single**	**Double**
Existing	STC-15	STC-13	STC-17	STC-16
Low Level Refurbishment	STC-20	STC-19	STC-22	STC-21
High Level Refurbishment	STC-23	STC-24	STC-23	STC-24
5mm Glass	STC-27	STC-27	STC-27	STC-25
6mm Glass	STC-31	STC-31	STC-30	STC-26
6.38mm Glass	STC-31	STC-31	STC-30	STC-27
6.76mm Glass	STC-25	STC-29	STC-25	STC-28

Some general comments on the test results are as follows :

- Overall, Contractor #1 yielded slightly better results. Even though Contractor #2's seals performed to a greater extent, it is important to note that they were modifying slightly better performing windows.
- Surprisingly, no extra benefit was realised by upgrading the 6mm thick glass to a laminated glass. The double interlayer (6.76mm) actually appeared to result in a relatively reduced performance.

- Although the provision of supplemental seals on existing windows resulted in a fair increase in transmission loss, this is probably a best-case scenario and should be treated as such. In practice, it is likely that the windows might generally perform 1 to 3 STC points lower than indicated.

5. WINDOW CONFIGURATION FACADE IMPROVEMENTS

In order to simplify results, Tables containing the window configurations and the corresponding minimum predicted improvements relative to the "existing window" base case are presented below.

Table 2 : Absolute Facade Noise Reduction Improvement For Different Acoustic Upgrades Relative to the Existing Window

Window Construction	Measured STC Increase Single		Measured STC Increase Double and Triple	
	Contractor #1	Contractor #2	Contractor #1	Contractor #2
Existing Window - 3mm	-	-	-	-
Low Level Upgrade	5	5	6	5
High Level Upgrade	8	6	11	8
5mm Glass	12	10	14	9
6mm Glass/6.38mm laminated	16	13	18	11
6.76 laminated	10	8	16	12

The nominal absolute acoustic improvement for each window upgrade relative to the previous one is shown in Table 3 below.

Table 3 : Facade Noise Reduction Improvement For Different Window Acoustic Upgrades Relative to the Previous Upgrade

Window Construction	Relative STC Increase Single		Relative STC Increase Double and Triple	
	Contractor #1	Contractor #2	Contractor #1	Contractor #2
Existing Window - 3mm	-	-	-	-
Low Level Upgrade	5	5	6	5
High Level Upgrade	3	1	5	3
5mm Glass	4	4	3	1
6mm Glass/6.38mm laminated	4	3	4	2
6.76 laminated	-6	-5	-2	1

6. DISCUSSION

As would be expected, the acoustic performance increase due to the upgrading of the windows in a facade will depend on the actual realised workmanship. The testing clearly showed that slightly better results were obtained from Contractor #1 than Contractor #2.

In terms of the STC improvement, most of the upgrades resulted in a measurable improvement. The most surprising results were (1) there was no effective improvement in upgrading from the 6mm to the 6.38mm laminated glazing and that (in upgrading from the 6.38mm laminated to the 6.76mm laminated, the acoustic performance **decreased.** Why this is so is not clear but the effect was clearly shown on a number of occasions.

The results show that it is practical to improve glazing in-situ and to achieve a significant acoustic performance increase in the noise reduction across a facade. The degree of the increase will depend on the initial acoustic performance. Our tests showed that a doubling of STC is possible in some circumstances.

7. CONCLUSION

The existing facade in an apartment complex was initially tested for noise reduction and then the facade glazing performance was progressively upgraded. Two separate contractors worked on two different apartment units simultaneously so as to ascertain the potential difference due to workmanship. The initial upgrades were with the existing glazing in place but with upgraded seals around the windows. Further upgrades included the use of thicker single panes and the use of a single laminated glazing. The results show that the results were dependent on the skills of the Contractor. The initial glazing did not perform well with an STC of the order of only STC-15 but that with care and an appropriate glazing, the STC could be increased to the order of STC-30 and above.

8. REFERENCES

AS2253 - 1979 Methods for Field Measurement of the Reduction of Airborne Sound Transmission in Buildings

AS1276 - 1979 Methods for Determination of Sound Transmission Class and Noise Isolation Class of Building Partitions

AUSTRALIAN ACOUSTICAL SOCIETY CONFERENCE

ACOUSTICS TODAY

Melbourne, 24 – 26 November, 1999.

AN INVESTIGATION OF NOISE FROM STAIRS BONDED TO AN APARTMENT BEDROOM

Graeme E Harding F.A.A.S., M.A.S.A., M.I.I.A.V.

Director, Graeme E. Harding & Associates Pty. Ltd.
Consultants in Acoustics Noise and Vibration

ABSTRACT

In a modern block of apartments without a lift, the apartment on the lowest floor adjoining the stairs received highly disturbing noise from the many occupants ascending and descending the stairs. There is an obvious airborne component and structureborne component of the noise. This paper gives the methods of testing, and results of tests which established that the staircase must be structurally disconnected from the building if an acceptable noise climate is to be achieved within the bedroom.

OWNER'S REQUIREMENTS/QUESTIONS

The owner lived overseas, and advised that tenants complained that the noise from footsteps on the stairs, and the sounds of people talking in the hall and stairway was so intrusive to sleep and living that few tenants stayed more than a few weeks before leaving with complaints of excessive noise intrusion.

What the owner wanted to know, was whether some door seals, or even an up-graded door would remedy the acoustical defect; and in the event that more extensive remedial work was required, what was appropriate.

The owner's complaints indicated that the noise intrusion was likely the result of both airborne sound transmission and structureborne sound transmission.

THE BUILDING & APARTMENT

The three storey building is only about three years old, and comprises a carpark on the ground floor, four apartments on the first floor with a further five smaller apartments on the second floor.

The apartment concerned was nearest to the stairs, and had the steel structure of the stairs supported by the blockwork wall of the bedroom. A quick inspection showed that

Aural tests were made that confirmed that both the airborne and structureborne paths contributed significantly to the noise intrusion.

FIRST REPORT TO OWNER, AND RESPONSE

The first report to the owner was that our brief assessment with the agent showed that the tenants were justified in leaving; but more importantly that remedial work would require structural building alterations at significant cost.

The owner asked how it was possible that a virtually un-inhabitable apartment could be built and sold having regard to the building regulations. We explained that the current Building Code of Australia had no requirements as regards isolation of the noise from impacts on floors or stairs, and in fact no requirements as regards the sound isolation of complete constructions. We were then asked to make what measurements were necessary to see if upgrading of the door and wall alone could achieve enough amenity for occupancy.

ACOUSTICAL MEASUREMENTS AND INTERPRETATIONS

One of the things we could not do was to use a standardised tapping machine as an impact source; not only would the impacts be completely different from footsteps, but we would damage the stairs with the hammers and disturb all occupants of the building. We determined to see how uniformly we could go up and down the stairs, and found we could do quite well enough; within a decibel or so in most octave bands.

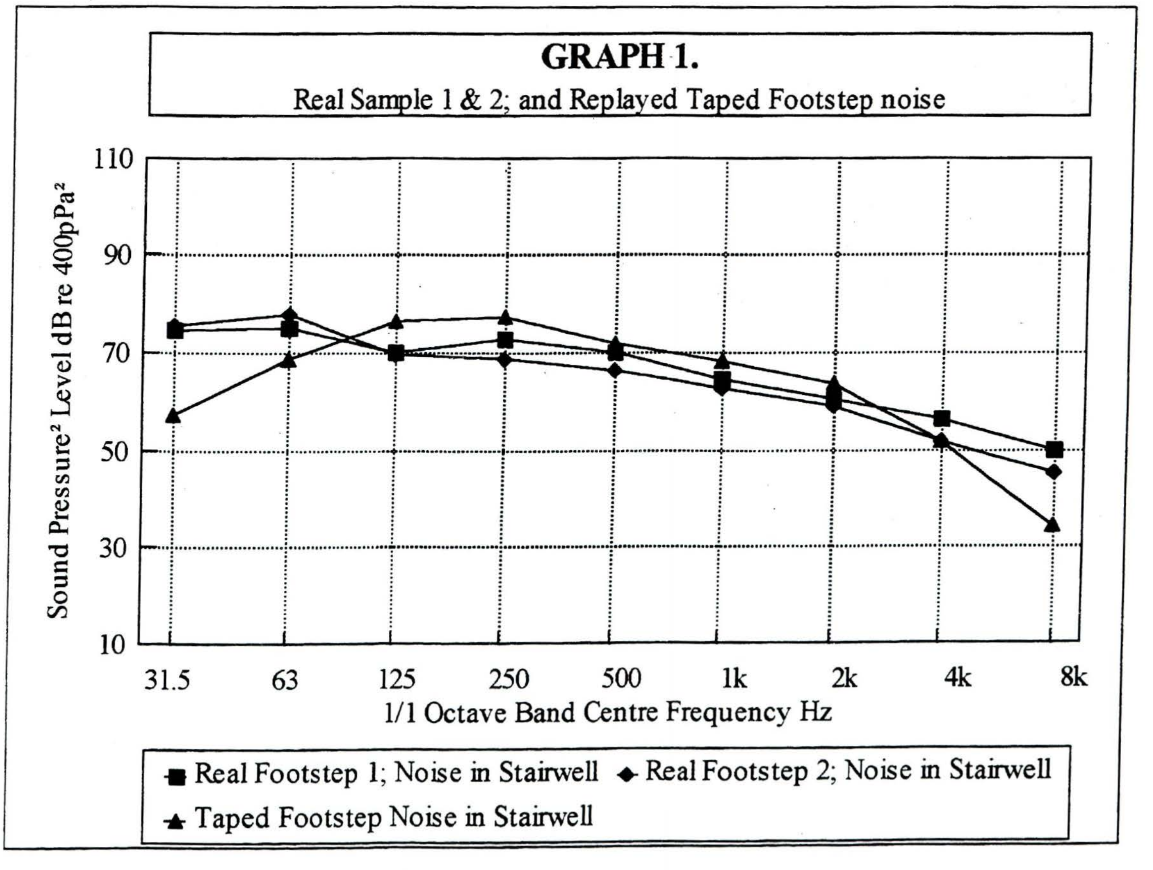

all the people from all the apartments in the building would traverse these stairs to go in or out of the building; and thus there would be plenty of footstep traffic.

Figure 1. below shows the arrangement of the apartment and stairs:

Figure 1. Arrangement of Apartment 4 and Stairs

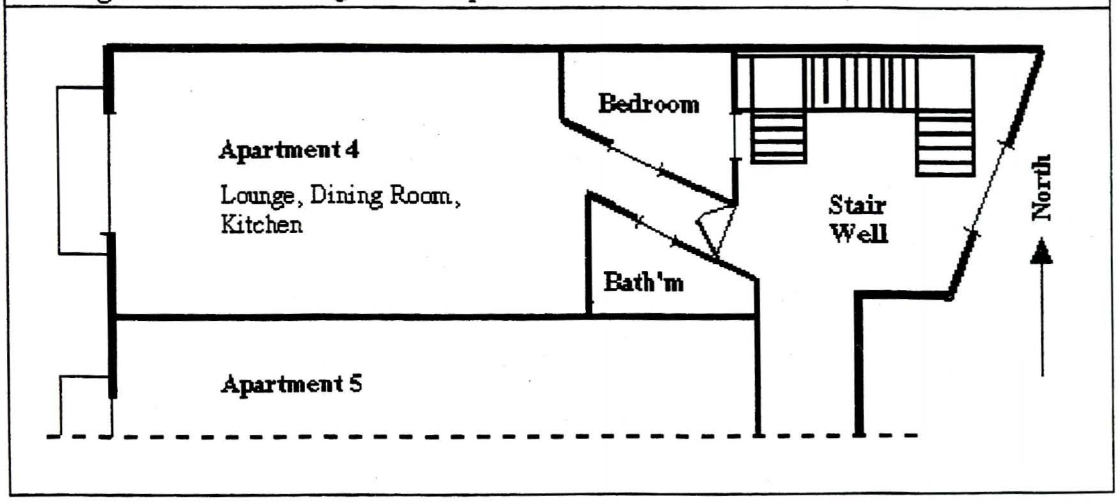

PRELIMINARY INSPECTION AND INVESTIGATION

The stairs are of hardwood with a polyester or other hard finish; no carpet. We tried out the stairs and found the hardwood steps and steel structure to be resonant and noisy. It was easy to see that in the quiet bedroom the structureborne footstep noise could be very disturbing.

The rolled steel channels supporting the stairs are bonded into, and supported by the 90mm block wall of the bedroom.

The light timber door to the apartment had a gap at the floor of at least 15mm, and a gap between the door face and the stop at the head of the of about 10mm; and hence would provide very little airborne sound isolation.

The door has a panel of glass bricks up the strike side of the door, and over the head of the door; and there is a larger panel of glass bricks in the bedroom wall just near the stairs.

The building fronts a small lane in a quiet part of West Melbourne, with the resulting background noise level being very low indeed. As later measurements showed the background noise level inside the apartment is typically 25dB(A).

It had taken but a few moments to appreciate that the noise intrusion was significant, and would most likely require noise control of both the airborne and structureborne paths.

Graph 1 shows the the 1/1 octave band noise levels for the real and taped footstep noise; the un-weighted overall noise level for the real footsteps was 80.2dB and 80.9dB, and for the taped and replayed noise 81.1dB.

An experimental technique used to separate the airborne and structureborne components, was to tape record the noise of the footsteps in the stairwell, and then replay the recorded footstep noise via a loudspeaker at the same overall level. Due to low frequency limitations of amplifiers and loudspeakers; and lack of a graphic equaliser we could not match the spectral noise levels. However we achieved a wholly airborne noise source with the same temporal characteristics as the real footsteps, and with no structureborne component.

Pink noise was also used as a controlled noise source and with no structureborne component.

A second experiment involved sealing the door perimeter; a direct measurement of the airborne noise reduction with and without the door sealed giving the limiting improvement possible if the structureborne component is negligible. Similarly measurement of the noise in the apartment with and without the door sealed resulting from real footsteps shows the limit of improvement possible with up-grading work limited to fixing sealing gaskets to the door.

Second result presentation Graph 2. shows the received noise in the bedroom both from the real and tape recorded footstep noise replayed in the stairwell.

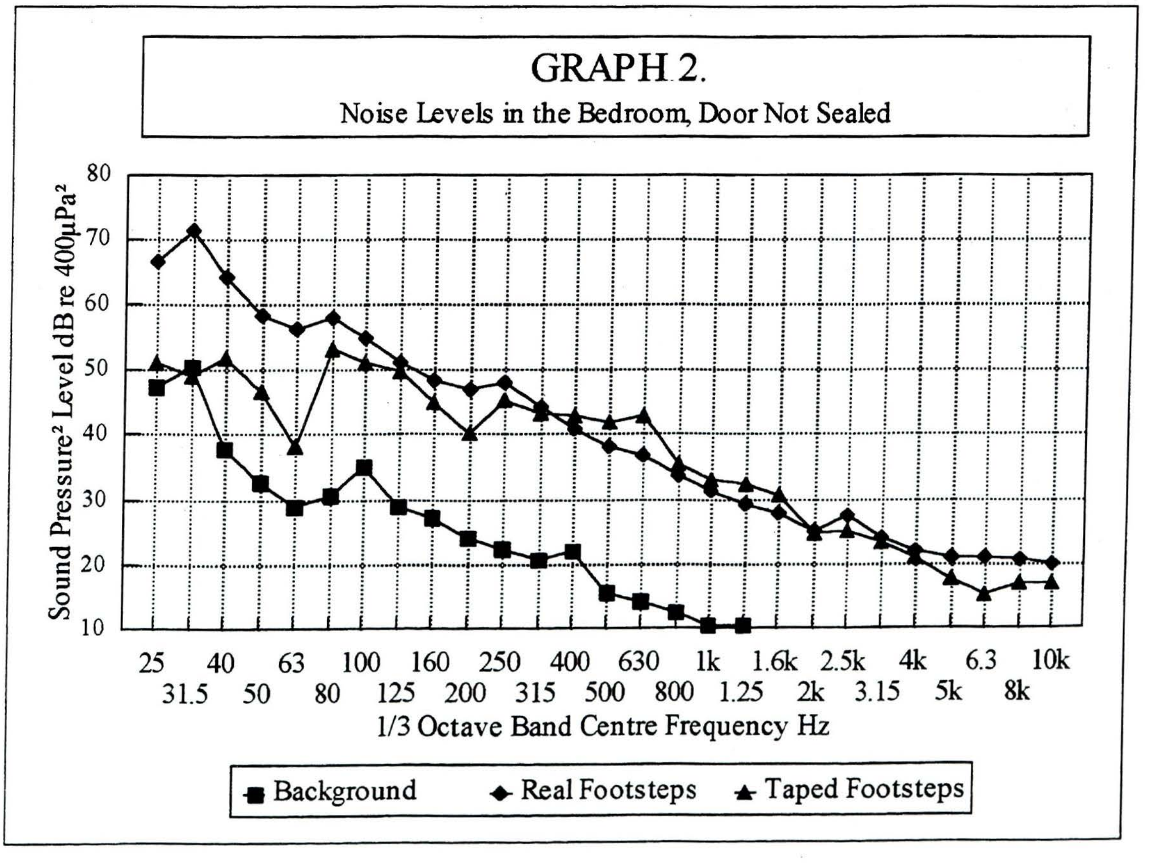

No correction has been made to correct the small mismatch between the real footstep noise and the taped footstep noise. The closeness of the results suggests that at least for frequencies above 63Hz the structureborne component is not as significant as judged.

Perhaps more importantly, Graph 2. shows that the footstep noise is typically about 20dB (and 27dB at 63Hz) above the background noise level. The overall noise level for the footstep noise is 47dB(A), whilst the background noise is 25dB(A). On both the ground of signal to noise ratio, and overall level of intrusive noise, the measurements justify the complaints that the apartment does not match the quality or expectations for the location or rent paid, and is basically too noisy for occupancy.

Third result presentation The results shown in Graph 3. were established with a pink noise source in the stairwell, the sending noise levels being measured in the stairwell about 600mm outside the apartment door, and the receiving noise levels being measured in the entry passage of the apartment.

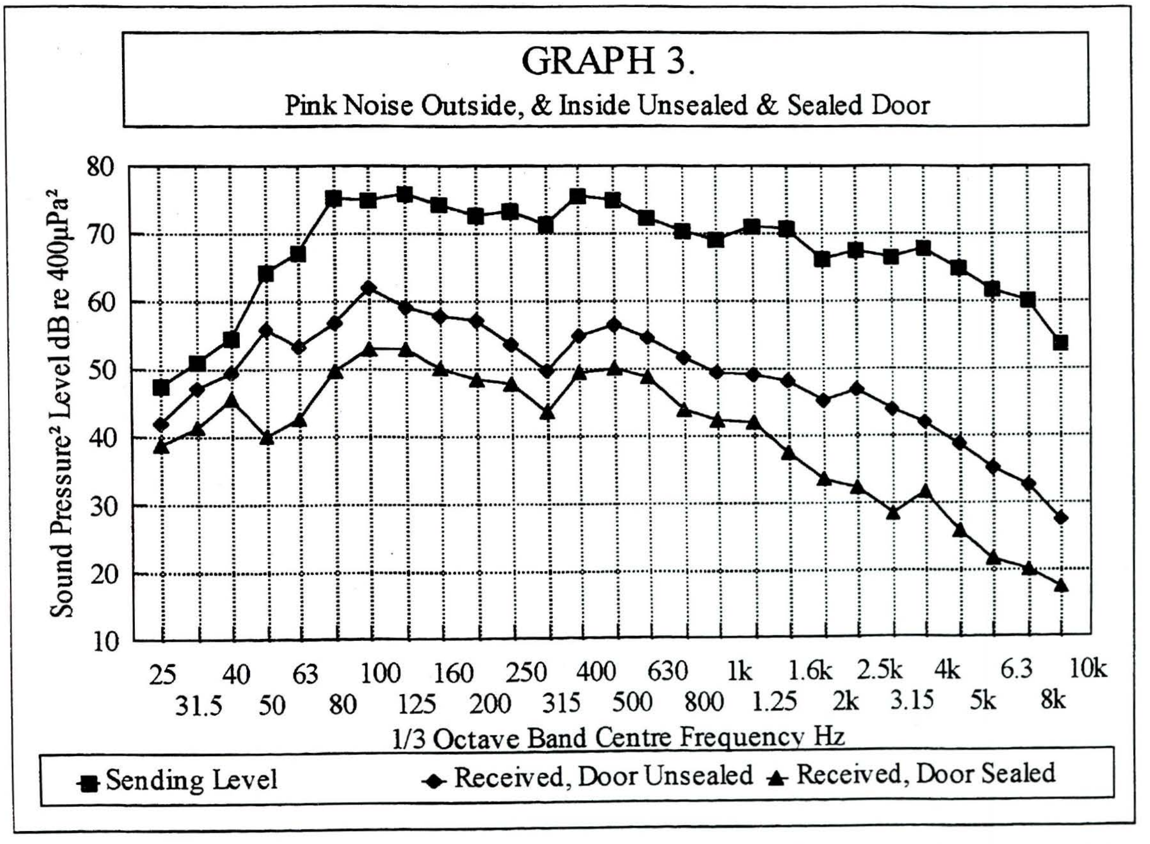

It will be noted that there is a worthwhile improvement in the noise reduction resulting from sealing the door perimeter. The average noise reduction from 100Hz to 4kHz with the door not sealed was 20dB, and with the door sealed was 28dB, an improvement of 8dB. With the measuring position in a passage just 1.5m inside the door, the sound transmission loss of the door is the dominating factor setting the noise reduction, and 28dB for the sealed door is what could be expected. No attempt was made to measure the receiving room absorption so that corrections could be made to the noise reductions to estimate the sound transmission loss of the construction.

The bedroom is only a little better off than the apartment entry passage. To provide ventilation the wall between the entry passage and the bedroom stops short of the ceiling by about half a metre. There is the additional weakness between the bedroom and the stairwell in the form of a panel of glass bricks in the nominal 90mm block wall.

Fourth result presentation The results shown in Graph 4. were determined with the same setup as for Graph 3., but with the receiving measuring position being in the bedroom rather than the entry passage of the apartment.

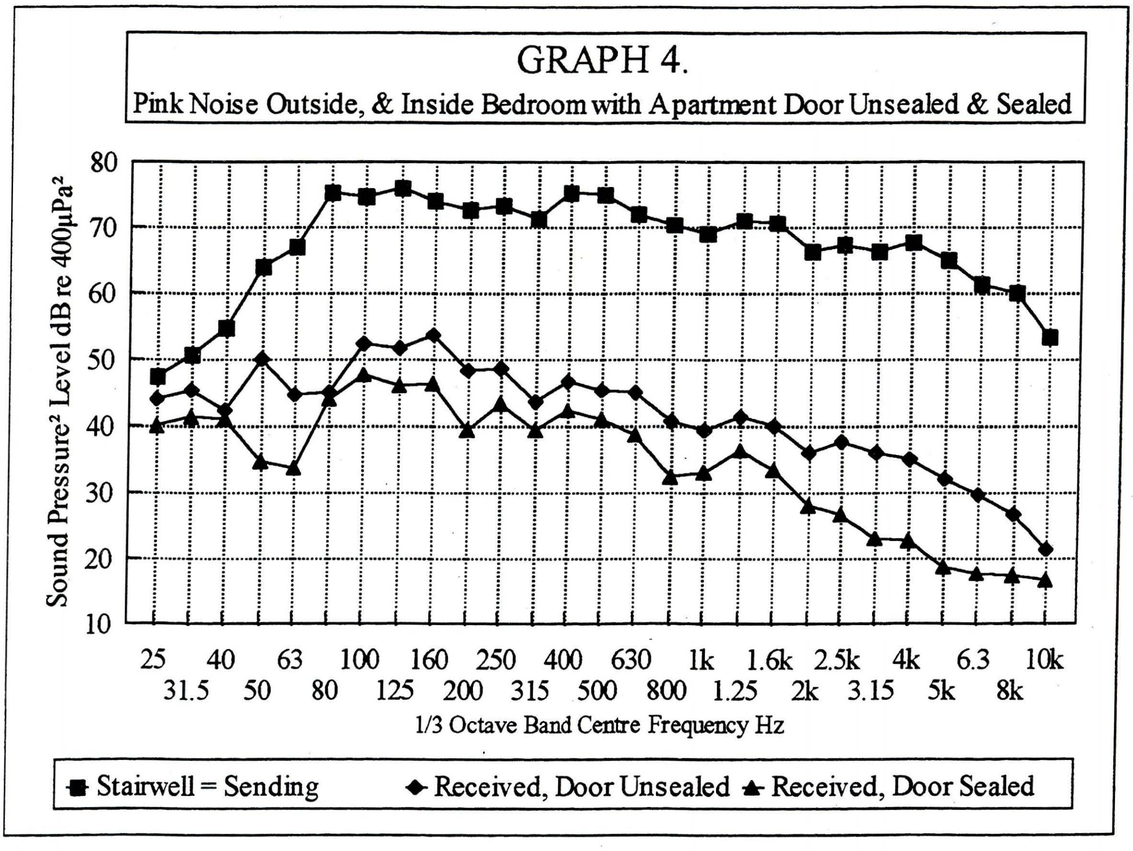

The noise reductions are higher than for the measuring position in the apartment entry passage, and consequently the noise levels are a little lower. More importantly the improvement obtained by sealing the door is slightly reduced. The average noise reduction from 100Hz to 4kHz was 26dB with the door not sealed, and 33dB with the door sealed, an improvement of 7dB.

Fifth result discussion The results shown in Graph 5. were determined by measuring the noise in the bedroom due to real footsteps firstly with no seals to the apartment door, and then with the door sealed.

In reading this graph it must be borne in mind that there are differences between the two sets of footsteps used for the apartment door not sealed, and apartment door sealed tests.

Not withstanding the different sets of footsteps used for the two tests; the results in Graph 5. clearly show that the possible improvement obtained by just sealing the front door of the apartment is not significant. The overall the (A) Weighted noise level fell by only 1dB, from 47dB to 46dB.

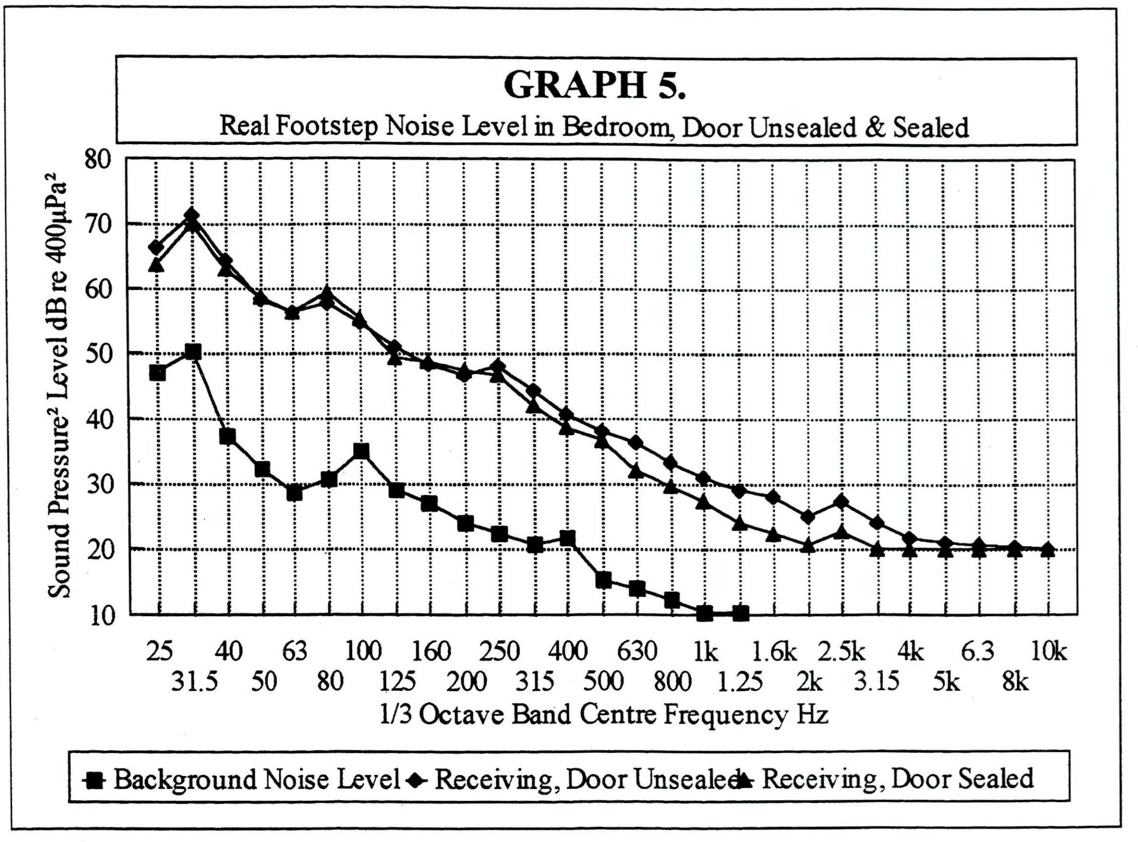

FINAL REPORT

The final report to the owner confirmed our initial advice that:

(a) That the noise disturbance was significant, and not such as a normal person would suffer for long.

(b) That the noise intrusion resulted from two distinct forms of deficiency: inadequate airborne sound isolation, and inadequate structureborne sound isolation.

(c) That as regards structureborne sound isolation, there were no specific requirements in the Building Code of Australia.

(d) That as regards the airborne sound isolation, the building did not conform to the minimum requirements of the Building Code of Australia for sound isolation of walls between dwelling units and passages or other common areas.

(e) That to upgrade the airborne sound isolation of the apartment would require a substantial upgrading of both the wall and entry, with a consequent smaller bedroom through increased wall thickness. In turn the bedroom would probably no longer conform to the minimum room size requirements of the Building Code of Australia.

(f) That to upgrade the structureborne sound isolation would require structural alteration of the building and stairs with steel columns; with attendant foundations and bracing; being provided to support the stairs. In turn this work; would require the consent of the body corporate;

would entail costs of foundation design, structural design etc, as well as the costs of construction.

The owner determined to take no action.

ACKNOWLEDGMENTS

The assistance of Paul Tierney and Jim Antonopoulos in making the site measurements is acknowledged.

AUSTRALIAN ACOUSTICAL SOCIETY CONFERENCE

ACOUSTICS TODAY

Melbourne, 24 – 26 November, 1999.

SENSING A BURIED OBJECT ACOUSTICALLY

Charles Don and David Lawrence[1]

Department of Physics, Monash University, Clayton 3168, Australia

[1]Current address: Department of Otolaryngology, The University of Melbourne

384-388 Albert Street, East Melbourne 3002

ABSTRACT

Since it was first reported at an AAS meeting in 1993, considerable refinement has been made to an acoustic method for detecting non-metallic objects at depths down to 10 cm in various types of soils. Based on an acoustic impulse source, the detector initially used two microphones to isolate the small pulse reflected back from, say, a land mine. The system evolved to using only one microphone and then to combining the outputs from an array of up to four microphones. Requiring accurate alignment and subtraction of pulse waveforms, the detecting algorithm has demanded a number of subtle problems be solved in order to detect the very small reflected pulse. The use of a pre-recorded ground reflection and a correlating pulse characteristic of the buried object has enabled a mine to be clearly located even when leaves and metal cartridge-cases litter the surface. Tuning the frequency spectrum of the pulse waveform has also decreased background noise due to surface roughness and spurious objects in the order of a few centimetres. However, the system suffers from false images produced by larger hills and hollows on the surface and a limited depth of penetration, especially in wet soils.

BASIC PRINCIPLES

One approach to detecting a buried object acoustically involves using two microphones spaced symmetrically on either side of a source of sound [1, 2]. Over uniform ground both microphones record essentially the same signal so the difference between their outputs should be zero. However, when one microphone is over a buried object the small delayed reflection from the object remains in the difference signal. In practice the challenge is to separate this from the background noise caused by factors such as signal misalignment and surface roughness.

There is a major advantage in using a pulse source compared to continuous waves as, in principle, the former can easily be aligned in time to achieve complete subtraction. Further, the components of the recorded signal can be readily identified. Our detector system [3, 4] uses a reproducible pulse of sound that emerges from a long thin tube attached to a loud speaker, Fig.1. The microphone is attached, via a vibration-isolated mount, to the tube at a fixed separation. This combination is referred to as the detector probe. Some of the energy from the source goes directly to the microphone, the '*direct pulse*' [A], while other energy is reflected from the surface, the '*surface pulse*' [B], and a lesser amount comes from any buried object, the '*object pulse*' [C]. The resultant signal is the sum of these components. In principle, the depth of the object can be determined from the delay between pulses B and C.

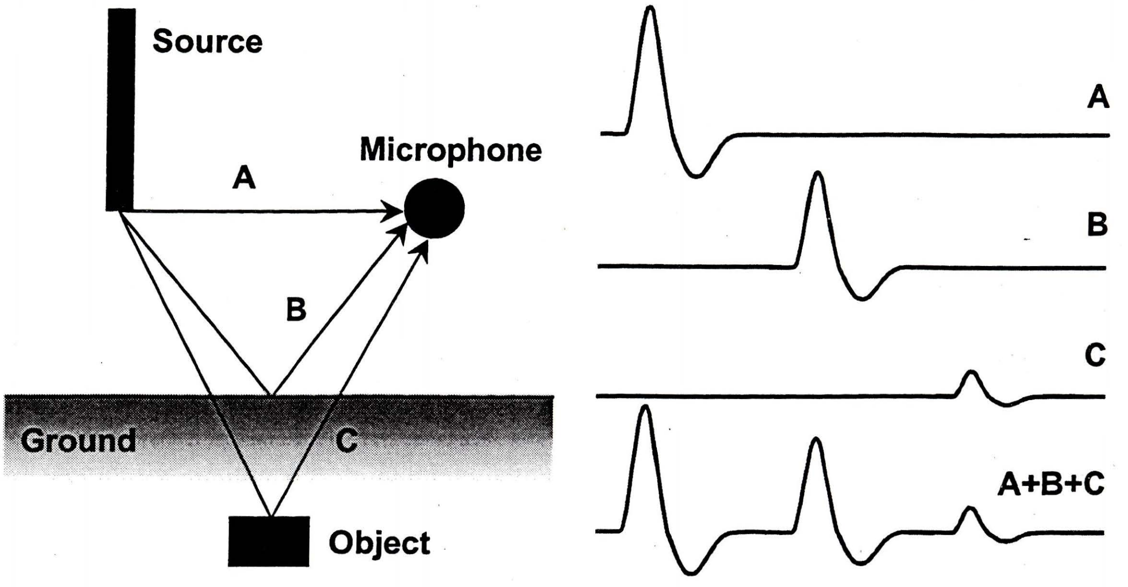

Fig.1: *Components of recorded pulse train: A is the free-field direct, B is an isolated ground reflection, and C is the desired object reflection obtained by subtracting A and B from the captured signal.*

The delay between the direct and the other pulses is dependent on the distance between the detector and the reflecting surfaces, which may not remain constant. Therefore two separate microphone outputs may not subtract correctly without first aligning the surface pulses in time. The problem is simplified by considering a single microphone output along with two pre-stored reference signals.

A reference direct pulse can be time isolated by raising the detector probe well away from the ground so that any surface reflection can be excluded by time isolation or windowing. A typical surface reflection for the ground being investigated is obtained by moving the system above an region known to contain no buried objects. The recorded signal also contains a direct pulse, which first must be subtracted. Six or more ground reflections are then averaged to obtain a representative reference surface pulse. These stored reference pulses are then subtracted from the signal recorded by the same microphone as it moves over the terrain being investigated.

A bonus is that the position of the surface relative to the detector probe can be determined from the delay of the surface reflection, and this position has been superimposed on the processed images that follow.

While the above ideas apply to any type of buried object, one important application is to the detection of non-metallic landmines [5]. The examples that follow are based on the detection of plastic landmines, about 8 to 15cm in diameter.

SOME PRACTICAL CONSIDERATIONS

Currently the detector is a laboratory-based instrument. Impulses of duration and with a peak energy at about are generated by feeding a horn driver with a pre- synthesised waveform. The object is buried in a large bed of sand or earth and the probe is held a few centimetres above the surface and moved in 2cm steps across the region to be investigated. The microphone output is recorded with a Data 6000 waveform analyser and after a sweep is transferred to a PC for processing using an algorithm which produces an image representing a cross-section through the ground.

Typically, a small object produces a hyperbolic pattern, caused by the detector sensing it as being "deeper" (i.e. more delayed) when the detector is at one side of the object.

Figure 2 shows such an image, which was considered to be a reasonable find about three years ago. The horizontal scale is such that this represents a scan across about 1m of the test bed, while the vertical scale images the ground down to a depth of 10cm. The darkest region near the middle of the scan represents the mine, which seems to be deeper than was the actual case, as the mine was just under the surface. A considerable amount of residual background noise is evident.

The region above the surface has been automatically set to white by the algorithm, which uses 256 grey levels and automatically makes the largest residue signal in the full image equal to black. The surface contour is added last so that it does not influence the choice of the grey scaling.

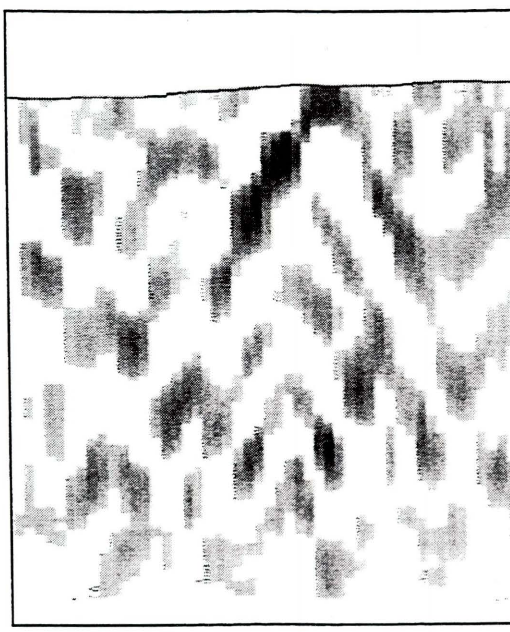

Fig.2: Image of mine obtained using an early detection algorithm.

A number of practical problems that had to be addressed in order to improve the detection algorithm will now be considered.

(a) Alignment of pulses

In principle, it is essential to optimise the alignment of the pulses to be subtracted as any residue may influence the background on which the object reflection is superimposed. In practice, alignment of the very reproducible direct pulses is not so crucial, as any residue is well before the surface reflection and can largely be time isolated. However, two types of shift may be needed before subtracting the surface reflected pulses. Firstly, a coarse movement is performed to allow for variations in the separation of the probe and ground surface. This is followed by a fine adjustment, which must allow for two factors.

(i) As the data is sampled with a resolution of 5 μs, there are few points during the rapid rise-time of the pulse. As these points may not occur at corresponding positions on the leading edge in different traces, alignment on these points may cause a sharp spike to remain after subtracting the leading edges. In worst case situations, these spikes can be larger than the object reflection, resulting in a spurious indication of a mine near the surface.

(ii) Even adjacent regions of ground often produce pulses with significantly different rise times, and these may all differ from that of the surface reference pulse even though the latter was derived from the same type of surface. The resulting mismatch typically leaves two large spikes of opposite sense in the residue.

To limit such effects, an algorithm was developed which shifted the alignment by fractions of a sampling period until the minimum residue over a narrow interval around the leading edge was achieved. It is important not to extend this summation beyond the leading edge as it may be influenced by effects due to the buried object itself.

As the probe is moved, the shape and magnitude of the surface pulse may vary due to surface irregularities and varying ground reflectivity. In general, to minimise the subtraction residue the peak of the reference is normalised to the surface reflection prior to subtraction.. However, an important possibility is that there may be a landmine at or very near the surface, producing a significantly enhanced reflection. A decision must be made whether or not to perform the normalisation and thereby possibly remove evidence of a surface mine. Further, if a highly reflective object is just below the surface, the ground reflection may appear as a double peak with a stronger second component. It is then necessary to scale on the first component to avoid eliminating evidence of the object. Another situation that may produce a complicated multi-peak ground reflection is when there is a hill or valley on the ground surface. In this case it is necessary to use additional information from the surface profile to try and reduce interference from the surface contour. In practice, it has been found necessary to have a number of selection rules built into the analysing algorithm, eg. if the peak value is outside a typical range then the scaling is bypassed. Incorrect subtraction, due to scaling or otherwise, can produce distinct features near the surface that may obscure the find. Attention to the above ideas has allowed the successful detection of a mine when covered by only a few grains of sand.

(b) Correlation techniques

Signal enhancement is achieved by correlating the subtraction residue with a predetermined object reflection or mask. A series of measurements were taken with the probe directly over a mine buried at a known depth. After subtracting the direct and surface peaks, the residue corresponds to the mine reflection. The average of a number of such results at a particular depth was stored and used as the mask. Because of different frequency-dependent soil attenuations, the appropriate mask changes with the type of soil and also varies with depth. Allowing for changing soil types just implies selecting a different set of masks, however, the depth variation is more complex because [at each position,] the residue contains information from all depths. Thus different correlation masks must be used at various parts of the one residue, as suggested in Fig. 3. Possible solutions include:

(i) processing the residue many times with different masks and choosing the result with the maximum "find",

(ii) changing masks at different sections of the residue and,

(iii) generating a continuously changing mask from knowledge of the acoustic parameters of the ground. Either of the first two processes can introduce steps, either between successive position scans or at the change-of-mask points along a residue. Generating the mask theoretically is potentially the best, but more difficult, approach and has not yet been attempted.

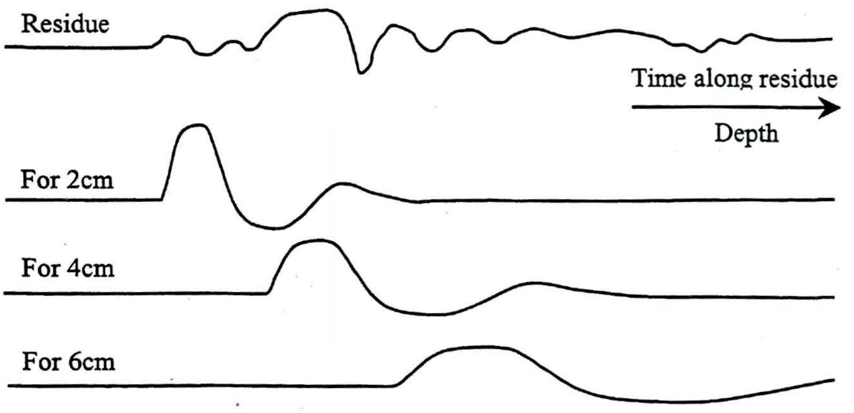

***Fig. 3**: Sketch showing a typical residue and the masks that must be applied at different depths in order to enhance the find.*

The improvement in the image of the mine that is possible by choosing the correct correlation mask at different depths is demonstrated in Fig.4. When a high correlation occurs, the find signal is so large that background noise is markedly suppressed. However, the use of an incorrect mask reduces the signal at the mine and allows the background to emerge more strongly, as in Fig. 4(d).

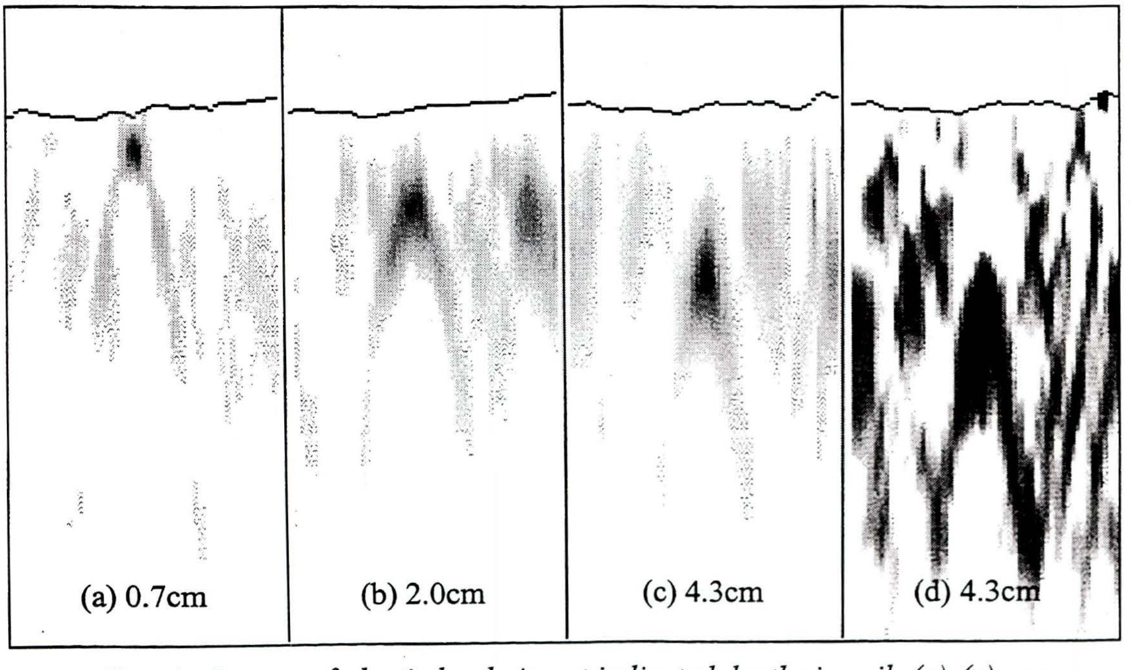

***Fig. 4**: Images of plastic landmine at indicated depths in soil: (a)-(c) use mask for that depth, while (d) uses the inappropriate 0.7cm mask. Because of the reduced find intensity in (d), scaling has enhanced the background noise. The horizontal distance is 1m in each image.*

(c) Surface problems

A well-defined hill or a hole in the surface can pose problems for the detector system. Both features produce a hyperbolic shaped artefact below the surface, which can be confused with the signal due to a mine, see Fig.5. However, the detector algorithm automatically obtains the ground surface profile which thereby locates the size and position of a hill or hole. In principle, the related hyperbolic pattern can then be subtracted to produce a cleaner image. However, there is the possibility that either a hole or a hill may be connected with the presence of a mine, so care needs to be taken not to remove evidence of the mine. The way around this problem would seem to be a series of additional checks similar to those used to prevent cancellation of effects due to a mine on the surface. While some work has been undertaken in this area, the algorithm to achieve these aims has not yet been completed.

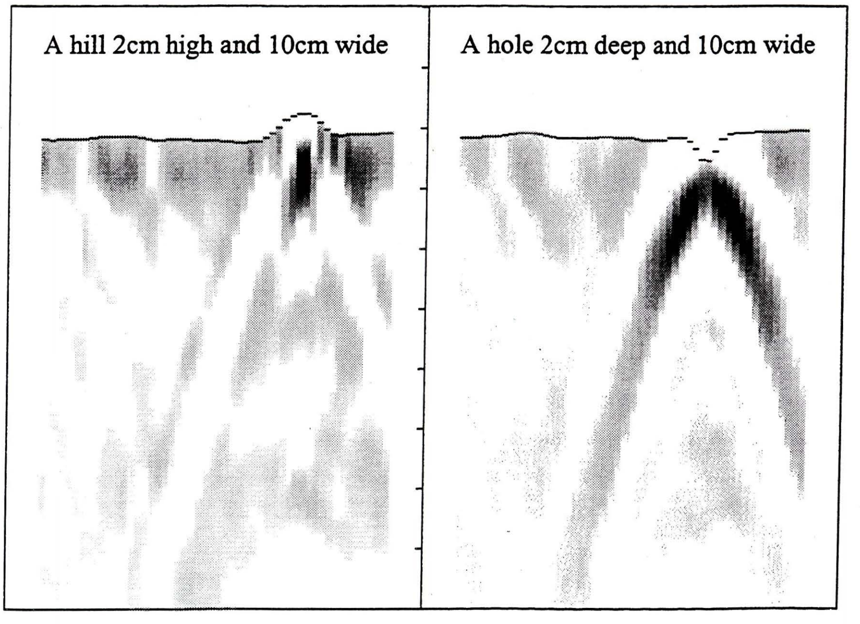

Fig. 5: *Characteristic hyperbolic signals from sharp surface features that might obscure the presence of a landmine. While these artefacts can be identified from the surface profile and therefore eliminated by the detection algorithm, the problem is to ensure that any evidence of a hidden landmine is not removed.*

(d) Multi-microphone techniques.

The detector originally was based on two microphones, then became a single microphone system. More recently, a system consisting of an array of four microphones positioned around a single source has been trialed. The output from each microphone is processed individually and the results are then combined to enhance common image features. As they all sense a slightly different area of ground, combining the outputs offers the potential to reduce the effect of near-the-surface differences while enhancing the signal from a deeper object such as a mine. Considerable effort has gone into finding the best positions for the microphones and to correctly combine the image from each microphone into a single image. One problem is the degradation of a find when only two microphones pass over the mine. If inappropriately combined, the resultant may significantly weaken the actual find by the other microphones. Linked with this is the question of whether to adjust the maximum of an image to full scale (black) in order to enhance a weaker find and thereby risk exaggerating unwanted residues. Several examples of four-microphone results will be presented as part of the talk.

ADVANTAGES AND DISADVANTAGES OF AN ACOUSTIC DETECTOR

This acoustic system has the advantage of being unaffected by extraneous metal objects, providing their size is small compared to the landmine, Fig. 6. In an old battlefield, where the ground may be littered with metal objects, such as cartridge cases or metal scrap, this is a major advantage over any metal-sensitive method.

By adjusting the frequency content of the pulse, it has been possible to eliminate the effect of soil lumps in the order of a few centimetres, and to reduce the effect of surface leaves and other debris. Combining multiple microphone outputs has markedly improved our ability to ignore surface irregularities. However, larger hills and hollows still pose a problem.

A major disadvantage of the acoustic method is that the high attenuation at depths of more than 5 to 10 cm makes detection difficult. This is particularly a problem in very wet soils where the ground pores are filled with water, inhibiting sound from penetrating. However, small cracks often appear once wet soil dries, permitting sound to once more enter.

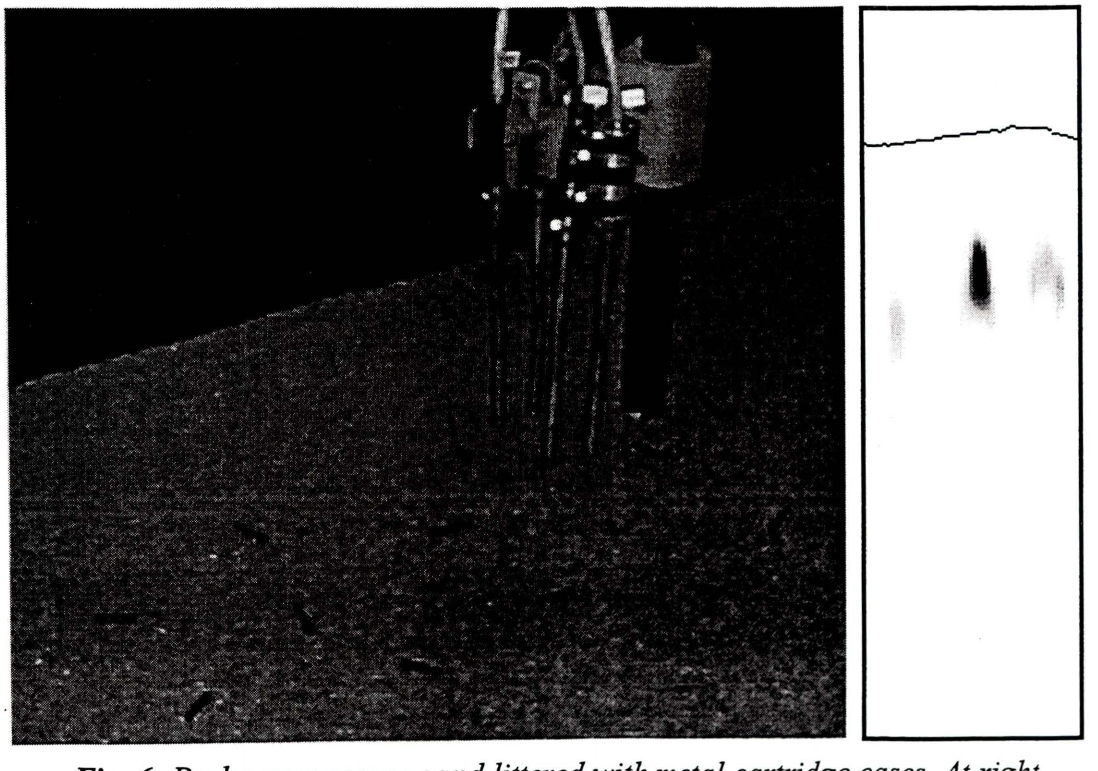

Fig. 6: *Probe over coarse sand littered with metal cartridge cases. At right is the corresponding detector image revealing the plastic mine at a depth of 5cm while uninfluenced by the metal objects.*

ACKNOWLEDGEMENTS

This work was supported, in part, by a Defence Science and Technology Organisation contract. The authors acknowledge the work of A.J.Rogers in developing the earlier version of the detector.

REFERENCES

1. A J Rogers,. and C G Don, 'Location of buried objects by an acoustic impulse technique.' Acoustics Australia, **22/1**, Apr 1994, p5.
2. C G Don and A J Rogers, 'Using acoustic impulses to identify a buried non-metallic Object,' 127th Meeting of the Acoustical Society of America, Boston, USA, Abstract 2aPA3, 1994.
3. U.S. Letters Patent, No 5,563,848 'Object detector for detecting buried objects.' Issued Oct.8, 1996.
4. C G Don, D E Lawrence and A J Rogers, 'Using acoustic impulses to detect buried objects,' 16th International Congress on Acoustics and 135th Meeting of the Acoustical Society of America, Seattle, Washington, USA, 20-26 June 1998.
5. C Bruschini and B Gros, 'A survey of current sensor technology research for the detection of landmines,' International Workshop on Sustainable Humanitarian Demining, Zagreb, Croatia, 6.18-6.27, 1997.

AUSTRALIAN ACOUSTICAL SOCIETY CONFERENCE

ACOUSTICS TODAY

Melbourne, 24 – 26 November, 1999.

A NEW INITIATIVE IN INTERNATIONAL METROLOGY:- ACOUSTICS, ULTRASONICS, VIBRATION, SONAR

Suszanne Thwaites

CSIRO
National Measurement Laboratory, Lindfield, NSW

ABSTRACT

International conformity of measurement in acoustics, ultrasonics and vibration has always rested on the assumption that if national measurement institutes use specified agreed methods for realising their internal references they will obtain equivalent results. International activity has been largely confined to the IEC, ISO and other standards defining groups. In 1997 the International Committee of Weights and Measures (CIPM), the organisation that administers the international Metric Treaty, conducted a survey of National Metrology Institutes holding these standards. This revealed a consensus view that there is a need for key international comparisons of primary standards to establish the degree of conformity between the realisation of these standards by the member nations. As a result the CIPM has formed a Consultative Committee in acoustics, ultrasonics and vibration (CCAUV) charged with setting up and coordinating a set of key comparisons of primary standards.

This paper gives a brief description of these key comparisons in acoustics, ultrasound and vibration. In addition the position of underwater acoustics (sonar) measurement in Australia, for which there is currently no measurement standards and conformance system, is discussed in detail.

1. CONVENTION DU MÈTRE (The Metric Treaty)

In today's society there exists a vast, often invisible, infrastructure of services, supplies, transport and communication networks. Their existence is usually taken for granted but their presence and smooth operation are essential for everyday life. Part of this hidden infrastructure is metrology, the science of measurement. Worldwide agreement on units of measurement and the practical provision of accurate measurement standards for all of these purposes is assured under the Convention du Mètre.

The Convention du Mètre, originally formed in 1875, is the diplomatic treaty between, at present, forty-eight nations, which gives authority to the Comité

International des Poids et Mesures (CIPM) to act as custodian of the international measurement system. The committee is elected by the member nations. The office, infrastructure and laboratories of the CIPM (the Bureau International des Poids et Mesures, BIPM) are located in Paris.

As the need has arisen the CIPM has created a number of Comités Consultatifs (CC) which bring together the world's experts in their specified fields as advisers on scientific and technical matters. Among the tasks of the CCs are the detailed consideration of advances in physics that directly influence metrology, the preparation of recommendations to the CIPM and the instigation of international comparisons of standards. At present there are nine CCs (Electricity, Photometry and Radiation, Thermometry, the Metre, the Second, Ionising Radiation, Mass, Units and Quantity of Substance). In 1998 the CIPM decided to form a CC in acoustics, vibration and ultrasound, CCAUV.

One of the most significant developments in the activity of the CIPM in recent years has been the establishment of a framework for a formal global recognition of measurements between treaty nations. Known as the Mutual Recognition Arrangement (MRA), this framework sets out principles for comparing primary standards and for documenting the results in a concise and useful form. These comparisons are known as Key Comparisons and are intended for only the highest level of absolute standards held at recognised national measurement institutes (NMI) such as the National Measurement Laboratory (NML).

2. CIPM SURVEY OF ACOUSTICS, VIBRATION AND ULTRASOUND

In 1997 the CIPM conducted a survey of the NMIs around the world on issues related to acoustic, vibration and ultrasonic standards, technology and measurement. Although these three areas differ greatly on most counts there were several areas of agreement.

- The use of acoustics, ultrasound and vibration is a growth area from the technical and industrial points of view.
- The level of activity and interest is sufficiently high for the CIPM to consider it a topic of metrological importance in which timely initiatives could be taken.
- Although other bodies (eg. IEC and ISO) are active there is a need for complementary, distinct initiatives which can address current concerns. CIPM could take ownership of these initiatives.

There was a strong consensus that there was no need for CIPM intervention or leadership in the development or compilation of documentary standards, this activity being well covered by IEC, ISO and other working groups. However, there was a perceived need for an independent international coordination of comparisons of first level measurement standards between NMIs. The CIPM was seen as a very appropriate organisation for this purpose. As it happened the CIPM was already in the process of coordinating international key comparisons for the global MRA program described in the last section.

3. KEY COMPARISONS

As a consequence of these conclusions the CIPM convened an ad hoc meeting of invitees from all responding NMIs in March 1998 at NPL in London. The participants were Netherlands, France, Australia, Poland, Germany, Japan, Slovakia, USA, South Africa, Switzerland, Italy, Canada, Mexico, Russia, India, UK and representatives of IEC TC 29(electroacoustics), TC 87(ultrasonics), ISO/TC 108/WG3 (shock and vibration pick-ups) and Euromet. The main purpose of this meeting was to initiate a small number of Key Comparisons of primary standards.

Towards this end the participants divided the acoustics/ultrasonics/vibration field into four subgroups, on the basis of transduction technologies, media and frequency range and selected a Key Comparison for each. Ultrasound was divided into high frequency applications (f > 1 MHz) as in medical and therapeutic use, and lower frequency applications (f < 500 kHz) as used in Sonar to be known as 'Underwater acoustics'. The categories are listed in Table 1 along with the type of Key Comparison selected, the artefact to be circulated and the pilot laboratory. The artefacts, with the exception of the USRD Hydrophone H52, are shown in Figure 1. Two Key Comparisons will be held in Ultrasonics due to the division of the field into medical diagnostic and therapeutic applications.

Figure 1. The transducers which will be used for the key comparisons. These are identified in Table 1. Note that these transducers are not all portrayed to the same scale.

NML has been invited to participate in all the comparisons except Underwater acoustics because it has primary level capability in these areas and it provides a strong link into the South East Asian region, both geographically and by virtue of its activities within the Asia Pacific Metrology Program. Since the March 1998 meeting all the Key Comparison details of timetables and reporting for the first four listed in Table 1 have been completed and the comparisons have commenced. The situation with regard to Underwater acoustics is discussed in the next section.

Table 1
Summary of Key Comparisons

Category	Key Comparison	Artefact	Pilot lab
Acoustics	Open circuit pressure sensitivity by coupler reciprocity, 125 Hz to 10 kHz, (IEC 61094-2)[1]	Bruel & Kjaer 4160 LSP1 1" condenser microphone.	NPL UK
Vibration	Charge sensitivity by interferometry or reciprocity, 30 Hz to 4 kHz, (ISO 5347-1)[2]	Bruel & Kjaer 8305 reference standard back-to-back accelerometer.	PTB Germany
Ultrasound Power. (therapeutic)	Power output between 10 mW and 10 W at 2, 6 and 10 MHz	Lithium Niobate transducers fabricated at PTB.	PTB
Ultrasound Sensitivity. (diagnostic)	Free field open circuit voltage sensitivity at 1, 2, 5, 10 & 15 MHz by interferometry	GEC Marconi membrane hydrophones, 1mm active area diameter.	NPL
Underwater acoustics	Free field open circuit voltage sensitivity by reciprocity, 1 kHz to 315 kHz (IEC 565)[3]	USRD H52 (low freqs), Reson 4034 (high freqs), Bruel & Kjaer 8104 (mid freqs), hydrophones.	NPL

4. UNDERWATER ACOUSTICS

Very few NMIs keep standards for underwater acoustics. The exceptions are UK, China and Russia. However, this does not reflect the amount of activity internationally in underwater acoustics but rather the concentration of this activity in the naval defence forces where it is used extensively for ranging, communications, imaging, detection etc. In fact many navies keep their own internal standards, including that of Australia. The quality of these standards is extremely variable as is the dissemination of the traceable measurements into the naval applications.

In order for an organisation to participate in international comparisons conducted through the BIPM, the organisation must be recognised formally as the holder of the national standard for the respective nation. (For instance in Australia ionising radiation standards are held by the Australian Nuclear Science and Technology Organisation (ANSTO.)) Most attendees at the March 1998 meeting of the CCAUV did not have any detailed information about local underwater acoustics activities so the underwater acoustics Key Comparison was deferred until member NMIs could survey their local capabilities.

4(a) Underwater acoustics in Australia

Over the last year an informal survey has been performed in Australia on underwater acoustic measurement. The information sought, initially, was the number of organisations performing measurements using underwater acoustics transducers, their field of application, the preferred transducers and the awareness of transducer calibration.

This revealed that the Royal Australian Navy Ranging and Assessing Unit (RANRAU) and the government organisation servicing defence, the Defence Science and Technology Organisation (DSTO), constitute some 80% of users. They maintain at least five testing ranges around the Australian seaboard and numerous laboratory installations as well. There are also several university departments involved in oceanography, a government research organisation involved in marine research and a few private companies. However, the navy is the principal client for the majority of the business of these companies and some of the government research as well.

The majority of the off-the-shelf transducers used are ITC (USA) or Bruel & Kjaer hydrophones, both reciprocal and containing preamplifiers, although a small number of Reson transducers are also in use. The favoured projectors are the J9 to J13 series of electrodynamic drivers made by the USA Navy's Underwater Sound Reference Detachment (USRD). There are also many systems especially constructed for military and civilian applications, both in Australia and by overseas manufacturers, containing combinations of commercial transducers and specially made elements. These include redeployable and fixed line sources for ranging and assessing of sonar systems and ship noise, large arrays for similar purposes, systems for monitoring sea noise and marine biology and arrays for underwater imaging.

4(b) Calibration and traceability in underwater acoustics in Australia

No consistent calibration or accreditation practices exist at present in Australia. Calibration is usually established by comparison with a 'reference' hydrophone either in house or by a third party. Organisations that do calibrations as part of their business vary in their policies ranging from maintaining reference hydrophones with their original calibrations supplied at time of purchase through to performing absolute measurements using underwater reciprocity on a reasonably consistent basis. In many cases the reference hydrophone can be informally traced to one of the facilities running the reciprocity calibrations. The reciprocity calibrations are generally based on the descriptions in Robert Bobber [4] although a standard describing the methods does exist, IEC-565.

Most hydrophones are supplied with claimed NIST (National Institute of Standards and Technology in the USA) traceable calibrations but NIST does not hold an underwater acoustics standard. Hydrophones claiming direct traceability to NIST do so via single frequency air acoustic measurements. In fact most hydrophone traceability is to the USRD which maintains extensive standards for the US navy. The USRD calibrations are traceable to NIST via current and voltage measurements and are accepted as a de facto standard within the USA that may be used internally to verify specifications, to show conformance with contractual obligations and to show conformance with environmental laws.

However, although this arrangement is legally acceptable within the USA, the USRD is not at present formally recognised by NIST to be the national standard in underwater acoustics. This means that although the traceability may be sufficient for some Australian naval applications such as the Data Exchange Agreements between the Australian navy and the USA Naval Underwater Warfare Center, it has doubtful legal validity outside the USA. For instance, the USRD cannot at present represent the USA in a Key Comparison for the CIPM MRA described above.

Unfortunately, since the reciprocity measurements performed in Australia are not traceable to an Australian standard, none of these hydrophone calibrations is unequivocally traceable to anything in the legal meaning of the word. In addition, use of calibration certificates more than two years old can be challenged on a metrological basis as can the lack of a formal traceability chain within Australia to the organisations doing reciprocity calibrations.

As a result of this situation it is common for Australian organisations to subcontract measurements assuming there are contractual requirements implied for calibration and verification of hydrophones when there are not. This problem also arises with acceptance testing being carried out by a third party where there is in fact no avenue available for demonstrated legal traceability, accreditation or competence. Some organisations have become aware of this only after experiencing problems over interpretation of contractual agreements.

Few organisations in the survey were aware of the ISO guide for the estimation of uncertainty in measurement [5] and no serious attempts at calculation of uncertainties or tolerances were encountered. Similarly, there is a general lack of awareness of the existence within Australia of a well-defined standards and conformance infrastructure or of the legal significance of measurement. For example, it is not widely realised that traceability to an Australian standard, if it existed, is an option that could be internationally acceptable, in place of the (non-existent) one at NIST if Australia took part in a Key Comparison as described above. All the groups spoken to expressed interest in the idea of an underwater acoustics standard in Australia. There is no doubt that it would considerably simplify the current situation.

4(c) Calibration of hydrophones

The recommended methods for absolutely determining the free field sensitivity of hydrophones, by reciprocity and by comparison measurements and for measuring low frequency pressure sensitivity, are described in IEC 565.

To calibrate hydrophones using the principal of reciprocity it is advisable to have at least two reciprocal transducers. Of the two groups doing this measurement in Australia one uses two Bruel & Kjaer 8103 standard reciprocal hydrophones (Figure 1) plus a J11 transmitter and the other group routinely calibrates two ITC 1042 standard reciprocal hydrophones.

In the first instance the calibrations are performed in a cylindrical tank 8.7 m deep and 7.6 m in diameter for frequencies up to 20 kHz. The 'open circuit' voltage sensitivity is measured with high input impedance preamplifiers (Ithaco 453) which are calibrated by a third party accredited test house. The test is performed once per year with results claimed to be good to within ±2 dB. This estimate represents the scatter of results from year to year not a formal calculation of uncertainty. The group performs hydrophone calibrations, designs and assembles complex systems and fabricates transducers.

The other group routinely calibrates the two ITC 1042 reciprocal hydrophones over the frequency range 500 Hz to 50 kHz. Less often a pair of ITC 6069 hydrophones are used for the range 1 to 100 kHz. The lowest frequency used is 63 Hz but the measurements are seriously affected by noise and are felt to be unreliable. The highest frequency used is 150 kHz. The calibrations are performed in a dam some 50 m deep with the hydrophones and transmitter mounted in a triangular arrangement approximately 3 m per side and 20 m below the surface. Fifteen cycle wave trains are usually used with a full range of calibrated instruments including SRS560 high input impedance preamplifiers. The temperature of the dam is routinely surveyed and varies only 2°C over most of its depth in summer and negligably in winter. The organisation's main business is calibrating hydrophones and projectors but they also operate as a platform for research measurements by other organisations.

5. CONCLUSION

The National Measurement Laboratory is participating in a set of Key Comparisons, run by the CIPM, of primary standards in acoustics, ultrasonics and vibration. The results will be entered into a database of key reference values as part of an international Mutual Recognition Arrangement set up under the Metric Treaty.

The infrastructure, both technical and administrative, to maintain an Australian standard of underwater acoustics already exists within the DSTO and NML. To bring the available facilities up to primary standards level requires

- improvement of the traceability paths of measurements to NML,
- fine tuning of the techniques used to align them with IEC 565,
- an assessment of uncertainties according to the ISO Guide and
- some intercomparisons of measurement of hydrophone sensitivity and frequency response with another national measurement institute.

However, a useful first step would be an informal intercomparison of measurements of hydrophone sensitivity amongst the organisations performing calibrations within Australia.

6. REFERENCES

[1] International Electrotechnical Commission Standard, 'Primary method for pressure calibration of laboratory standard microphones by the reciprocity technique.', Publication IEC 61094-2.

[2] International Organisation for Standardisation, 'Methods for the calibration of vibration and shock pick-ups,-Primary calibration by laser interferometry', Publication ISO 5347-1.

[3] International Electrotechnical Commission Standard, 'Calibration of Hydrophones', Publication IEC 565-1977.

[4] R.J.Bobber, *Underwater Electroacoustic Measurements*, Los Altos, Calif.: Peninsula Publications, 1988.

[5] Guide to the Expression of Uncertainty in Measurement: International Organisation for Standardisation, 1993.

AUSTRALIAN ACOUSTICAL SOCIETY CONFERENCE

ACOUSTICS TODAY
Melbourne, 24 – 26 November, 1999.

CONTOURED FOAM ABSORBERS

J P Parkinson[1], M D Latimer[2] and J R Pearse[1]

[1]Department of Mechanical Engineering, University of Canterbury, Christchurch, New Zealand
[2]D G Latimer and Associates Ltd, P O Box 12 032, Christchurch, New Zealand

ABSTRACT

The noise absorbing properties of two and three-dimensional contoured foam absorbers were investigated. The sound absorption of five differently shaped foams was measured in a reverberation room and comparisons made to a plain foam of equivalent volume. The effect of painting the foam surface and fabric coverings on acoustic performance were also investigated. The amount of absorption can be related to the volume and surface area of each foam. It was found that painting the absorbers had very little effect on their acoustic performance. Two and three-dimensional finite element models are being developed to further investigate the effect of surface shape on absorption.

1. INTRODUCTION

Contoured or shaped foam absorbers have been used extensively in architectural acoustics. Shapes such as pyramids or corrugations are typically used for aesthetic reasons as well as to improve the acoustic absorption. It is commonly thought that shaped absorbers have a greater surface area available to incident sound waves and hence greater absorption than equivalent plane absorbers of the same volume. This was investigated along with the effect of painting the absorber surface.

2. MATERIALS

Shapes

The foam was an open cell flexible polyurethane of the polyether type, figure 1. It typically has 35–40 cells per 25 mm, a density of 34 kg/m^3 and a flow resistivity of 13800 mks rayls/m.

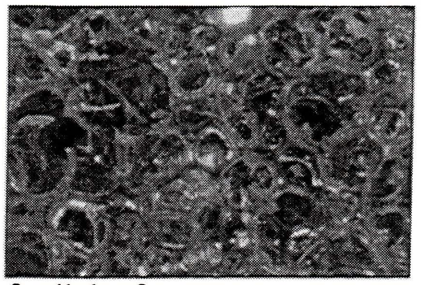

Figure 1 Micrograph view of cellular foam

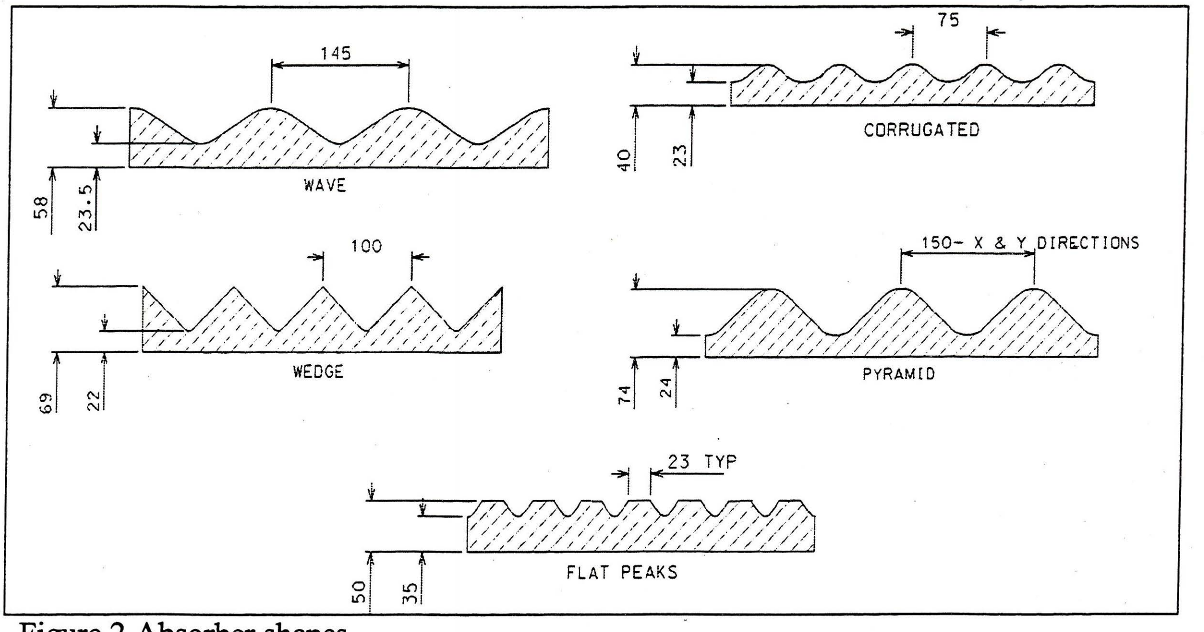

Figure 2 Absorber shapes

3. PROCEDURES

The absorption properties of five differently shaped foams (three 2-dimensional and two 3-dimensional shapes) were investigated, figure 2. The absorption of plane foams corresponding to the same total volume of the pyramid and corrugated shapes was also measured. The surface of each shaped foam was then painted and the absorption determined.

Absorption coefficients were measured according to ISO 354:1988 [1]. A sufficiently diffuse sound field was established in the reverberation room by the inclusion of five stationery diffusers.

Table 1 Reverberation Room Dimensions

	Reverberation Room
Floor area (m^2)	60.1 +/- 0.1
Total surface area (m^2)	270.5 +/- 0.6
Room volume (m^3)	216.8 +/- 0.7

The sound source was a loud speaker placed at four consecutive positions in the room. The test signals were random pink noise generated by a Bruel and Kjaer 2260 Investigator. The sound field was measured using a Bruel and Kjaer 2260 Investigator loaded with a Bruel and Kjaer BZ7204 Building Acoustics software package. The reverberation times were determined from decays of the sound field both for the empty room and for the room containing the specimen being tested. Two reverberation decays were measured at each of four microphone positions within the room.

The samples were positioned centrally in the reverberation room. Each sample was enclosed within medium density fibreboard frames. The area of each specimen was 11.52 m^2, consisting of eight 1.2m square panels placed together.

The weight of each absorber type was measured and the foam volume determined from the previously determined density.

4. RESULTS

The volume and average height of each contoured absorber is shown in table 2. The average height in table 2 was calculated by dividing each volume by the total absorber area (11.52 m^2).

Table 2

Shape	Shape variation	Volume (m^3)	Average Height (mm)
Flat Peak	3D	0.569	49
Wedge	2D	0.531	46
Pyramid	3D	0.487	42
Wave	2D	0.427	37
Corrugated	2D	0.371	32

The average one-third octave band absorption of each of the contoured foams is shown in descending order in table 3. The results for individual frequency bands are shown in figure 3. It is clear from table 3 that the average absorption corresponds to the average height (or volume) of foam of the subject absorber shape.

Table 3

Shape	Average Height (mm)	Average Absorption of One-third Octave Band Centre Frequencies	$V\ m^3$
Flat Peak	49	0.74	.57
Wedge	46	0.68	.53
Pyramid	42	0.64	.49
Plane 1	42	0.63	
Wave	37	0.63	.43
Corrugated	32	0.55	.37
Plane 2	32	0.54	

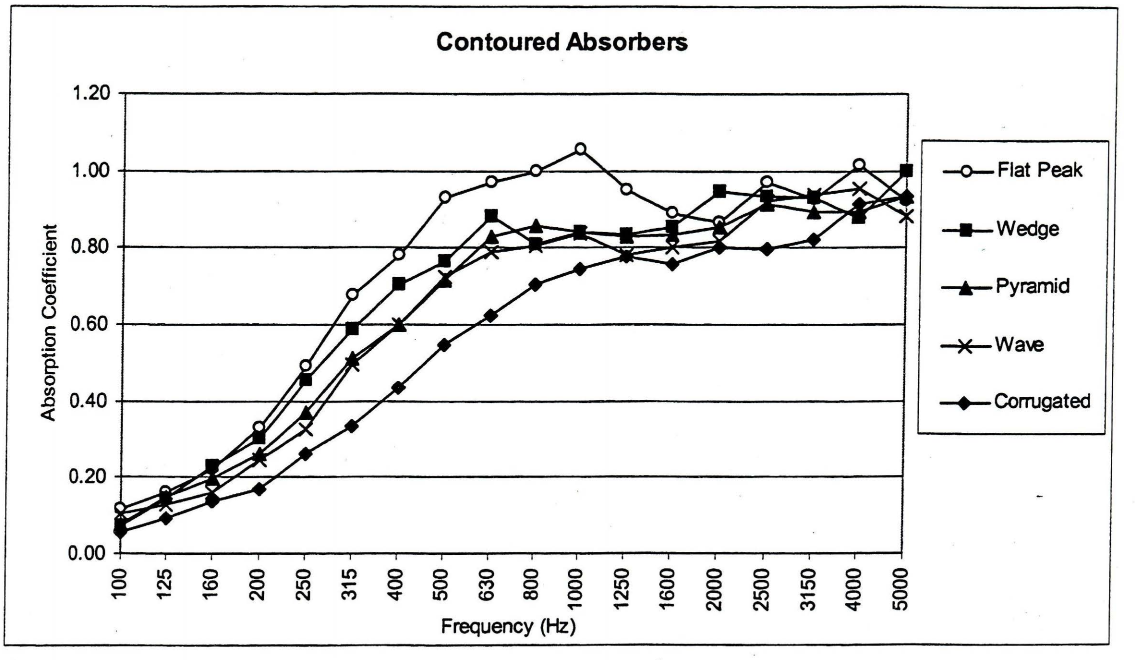

Figure 3 Contoured absorbers

The pyramid absorber is compared to a plane absorber (42mm thickness) in figure 4. It is clear that these two absorbers have very similar absorption trends. Similarly, the corrugated absorber has very similar absorption to the plane absorber (32mm thickness) as shown in figure 5. These results indicate that it is the volume of foam, not the surface profile, that is critical to the amount of absorption.

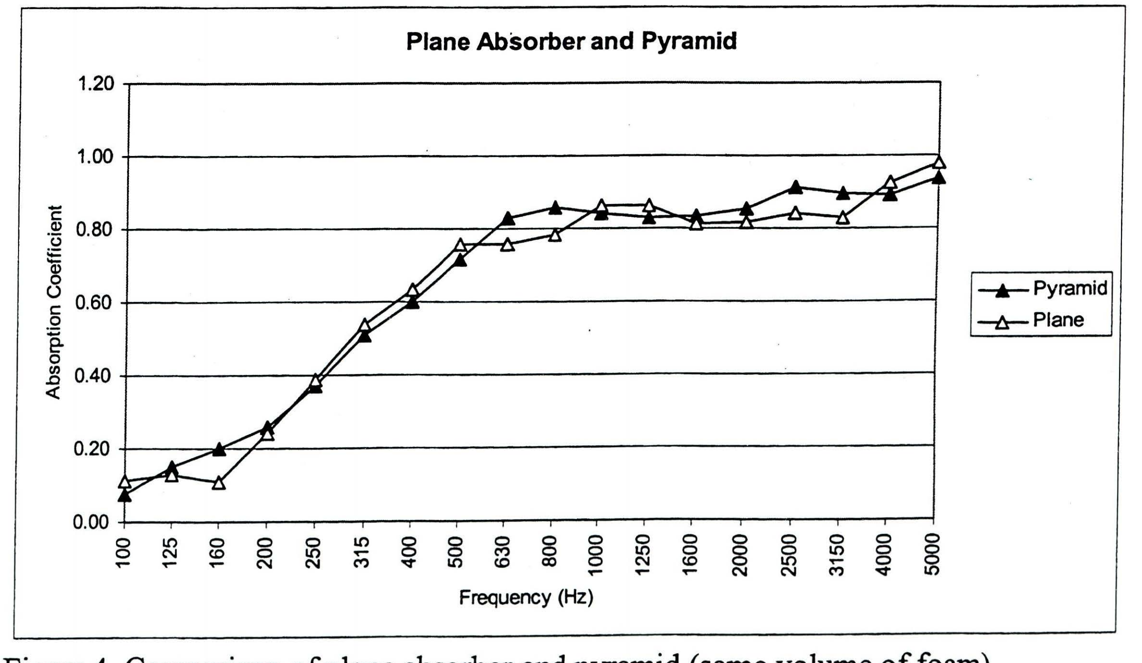

Figure 4 Comparison of plane absorber and pyramid (same volume of foam)

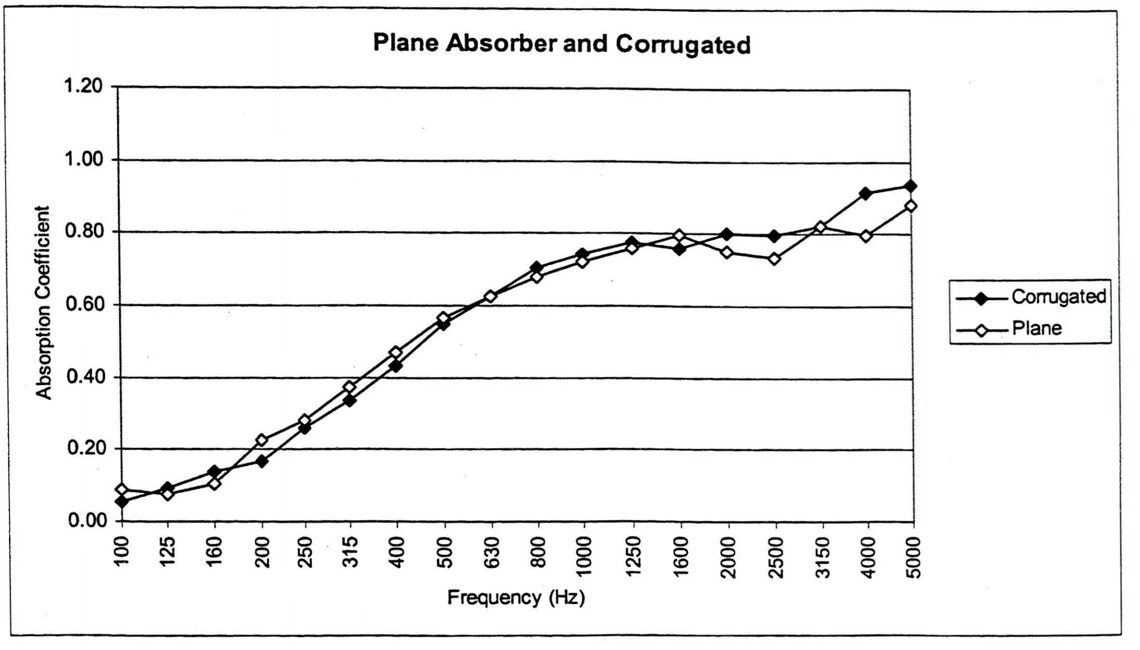

Figure 5 Comparison of plane absorber and corrugated (same volume of foam)

The effect of painting the absorbers' surface can be seen in figure 6. The painted absorbers show very similar absorption trends to the original foams in figure 3; this is illustrated for the pyramid shaped absorber in figure 7.

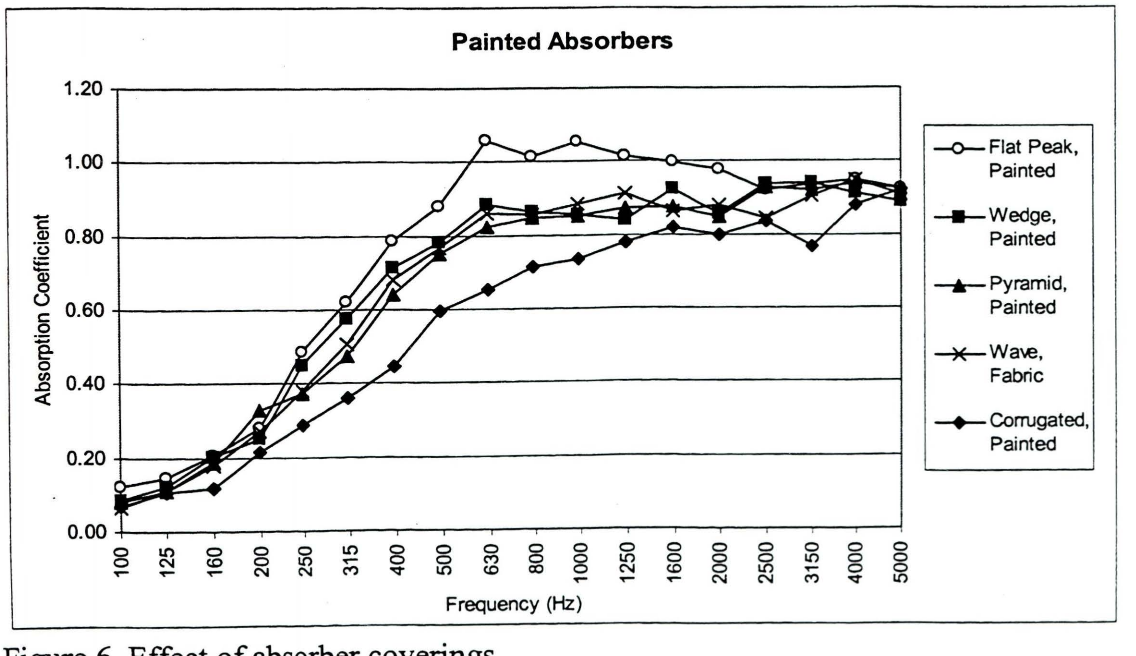

Figure 6 Effect of absorber coverings

It is clear that the pyramid foam's absorption changed only slightly across the whole frequency range, figure 7. Similar trends were observed in the results of the other painted absorbers.

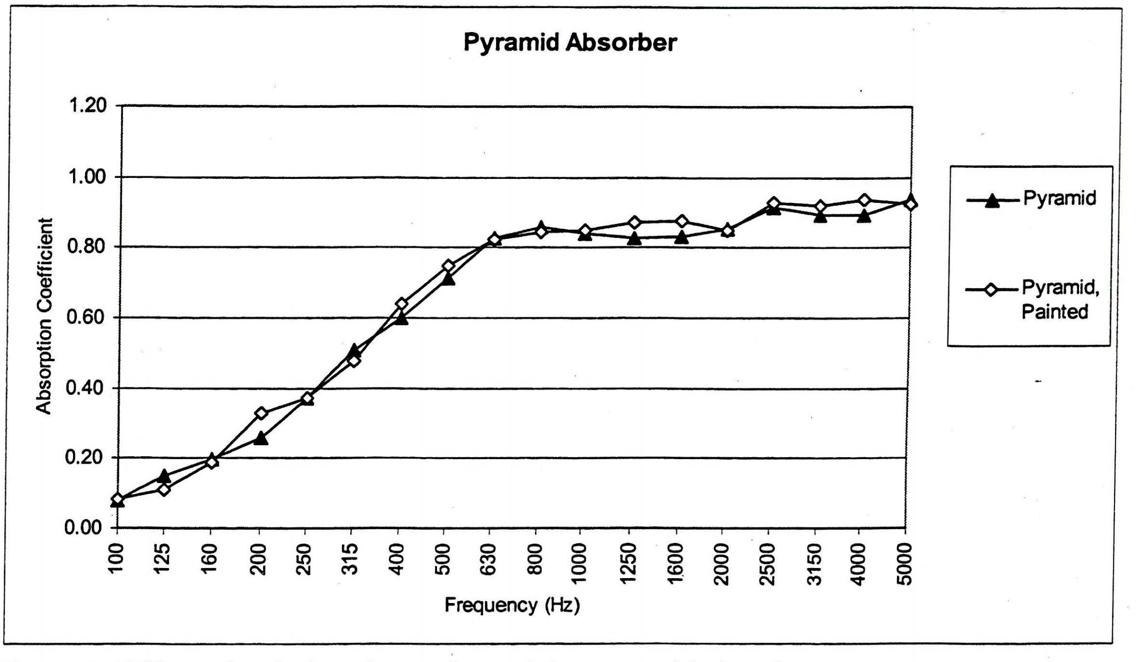

Figure 7 Effect of painting the surface of the pyramid absorber

The fabric covered wave absorber had greater absorption in the mid-frequency range than the original wave foam, figure 8.

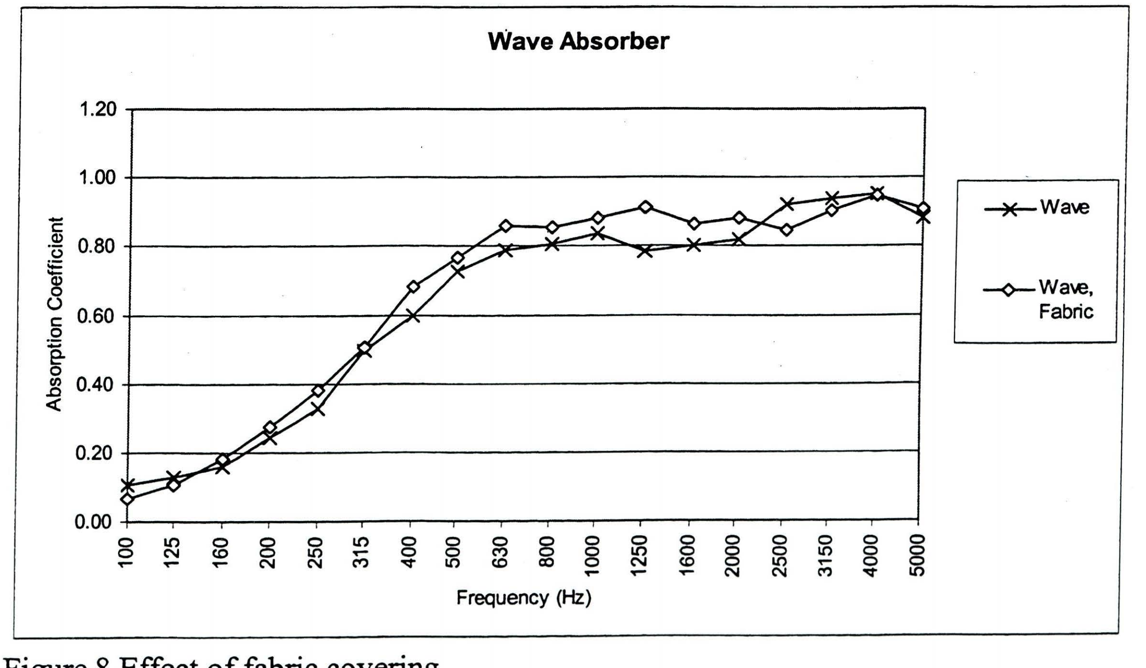

Figure 8 Effect of fabric covering

5. CONCLUSIONS

The sound absorption of contoured foam absorbers has been investigated. The sound absorption was strongly dependant on the volume of foam and relatively independent of the shape of the foam. Painting the surface of the absorbers only slightly changed the absorption. Fabric coverings can be used to increase the absorption.

REFERENCES

[1] International Standard ISO 354:1988, Acoustics - Measurement of sound absorption in a reverberation room, International Organisation for Standardisation, Switzerland, 1988.

AUSTRALIAN ACOUSTICAL SOCIETY CONFERENCE

ACOUSTICS TODAY
Melbourne, 24 – 26 November, 1999.

'PSYSOUND': A COMPUTER PROGRAM FOR PSYCHOACOUSTICAL ANALYSIS

D. Cabrera

Department of Architectural and Design Science, University of Sydney

ABSTRACT

This paper outlines the capabilities of a computer program called 'PsySound' (written by the author), which implements a range of psychoacoustical models.

1. INTRODUCTION

The relationship between an acoustic stimulus and the corresponding sensation is no simple matter. While physical measurements are relatively easy to perform, psychoacoustical models are principally available in limited or expensive forms, and in that sense, are unavailable to all but the most specialised researchers. This is a matter of some frustration to researchers, students and educators with limited resources.

This paper describes a program called 'PsySound', in which several psychoacoustical models are implemented. PsySound is compiled for Macintosh PPC, and is freely available from this author's web site (http://members.tripod.com/~densil/). This paper primarily refers to the current version of PsySound (version 2.x), which combined what were previously five separate programs into one.

PsySound reads 16-bit signed integer sound files, with a sample rate of 44100 Hz, and either 1 or 2 channels. Sound Designer 2, AIFF, and Microsoft Wave formats can satisfy these criteria. It analyses the files in a succession of overlapping 93 ms windows. Results are recorded in four tab-delimited text files: one for level, spectrum and cross-channel time series data; one for loudness and related time series data; one for pitch and related time series data; and one for summary data. The broad structure of the program is shown in Fig. 1.

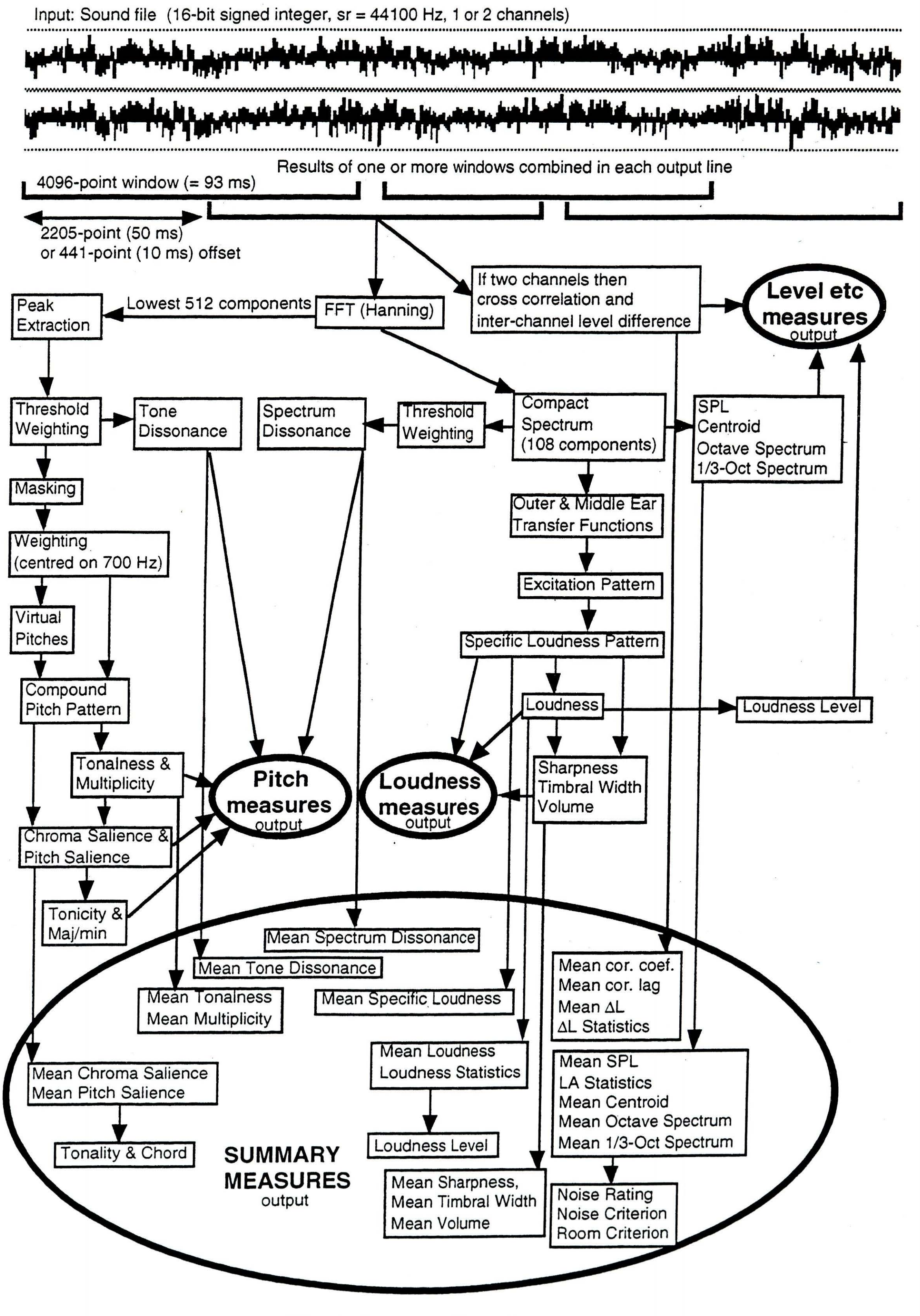

Fig. 1: Program flow diagram.

2. MEASURES

Level, spectrum and cross-channel measures

Frequency analysis is achieved initially by a 4096-point Fourier transform. In order to speed up processing, the frequency spectrum is reduced to a compact form: linear frequency distribution is retained at low frequencies, while twelfth-octave distribution applies to higher frequencies (reducing the spectrum from 2048 to 108 components). From this, octave (from 31.5 Hz) and third-octave (from 125 Hz) spectra are derived, as well as L_A, L_B, L_C, L_{lin}, and spectral centroid. Summary measurements also include statistical A-weighted levels and background noise measures (NC, NR, and RC).

All of the abovementioned measures are easily obtainable by other means. Nevertheless, their presence in PsySound output is important for program calibration. It can also be useful to compare physical and psychoacoustical measures in an effort to understand how various dependencies interact. For example, a comparison between NR and loudness level measurements for a range of sounds having the same SPL but varying bandwidth might show that NR decreases with a smoother spectrum, while loudness level increases.

The two audio channels of a sound file are compared by calculating the unweighted inter-channel level difference and their cross correlation function (for lags between ±1 ms). Only the maximum absolute value of the function is recorded, together with the corresponding lag time. A slight central tendency is applied in an effort to produce meaningful results for periodic cross correlation functions. In some circumstances, the lag time and level difference could be interpreted in terms of lateralisation, especially when their signs match. The cross correlation coefficient might be interpreted in terms of the spread of sound in the horizontal plane (in a manner similar to auditory spaciousness measures in auditoria). Statistical level difference measures are calculated for the summary. In some situations, ΔL_{10}-ΔL_{90} or ΔL_{20}-ΔL_{80} could be used to quantify the lateralisation range in the sound.

Measures related to loudness

The Australian Standard [1] procedures for calculating loudness have a number of deficiencies which have been accounted for by the 'Cambridge School' of psychoacoustics. Stevens' method (ISO 532A) is only suitable for sounds without tonal components. Zwicker's method (ISO 532B) has broader application, but is based on an auditory filter model that is challenged by more recent research. In addition to using the more sophisticated auditory filter model of Glasberg and Moore [2], the loudness model of Moore et al [3] takes a more detailed approach to ear transfer functions and the loudness function. This model is implemented in PsySound. The free field, diffuse field or field at the eardrum can be assumed.

Specific loudness is the loudness attributable to an auditory filter. The specific loudness function extends from the low frequency filters (with centre frequencies at around 50 Hz) to the high frequency filters (with centre frequencies around 15 kHz). A psychoacoustical 'frequency' scale accounts for the distribution of sound in the cochlea. Following Moore et al [3], the Erb unit is used for this 'Erb-rate' scale, with values ranging between 2 and 39 Erbs. PsySound calculates specific loudness at 0.25

Erb intervals.

When read directly, the specific loudness function shows the parts of the frequency spectrum that make the strongest contribution to loudness. The specific loudness function also contributes to several higher level measures: PsySound calculates loudness, sharpness, timbral width and volume from the specific loudness function.

Loudness is the integral of specific loudness, or the area under the specific loudness curve. Figure 2 shows the specific loudness functions produced by a narrow band and broad band sound, both presented at 60 dB(SPL). While the A-weighted level is a little lower for the pink noise, its loudness is more than four times that of the 1 kHz tone. These results were calculated by PsySound, assuming a free field.

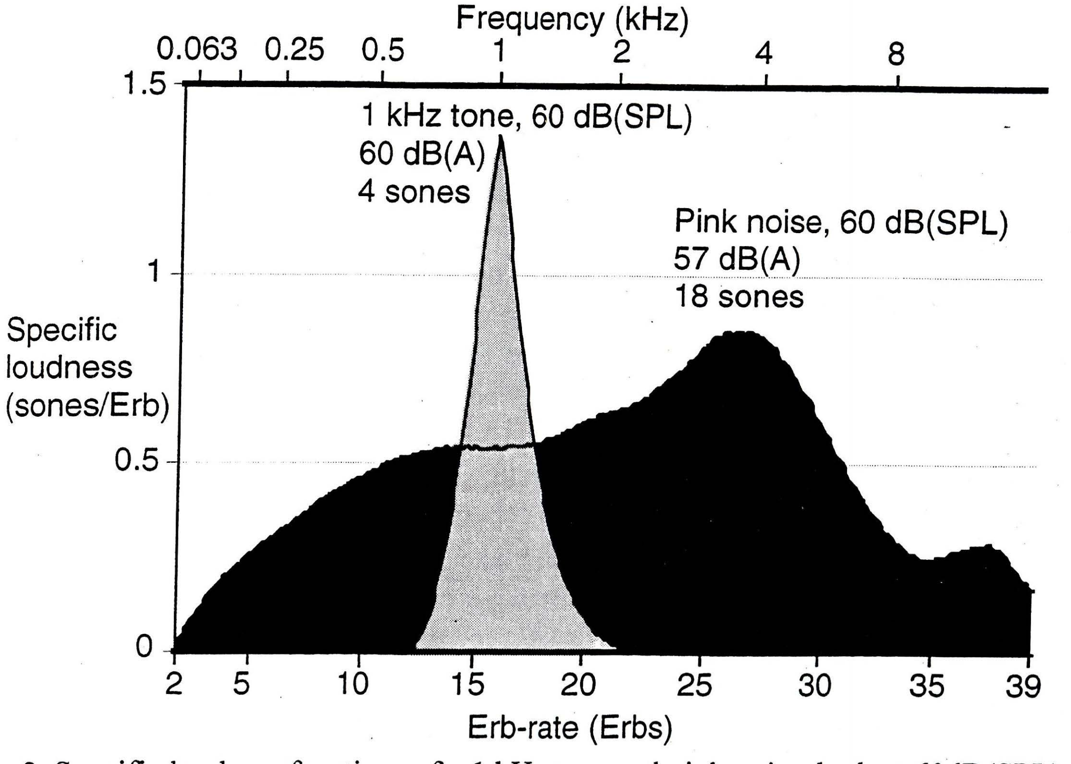

Fig. 2: Specific loudness functions of a 1 kHz tone and pink noise, both at 60dB(SPL).

Statistical loudness measures are calculated for the summary results. These might be manipulated in a manner akin to the more familiar statistical SPL measures, except that ratios are used instead of differences. Zwicker and Fastl [4] find a high loudness percentile, such as N_5 or N_{10}, usually gives the best representation of overall loudness, the louder moments of a sound being more salient than its quieter moments.

Sharpness is a subjective measure of sound on a scale extending from dull to sharp - sometimes it is thought of as a pitch-like (low-high) aspect of timbre. 'Brightness' and 'density' are two other terms that have been used to denote equivalent or closely related attributes by, for example, Boring and Stevens [5] and Lichte [6]. PsySound implements the sharpness models of Zwicker and Fastl [4] and Aures [7].

Zwicker and Fastl's model is simply a weighted centroid of specific loudness, while Aures' model is more sensitive to the positive influence of loudness on sharpness. Both models use the Bark (rather than Erb) scale of critical-band rate, so PsySound simply transforms Erbs to Barks, using the specific loudness function already generated, producing minor deviations from the original models.

Timbral width is a simple measure proposed by Malloch [8], inspired by Pollard and Jansson's [9] tristimulus method of timbre analysis. It measures the flatness of the specific loudness function. Its implementation in PsySound had to be changed from that of Malloch because Malloch used Stevens' [10] loudness calculation method, which has broader frequency components than Glasberg and Moore's auditory filters.

Volume is a subjective measure of sound on a scale extending from small to large. It is a rather old-fashioned measure, and was the subject of Stevens' PhD thesis [11]. A model of the volume of pure tones was developed by Terrace and Stevens [12]. Large volume is associated with low frequency, high intensity, and broad bandwidth. Volume and spaciousness have very similar subjective definitions (the apparent size of the sound), suggesting a binaural component to volume. Recently this author [13] has derived a preliminary model of auditory volume using the specific loudness function, which is implemented in PsySound.

Dissonance

Musical dissonance is determined by a combination of acoustic and contextual factors. The contextual factors relate to what might be called 'musical language'. To measure them would be a complex task, possibly suited to neural network modelling. However the measurement of the acoustical component of dissonance is relatively simple, and models have been proposed by Kameoka and Kuriyagawa [14], Hutchinson and Knopoff [15], Greenwood [16] and Sethares [17]. These models assume that acoustical dissonance is caused by interference (roughness) between frequency components within the auditory filters.

Dissonance is a type of roughness, and fairly sophisticated roughness models have been developed by Aures [18] and Daniel and Weber [19]. Unlike 'dissonance' models, these are sensitive to amplitude and frequency modulation effects, and model the effect of loudness on roughness. However the computational complexity of such models precluded them from the present version of PsySound.

PsySound calculates dissonance in four ways. It calculates dissonance using all the components of the 'compact spectrum', and also using just the tonal components extracted in the early stages of Terhardt et al's [20] pitch model. In both of these cases, the algorithms of Hutchinson and Knopoff [15] and Sethares [16] are applied. The former algorithm normalises the results, and uses linear intensity. The latter algorithm does not normalise the results, and uses scaled decibels (following personal communication with Sethares). When applied to the compact spectrum, these algorithms measure the noisiness of the sound; when applied to the tonal components, they come closer to measuring musical dissonance. Sethares [21] and Malloch [8] give detailed examples of how dissonance models can be used in music analysis.

Pitch Measures

Pitch, here, is used in the psychoacoustical sense: it refers to the *perceived* pitch(es) of sound. This type of analysis is to be distinguished from 'pitch tracking' (musical score or MIDI sequence extraction), and from frequency analysis.

Pitch is multidimensional, at least involving the components of pitch height and pitch strength (or salience). Shepard [22] has developed much more sophisticated models of the structure of 'pitch space', accounting for pitch height, octave similarity and the cycle of fifths. Including pitch strength and the temporal dimension renders futile the reduction of such structures to a flat piece of paper.

The pitch model of Terhardt et al [20] was chosen for PsySound, primarily because of its track record in music analysis, especially in the work of Parncutt [23]. This relatively simple model (based on frequency spectrum analysis rather than auto-correlation), predicts pitch height and strength, virtual pitches and pitch shifts. Additional measures proposed by Parncutt allow the estimation of two types of tonalness (how tone-like the sound is) and multiplicity (the number of pitches heard).

PsySound quantises the results to fit the 12-tone equal temperament scale (saliences of out-of-tune pitches are shared between the adjacent pitch categories). By default it does not implement Terhardt's pitch shifts, as these degrade the results for such a coarse quantisation. Pitch salience patterns are expressed linearly over the pitch height range, and circularly over the chroma range. Fig. 3 shows how these aspects of pitch might be combined. It shows the mean pitch salience of the entire final movement of Mahler's Ninth Symphony, as analysed by PsySound. Even in such a chromatic movement, its tonic of D flat is clearly discernible, although whether the key is major or minor is unclear.

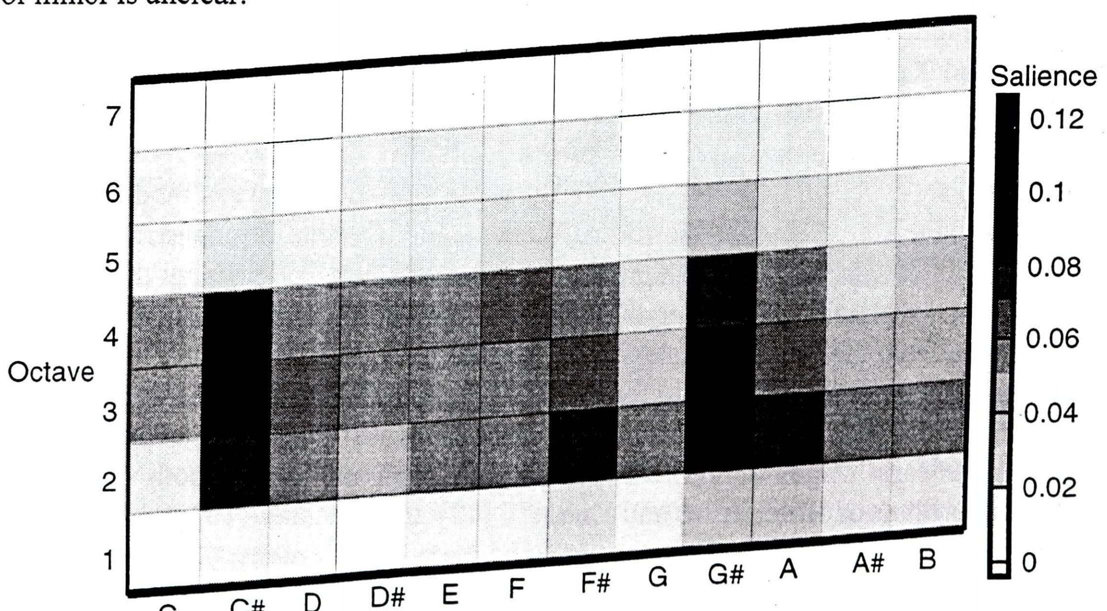

Fig. 3: The mean pitch salience of the fourth movement of Mahler's Ninth Symphony.

PsySound correlates measured chroma saliences with those of 24 keys and 27x12 octave-spaced chords, thereby conducting a crude automatic harmony analysis.

3. APPLICATIONS

PsySound was designed for use in research and education, particularly in areas related to music. Earlier versions of PsySound have been used as part of a course 'Musical Applications of Psychoacoustics', taught as an elective at the University of Sydney's Conservatorium of Music in 1988.

In research it has been applied by Jeong [24] in the analysis of stimuli used in just-noticeable difference experiments in room acoustics. A very early version was used by Schubert [25] in a time series analysis of musical emotion. It is being used by Neil MacLachlan (RMIT University) for the perceptual modelling of bells with harmonic series. This author is using PsySound to analyse music recordings, as well as for the analysis of listening test experiment stimuli (using a dummy head microphone).

4. CONCLUSION

PsySound aims to provide an accessible platform for psychoacoustical analysis, oriented towards musical measures. It combines several models in a single program. It provides interfaces so that the models can be applied directly to sound files, and produces relatively detailed results for spreadsheet, statistical and graphing programs.

The large number of measures implemented in PsySound could mislead a reckless correlation hunter. Nevertheless they allow several measures of related phenomena to be compared, and in this capacity PsySound is an efficient exploratory and educational tool. While PsySound almost presents itself as a ubiquitous analysis program, it would benefit from the inclusion of more sophisticated spatial measures, as well as roughness, fluctuation strength and rhythm models. Proper temporal integration of loudness, and pitch streaming would greatly enhance the present measures.

ACKNOWLEDGMENTS

The author is thankful to Stephen Malloch, Brian Moore, Richard Parncutt, William Sethares and Ernst Terhardt for their advice and permission to include their algorithms. This research was conducted under an Australian Postgraduate Award and a Department of Architectural and Design Science Supplementary Scholarship.

REFERENCES

[1] Australian Standard AS 3657-1996, Acoustics-Expression of the subjective magnitude of sound or noise, Part 2: Method for calculating loudness level, Standards Australia, 1996 (ISO 532:1975, Acoustics-Method for calculating loudness level)

[2] B Glasberg and B Moore, 'Derivation of auditory filter shapes from notched noise data', Hearing Research, 47, pp 103-137

[3] B Moore, B. Glasberg and T Baer, 'A model for the prediction of thresholds, loudness, and partial loudness', Journal of the Audio Engineering Society, 45/4,

1997, pp 224-240
[4] E Zwicker and H Fastl, *Psychoacoustics* (Springer, Berlin, 1999)
[5] E Boring and S Stevens, 'The nature of tonal brightness', Proceedings of the National Academy of Science, 22, 1936, pp 514-521
[6] W Lichte, 'Attributes of complex tones', Journal of Experimental Psychology, 28/6, 1941, pp 455-480
[7] W Aures, 'Berechnungsverfahren für den sensorischen Wohlklang beliebiger Schallsignale', Acustica, 59, 1985, pp 130-141
[8] S Malloch, *Timbre and technology* (PhD thesis, University of Edinburgh, 1997)
[9] H Pollard and E Jansson, 'A tristimulus method for the specification of musical timbre', Acustica, 51, 1982, pp 162-171
[10] S Stevens, 'Perceived level of noise by mark VII and decibels (E)', Journal of the Acoustical Society of America, 51/2, 1972, pp 575-601
[11] S Stevens, *The volume and intensity of tones* (PhD thesis, Harvard University, 1933)
[12] H Terrace and S Stevens, 'The quantification of tonal volume', American Journal of Psychology, 75, 1962, pp 596-604
[13] D Cabrera, 'The size of sound: auditory volume reassessed', Proc 1999 Australasian Computer Music Association Conf, Wellington NZ, pp 26-31
[14] A Kameoka and M Kuriyagawa, 'Consonance theory, part II: Consonance of complex tones and its calculation method', Journal of the Acoustical Society of America, 45, 1969, pp 1451-1459
[15] W Hutchinson and L Knopoff, 'The acoustical component of western consonance', Interface, 7, 1978, pp 1-29
[16] D Greenwood, 'Critical bandwidth and consonance in relation to cochlear frequency-position coordinates', Hearing Research, 54/2, 1991, pp 164-208
[17] W Sethares, 'Local consonance and the relationship between timbre and scale', Journal of the Acoustical Society of America, 93/3, 1993, pp 1218-1228
[18] W Aures, 'Ein Berechnungsverfahren der Rauhigkeit', Acustica, 1985, 58, pp 268-281
[19] P Daniel and R Weber, 'Psychoacoustical roughness: Implementation of an optimized model', Acustica, 83, 1997, pp 113-123
[20] E Terhardt, G Stoll and M Seewann, 'Algorithm for extraction of pitch and pitch salience from complex tonal signals', Journal of the Acoustical Society of America, 71/3, 1982, pp 679-688
[21] W Sethares, *Tuning, timbre, spectrum, scale* (Springer, London, 1998)
[22] R Shepard, 'Geometrical approximations to the structure of musical pitch', Psychological Review, 89/4, 1982, pp 305-333
[23] R Parncutt, *Harmony: a psychoacoustical approach* (Springer, Berlin, 1989)
[24] D Jeong, *Just noticeable differences in tonal quality as a measure of room acoustics* (PhD thesis, University of Sydney, 1998)
[25] E Schubert, *Measurement and time series analysis of emotion in music* (PhD thesis, University of New South Wales, 1999)

AUSTRALIAN ACOUSTICAL
SOCIETY CONFERENCE

ACOUSTICS TODAY
Melbourne, 24 – 26 November, 1999.

ADVANCES IN THE CONTROL AND CALIBRATION OF TRANSDUCER INSTALLATIONS

Poul Svensgaard[1] and Bernard Ginn[2]

[1]Brüel & Kjær, Australia
[2]Brüel & Kjær, Denmark

Brüel & Kjær has introduced a configurable Signal Conditioning Amplifier system known as NEXUS which can be used with a wide range of acoustical and vibrational transducers. The technological advances incorporated in the unit mean that less time is required than previously to install, check, calibrate and measure. Compared to traditional instrumentation, the use of a NEXUS conditioning amplifier means that the probability of getting the measurements "right first time" is greatly increased.

Introduction

It is usually true that the length of time taken to install, calibrate and test a transducer installation is far longer than the time needed to perform the measurements. Especially for measurements in remote locations (e.g., on board ships, on drilling rigs), the measure-ments must be right first time.
The incorporation of techniques into the measurement system to check the integrity of the transducers and the quality of the signals would greatly enhance the cost effectiveness of the task. This article presents a signal conditioning amplifier, known as NEXUS, which incorporates significant advances in the fields of computer control, transducer calibration and channel verification (with two patented techniques) and extensive overload detection.

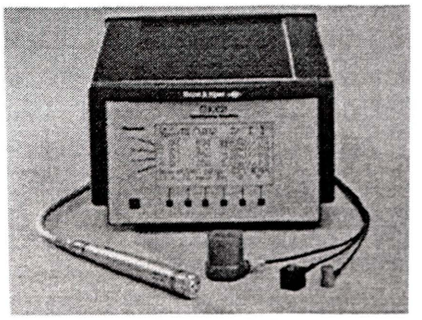

Fig.1. Configurable conditioning amplifier for microphones, charge accelerometers, DeltaTron transducers and direct voltage input with up to 4 channels per unit.

Calibration and verification techniques for acoustical systems

For acoustical measurements, an acoustical calibration using a type 1 pistonphone or type 1 sound level calibrator, is indispensible. However, if there are many acoustical transducers (microphones or hydrophones) or if the acoustical transducers are positioned where access is difficult, then remote, electrical verification is desirable. Two commonly used electrical verification methods are the use of an electrostatic actuator and the insert voltage calibration technique. The actuator produces an electrostatic force which simulates a sound pressure acting on the microphone diaphragm. Compared to sound-based methods, the actuator method has an advantage in that it provides a simpler means of producing a well-defined calibration pressure over a wide frequency range without the special facilities of an acoustics laboratory. For practical monitoring systems, the actuator needs to be an integral part of the micro-phone system. The Insert Voltage Calibration (IVC) method is primarily intended for use in calibration laboratories for determining open-circuit sensitivity of condenser microphones. This facility is incorporated into some of Brüel & Kjær's preamplifiers (Types 2645 and 2673) and in Hydrophone Type 8106. The IVC technique may also be used to provide a field-check of a measurement system including a preamplifier and cables. This is sufficient to verify the electrical part of a measurement system, but not for verifying the microphone cartridge.

The Brüel & Kjær patented Charge Injection Calibra-tion (CIC) technique, implemented in NEXUS (Fig.2), offers considerable advantages compared to the IVC method. CIC enables a complete measurement chain to be verified, including the microphone. The patent includes the measurement method and the practical realisation of a high quality, stable capacitance which is built into the preamplifier (Cc). The main applications are the monitoring of remote microphones and microphone arrays. The small, built-in capacitor makes an attenuator together with the impedance of the combined microphone and preamplifier input circuit. The ratio between the output (Vo) and input (Vi) voltages can be used to monitor the stability of the whole measurement system, including the microphone, preamplifier and cables. The method can be used to monitor the pre-amplifier input resistance (Ri) at low frequencies and the microphone capacitance (Cm) in the mid- and high-frequency range. The user is interested not in the actual level but in relative changes in level. Ideally, the user can perform CIC on his system and build up a library of results for the normal system and for a faulty system. When a fault occurs, the user will have a good indication of its location. Generally speaking, acoustical calibration is much more costly than CIC in time and resources. It must be stressed that CIC cannot replace acoustical calibration. However, the number of times that the user needs to make an acoustical calibration can be reduced, thus saving time and money.

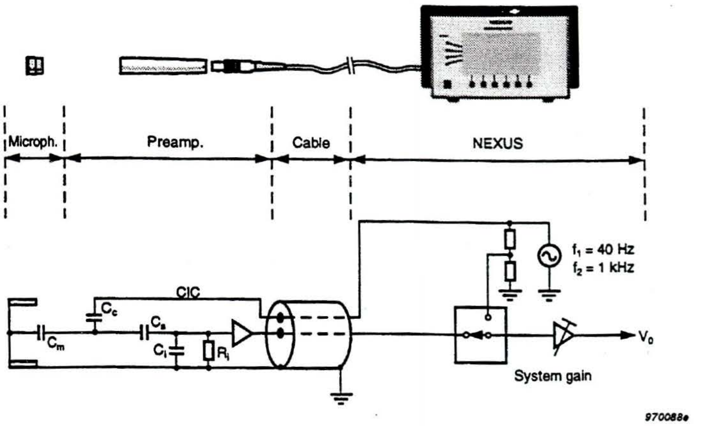

Fig. 2. Implementation of the patented CIC technique;
Cm = capacitance of microphone Cc = stable, inserted capacitance;
Vo = voltage out; Vi = voltage in

Implementation of Charge Injection Calibration technique

The necessary signal conditioning and accuracy is obtained by implementing an extremely accurate and stable digital gain combined with stable analogue components (e.g., NP0 (negative-positive-zero temperature coefficient) capacitors. The processing power for controlling the gain and all necessary set-ups is provided by an 80C528 main processor. An 87C51FB processor deals with transducer calibration and generation of reference frequencies. The sine tone generator provides the two test frequencies of 40Hz and 1kHz with an output level of 10V peak corresponding to an SPL of more than 100dB when using a micro-phone with a sensitivity of 50mV/Pa. This high level means that CIC can be used even where the background acoustical noise is high. Both the generator signal (Vi from NEXUS to the transducer) and the returned signal (Vo from the transducer to NEXUS) are passed through the same amplifier chain. In combination with the digital gain, this permits the detection of very small changes in the transducer's condition, down to fractions of a dB in the frequency response of the microphone, preamplifier and cable system. The same circuitry can also be used to support the IVC method.

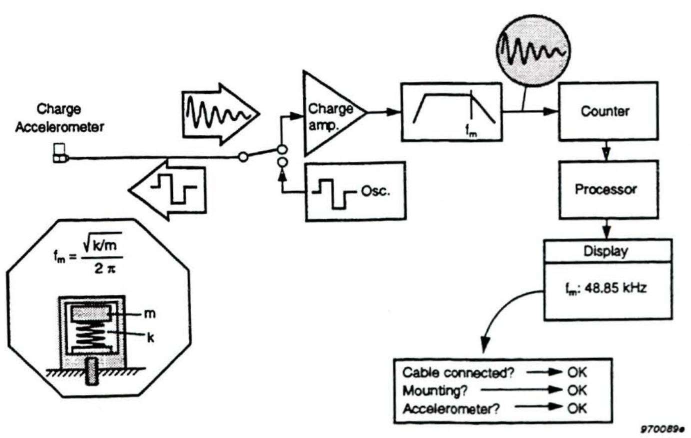

Fig. 3. Implementation of patented Mounted Resonance technique

Implementation of mounted resonance technique

For vibrational measurements, the accele-rometer is calibrated using a known vibrational level before being mounted on the surface of interest. The quality of the mounting can have an enormous influence on the quality of the results. For charge accele-rometers which act in a reciprocal way, the mounting can be investi-gated using the Mounted Resonance technique.

Accelerometers with built in electronics, such as Delta-Tron, cannot be used with Mounted Resonance technique. In this technique a short voltage pulse is sent to the charge accelerometer. The electrical pulse is converted to a mechanical pulse by the piezoelectric element(s) and causes the accelerometer's seismic mass to vibrate which produces a response. The conditioning amplifier then filters the returned signal to remove any DC component and higher resonances; then the resonance frequency of the exponentially decaying response is measured (Fig.3). Before using the technique, the known resonance frequency of the accelerometer is keyed into the conditioning amplifier. The internal processor then sets the correct pulse length and low-pass filter. Poor mountings yield resonance frequencies which differ from the mounted resonance frequency stated on the accelerometer's calibration chart. Faulty cables can also be detected. When an accelerometer is correctly mounted on a thin panel, the mounted resonance will be somewhat lower than the value on the calibration chart due to the effect of mass loading. In this case, the mounted resonance technique can be used to ensure that the resonance frequency remains constant during the measurements.

Overload detection

Once the transducers in a measurement system have been calibrated correctly, verified with Charge Injection Calibration and Mounted Resonance techniques and the measurements commenced, there is still a chance for erroneous readings due to overloads. A minimum requirement for a measurement system is that there should be an instantaneous (i.e., an overload is occurring) and a latched (i.e., an overload occurred) indication on each channel. More extensive overload facilities (e.g., transducer current and transducer voltage overload, Fig.4) vastly reduce the occurrence of false readings. Overloads can occur in the transducers in the cabling and in the conditioning amplifier itself. Transducer current overload is usually not a problem. However, with long cables and signals with a high frequency content, then one approaches the limit for the voltage which the transducer can deliver without distorting the signal (Fig.5). With 1000m of cable it is possible to reach the limit for a "current overload" (i.e., the transducer distorts the signal) at 1V. A signal of 1V would not be detected by a normal signal overload. Therefore a special "transducer current overload" has been implemented which continuously calculates whether the transducer can handle the incoming signals. The transducer overload is measured and calculated as a function of the transducer type, cable length and supply current. The Transducer Voltage overload facility for DeltaTron preamplifier inputs (Fig.6) can also be used to continuously monitor such faults as broken cables.

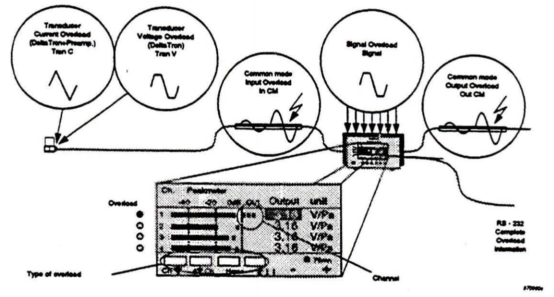

Fig. 4. Extensive overload capabilities in an advanced signal conditioning amplifier

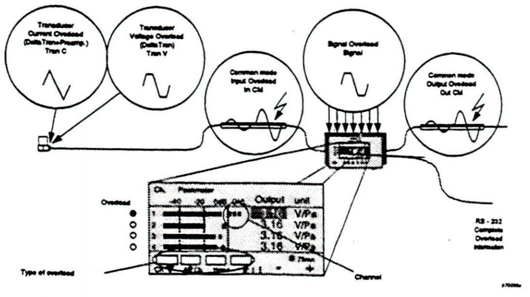

Fig. 5. Transducer current overload: causes and possible solutions

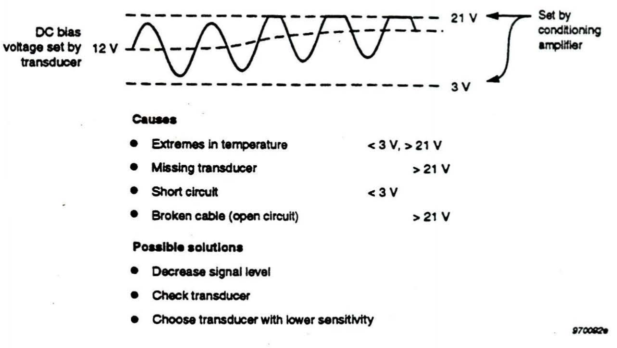

Fig. 6. Transducer voltage overload: causes and possible solutions

In machines, there is always the possibility that the machinery housing is not at earth potential (Fig.7), which present problems for multichannel accelerometer measurements. It should be noted that similar problems can also occur with multichannel microphone arrays if the frame of the array is an electrical conductor and makes contact with the housing of the microphone preamplifiers.
Consequently, the accelerometer housing and the cable screen will not be at earth potential either and a voltage drop will exist along the cable. Electromagnetic interference also causes a similar voltage drop along the cable. The solution to these problems is to employ the "floating input" together with only one grounding cable from the machinery housing to the signal conditioning amplifier. The conditioning amplifier described here, can cope with earth potential differences of up to ± 5 V. If these levels are exceeded, then a "common mode overload" is indicated on the graphical display and remains there until the amplifier is reset. Common mode rejection of ground loops of up to 50dB can be obtained compared to single-ended operation.

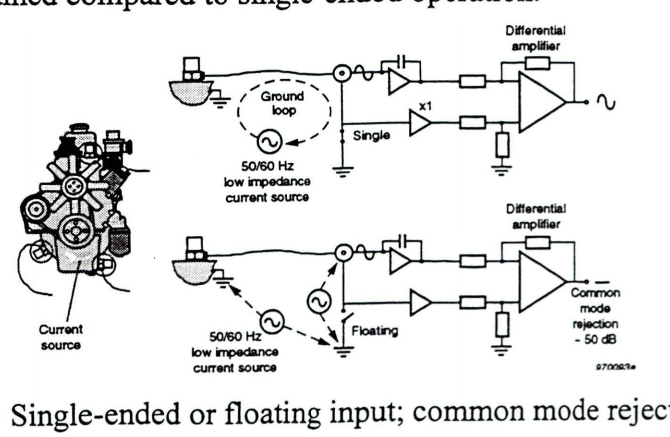

Fig.7. Single-ended or floating input; common mode rejection

Using predefined set-ups to keeping installation time to a minimum

The time taken to install the measurement system can be kept to a minimum by using the predefined set-ups in the conditioning amplifier. Three examples are:

1. The unit "wakes up" in the same state as when it was switched off.
2. Where many standard measurements are to be performed, then user-definable set-ups saved in a non-volatile memory greatly simplify measurement procedures.
3. A PC can be used to send predefined set-ups from a database to the unit(s). The unit can be locked to avoid unwanted tampering or accidental changes of settings during, for example, field measurements.

Remote control of measurement system

The conditioning amplifiers can be daisy-chained together (up to 99 channels) via one RS-232 port which means that the set-ups of each channel can be remotely controlled via a PC. Furthermore, the RS-232 also enables transducer tests (i.e., Charge Injection Calibration and Mounted Resonance techniques) to be performed from distant control centres as well as the monitoring of all overload information (i.e., instan-taneous and latched indications, overload type and channel number). Remote control of autonomous systems (such as a conditioning amplifier(s) and an associated DAT recorder for use for example inside moving vehicles) can be done using a palm-top computer (Fig.8).

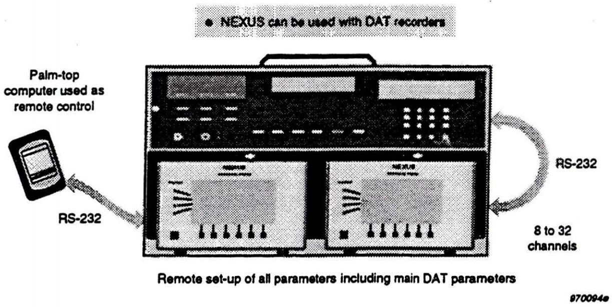

Fig. 8. Two NEXUS signal conditioning amplifiers used in conjunction with a SONY DAT recorder and a remote control unit

Conclusion

Advances in instrumentation means that many other techniques have been incorporated to check the integrity of the transducers and the quality of the system.

Not only can transducers be tested using Charge Injec-tion Calibration and Mounted Resonance techniques, but also the system can be continually monitored using extensive overload facilities. Remote computer control and user definable set-ups reduce installation time and increase the reliability of transducer installations considerably without compromising accuracy.

References

1."The NEXUS range of Conditioning Amplifiers", Product Data sheet (BP 1702), Brüel & Kjær.

2. "A new technique for monitoring condenser microphones", Sound & Vibration, Dec.1996.

AUSTRALIAN ACOUSTICAL SOCIETY CONFERENCE

ACOUSTICS TODAY

Melbourne, 24 – 26 November, 1999.

LOW FREQUENCY NOISE LOUDNESS VS ANNOYANCE

N.Broner[1] and R.Hellman[2]

[1]Vipac Engineers and Scientists Ltd., Private Bag 16, Port Melbourne, Melbourne, Australia 3207

[2]Auditory Perception Laboratory, Northeastern University, Boston, MA02115, USA

ABSTRACT

Over recent times, there has been some on-going discussion in the acoustical fraternity in relation to Beranek's NCB curves and as to whether these curves are appropriate for low frequency noise assessment below 63 Hz. Beranek has assumed that at low frequencies, loudness and annoyance are equal. As part of an on-going research project sponsored by ASHRAE, the Loudness and Annoyance of samples of HVAC noises with dominant energy due to low frequency energy (eg due to VAV systems) was compared using a psycho-acoustical technique. The test subjects sat in a test room simulating a standard office situation. The Loudness and Annoyance assessments were compared and related to objective measures of the HVAC stimuli. The results will be presented and conclusions regarding low frequency noise assessment indicated.

1. INTRODUCTION

Over recent times, there has been some on-going discussion in the acoustical fraternity in relation to Beranek's NCB curves and as to whether these curves are appropriate for low frequency noise assessment below 63 Hz. Confusion has occurred following the inclusion of both the RC and NCB criteria methods in ANSI S12.2-1995. The main divergence between the two criterion curves occurs at low frequencies, i.e. below 100 Hz. The reason for this divergence is that the NCB curves are based on the assumption that loudness and annoyance are equivalent while the RC is empirically based and reflects the assumption that, at low frequencies, in particular, loudness and annoyance are not equivalent [1,2]. The great interest in achieving an acceptable Sound Quality environment, has led to a recognition by many researchers that annoyance is more than just loudness. For example, Zwicker [3] pioneered recognition that to determine annoyance, sound quality factors such as fluctuation strength and sharpness would need to considered in addition to a simple loudness metric. This recognition has not yet resulted in a change away from the old and purely loudness-based assessment metrics such as the dBA or NCB.

As part of an on-going research project "The Determination of the Relationship Between Low Frequency HVAC Noise and Comfort in Occupied Spaces - Subjective Phase" sponsored by ASHRAE, the Loudness and Annoyance of samples of HVAC noises with dominant energy due to low frequency energy (eg due to VAV systems) was compared using a psycho-acoustical technique. Below we report some of the results of the pilot study which shed some light on the assessment of low frequency noise.

2. NOISE STIMULI

For the purpose of the testing, 12 samples of HVAC noise (8 actual recorded samples as collected during Phase 1 of the ASHRAE sponsored research [4]and four synthesized samples based on actual recordings) with varying degrees of low frequency content were used. The four synthesized samples had "tones" added at one of the centre frequencies of 25, 31.5, 50 and 63 Hz. For al the spectra, the maximum energy is below 250 Hz. Figure 1 shows the spectra for the 12 samples.

For this testing, three sequences of the 12 test stimuli, were generated with the only proviso being that the Sound Pressure Level difference between any two samples should not be more than 40 dB. Within each sequence, each noise stimulus was presented for 10 seconds, followed by a 7 second period of silence during which the subjects rated the test stimulus.

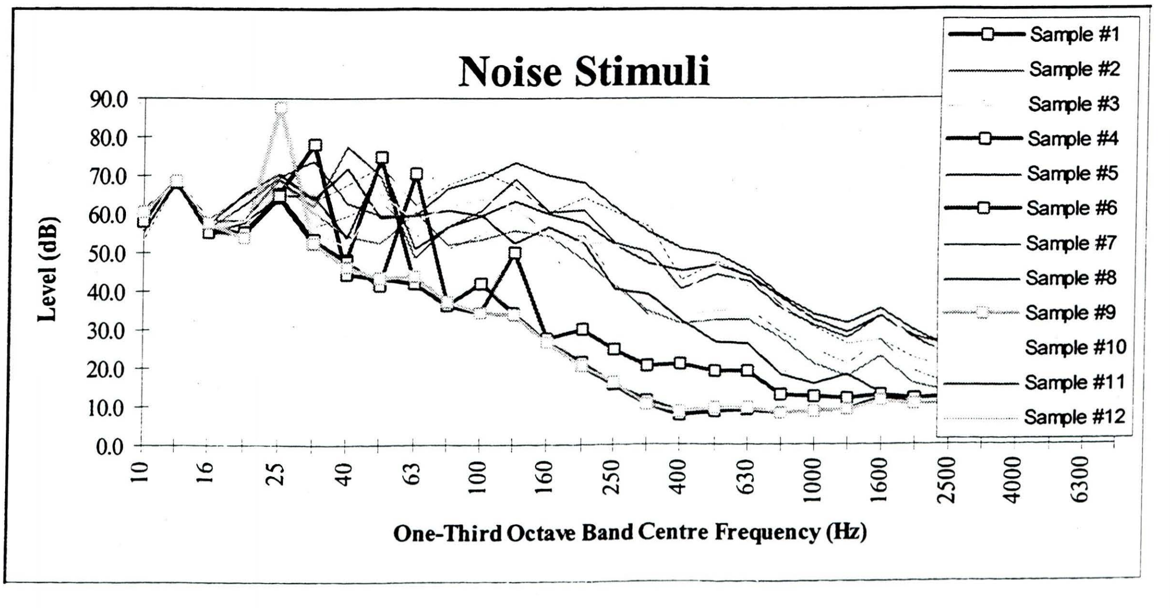

Fig.1 - The twelve noise stimuli used in the Pilot Study

3. RESPONSE RATING

To determine the subjective response of subjects for both loudness and annoyance, the Absolute Magnitude Estimation method was used. In this psycho-acoustical method, the subject assigns a rating number to the perceived loudness or annoyance without the use of a reference. This method has been used previously to characterise perception of loudness eg [5]. For this testing, the subjects were asked to rate loudness as follows. "For each of the sounds, record its loudness as defined as the perceptual aspect of the noise that is changed by turning the volume knob on a radio or T.V." For annoyance, the task was to "record the annoyance defined as the nuisance aspect of the sound experienced. Imagine you are in an office and are seated in your chair while working. Please estimate how annoyed **you** would feel when exposed to each sound". All the judgements were made after each of the noise stimuli were turned off.

4. TEST METHOD

The subjects were seated in the ASHRAE test room. This room has a double wall construction and is floated on isolators so as to minimise any noise intrusion from the outside. The room is 6700 long by 3100 wide by 2350 high and is a reasonably sized meeting room. The noise stimuli are played back to the subjects via two loudspeakers, each one located above a diffuser located in the ceiling on either side of the room width-wise. The subjects sat in one of three seats at a desk, these seats having been pre-qualified as nominally providing the same acoustic stimulus to the subjects independent of seat location. Up to three subjects were tested at any one time.

To aid in the response rating, a cue light located on the desk came on when the noise stimulus ended so as to indicate to the subjects that the time to fill in the response ratings had begun. In this way, no stimuli were missed.

5. TEST SUBJECTS

For the December, 1997, tests there were four male subjects, average age 23 years. For the April, 1998, tests, there were 7 subjects, 3 males, 4 females, average age 28.3 years. All subjects had normal hearing.

6. TEST RESULTS

During each session, each test subject judged the Loudness and Annoyance of the 12 samples three times in a quasi-random order that differed for each of the three runs. The latter two judgements produced by each listener were geometrically averaged and the individual geometric averages were then used to determine the group geometric means.

Figure 2 shows the correlation between the group loudness estimation data and the A-weighting while Figure 3 shows the correlation of group loudness estimation data with loudness predictions in Sones according to Zwicker's model [6]. It can be seen that the correlation with the A-weighted Sound Pressure Level (SPL) is poorer ($r^2 = 0.74$) than with Zwicker Sones ($r^2 = 0.90$).

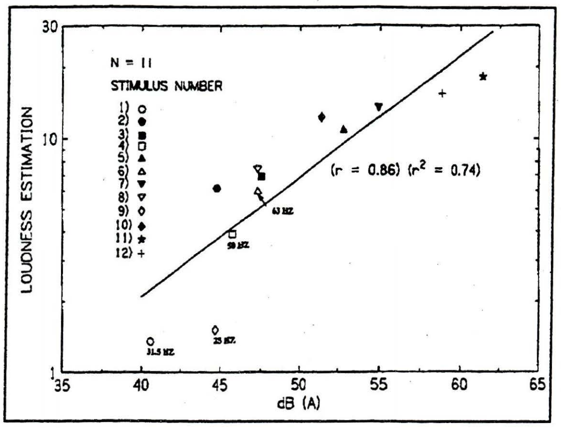

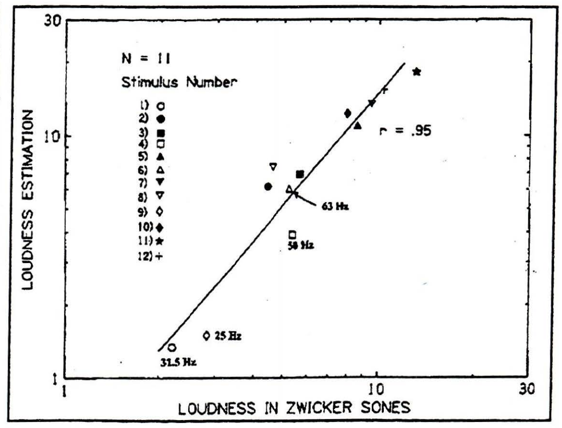

Fig. 2 - Loudness vs A-wtd SPL

Fig. 3 - Loudness vs Zwicker Loudness

To investigate the results further, we plotted the Annoyance/Loudness ratios for each sample - see Figure 4. An examination of the A/L ratios indeed reveals the extent to which annoyance may differ from loudness for each of the 12 spectra. For eight of the spectra, the ratios of A/L are about 1.0 indicating that for these stimuli, annoyance can be well accounted for by our knowledge of loudness. But for four of the spectra, viz those which were characterised by the low frequency "tones", the A/L ratios were all significantly greater than 1.0, ranging from 2.0 to more than 7.0. Further analysis showed that the Loudness Level in accord with Zwickers model [6] provided a better account of the A/L relation than the A-weighted SPL.

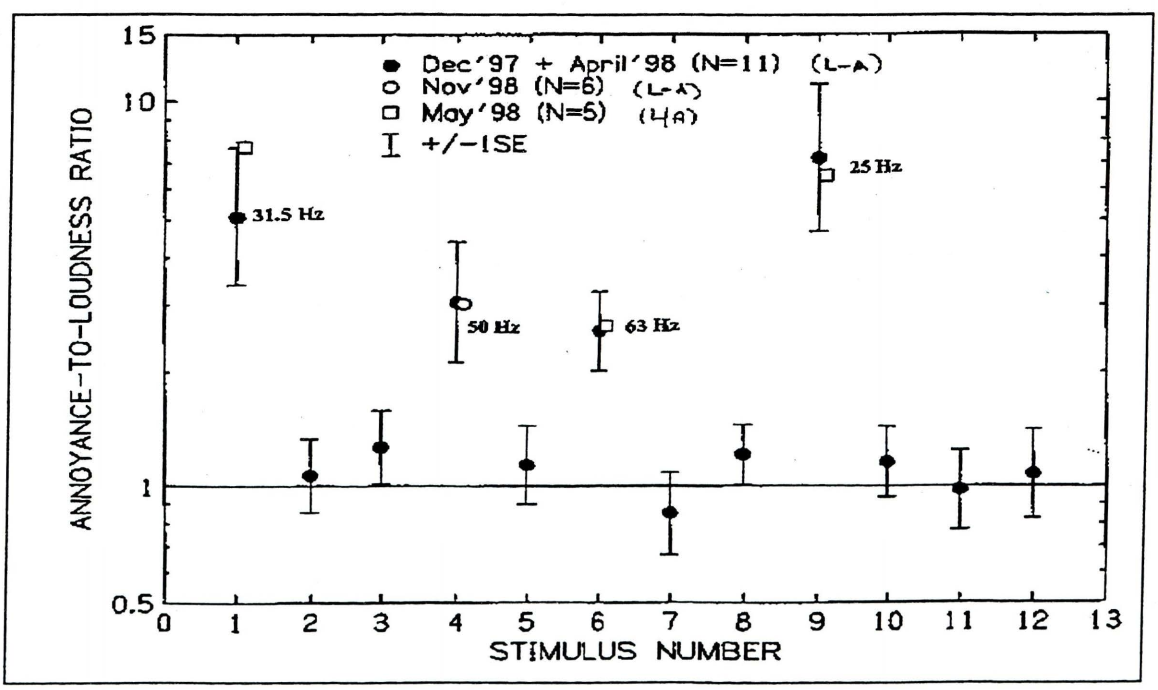

Fig. 4 - Annoyance/Loudness Ratios for the twelve stimuli

7. LOUDNESS VS ANNOYANCE AND THE dBA

Figure 2 showed the relationship between the perceived Loudness and A -weighted SPL while Figure 5 shows the relationship between the perceived annoyance rating and the A-weighted SPL. Neither of the correlations are very strong with an r^2 value for Loudness of 0.74 and an r^2 value of 0.62 for Annoyance but the correlation was better for Loudness than for Annoyance (a similar result of a higher correlation with Loudness than for Annoyance was replicated for other purely loudness-based metrics and, in particular, for the Stevens Mark 7 loudness metric which forms the basis for the NCB) Neither of the correlations is as strong as the correlation between Perceived Loudness and Zwicker Sones which had an r^2 value of 0.90.

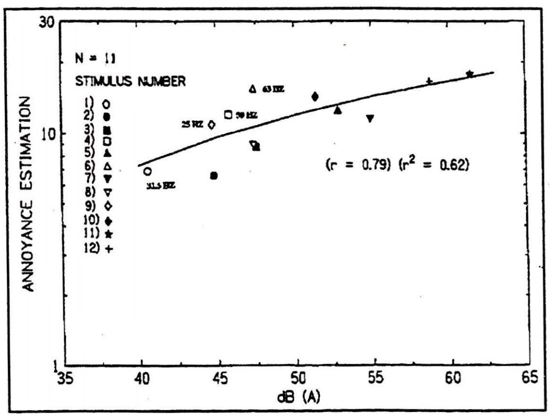

Fig. 5 - Annoyance vs A-weighted SPL

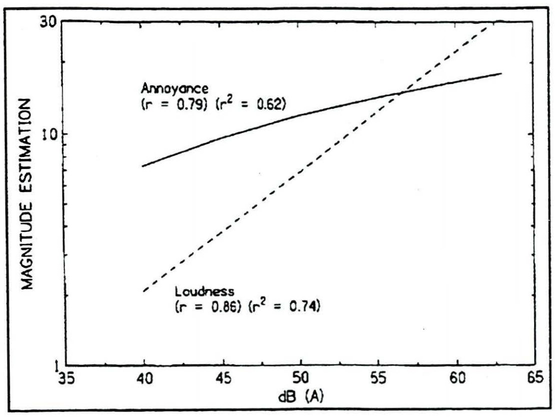

Fig. 6 - Annoyance and Loudness Lines of best fit against A-weighted SPL

Figure 6 shows both the Loudness and Annoyance versus A-weighted SPL. Note the much smaller range of numerical estimates for Annoyance than for Loudness. It can also be seen that the Annoyance is high at lower dBA values and then increases slowly with increasing level. Consequently, the Annoyance exceeds the Loudness at lower A-weighted SPL's while at higher SPL's, the reverse is true i.e. the Loudness exceeds the Annoyance. All of this is consistent with the finding that the A/L ratio is largest for sounds containing prominent low frequency energy. And these sounds are generally those with the lowest A-weighted SPL's.

8. CONCLUSION

The A-weighted sound pressure level has been shown to not be a good predictor of Annoyance due to sounds with rumble. The A-weighted SPL is, however, a somewhat better predictor of Loudness. The strong implication of the results of the pilot study is that, for HVAC noises with rumble, the loudness and annoyance cannot be assumed to be the same as has been assumed in the derivation of the NCB curves. The shape of the NCB curves at low frequencies (< 63Hz) therefore needs to be reviewed.

9. REFERENCES

1. L. L. Beranek, J. Acoust. Soc. America, “Balanced Noise - Criterion (NCB) Curves”, **86(2)**, 650-664, (1989).
2. W. E. Blazier, J Noise Control Eng., “RC Mark II: A Refined Procedure for Rating the Noise of Heating, Ventilating, and Air-conditioning (HVAC) systems in Buildings”, **45(6)**, 243-250, Nov-Dec, (1997).
3. E. Zwicker, Proc InterNoise 89, “On the Dependence of Unbiased Annoyance on Loudness”, 809-814, (1989).
4. N. Broner, ASHRAE 714-RP (Vipac Report 38114, April 1994) ”Determination of the Relationship Between Low Frequency HVAC Noise and Comfort in Occupied Spaces - Objective Phase”, (1994).
5. G. Canevet, R. Hellman. and B. Scharf, Acustica, “Group Estimation of Loudness in Sound Fields”, **60**, 277-282, (1986).
6. ISO R532B “Method for calculating loudness level”, Intl. Org for Standardisation, Geneva, (1966).

10. ACKNOWLEDGMENT

This work was conducted as part of the Research Project 879RP sponsored by ASHRAE.

AUSTRALIAN ACOUSTICAL SOCIETY CONFERENCE

ACOUSTICS TODAY
Melbourne, 24 – 26 November, 1999.

THE DEVELOPMENT OF A HIGH PERFORMANCE ABSORPTIVE ROADSIDE NOISE BARRIER

J.F. Upton

Principal Consultant
Shelburg Acoustics Pty. ltd.

ABSTRACT

It seems that for many years, the solution to reducing highway and freeway noise for residential housing that in many cases borders on the highway precinct, has been to erect a proliferation of solid, reflective, roadside noise barriers that have been either sculptured concrete in a variety of shapes and forms or solid, treated pine with close fitting palings, also in various shapes and heights. The Department of Main Roads in Queensland and the Road Traffic Authority in NSW have been looking at the use of absorptive panels that will offer a complete sound reduction solution by ensuring that not only are residents subject to levels no higher than 63 dBA but that the general level of noise on the freeway itself is also reduced.

1. INTRODUCTION

There have been some recent developments in the use of absorptive panels for roadside use, particularly with a joint project between BHP and Ingal Highway Products. The development of their panel has started a chain of research by other companies who are keen to offer an alternative product.
On this basis, Shelburg Acoustics P/L commenced development of their own version of an absorptive panel in 1998.

2. REQUIREMENTS

The Queensland Department of Main Roads in particular has a stringent specification that contains clearly prescribed requirements in terms of both acoustic and mechanical performance.

In essence the acoustic requirement is :

(a) the Sound Transmission Class shall be not less than 30

(b) that the minimum Coefficient of Absorption shall be;

Sound Frequency (Hz)	Coefficient of Absorption
125	0.5
250	0.8
500	0.9
1000	0.9
2000	0.7
4000	0.6

(c) the absorptive face shall be on the traffic side of the barrier

The mechanical requirements are;

(a) that the panels shall have a serviceability life expectancy of *40 years*

(b) that the panel shall be able to withstand the impact of a 4 Kg steel ball dropped from a height of 3 metres when the panel is supported horizontally above the ground. The impact shall only cause superficial scratches and marks.

(c) the panel shall not rattle in any breeze or wind and no noise shall emanate from the barrier

(d) all steel components shall be galvanised after fabrication in accordance with AS 1650 with a Z600 coating and design strength shall be in accordance with AS 4100 & 4600

In addition to these, the falling ball test must be applicable to *both* sides of the panel and where panels are stacked one on top of the other, any panel should be able to be removed without causing the collapse of any others !!

3. GENERAL INSTALLATION METHOD

The panels are generally required to be 4 metres long by 1 metre high, mounted on top of concrete panels or Pittsburgh barriers, in between 'I' beams. In this way the panels can be stacked one on top of the other to produce a barrier of the required height.

4. THE DEVELOPMENT OF THE BARRIER

The falling ball requirement is simply to assure DMR that the panel is reasonably vandal proof. It was therefore clear that to satisfy this and the longevity requirements, the panel would have to be quite strong. Various frame materials were tried and tested but it was found that the most satisfactory was a fully welded 3 mm cold formed steel channel. Stiffeners were included over the 4 metre length and it was found that heavy duty 4mm 30% open area steel mesh provided a very satisfactory front protective layer.
This whole structure was then hot dipped galvanised in one single piece, according to the provisions of the specification. This combination of steel channel and front face was found to easily comply with the falling ball test and was an integral part of fulfilling the requirement of a 40 year life.

To establish a baseline, the acoustic performance was tested firstly with 50mm rockwool and although the performance was quite good, it fell short of the mark, particularly at 125, 250 and 500 Hz. The use of 100mm thick rockwool gave excellent preliminary absorption results when checked with an impedance tube and made a vast improvement to the absorption at lower frequencies. A special hydrophobic grade of rockwool was used to compensate for ingress of moisture.
The back panel, which is screwed on after the rockwool has been put in place, also needed to be galvanised. A single sheet of 1.6mm galvanised steel was found to be suitable for this purpose. The join was sealed with a proprietary brand acoustic sealant approved by DMR, to ensure a complete weatherproof and acoustic seal between the two surfaces.

The use of a 1.6mm steel backing provided a suitable barrier to obtain the STC that was nominated in the specification. Final testing was carried out by the CSIRO Division of Building, Construction & Engineering at Highett in accordance with the provisions of AS 1045-1988, on a 10.6m^2 sample to achieve the results as shown below.

Testing for airborne sound transmission loss was conducted by RMIT under the procedures laid down in AS 1191-1985, and a NATA test certificate was issued.

5. RESULTS

The results are shown below:

Requirement:			**Our panel**
STC shall be not less than 30			**STC of 43**
The minimum Coefficient of Absorption shall be:			The development panel:
	125 Hz	0.5	**0.65**
	250 Hz	0.8	**1.15**
	500 Hz	0.9	**1.15**
	1000 Hz	0.9	**1.05**
	2000 Hz	0.7	**1.00**
	4000 Hz	0.6	**0.90**

5. CONCLUSIONS

From fundamental laws of physics and acoustics, the material that is used to make up the absorptive infill must be reasonably pliable and not too dense to absorb a wide range of frequencies and it must also be quite thick to give extra absorption at the lower frequencies of interest. For this reason, 100mm rockwool gives optimum performance to comply with the coefficient of absorption figures required by the DMR specification.

The advantages of this absorptive panel are:

(a) superior absorption coefficient performance in excess of the requirement
(b) excellent dead load and wind load combinations as determined from AS 1170.1
(c) better than required STC performance
(d) superior mechanical strength and outstanding longevity expectation in all climate conditions

REFERENCES

[1] Australian Standard AS 1045-1988 "Measurement of Sound Absorption in a Reverberation Chamber"

[2] Australian Standard AS 1191-1985 "Method for Laboratory Measurement of Airborne Sound Transmission Loss of Building Partitions "

[3] Queensland department of Main Roads Standard Specification " Noise Barriers " No. MRS11.15 Interim 10/98

AUSTRALIAN ACOUSTICAL SOCIETY CONFERENCE

ACOUSTICS TODAY

Melbourne, 24 – 26 November, 1999.

OCCUPATIONAL NOISE MANAGEMENT – EDUCATING THE WORKFORCE

N Koolik[1], D Eager[2] and R Tonin[3]

[1]Renzo Tonin & Associates Pty Ltd
[2]University of Technology, Sydney
[3]RTA Techvision Pty Ltd

ABSTRACT

The education of employees, those who are at risk and exposed to high levels of noise in the workplace, about the potential for hearing loss damage remains a difficult task for those charged with this responsibility. It is an accepted fact that training at all levels of an organisation about the effects and control of industrial hearing loss is essential to the implementation of a successful occupational noise management program within an organisation. This paper presents the results of research into development of an interactive CD teaching aid specifically designed to address this need, culminating in the production of an Industrial Hearing Loss Educational Pack.

1. INTRODUCTION

Implementation of the occupational health and safety noise guidelines requires a high degree of worker cooperation and input. Health and safety officers, and management to a certain degree are generally fully aware of the consequences of high noise exposure over time. Often a person's motivation to undertake a tedious or seemingly unnecessary task changes if they understand the reasons behind it. Difficulties arise in helping the workforce become aware of the rationale behind the occupational health and safety guidelines. ?

Discussions with health and safety officers and workers involved in noisy industries, in addition to discussions with various professional acoustical consultants highlighted the need for interactive educational media in this occupational health area. The development of an educational package to meet this perceived gap in educational products was therefore proposed as a final year engineering thesis in conjunction with RTA Techvision Pty Ltd, a company specialising in the design and production of interactive multi-media presentations for engineering based projects.

The aim of this project was to combine interesting and relevant information into a CD-ROM package ("the project"). The objective of the project was to use multimedia presentations such as text, pictures, sound, graphics, video, animation and interactivity. The combination of a range of media types would be likely to keep interest levels high and help the audience to appreciate the value of their hearing and to improve the acceptance of hearing protection devices. In addition, by use of multiple choice questions and answers at the conclusion of the presentation, it is possible to provide anonymous feedback to management regarding workers attitudes.

2. BACKGROUND

RTA Techvision Pty Ltd has understood the opportunities available to companies willing to use the recent advances in technology. This technology now provides the capability to present comprehensive visual and aural information and accurate simulations of the desired information. RTA Techvision Pty Ltd believes that the use of interactive computer based systems is ideal for both disseminating information to the public and for feeding back information to the project team.

The project is taken from the initial concept through the development cycle to the final product by a team comprising the following personnel:

- Project manager – The project manager is involved in the initial concept development, liaison with the client, ensuring compliance with the base objectives, monitoring production timing and costs and ensuring the final result is a quality product;
- Design manager – The design manager organises the technical team members and is primarily involved with technical co-ordination of the project. He or she works closely with the client to understand the issues involved and familiarises himself or herself with appropriate background information. Script development and site visits to gain input from appropriate sources is usually undertaken by this role;
- Graphics designer – The graphics designer prepares the layout and graphics associated with the particular project;
- Technician – The technician prepares all the video, photo and audio files and incorporates these into the program; and,
- Programmer – The programmer makes modification to the software code as necessary.

The use of multi-media technology to communicate the information is considered of the upmost importance. The development of the product makes use of digital photos and video, software packages (eg Visual Basic, Adobe and Corel), and a computer based recording studio system. The final product is presented in a specially designed portable kiosk. The kiosk incorporates a multi-media computer and touch screen enabling users to interact with it. Attached to the kiosk is a set of special-purpose headphones calibrated in an anechoic chamber in accordance with appropriate Australian Standards (see Figure 1).

Figure 1: View of kiosk

The concept has been used previously to develop information kiosks related to the Sydney International Kingsford Smith Airport third runway and the Sydney M5 freeway project. The main purpose of these products was to provide the community with information about the changes associated with these developments.

3. METHODOLOGY

The research and development of the project took many months. Research involved industrial site visits and collation of informative material while the development side focused on graphics layout and programming. The following points briefly describe the process undertaken:

- Industrial Input – Industry input into the project was considered important because of the expected final market and audience. This is further described in detail in Section 4 below;
- Research – Research involved a wide reading program from both the print and electronic media. Reading included current legislation, standards, guidelines, text and case studies from both Australia and overseas. Discussions were also undertaken with a number of consultants and workers within the industry. A summary table presenting the topics covered is shown in Section 6 below;
- Graphics – The graphics production includes the overall layout, touch screen buttons, animations and other special affects as required. The animations in the package include how noise interacts with the ear and how damage can occur; and
- Programming – The project is programmed in Visual Basic. The programming includes organising the video and sound input/output and development of the database to store and report responses from the questionnaire.

4. INDUSTRIAL INPUT

Industry input into this educational package was considered of vital importance. Industrial occupational health and safety officers understand the issues associated with educating the workforce and have a working knowledge of the educational process. For these reasons a number of industry site visits were conducted during the course of researching and producing this Industrial Hearing Loss Educational Pack.

Liaison with a cross section of industries was undertaken. In addition, site visits were made to Cottees Hepburn Spa in Alexandria and the BHP steel works in Port Kembla. At both locations, discussions with occupational health and safety staff provided valuable input and an inspection of factory noise conditions was possible. The issues discussed with representatives of both companies included:

- The history of their hearing protection programs;
- Initial and on going acceptance by employees of hearing protection programs;
- Changes in occupational health and safety approaches over the years;
- Future direction of noise guidelines and how this relates to health and safety;
- Noise reduction measures that have been implemented at the plants or are being developed for future application;
- Site tour with discussions about noisy plant items, signposting and other site-specific issues;
- Hearing protection devices used on site, and the acceptance of them by workers; and
- Ideas for the project, the likelihood of it being accepted as an educational tool and input to the script text.

These discussions proved invaluable to the development and production of this project which is formally known as the Industrial Hearing Loss Educational Pack. The input and help provided in gathering information gave a good perspective of the industry and the issues facing it.

5. AUDIENCE

The perceived final audience played an extremely important role in the research and development of this project. The audience dictated the type and quantity of technical content. This section describes the methodology applied to the selection of the final content of the project.

Discussions with people involved in occupational health and safety revealed that there was a reasonably high awareness in the workforce about noise and its potentially harmful effects. Therefore, any presentation would need to be technically competent and reasonably informative. Whilst the level of awareness was high, the technical issues would no doubt not be clearly understood and hence it was decided that the target audience would predominantly be employees on the workshop floor having little or no acoustic knowledge.

By targeting this market though, the potential to aim it at students, managers and employers who may not understand the processes involved in hearing or why hearing protection must be taken seriously in noisy work environments became evident. It was resolved to target this audience as well.

During various interviews with company representatives an awareness of related and relevant workplace issues was obtained. One very important issue is the non-English speaking backgrounds of some of the employees. There is clearly potential for the project to be developed to cater for a range of ethnicity, however, this is beyond the scope of this project.

6. CD-ROM CONTENTS

The actual contents of the project evolved and changed considerably over the development cycle. The final product is broken up into a number of distinct sections, an overview of which is presented in Table 1 below reproduce from Koolik [1]. Figures 2 and 3 on the following page provide sample screen shots that taken from the project produced by © RTA Techvision Pty Ltd [2].

Table 1 – Summary of CD-ROM Educational Package Contents

Section	Contents
Prompt	Opening comments and music repeating until the Introduction button is pressed.
Introduction	Commentary on how health can be affected by noise and its impacts on family and social life.
Noise Simulation	Description of noise and simulation of industrial sound at 60, 70, 80, 85 and 90 dB(A). This simulation must be calibrated to hear represented noise levels.
Hearing Damage	Animation and description of how the ear works. Outlining the need to have a noise criterion. Permanent and temporary threshold shifts. Normal hearing loss (presbycusis), tinnitus, noise induced hearing loss and deafness.
Legislation	Brief overview of the role of National and State based legislation as well as Australian Standards. Graphs of various statistics.
Simulation of Hearing Damage	Demonstration of different situations, and relative hearing losses (2%, 15%, 35% and tinnitus) and how they would sound.
Noise Mitigation	Case studies of industry implemented hearing conservation programs. Hearing protection and introduction to noise mitigation techniques.
Questionnaire	Questions related to current perception of workers hearing, the perceived importance of wearing hearing protection and the acceptance of hearing protection.
Conclusion	Concluding statements, thanks and credits.

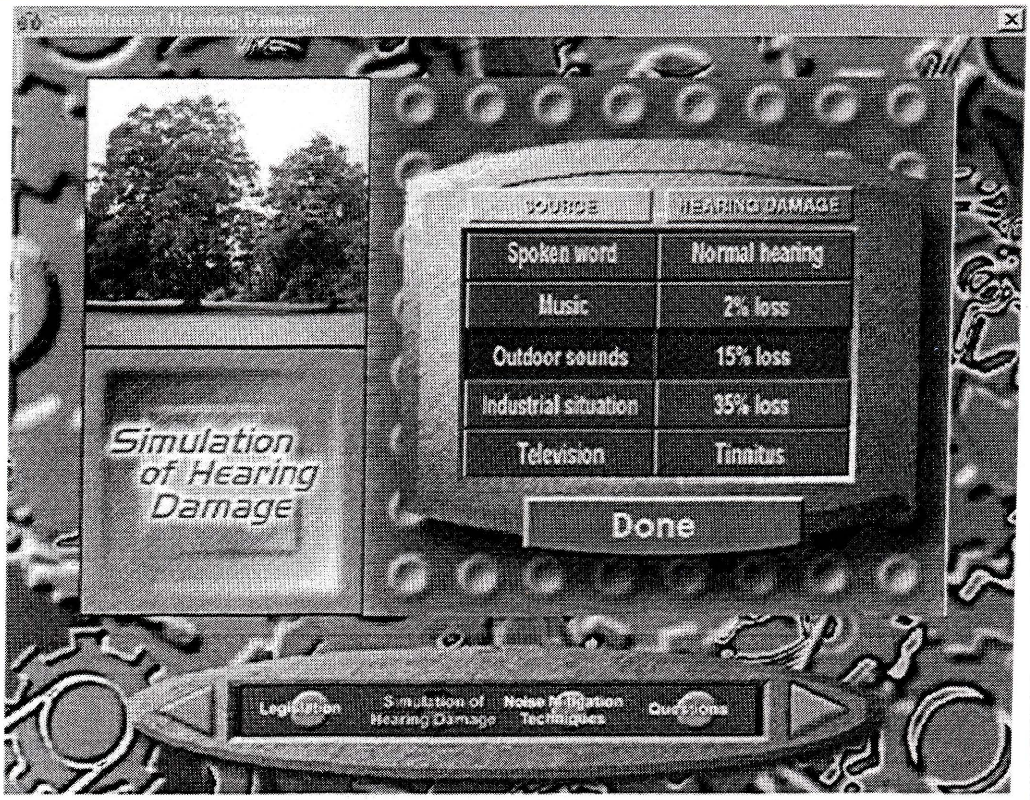

Figure 2: Screen shot of simulation of hearing damage

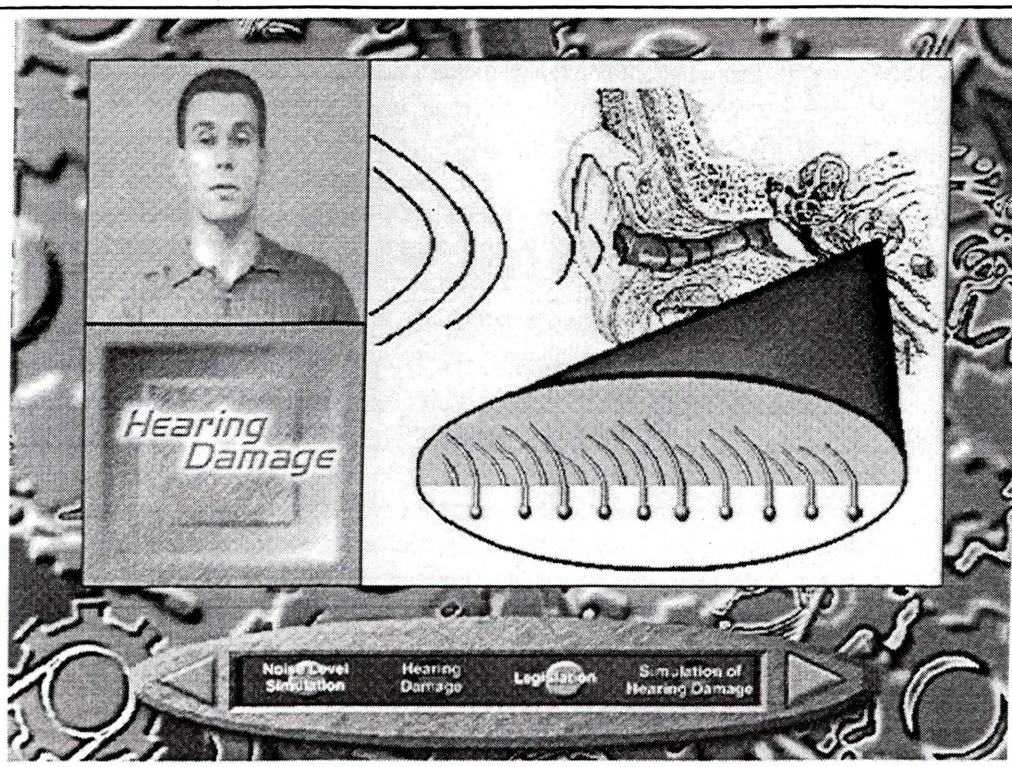

Figure 3: Screen shot of ear animation

7. APPLICATION

The RTA Techvision Pty Ltd, Industrial Hearing Loss Educational Pack is offered for sale in CD-ROM format and the kiosk is available for hire. It is expected that workplace environments may provide important feedback on the content and presentation of the project. The kiosk design and setup is robust and secure enough to be placed in most work environments.

The deployment of the kiosk within a workplace environment is anticipated to follow the basic procedure:

1. Briefing of health and safety officer of the concerned workplace as to the contents and capabilities of the educational package;
2. Presentation to workers by health and safety officer of the package and contents and explanation of aims and expectations of the package;
3. Kiosk to be set up in lunch or recreational room and workers requested to view CD-ROM presentation in a group or individually within a specified time frame;
4. Health and safety officer reviews responses to questionnaire and uses information to assess impact of current hearing protection program; and
5. Review of kiosk impact and hearing protection program with consultants if required.

The successful application of this process will require cooperation and understanding between employers and employees.

8. CONCLUSION

The Industrial Hearing Loss Educational Pack may assist in making workers and employers aware of the consequences of high noise exposure over time and the importance of occupational health and safety programs. It is hoped, as a consequence, they will take hearing conservation more seriously.

9. ACKNOWLEDGEMENTS

The authors acknowledge the support of Cottees Hepburn Spa and BHP Steel who allowed generous access to their workplace and employees. The authors also extend their gratitude to the staff at RTA Techvision Pty Ltd who assisted with the development and production of the project.

10. REFERENCES

[1] N Koolik, *Industrial Hearing Loss Information Pack*, BE (Hons) Thesis, University of Technology, Sydney, Australia, January 1999.

[2] © RTA Techvision Pty Ltd, *Industrial Hearing Loss CD-ROM Educational Pack*, Sydney, Australia, November 1999.

- 1 Do workers/etc understand the cumulative effect of noise exposure
- 2 Still "personal choice" - the problem: "wear your HPs or you'll go deaf"
- 3 Assumes HPs work

AUSTRALIAN ACOUSTICAL SOCIETY CONFERENCE

ACOUSTICS TODAY
Melbourne, 24 – 26 November, 1999.

TRAFFIC NOISE REVISITED

C L Fouvy

Fouvy Consulting Services

ABSTRACT

The noise of motor vehicles from heavily-trafficked roadways is one of the most annoying sounds of recent times. Some reduction has been achieved ; but apart from questionnaire surveys (some correlated with noise measurements, some not) involving those living or working near such noise sources, not all that much research seems to have established why it is so annoying.

Frequency and statistical analyses provide such answers, for establishing satisfactory noise control criteria, and developing traffic noise estimating equations.

Traffic noise becomes annoying for, as vehicle flows increase from 250 to 1000 veh/h, the noise changes from occasional foreground noise to intrusive background. Two control criteria (eg, L_{90} and L_{10}) are the necessary minimum. One criterion alone is statistically completely inadequate for noise levels with instantaneous values varying widely between 30 and 110 dB(A). Its problems are, however, likely to be solved by other than acoustical criteria.

1. INTRODUCTION

The noise of motor vehicles is among the most annoying sounds of recent times. A notable early report drawing attention to this was the 1963 Wilson *Final Report on Noise* [1]. More recently, *AAS Bulletins* (1971-84), and *Acoustics Australia* (1985-) have regularly included articles on this subject ; and AAS conferences from the 1971 *Noise Zoning Conference* onwards have included papers on this noise, with the 1985 Conference devoted entirely to *Motor Vehicle and Road Traffic Noise* : providing a rich resource of at least 37 AAS articles and papers on aspects of vehicle and traffic noise

2. PREVIOUS RESEARCH

Previous research on this subject has been of wide scope, covering both traffic and individual vehicle noise, their measurement and estimation, their effects on people and communities, the setting of suitable statutory noise criteria, and means of reducing the noise.

Noise measurement.

Earlier articles and reports were primarily concerned with noise from individual vehicles. Ch VI of the *Wilson Report* [1] recommended maximum noise levels for individual vehicles [85 dB(A) for 4- and more-wheeled vehicles, and 90 dB(A) for 2-wheeled vehicles] tested according to the method of ISO 362 ; and assumed that, in traffic, the resulting noise would be less with quieter vehicles. Two papers on motor vehicle noise were contributed to the 1971 AAS Noise Zoning Conference. Bryant's on *Highway Noise* [2], while concerned with quantitative measures of vehicle noise, also discussed in a more qualitative way means of reducing the noise of concentrations of traffic from expressways. Challis' on *Traffic Noise Criteria in Australia* [3] surveyed the sources of vehicle noise (speed, acceleration, payload, road surface) in order to include a simpler test in addition to the ISO 362-compatible standard test in the then forthcoming Australian Standard on measuring motor vehicle noise {issued in draft form as DR75075, *Measurement of the determination of motor vehicle noise emission* [30], published as AS 2240-1979, then withdrawn in Jul 99} [4]. After this, most later articles have been concerned with noise from traffic rather than from individual vehicles, but with the papers given at the 1985 AAS Conference on *Motor Vehicle and Traffic Noise* nearly equally divided between the two.

AS 2240-1979 [4] usefully specified, as well as the ISO 362-compatible moving vehicle acceleration test, five additional types of test for measuring vehicle noise : from a stationary vehicle, during acceleration from a standing start, from low and high speed drive-by tests, and of body noise. AS 2702-1984 [5] prescribes methods for the measurement of road traffic noise. In addition, Saunders and Taylor [6], Dunlop et al [7], and Lawrence [8] published series of recorded traffic noise levels (giving at least L_{90} and L_{10}) which are useful for comparison with later measurements or testing traffic noise estimating equations. Lawrence's data are given in TABLE 3 below.

Not much Australian research on individual vehicle noise sources appears to have been published apart from the work of Samuels and Alfredson [9], Samuels [10], and Samuels and Sharp [11], who over more than 10 years investigated how tyre-on-road noise (loud at higher vehicle speeds) is influenced by tread pattern and road surface macrotexture.

Noise estimation.

Much research on vehicle and traffic noise has been on estimating its noise levels, or on surveys for predicting human and community response to it. Alfredson [12] compared observed traffic noise levels with estimates using the Johnson (UK) and Gordon et al (USA, FHWA) equations to predict L_{50} under similar conditions, found them unsatisfactory, and developed his own equations for estimating L_{50} and its standard deviation. Hothersall and Jones [13], in a similar investigation, found the UK Dept of the Environment (DoE) method of estimating traffic noise generally satisfactory. This author in a paper concerned with various aspects of traffic noise [14], reviewed the Johnson, Gordon and Alfredson equations, and discussed the SATS equations for estimating L_{90} and L_{10} [15]. That paper also discussed the way in which L_{min}, L_{90}, L_{50}, L_{10} and L_{max} vary with traffic flow for the case of uniform flows of vehicles of acoustically identical power level at uniform speed.

Lawrence & Burgess [16] introduced two further traffic noise equations (due to Delaney, and Burgess) for estimating L_{10}, and concluded that *"effective urban planning, traffic management and strict vehicle noise emission controls appear to be the most profitable long-term solutions to the traffic noise problem in both existing and new areas"*. Burgess, in *Traffic flow and noise levels at one site* [17], discussed the advantages and disadvantages of shorter and longer time noise samples, and the considerable variation occurring between observed and estimated L_{10} traffic noise levels at different values of traffic flow, and concluded that large errors can occur when estimating equations are used outside their range of validity. Samuels [18], in commenting on this article, discussed sources of variability in traffic noise levels beyond sampling time interval (such as variations in instantaneous traffic flows and speeds). Modra [19] discussed the UK DoE method of estimating $L_{10(18h)}$, whether measurement or estimation is to be preferred, and whether $L_{10(18h)} = 68$ dB(A) is a satisfactory traffic noise limiting criterion for Australian conditions. Kato et al in two articles [20,21] described their development of digital simulation methods for estimating the statistical distribution of traffic noise levels. One of their conclusions was that L_N is more likely to be non-Normally rather than Normally distributed about L_{50}. North and Samuels [22] discussed, inter alia, the more recent (1988) UK Dept of Transport method of estimating road traffic noise levels, and introduced the useful traffic noise relationship,

$$L_{10(1h)} = L_{eq(1h)} + 3 \quad \text{dB(A)} \qquad (1)$$

Human response to traffic noise.

Brown & Law [23] conducted a survey near a Brisbane expressway to discover the extent to which people were annoyed by the nearby traffic noise, but did not report the concurrently made noise measurements. One useful conclusion was that people living further than 70 m from the expressway reported an annoyance score no higher than 3 out of a maximum of 7. Bryant [24] reported on an ARRB seminar on *Measuring social behavior in road research*, in which researchers described their surveys to relate people's degree of traffic noise annoyance to various noise measures, of which one interesting outcome was that the much used $L_{10(18h)}$ was found to be an insensitive indicator of annoyance. Hede [25] reported that both traffic and individual vehicle noise provoked community annoyance, and concluded that worthwhile reductions in annoyance would result from quietening all, not just noisy vehicles. Hede et al [26] commenting on the 1986 Community Noise Survey reported that its results showed that noise was the most serious form of environmental pollution, and confirmed that traffic noise was still very much a major source of community disturbance, that complaint data are a poor indicator of the community impact of noise, and that people's reaction to noise generally decreased with age and increased with education level. Job and Hatfield [27] agreed, and recommended that solutions to noise problems included the importance of psychological approaches as well as physical noise abatement measures.

Noise criteria.

Noise control criteria are either general (such as those rating sounds according to their loudness, or the *Maximum Permissible Speech Interference Levels* of AS 2822), or particular (such as those developed for vehicle and traffic noise) [28].

Lawrence [29] reported that in the UK the statutory traffic noise limit had by 1973 been set at $L_{10(18h)} = 70$ dB(A). Because it was considered higher than desirable it would soon be reviewed. At the same time, L_{eq} in dB(A) was being used in Austria, L_{50} in France, and L_{50} and L_{10} in Poland. Mather, in two papers, discussed both vehicle and traffic noise limiting criteria. The first [30] gave the ADR 28 maximum noise levels for various vehicle types, and showed the SAA DR75075 proposals for progressively reducing them in 3 stages, with those of the last stage being at least 10 dB(A) below those of ADR 28. The second, on *Human criteria--noise measures* [31], reviewed the many available noise criteria covering sleep disturbance, task interference, health damage, traffic noise, etc ; noted that, although in the UK the $L_{10(18h)}$ traffic noise limit had by 1979 been reduced from 70 to 68 dB(A), no similar limit had been adopted in Australia ; and recommended that, because there was no single agreed-on measure for the "integrated effect of environmental noise on human health and well-being", there was a need for multiple noise measures.

Alexandre, in the 1985 AAS NSW Conference keynote paper, *Strengthening motor vehicle noise abatement policies* [32], said that 16% of the OECD countries' populations were daily exposed to *unacceptable* levels of noise [> 65 dB(A)], with a further 34% suffering *acoustic discomfort* [ie, levels between 55 and 65 dB(A)] ; that between 1970 and 1985 very little vehicle and traffic noise reduction had been achieved [c. 3 dB(A)] ; and concluded that, if stringent motor vehicle noise limits, better methods of traffic management, and infrastructure and building modifications were seriously enforced, continuing increases in noise would not be inevitable. Griefahn [33], concluded that sleep would probably not be disturbed with levels less than $37 > L_{eq} > 45$ dB(A) for continuous noise, and, for intermittent noise, levels less than 59,4 dB(A) for 2 events per night, 54,1 (10 events) or 53,5 (30 events).

The $L_{10(18h)}$ traffic noise limit began (in the UK) at 70 dB(A), and has been progressively reduced to 68 dB(A)(as adopted in Australia) and in c. 1993 to 63 dB(A). The author [34,35] and others have begun to seriously question the usefulness of $L_{10(18h)}$ alone as a traffic noise limiting criterion. Murray [36] indicated a need to measure L_{90} as well as L_{10}. Others have suggested that L_{50} or L_{eq} might be more appropriate.

Traffic noise reduction.

Reducing traffic noise at its source, and modifying the sound path between source and hearer have both been investigated, with most work on modifying the sound path. Crocker [37], argued that reducing this noise is of the highest priority. With the NSW State Pollution Control Commission's traffic noise control program [38], this noise was to be reduced by new controls designed to reduce vehicle noise at its source by ensuring compliance with the Noise Control Act, careful land use planning, traffic management and road design to reduce its impact, and traffic management schemes and noise barriers in residential areas. Hede [39] recently argued that the 'collaborative' rather than the 'technofficial-centred' approach would achieve more effective noise control.

Bullen [40], reviewing Alexandre et al, *Road traffic noise*, London, 1975, quoted that *the most promising method for the reduction of noise is by suitable town planning and orientation of houses, which could reduce current noise levels by 15 dB(A). In comparison, noise barriers at the sides of major roads could reduce levels by only 8-10 dB(A), as well as being visually unattractive, and noise from vehicles themselves can be expected to be reduced by only about 5 dB(A) in the near future. Unfortunately, it would appear that legislators and administrators have investigated these solutions in the reverse order of priority, indicating the need for an interdisciplinary approach.* Radwan and Oldham [41] proposed a computer method for simulating the generation and propagation of traffic noise in built-up areas so that land use planners can plan and zone urban areas more effectively.

In four papers describing the use of building elements for optimum attenuation of traffic and other noise, Fricke [42] demonstrated this with a courtyard house design. Dubout [43] found dB(A) still the most useful measure for rating the sound transmission loss of building partitions and envelopes against interior and exterior noise. Lawrence and Burgess [44] described the success of their experimental building in determining the attenuation of walls, doors and windows against traffic noise. Mizia and Fricke [45] showed how to locate windows for both maximum ventilation and attenuation of exterior traffic noise.

Of the two methods for calculating the excess attenuation of barrier screens alongside busy roadways, Method A [46,47] gives the effective or excess height of the barrier as its height normal to and above the direct line between noise source and hearer. The excess attenuation is obtained from a graph of attenuation vs excess barrier height in wavelengths for various angles-into-the-sound-shadow. In Method B [48,49], the excess height is the vertical height above the direct line between source and hearer. The excess attenuation is calculated from a parameter, x, depending on the wavelength of the noise, the barrier's excess height, and the two horizontal distances between source, barrier and hearer, then obtained from a graph of excess attenuation vs x [49]. Several calculations showed that Method A tends to give higher excess attenuations than Method B, particularly at lower frequencies. However, the author has found that attenuations calculated by Method B are in quite close agreement with the corresponding measured values. Saunders [50], discussed several ways (by noise zoning, barriers, etc) of suitably locating and isolating major arterial roads and expressways to reduce the adverse effects of their traffic noise, particularly in residential areas. West [51] described a recently developed concrete barrier with one sound-absorptive side having coefficients of acoustic absorption of around 0,9 and 1,0 at frequencies between 100 and 1000 Hz. These articles and papers, many in AAS publications, are valuable. Taken together, they significantly increase our understanding of traffic noise problems.

3. TRAFFIC NOISE MEASUREMENTS

Traffic and vehicle noise levels are measured for three basic purposes : to characterize, at any particular location, a sound source or acoustic environment ; to check a sound source for compliance with specifications or regulations ; or to obtain data for noise prediction purposes. The author, in order to obtain information about the traffic noise from vehicles on a busy expressway, recently carried out several statistical and frequency analyses (both octave and one-third octave) ; and, for comparison, made similar measurements in a quiet residential street. The results of the statistical analyses are given in TABLE 1 ; those of the frequency analyses are given in Figures 1 and 2.

4. ESTIMATING TRAFFIC NOISE

Of equations developed for estimating traffic noise levels, giving L_N in dB(A) in terms of traffic flow, Q veh/h, mean traffic speed, V km/h, distance to the traffic flow, D m (not always precisely specified), and percentage of heavy vehicles, P, Alfredson [12] quoted his own, (2) and (3), for estimating L_{50} and its standard deviation, σ, as well as those developed by Johnson (UK) and Gordon (USA, Federal Highway Administration, FHWA).

$$L_{50} = -4{,}5 + 16{,}4 \log Q - 14{,}3 \log D + 17{,}4 \log V + 0{,}16\, P \ \text{dB(A)} \quad \text{.............(2)}$$

$$\sigma = 8{,}7 - 2{,}1 \log Q - 3{,}7 \log D + 3{,}84 \log V + 0{,}04\, P \ \text{dB(A)} \quad \text{...................(3)}$$

Lawrence and Burgess [16] quoted the following two equations for estimating L_{10} (due to Delaney, and Burgess resp, using the above variables).

$$L_{10} = 31{,}0 + 8{,}9 \log Q - 14{,}7 \log D + 16{,}2 \log V + 0{,}117\, P \ \text{dB(A)} \quad \text{.............(4)}$$

$$L_{10} = 56{,}0 + 10{,}7 \log Q - 18{,}5 \log D + 0{,}3\, P \ \text{dB(A)} \quad \text{..................................(5)}$$

The US FHWA environmental assessment section of its transport planning package included traffic noise estimating equations ; so also did the Sydney Area Transportation Study (SATS) Report [15], with the following equations for estimating L_{90} and L_{10}.

$$L_{90} = -19{,}0 + 21{,}3 \log Q - 6{,}1 \log D + 9{,}8 \log V + 0{,}075\, P \ \text{dB(A)} \quad \text{............(6)}$$

$$L_{10} = 26{,}8 + 8{,}9 \log Q - 10{,}5 \log D + 16{,}2 \log V + 0{,}117\, P \ \text{dB(A)} \quad \text{............(7)}$$

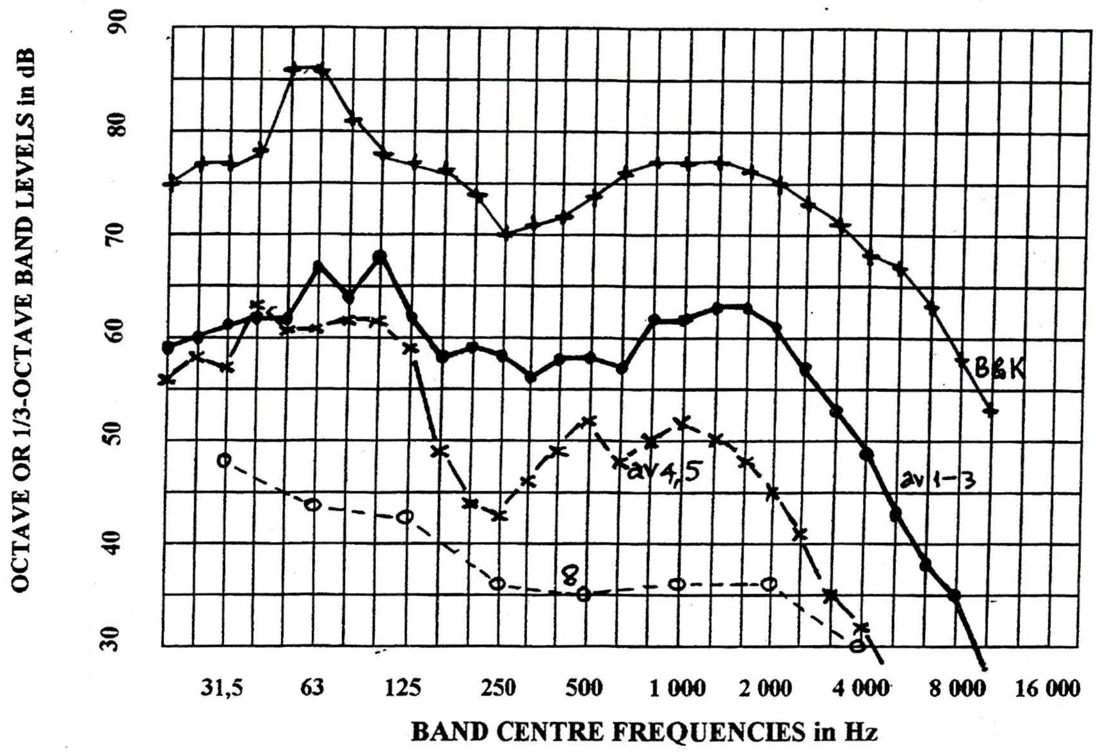

FIGURE 1 —TRAFFIC NOISE SPECTRA [numbered as in TABLE 1]

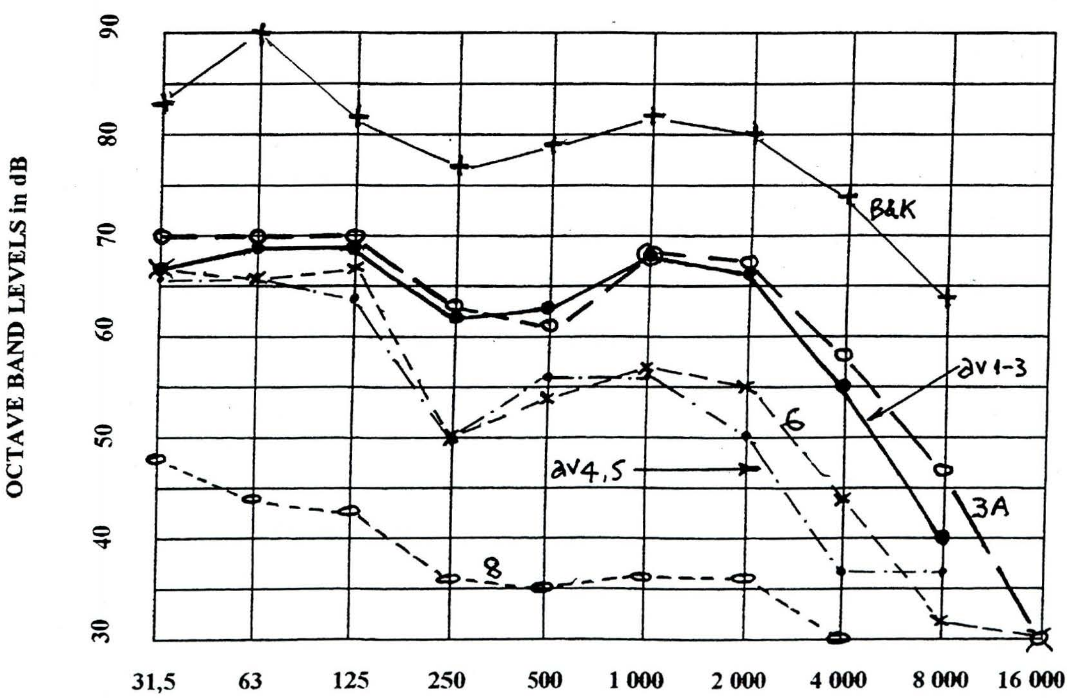

FIGURE 2--TRAFFIC NOISE OCTAVE BAND SPECTRA [numbered as in TABLE 1]

These equations, combined with the values of Q, D, V and P from Lawrence's data [8], were used by the author to obtain corresponding estimates of L_{90}, L_{50} and L_{10}, to assess the equations' performances against each other. The data and estimates are included in TABLE 3 below. The estimates obtained using equation (5), were not included as they did not appear directly comparable with the other estimates.

5. DISCUSSION

Traffic noise characteristics, control criteria, and its reduction are discussed here in terms of the author's recent traffic noise measurements and estimates, and the previous research.

Traffic noise characteristics

Traffic noise characteristics are given by frequency analysis, and from its variation with time, vehicle speed, distance between source and hearer, from vehicle to vehicle, instantaneous traffic flow, and the proportion of heavy vehicles in the traffic stream.

Frequency spectra. Because vehicle and traffic noise are basically broad band sounds, their frequency spectra can be adequately obtained from octave and one-third octave band analysis, with one-third octave analysis also indicating the presence of tonal components (through the band containing the tonal component having a level at least 3 dB above the mean of those in the two adjacent bands).

The author's frequency analyses of the noise of traffic on a busy expressway, are given as one-third octave (L_{eq}) spectra in Figure 1 and octave spectra in Figure 2. Of these, spectra nos. 1 to 3 were within direct sight of the expressway, about 20 m from the nearest traffic lane ; while spectra nos. 4 and 5 were obtained at about 30 m from this lane, but behind an acoustic barrier screen with, for this location, an effective height of about 15 m. Spectrum no. 6 was at about 50 m on an adjacent arterial road. Their spectrum shapes are similar but with the noise levels of the screened traffic (spectra ## 4-6) attenuated by about 10 dB at frequencies above 250 Hz. Between 800 and 2 500 Hz (the band of maximum interference to speech) the higher levels are typical of tyre-on-road and wind noise from traffic at speeds at 80 to 100 km/h. Though these spectra suggest the presence of tonal components from engine and exhaust noise at 63 and 100 Hz (spectra ## 1-3), and 40 Hz (spectra ## 4,5), the presence of tonal components cannot be confirmed because these band levels were measured sequentially rather than at the one moment (as when instruments equipped with FF transformation are available), and traffic noise levels were varying. The Hassall and Zaveri [53] traffic noise spectrum (labelled *B&K*) shows a similar spectrum shape. By contrast, the octave spectrum of background noise in a quiet residential street does not show significant increases in level above 500 Hz.

Statistical measurements. The author's statistical noise measurements made the next day at the same locations over periods of 5 minutes' duration are given in TABLE 1. The L_{eq} marked ‡ of the corresponding frequency analyses of Figures 1 and 2 are generally similar, except that at location 8 the statistical noise levels include two motorcar passes. At locations nos. 1 to 7 near the expressway, with traffic flows not greatly varying, the differences, $L_{10} - L_{90}$ were small, varying only between 3,0 and 7,0 dB(A). The way in which the various L_N vary with measurement distance, traffic flow, traffic speed, etc will show the significance of this.

Variation of noise level with measurement distance, traffic flow, etc. In general, the various L_N of traffic noise decrease with increasing measurement distance, and increase with increasing traffic flow, traffic speed and percentage of heavy vehicles in the traffic stream.

These are conveniently shown in equations for estimating traffic noise levels. Alfredson [12], Burgess [17] and Samuels [18] stressed the need for careful control while measuring statistical traffic noise levels to minimize the effects of variations in instantaneous traffic flow and speed, and discussed the merits of measuring noise levels over shorter or longer sampling periods. While longer periods of from 1 to 24 hours are necessary to characterize an acoustic environment, short periods are desirable for minimizing the effects of those independent variables which can be precisely measured. For, when accurate means of measuring instantaneous traffic flows and speeds are available, the shorter noise sampling periods, in which there is minimum variation of flow and speed, will provide the more satisfactory data. Under these circumstances, even at a uniform low traffic flow of around 250 veh/h (= 4 veh/min), a sampling time of 1 minute would be quite sufficient, because during this time L_N would provide 4 minima and 4 maxima, with only the noise outputs of individual vehicles being variable.

TABLE 1 — TRAFFIC NOISE STATISTICAL ANALYSES

NOISE LEVEL L_N, L_{eq}	STATISTICAL NOISE LEVELS, L_N, in dB(A), and L_{eq} in dB(A) and dBflat, and SIL in dB at Location no.							
	[1]	[3]	[4]	[5]	[6]	[7]	[8]	B&K
L_{min}	67,8	63,5	53,2	53,2	55,3	56,0	33,6	—
L_{99}	69,5	66,0	53,5	54,0	57,0	57,5	34,5	
L_{90}	71,0	70,0	54,5	55,0	59,5	60,0	35,5	
L_{50}	73,5	73,0	56,0	56,5	62,0	62,5	38,0	
L_{10}	75,0	75,5	57,5	58,5	66,5	66,0	47,0	
L_1	77,0	77,0	59,5	61,5	72,0	72,0	62,5	
L_{max}	80,8	78,5	62,1	67,3	76,1	74,1	69,3	
L_{eq} in								
dB(A)	73,4	73,2	56,3	56,9	64,0	63,7	49,0	—
dB(A) ‡	71,0	72,3	56,5	62,2	60,6	—	41,1	85,5
dBflat ‡	77,0	77,1	68,9	72,3	71,9	—	51,0	92,3
SIL, dB ‡	62,2	64,3	46,9	52,6	52,5	—	34,2	78,6

NOTES :

[1] Locations of ## **1-3** were above the E Fwy (8-lane, flow = 4 000-5 000 veh/h, flowing freely at 80-100 km/h) in Kew (Melb), 50 m E of Belford Rd, at c. 20 m from the nearest S traffic lane, of ## **4,5** were c. 300 m further E, in a hollow behind an acoustic barrier screen (5 m below road level, 30 m from the nearest traffic lane, and c. 15 m below the top of the barrier), of ## **6,7** opposite # 3 at the Kilby Rd N property line (at c. 50 m), and of # **8** in a quiet residential street (Bowyer Av, Kew).

[2] For ## 6 and 7 the local Kilby Rd traffic flow was of the order of 400 veh/h. Measurement # 6 includes this traffic noise (at the N property line) ; # 7 includes only the expressway traffic noise (at 50 m in the cutting just E of Belford Rd), local traffic noise was excluded by the meter interrupt.

[3] ‡ signifies that these L_{eq} were measured at the same location on the previous day but at approximately the same time of day. For # 8 the later L_{eq} is higher on account of two vehicle passes.

The study of masses of L_N data is time-consuming ; so it is simpler to synthesize the instantaneous noise levels of a succession of vehicles passing a measuring point, or to combine a set of carefully measured data into estimating equations. These show how the various L_N vary with traffic flow (Q), measuring distance (D), vehicle speed (V) and percent of heavy vehicles (P).

In 1976, this author [14], in a synthesis for the simple case of identical vehicles passing a point at uniform speeds and flows, which indicated how L_{min}, L_{90}, L_{50}, L_{10} and L_{max} varied with traffic flow, showed that while L_{min}, L_{90} and L_{50} increased by 4 to 5 dB for each doubling of the traffic flow, L_{10} and L_{max}, increased by only about 1 to 2 dB for each doubling of traffic flow, apart from an increase in L_{10} of around 3 dB for a doubling of flow from 250 to 500 veh/h.

$L_{10} - L_{90}$ is thus greater at lower than at higher traffic flows, varying from 13 dB (at 5 m) and 8 dB (at 20 m) at flows of 200 veh/h, to almost zero at flows of 4000 veh/h. Also, the difference, $L_{50} - L_{90}$, varied very little as the traffic flow increased, varying from 2 dB at 200 veh/h to almost zero at 4000 veh/h. These traffic noise characteristics mean that, while at low flows of 200 veh/h (3 to 4 veh/min) the noise of each passing vehicle is heard as foreground noise, at high flows the noise of individual passing vehicles have coalesced, and has become a louder, intrusive, background noise. This change from foreground to intrusive background noise occurs at around 500 veh/h.

The traffic noise equations given above show similar relationships. TABLE 2 below summarizes, for the synthesized and estimated levels, the changes which occur when traffic flow, source-to-hearer distance, and traffic speed are doubled. L_{90} is greatly influenced by traffic flow (by + 4 to over + 6 dB per doubling of Q), noticeably influenced by traffic speed (by + 3 dB per doubling of V), but less by distance (by – 1,8 dB per doubling of D) ; whereas L_{10} is significantly less influenced by Q than L_{90} (by + 1 to + 2,7 dB per doubling of Q), and more influenced by D and V than L_{90} (– 3,2 to – 4,4 dB per doubling of D, and + 4,9 dB per doubling of V). Apart from the equation (1) quoted by North and Samuels [22], which could be alternatively given as

$$L_{eq(1h)} = L_{10(1h)} - 3 \quad dB(A) \quad \text{...(1A)}$$

there appear to be no equations for estimating L_{eq} in terms of Q, D, V and P. Experience shows that with traffic noise, L_{eq} is usually close to L_{15}.

The Johnson, Gordon and Alfredson [12] equations for estimating L_{50} and standard deviation, σ, assumed that instantaneous L_N were Normally distributed about L_{50}. In statistical fact, these L_N would be, if Normally distributed at all, so distributed about the arithmetic mean, L_{mean}, rather than the median, L_{50}. While some statistical noise measurements do show L_{50} lying approximately midway between L_{90} and L_{10}, others, including the author's traffic noise synthesis for the case of uniform flows of acoustically uniform vehicles, show L_{50} lying noticeably closer to L_{90}, indicating a distribution of instantaneous noise levels upwardly much more skewed than with Normally-distributed levels, whether about L_{mean} or L_{50}. Kato et al [20,21] also found that non-Normal distributions of noise levels are more probable.

Comparison of L_{90} and L_{10}, as in TABLE 3 below, shows that the measured $L_{10} - L_{90}$ are usually greater than the estimated differences. This probably occurs because, in developing estimating equations, the noise levels are for as constant as possible traffic flows, speeds and percentages of heavier vehicles, whereas with the measurements, the observed flows and speeds are averages measured over probably five minutes or more, during which Q, V and P could have greatly varied. The Lawrence data [8] acknowledged this variability in Q and P by giving averaged values with their standard deviations (as ± σ), indicated in TABLE 3 by a ± sign after each Q or P. The measured L_{90} would then be lower than the estimated during moments of lower than average flow, and L_{10} higher during moments of higher flow. The additional estimates at the bottom of TABLE 3 thus confirm that, for this measurement, the average traffic flow of 2899 veh/h could have represented flows varying from 1600 to 4200 veh/h.

TABLE 2 — TRAFFIC NOISE LEVEL CHANGE WITH CHANGE IN Q, D and V

EQUATION		CHANGE IN TRAFFIC NOISE LEVEL [dB(A)] for a two-fold change in		
		Flow, Q veh/h	Distance, D m	Traffic speed, V km/h
Fouvy synthesis [14]	for L_{90}	+ 4 to + 5	(adopted as – 4,3)[14]	—
	for L_{50}	+ 4 to + 5		—
	for L_{10}	+ 1 to + 2		—
Alfredson [12]	eqn (2) for L_{50}	+ 4,9	– 4,3	+ 5,2
	eqn (3) for σ	– 0,6	– 1,1	+ 1,2
Delaney [16]	eqn (4) for L_{10}	+ 2,7	– 4,4	+ 4,9
Burgess [16]	eqn (5) for L_{10}	+ 3,2	– 5,6	—
	eqn (5A)	+ 5,6	– 3,2	—
	eqn (5B)	+ 2,6	– 3,2	—
SATS [15]	eqn (7) for L_{10}	+ 2,7	– 3,2	+ 4,9
SATS [15]	eqn (6) for L_{90}	+ 6,4	– 1,8	+ 2,9

NOTES :

[1] Reference sources for each equation are as given above in the TABLE

[2] The Burgess equation (5) as originally given [16] appears to contain an inadvertent (eg, printing) error. Possible alternatives are $L_{10} = 29{,}0 + 18{,}5 \log Q - 10{,}7 \log D + 0{,}3\,P$......(5A), and

$L_{10} = 69{,}0 + 8{,}5 \log Q - 10{,}7 \log D + 0{,}3\,P$.......(5B)

Comparing the measured with estimated values of L_{90} and L_{10} also indicates the faithfulness with which any of these equations can reproduce the measured data. Of the various equations, all of which appear to satisfactorily reproduce the measured data, the SATS equations [nos. (6) and (7)] have the advantage of being a matched pair for estimating L_{90} and L_{10}, which not only satisfactorily reproduce the measured values, but also reproduce the way in which the difference, $L_{10} - L_{90}$, decreases as traffic flow increases. The Delaney equation, (4), though estimating L_{10} similarly to the SATS equation, (7), suffers in not having a paired equation for estimating L_{90}. The Alfredson equations, (2)and (3), suffer through estimating L_{90} and L_{10} from L_{50} and a standard deviation instead of directly, and the doubtful assumption that the instantaneous L_N are Normally distributed about L_{50}. The SATS equations [15] thus currently appear the most useful.

Measures for characterizing traffic noise

Sound levels in dB(A) and dBflat, together with octave and one-third octave band levels, and the Speech Interference Levels (SIL) derived from them, are those most used for characterizing either the instantaneous or time-averaged frequency spectra of traffic noise ; while its statistical levels, L_{90} and L_{10}, and its time-averaged L_{eq} are the most widely used for characterizing its varying intensities at any location. L_{min}, L_{99}, L_{50}, L_1 and L_{max} can also be used if a more complete statistical characterization is required.

With these three main noise levels, L_{90} and L_{10} provide stable measures of the near-minimum and near-maximum values of the traffic noise at any location (unlike L_{min} and L_{max} which give only the extreme minimum and maximum), while L_{eq} gives a suitable measure of

TABLE 3 — TRAFFIC NOISE MEASUREMENTS AND ESTIMATES

SITE AND TRAFFIC DETAILS [note 1]			STATISTICAL NOISE LEVELS in dB(A)											
			MEASURED				ESTIMATED [note 2]							
			Lawrence data[note 1]				Alfredson method				Del	SATS method		
Year	Q veh/h	P%	L_{90}	L_{eq}	L_{10}	L_{10}-L_{90}	L_{90}	L_{50}	L_{10}	L_{10}-L_{90}	L_{10}	L_{90}	L_{10}	L_{10}-L_{90}
Site 1–19,5 m to road c/l														
1978	2715	8,97	62,5	74,3	77,5	15,0	63,6	69,7	75,8	12,2	76,0	66,7	77,2	10,6
1984	2899±	8,10±	61,8	75,3	78,7	16,9	64,1	70,0	75,9	11,8	76,1	67,1	77,3	10,2
Site 3														
1975	2368±	8,98±	62,8	76,3	79,1	16,3	62,2	68,5	74,8	12,6	75,5	65,4	76,7	11,3
1985	2252±	8,77±	61,1	74,8	78,0	16,9	61,8	68,2	74,6	12,8	75,2	65,0	76,4	11,4
Site 4														
1977	2088	20,10	61,1	75,2	78,8	17,7	62,6	69,5	76,4	13,8	76,4	65,0	77,6	12,6
1985	1937±	15,14±	62,2	75,6	78,8	16,6	61,4	68,2	75,0	13,6	75,4	63,9	76,6	12,7
Site 5														
1985	1854±	18,52±	64,1	75,7	79,0	14,9	61,5	68,4	75,3	13,8	75,7	63,7	76,9	13,2
Site 2a–12,8 m to road c/l														
1977	363±	5,18±	47,2	65,6	69,0	21,8	48,2	57,3	66,2	18,2	66,9	46,5	67,4	20,9
1984/5	279±	3,31±	42,8	64,4	68,5	25,7	45,8	55,1	64,4	18,6	65,7	43,9	65,2	21,3
Site 2b														
1977	363±	5,18±	47,6	66,1	69,2	21,6	48,2	57,3	66,2	18,2	66,9	46,5	67,4	20,9
1984/5	279±	3,31±	42,8	65,7	68,9	26,1	45,8	55,1	64,4	18,6	65,7	43,9	65,2	21,3
Site 6														
1984	490±	4,76±	45,3	65,6	69,5	24,2	50,6	59,4	68,2	17,6	68,1	49,3	68,6	19,3
Site 1 [additional estimates]														
1984	2899±	8,10±	61,8	75,3	78,7	16,9	64,1	70,0	75,9	11,8	76,1	67,1	77,3	10,2
	2400}	2900										65,4	76,6}	12,5
	3400}											68,6	77,9}	
	1900}	2900										63,2	75,7}	15,3
	3900}											69,9	78,5}	
	1600}	2900					59,0	65,6	72,2}	17,9		61,6	75,0}	17,1
	4200}						68,3	72,6	76,9}			70,5	78,7}	
[flow = 2899 ± 172]										[note 3]				[note 3]

NOTES :

[1] The site details, measured traffic flows (Q), percentages of medium plus heavy vehicles (P), etc are from Lawrence [8], TABLE II. Q and P followed by ± gave the corresponding standard deviation. Sites 1, and 3 to 5 were at 6-lane divided arterial roads, and sites 2 and 6 at 4-lane roads. Average traffic speeds have been taken as 100 and 60 km/h, respectively, for the 6-lane and 4-lane roadways. Microphone to road centreline distances were estimated from the original distances to centreline of nearer traffic flow. Time periods (20 to 240 min) for the measured noise levels are from TABLE I [8].

[2] The Alfredson method [12], gives estimates of L_{50} and its standard deviation, σ, from equations (2) and (3) above. L_{90} and L_{10} were calculated from $L_{50} \pm 1{,}28$ s. The Delaney equation (4) for L_{10} is from Lawrence and Burgess [16]. The Sydney Area Transportation Study (SATS) [15] equations (6) and (7) give direct estimates of L_{90} and L_{10}.

[3] The three composite values of L_{10} - L_{90} shown are the differences between the higher L_{10} and the lower L_{90} of each estimated pair.

the average traffic noise level, as it is the level which would have been measured had the noise been unvarying. Though equation (1) above suggests a fixed (but approximate) relationship between L_{eq} and L_{10}, these two related levels are by derivation independent of oneanother. All these three are important as the minimum to be obtained ; no traffic noise measurement is either adequate or satisfactory without any one of them.

Noise criteria applied to traffic noise

The most general noise criteria are those that rate sounds with a level above 60 dB(A), 80 dB(A) and 100 dB(A) as, respectively, *loud*, *very loud*, and *deafening* ; and the early criterion that sounds of level below 80 dB(B) [equivalent to about 75 dB(A)] are unlikely to cause hearing damage, even with prolonged exposure, or if the sound is a pure tone. Amongst the most useful and readily applied criteria when an octave spectrum of the noise is available are the *Maximum Permissible Speech Interference Levels for Reliable Speech Communication* of AS 2822-1985 [28].

Other criteria besides the current $L_{10(18h)}$ noise limiting criterion of 63 dB(A) can be applied to traffic noise. Reducing $L_{10(18h)}$ from 68 to 63 dB(A) changed this noise, in Alexandre's terms [32], from being "unacceptable" to causing "acoustic discomfort". Griefahn's criteria [33] that sleep is not likely to be disturbed by continuous noise of level less than 37 > L_{eq} > 45 dB(A), or by intermittent noise of level less than 59,4 dB(A) (2 events per night), 54,1 dB(A) (10 events) or 53,5 dB(A) (30 events) are applicable to traffic noise at night.

AS 3671-1989, *Acoustics–Road traffic noise intrusion–Building siting and construction* [54] (which also refers to the design levels for building interiors of AS 2107-1987) gives $L_{10(18h)}$ = 45 dB(A) as a general indoor noise limit. The AS 2107 recommended *'desirable'* design sound levels for rooms and other building interiors where reliable speech communication is essential, vary from 25 to 40 dB(A), with the corresponding *'maximum'* levels as mostly 5 dB(A) higher.

With a sound's Speech Interference Level (SIL) on average 8 dB less than its A-weighted sound level (AS 2822), this level of 40 dB(A) from AS 2107 has an equivalent estimated SIL of 32 dB, indicating that reliable speech communication is possible between people using 'normal' voice level up to 20 m apart. For the AS 2107 noise level of 45 dB(A), and its equivalent SIL of 37 dB, this distance falls to 11 m. At 55 dB(A) (the onset of "acoustic discomfort") with equivalent SIL of 47 dB, the corresponding maximum distance is 3,5 m. The maximum permissible SILs of AS 2822 thus demonstrate the essential reasonableness of 40, 45 and 55 dB(A) as criteria for limiting background noise to a desirable or maximum level, or to the onset of "acoustic discomfort".

Relation between traffic noise levels and degree of annoyance

Because people tend to become annoyed when they cannot communicate reliably against excessive background noise, SIL criteria are useful for identifying this form of noise annoyance. Other annoying characteristics of traffic noise include

--- its loudness (for motor vehicles rarely run quietly),
--- its harshness (particularly tyre-on-road noise from vehicles at higher speeds),
--- its duration (in some locations it lasts for much of the day),
--- its relentlessness (it continues almost constantly with little or no respite),
--- it is unnecessary (for we assume that vehicles don't have to be noisy or driven noisily),
--- heavily-trafficked roadways don't have to be located within residential areas.

Of these other annoying characteristics of traffic noise, the first four can be directly related to one or other of its measurements.

--- Traffic with noise levels of 60 dB(A) and above is *loud*; while traffic noise levels of 65 dB(A) and over are *unacceptable* [32].

--- The harshness of traffic noise, mostly from wind, and tyre-on-road noise, arises from its significant high frequency noise (500 to 2 000 Hz, the band of maximum interference to speech), as shown in Figures 1 and 2 above.

--- The high morning and evening peak period traffic flows on major arterial roads and expressways now often continue throughout the day, particularly on expressways.

--- That traffic noise is relentless is readily shown by the low values of $L_{10} - L_{90}$, which are typical of flows above 2000 to 3000 veh/h. For, when $L_{10} - L_{90}$ is less than around 5 dB(A), as at most locations in TABLE 1, the "near-minimum" level of any noise is almost as high as its "near-maximum". In other words, the traffic flow is constantly high, without gaps which would afford even short temporary relief from its constant roar (noted as harsh close to the traffic, or as dull at a distance, a distance greater than about 70 m according to Brown and Law) [23].

--- That traffic noise is unnecessary, and that vehicles don't have to be noisy or driven noisily raises questions of the existence and enforcement of statutory vehicle and traffic noise limits. That heavily-trafficked roadways don't have to be located within residential or other noise-sensitive areas raises questions of Noise Zoning, involving the close co-operation of land use and transport planners and the corresponding government and municipal planning authorities.

Traffic noise criteria

Statutory vehicle noise criteria are established because quieter motor vehicles result in lower road traffic noise levels. The most recent known statutory vehicle noise limits are any EPA criteria plus those of 1980/81, which are 3 to 4 dB(A) lower than the ADR 28/28A limits [8], and represent approximately the first stage limits of DR75075 [30]. There is now no reason whatever why after a further 18 years the DR75075 stage 3 vehicle noise limits should not be in force as the current statutory criteria.

Currently, $L_{10(18h)}$ = 63 dB(A) is the only criterion for limiting traffic noise, and only during the 18 hours from 0600 to 2400h. Other additional limits, such as a night-time L_{eq} limit of 55 dB(A), have been suggested but not adopted. $L_{10(18h)}$ as a noise limit is, by itself, unsatisfactory, for although it places a limit on the near-maximum traffic noise levels, it has no corresponding $L_{90(18h)}$ limit for controlling the near-minimum noise levels. Exactly the same would apply to L_{eq} used alone as a traffic noise criterion. Thus, in situations with a measured $L_{10(18h)}$ of 63 dB(A), those in which the corresponding $L_{90(18h)}$ were 60 dB(A), with little relief from the continuous noise, would most probably be considered noticeably more annoying than those in which the $L_{90(18h)}$ were 40 dB(A), with much more relief, giving credence to the report that $L_{10(18h)}$ is an insensitive indicator of noise annoyance [24].

The use of $L_{90(t)}$ as a noise limiting level significantly below $L_{10(t)}$ takes account of the fact that, as traffic flows increase and the noise becomes more continuous and so more annoying, the difference, $L_{10} - L_{90}$, decreases (from around 15 dB(A) at 500 veh/h to around 5 dB(A) at 4000 veh/h), and so provides a useful measure of traffic noise annoyance. $L_{10} - L_{90}$ has been ambiguously interpreted, as shown by the Traffic Noise Index, TNI [14]. For, the TNI, which included an $L_{10} - L_{90}$ term, did so on the grounds that traffic noise of more widely varying level was thought to be ***more*** annoying than noise of more constant level, not less so as assumed above.

Any useful traffic noise criterion must take account of speech interference criteria, Alexandre's "unacceptable" noise and "acoustic discomfort" criteria [32], and Griefahn's sleep disturbance criteria [33]. Within the framework of the usually adopted time periods for day (0700-1800h), evening (1800-2200h) and night (2200-0700h), traffic noise criteria such as $L_{10(15h)max}$ = 63 dB(A) and $L_{90(15h)max}$ = 43 dB(A) for daytime and evening (0700 to 2200h), and $L_{10(9h)max}$ = 53 dB(A) and $L_{90(9h)max}$ = 33 dB(A) for night-time (2200 to 0700h) would generally achieve these aims.

The day/evening $L_{10} = 63$ dB(A) would limit noise to causing "acoustic discomfort" rather than being "unacceptable" ; and the night L_{10} criterion of 53 dB(A) is just below the Griefahn sleep disturbance limit of 53,5 dB(A) for intermittent noise (30 events per night). The corresponding estimated SILs of 55 and 45 dB mean that two people up to, respectively, 1,3 or 4,3 m apart could converse reliably using no stronger than "normal" voice, or at up to double these distances using "raised" voice.

From equation (1) above, the corresponding estimated L_{eq} limits would be 60 and 50 dB(A) ; and from experience that *measured* values of L_{50} for traffic noise tend on average to lie approximately midway between L_{90} and L_{10}, corresponding estimated L_{50} limits would be 53 and 43 dB(A). The SILs of 52 and 42 dB corresponding to these L_{eq} would mean that two people up to, respectively, 2,0 and 6,3 m apart could converse reliably using "normal" voice, and the SILs of 45 and 35 dB corresponding to these L_{50} would mean that for 50% of the time two people up to 4 and 14 m apart could do so. These conditions become possible only because there are L_{90} as well as L_{10} limits for both the day/evening and night periods. These examples also show the usefulness of the AS 2822 speech interference criteria for characterizing an acoustic environment in which there are significant levels of background noise. However, because the night estimated L_{eq} limit of 50 dB(A) is somewhat above the Griefahn sleep disturbance limit for continuous noise of $37 > L_{eq} > 45$ dB(A) [33], the L_{90} and L_{10} night limits may need to be decreased by 5 to 10 dB(A).

Traffic noise reduction

Traffic noise is loud : as described by Lawrence [8], *pervasive, invasive and intractable. The technology is available to enable passenger car noise limits to be reduced by at least 5 dB(A) and truck noise limits could be reduced by at least 10 dB(A).* Suitable noise limiting criteria and statutory regulations are already available. Traffic flows, which are noisy, can be reduced by encouraging people, especially in urban areas, to travel instead by public transport, which is less noisy, and significantly more space- and fuel-efficient than car travel.

Land use and transport planners, when they co-operate, can apply the numerous available methods of noise zoning, known at least since 1971, the year of the AAS Victoria Division Noise Zoning Conference. Bryant's and Challis' papers [2,3] have already been referred to. Bullen [40] quoted Alexandre et al as claiming that suitable town planning and orientation of houses could reduce traffic noise levels by up to 15 dB(A), compared with 8 to 10 dB(A) with barrier screens or 5 dB(A) with quieter vehicles. Lawrence & Burgess [16] stressed that *effective urban planning* was essential to *the most profitable long-term solutions to the traffic noise problem.* Saunders [50] reported that it has been possible to apply noise zoning in locating several of Melbourne's expressways. Fricke's courtyard house design [42] used a 'domestic' form of noise zoning to effect significant noise attenuation. This author, in a paper [56] given to the 1971 AAS Noise Zoning Conference, concluded that, while noise zoning of some public transport operations (such as railway goods shunting) is practicable, with passenger services it is not, because, in order to provide optimum service, vehicle stations and stops need to be centrally located in close contact with the general public, requiring that vehicles operate quietly. When noise zoning to separate noisy activities from noise-sensitive areas cannot be applied, reduction of noise at its source is then essential.

Though noise zoning is more effective than barrier screens, some situations still require them, with at present extensive use of them being made alongside expressways. In Melbourne, for example, barrier screens (usually no more than 2 m in height) were being used from the mid-1980s until 1994, when, following the Environmental Effects Hearings into to the W and S City Bypasses, they began to proliferate, sometimes with heights over 5 m..

These screens are acoustically effective, particularly when those with high coefficients of acoustic absorption described by West [51] are used with the non-sound-reflecting side facing the roadway. But they are unsightly : those that are transparent being somewhat less so (including the partial roof over the Mt Alexander Rd overpass).

In spite of this, the current commercial climate gives us no impetus to continue reducing the noise. Factors other than acoustical – declining supplies of cheap oil [52,35], and that future activity must be ecologically sustainable [55] – will change the future. It will no longer be "business as usual" or "more of the same".

Retrospect and prospect.

As acousticians we are also environmentalists, responsible for doing what is ecologically sustainable, as well as maintaining a satisfactory aural and audible environment so that the speech, music and other communication and warning sounds we need to hear are clearly heard, and if necessary amplified or reinforced ; and that the other sounds – noise – which we don't want or need to hear are minimized, either by eliminating or significantly reducing them at their source, or significantly limiting their transmission. Architectural and musical acoustics are amongst the oldest branches of the science and art of Acoustics, dating back to the Greeks of around the 5th cent BC. By contrast, our problems of road traffic noise are modern, having a post-World War II existence of only around 40 years.

As a particularly urban problem, private car travel and the movement of goods by truck with their inefficient use of space and fuel, and accompanying vehicle and traffic noise became possible only with the advent of cheap petroleum products, and will therefore decline again with the forthcoming eventual disappearance of cheap oil within the next 10 to 15 years [52, 35]. As supplies of cheap oil become more scarce, and the needs of rural and commercial transport take priority over urban private car travel, car travel and its major contribution to traffic noise will be the first to decline, which will bring with it substantial changes not only to national and state economies and all transport operations, but to rural and urban activities far beyond transport. Within the next 50 years the *"Petroleum Age"*, with its particular style of travel convenience, its material affluence for some and unemployment for others, and its appalling environmental devastation and onset of global warming, will be at, or near its end. In later times, this Age may well be seen as an historical aberration, which could have been considerably longer than 150 years had we not been so eager to "eat our future" [52].

The future will bring not only considerable change, but significant challenges, as more efficient agricultural and industrial processes, and vehicles powered by electrical energy rather than petroleum fuels (eg, modern electric rapid transit trains, trams and trolley buses, all of which are significantly more space-, fuel-, and transport-efficient than private car travel) supersede our currently much less efficient processes and vehicles [35]. Following Hede [39], are we as acoustical technocrats giving government, municipal and other statutory authorities the advice we can and should give?

6. CONCLUSIONS

Traffic noise, the combination of many noisy vehicles travelling along heavily-trafficked major roads and expressways, is one of the harshest and most relentless of urban noises. Even at 200 m from a roadway with traffic flows of 2000 veh/h or more at speeds of 80 km/h, noise levels of L_{90} = 57 and L_{10} = 65 dB(A) are likely.

Traffic noise is annoying because, at flows above around 500 veh/h, it is heard not as the occasional foreground noise of individual vehicles, but as constant intrusive background noise [with $L_{10} - L_{90}$ less than 10 dB(A) and speech interference levels (SILs) above 50 dB]. It is annoying, also, because of its harsh high frequency content [500 to 2000 Hz] mainly from tyre-on-road noise, which contributes to these high SILs.

The now considerable body of knowledge accumulated over more than 30 years shows us how to solve these noise problems, with only tyre-on-road noise as one of the more difficult. With many recorded measurements of traffic noise levels, and equations such as the SATS equations for estimating L_{90} and L_{10}, and with the DR75075 stage 3 maximum vehicle noise limiting levels, and traffic noise limiting criteria of L_{90} = 43 and L_{10} = 63 dB(A) for daytime and evening, and L_{90} = 33 and L_{10} = 53 dB(A) for night time, together with our extensive understanding of noise zoning and of how to reduce vehicle and traffic noise at its source, rather than merely using acoustic barrier screens alongside expressways, we need only the will to do so.

However, the future of the road traffic noise problem can no longer be determined only by the acoustical issues discussed in this paper. It will be largely determined by the near-future decline of cheap oil, and the environmental imperative that our future action in all spheres of rural and urban life will need to be ecologically sustainable. No longer can we expect a future of "more of the same" ; momentous changes lie ahead, with much to challenge us as acousticians.

REFERENCES

[1] Wilson, A, *Noise : final report*, London, HMSO, 1964

[2] Bryant, J F M, 'Highway noise', proc 1971 AAS Conf, Vic, pp 6.1-6.21

[3] Challis, L, 'Traffic noise criteria in Australia', proc 1971 AAS Conf, Vic, pp 7.1-7.8

[4] AS 2240, Measurement of the sound emitted by motor vehicles, Standards Aust, 1979

[5] AS 2702, Measurement of road traffic noise, Standards Aust, 1984

[6] Saunders, R E & Taylor, I, 'A data-base of traffic noise in Melbourne streets', proc 1974 AAS/Monash Uni Noise, Shock & Vibration Conf, Melb, pp 79-87 & app^{x}

[7] Dunlop, J et al, 'Some characteristics of traffic noise', Bulletin AAS, 11/1, IV/83, pp 33-34

[8] Lawrence, A, 'Road traffic noise : 1975-1985', proc 1985 AAS Conf, NSW, pp 37-42

[9] Samuels, S E & Alfredson, R J, 'The effect of tread pattern on tyre noise', proc 1974 AAS/Monash Uni Noise, Shock & Vibration Conf, Melb, pp 62-70

[10] Samuels, S E, 'Traffic noise--a study of a tyre/road noise mechanism', proc 1976 ARRB Conf, WA, vol 8, pt 6, session 33, pp 1-7, 47-50

[11] Samuels, S E & Sharp, K G, 'Passenger car noise on a concrete block pavement', proc 1985 AAS Conf, NSW, pp 124-129

[12] Alfredson, R J, 'Prediction of noise levels from Aust freeways', proc 1974 AAS/Monash Uni Noise, Shock & Vibration Conf, Melb, pp 71-78

[13] Hothersall, D C & Jones, R R K, 'Observed & predicted noise levels around road junctions in the UK', proc 1976 ARRB Conf, WA, vol 8, pt 6, session 33, pp 31-35, 47-54

[14] Fouvy, C L, 'Traffic noise & residential noise criteria', proc 1976 ARRB Conf, WA, vol 8, pt 6, session 33, pp 36-47, 54-59

[15] Sydney Area Transportation Study (SATS), *SATS report-vol 2*, Sydney, 1974, p V-9

[16] Lawrence, A & Burgess, M, 'Road traffic noise--the outlook for the future', Bulletin AAS, 4/4, XII/76, pp 21-24

[17] Burgess, M, 'Traffic flow & noise levels at one site', Bulletin AAS, 12/2, VIII/84, pp 51-53

[18] Samuels, S E, 'Comments on Burgess' *Traffic flow & noise levels at one site* [17]', Bulletin AAS, 12/3, XII/84, pp 101-102
[19] Modra, J, 'Traffic noise predictions & levels in Melb', proc 1979 AAS Conf, Vic, 2.1-2.7
[20] Kato, Y et al, 'A statistical estimation method of noise level probability distribution of arbitrary type based on the observed L_{50} data' AcAust, 13/2, VIII/85, pp 69-72
[21] Kato, Y & Yamaguchi, S, 'A prediction method for probability distribution of road traffic noise at an intersection', AcAust, 18/2, IX/90, pp 45-50
[22] North, J & Samuels, S E, 'Establishment of an outdoor learning environment for young deaf children in an acoustic climate dominated by road traffic noise', proc 1993 AAS Conf, NSW, pp 171-177
[23] Brown, A L & Law, H G, 'Effects of traffic noise : SE Fwy, Brisbane', proc 1976 ARRB Conf, WA, vol 8, pt 6, session 33, pp 8-30, 47, 50-52
[24] Bryant, J F M, 'Research on annoyance from road traffic', Bulletin AAS, 8/2, VIII/80, pp 24,26
[25] Hede, A, 'Factors determining traffic noise annoyance', Bulletin AAS, 12/3, XII/84, pp 81-87
[26] Hede, A et al, 'National noise survey--1986', AcAust, 15/2, VIII/87, pp 39-42
[27] Job, R F S & Hatfield, J, 'Community reaction to noise', AcAust, 26/2, VIII/98, pp 35-39
[28] Fouvy, C L, 'Noise control criteria', proc 1992 AAS Conf, Vic, pp 105-163
[29] Lawrence, A, 'Community noise studies overseas', Bulletin AAS, 2/1, 1973, pp 7-10
[30] Mather, C E, 'Requirements & recommendations for motor vehicle noise emission in Aust', Bulletin AAS, 4/1, III/76, pp 19-22
[31] Mather, C E, 'Noise measures', proc 1979 AAS Conf, Vic, pp 1.1-1.11
[32] Alexandre, A, 'Strengthening motor vehicle noise abatement policies', proc 1985 AAS Conf, NSW, pp 1-11
[33] Griefahn, B, 'Noise control during the night', AcAust, 20/2, VIII/92, pp 43-47
[34] Fouvy, C L, 'Notes on traffic noise & vehicle fuel consumption', submission to XII/94 VicRoads EES hearings on W & S Bypasses, Melb (unpublished)
[35] Fouvy, C L, 'Electric vehicles : transport vehicles for the future', proc 1998 CITIA symposium on *Beyond oil : transport & fuel for the future*, Tas, pp 11.1-11.51
[36] Murray, B, 'Comments on environmental noise assessment', AcAust, 24/2, VIII/96, pp 67-69
[37] Crocker, M J, 'Priorities in noise reduction' Bulletin AAS, 4/2, VI/76, pp 13,15
[38] State Pollution Control Commission, 'The SPCC's traffic noise control program', AcAust, 11/2, VIII/83, pp 73-74
[39] Hede, A, 'Towards a normative model of public policy for environmental noise', AcAust, 26/3, XII/98, pp 95-100
[40] Bullen, R, 'Review of Alexandre et al, *Road Traffic Noise*', Bulletin AAS, 4/1, III/76, p 25
[41] Radwan, M M & Oldham, D J, 'Application of computers to the study of urban noise problems', AcAust, 13/3, XII/85, pp 93-96
[42] Fricke, F, 'The use of walls & barriers against motorway noise', Bulletin AAS, 3/3&4, 1975, pp 22-26
[43] Dubout, P, 'Descriptors & criteria of performance of building partitions & envelopes', proc 1979 AAS Conf, Vic, pp 4.1-4.7
[44] Lawrence, A & Burgess, M, 'Experimental building for façade attenuation measurements', Bulletin AAS, 10/3, XII/82, p 117

[45] Mizia, U & Fricke, F, 'Putting windows where they ought to be', AcAust, 11/3, XII/83, pp 105-109
[46] Harris, C M (ed), *Handbook of noise control*, McGraw-Hill, New York, 1957, p 3.4
[47] Randall, R B, 'Noise zoning in industry', proc 1971 AAS Conf, Vic, pp 12.1-12.10
[48] Beranek, L L, *Noise reduction*, McGraw-Hill, New York, 1960, pp 193-194
[49] Brit std, BS CP3 : pt 2 : 1972 : ch III, Code of basic data for the design of buildings, ch III, sound insulation & noise reduction, BSI, 1972, Fig 10
[50] Saunders, 'Traffic noise--its effect on road design', Bulletin AAS, 9/1, IV/81, pp 18-28
[51] West, P, 'Traffic noise barrier development', AcAust, 17/3, XII/89, pp 71,73
[52] Fleay, B J, 'Climaxing oil--how will transport adapt?' proc 1998 CITIA Symp, Tas, pp 2.1-2.60
[53] Hassall, J R & Zaveri, K, *Acoustic noise measurements*, Brüel & Kjær, 1988, p 212
[54] AS 3671, Acoustics–Road traffic noise intrusion–building siting and construction, Standards Aust, 1989
[55] Greene, D, 'Environmental protection--sustainability', Env Engg Soc Nat Newsletter, IX/99, p 1
[56] Fouvy, C L, 'Public transport system noise and noise zoning', proc 1971 AAS Conf, pp 5.1-5.43

[NOTE : *Acoustics Australia* has been abbreviated as *AcAust*]

AUSTRALIAN ACOUSTICAL SOCIETY CONFERENCE

ACOUSTICS TODAY

Melbourne, 24 – 26 November, 1999.

EVALUATING THE AMERICAN FHWA TRAFFIC NOISE MODEL IN MELBOURNE

Neil Huybregts[1] and Stephen Samuels[2]

[1]Marshall Day Acoustics, Collingwood, Victoria
[2]OLSAN Consulting, Cronulla, NSW

ABSTRACT

The present paper outlines an evaluation study of the American FHWA Traffic Noise Model (TNM) conducted in Melbourne under contract to VicRoads. Following well-established scientific procedures, traffic noise measurements and TNM predictions were conducted at a range of sites in and around the Melbourne metropolitan area. Analyses of these data have allowed determination of estimates of the accuracy of TNM under typical conditions of particular interest to VicRoads. The results indicated that TNM is about 1dB(A) more accurate than the UK Calculation of Road Traffic Noise (CRTN) method and that TNM can be used to predicted L_{10}(18hr) at least as accurately as CRTN.

1. INTRODUCTION

Prediction of road traffic noise is a process that forms a routine component of procedures, such as the assessment of the environmental impacts of a new road proposal. These predictions have traditionally been conducted throughout Australia utilising the well-known UK Calculation of Road Traffic Noise Method (UK DoT 1988), modified for Australian conditions. More recently, however, several alternative methods have been adopted as the previous requirement to use only the UK Method has been progressively relaxed. Particular applications of these models have also been in the design of roadside noise abatement barriers. In this context, there is considerable interest in the American FHWA Traffic Noise Model (TNM) which, after many years in development, was finally released during 1998 (Menge et al 1998).

The present paper outlines the conduct and results of a study undertaken recently in Melbourne aimed at reviewing a wide range of traffic noise prediction methods, selecting one method for detailed evaluation and investigating the performance of the selected method at sites along major highways and freeways that are under the jurisdiction of VicRoads, the Victorian road and traffic authority.

The study dealt with two traffic noise parameters in particular, namely the L_{eq}(16 hr) for daytime noise assessment and the L_{eq}(8hr) for night-time. These parameters were nominated by VicRoads as being likely candidates to be adopted in the future. The method evaluated in detail was the FHWA TNM. In order to provide a meaningful comparison with CRTN, the accuracy of CRTN was evaluated at the same sites using the same methodology.

2. COMPARISON OF CURRENT MODELS

The initial phase of the study involved a comparison of currently available models sourced from within Australia and internationally. This desktop exercise involved considerations of both the technical, scientific merits of each prediction method and the computer software packages that implement the methods. A total of 18 methods were investigated while some 30 computer packages were included.

The software review and prediction method evaluation began with a set of evaluation criteria for both the software packages and for the prediction methods. Within each of the criteria, a series of detailed questions was developed and the software packages and prediction methods were evaluated against these questions. Each question was weighted individually, and each criterion also had its own weighting. One criterion for the prediction methods was the quality of the software packages that implement the methods. The score under this criterion was based on the outcome of the software package review.

Space limitations do not allow a detailed discussion of this evaluation to be included herein, but it is comprehensively documented in Huybregts and Samuels (1998). In summary, three noise prediction methods were finally shortlisted together with ten software packages. The final outcomes of the evaluation, in terms of rankings of the methods, are reproduced in Table I. The three prediction methods were as follows:

- Scandinavia: Road Traffic Noise, Nordic Prediction Method (Nielsen 1996)
- UK: Calculation of Road Traffic Noise, modified to predict L_{eq} (UK DoT 1988)
- USA: FHWA Traffic Noise Model (Menge et al 1998)

Table I
Ranking of traffic noise prediction methods

Criterion	Nordic	CRTN	FHWA TNM
How is the sound path geometry handled?	32	32	40
How is the noise source modelled?	13	11	23
Noise source: what factors are considered in calculating noise emission?	12	13	21
Noise source: spectrum or dB(A)?	8	8	32
How accurate is the method?	176	176	220
What is the status of the calculation method?	20	20	20
Propagation: which factors are considered?	81	60	135
Propagation: spectrum or dB(A)?	8	8	32
Which descriptors will it calculate?	100	57	86
Modification of the method	40	35	60
Quality of software packages that implement the method	94	121	95
TOTAL	584	541	763
RANK	2	2	1

It is apparent that TNM rated higher than the other two against almost all criteria. While this suggests that TNM is the superior method, both the Nordic and CRTN Methods are clearly acceptable prediction methods.

Note that CRTN ranks highly for the quality of the software packages. This is because of the large number of packages that implement the CRTN method. TNM is currently only implemented on one software package produced by the FHWA, although a TNM module is currently under development for SoundPLAN. Amongst software packages, TNM and SoundPLAN were found to be equally superior, while a couple of other packages such as T-Noise and ENM rated as clearly acceptable. Overall, it was concluded that the study should subsequently focus on a detailed evaluation of TNM.

3. EVALUATION OF TNM

3.1. Overview

Evaluation of TNM under Victorian conditions was approached on the basis of an established scientific procedure (Saunders et al 1983) which had previously been successfully adopted in Australia in evaluating the UK CRTN method. This procedure involved the following components:

- Selection of suitable measurement sites
- Simultaneous measurement of noise levels, traffic conditions and weather conditions
- Measurement of physical conditions, including the road/receiver cross-section, road gradient, pavement type, ground surface details and the location of reflecting surfaces
- Filtering of the measurements to exclude days where the weather conditions were not suitable, or where the measurement data were not reliable
- Input of the traffic and physical conditions into the TNM software package and subsequent prediction of the traffic noise indices $L_{eq}(16hr)$ and $L_{eq}(8hr)$
- Comparisons and analyses of the measured and predicted noise levels to effect the TNM evaluation.

The difference between each predicted noise level and its corresponding measured noise level is referred to as the prediction difference (PD), which is given by the following simple relationship.

PD = Predicted noise level - Measured noise level

For the TNM evaluation, prediction differences were calculated for all $L_{eq}(16hr)$ and $L_{eq}(8hr)$ data. For the evaluation of CRTN, the same methodology was implemented, using CRTN and $L_{10}(18hr)$.

3.2. Data collection and verification

Noise levels were measured at 26 sites. Two sets of measurements were made at 5 sites, giving a total of 31 sets of measurements. Data collected at several of the sites were rejected due to either unforeseen site conditions or equipment failure. In total, 87 valid days of measurements and predictions were undertaken at 19 sites. The sites were all in or near the Melbourne metropolitan region, with most being adjacent to freeways. The predominant pavement type was Open Graded Asphaltic Concrete (OGAC), with Dense Graded Asphaltic Concrete (DGAC), Chip Seal(CS) and Portland Cement Concrete (PCC) at other sites. Mean traffic speeds were generally in the range 90-100km/h, with lower speeds at 3 sites. Road-receiver distances were around 20-120m, with all measurements taken at the façade of a building on a residential property. The sites cover a range of shielding by barriers, including some sites with no barriers. Data validity was regularly monitored through instrument calibration, checks for internal data consistency and by comparison with manual measurements. Days with excessive wind speeds or rainfall rates were rejected.

3.3. Preliminary data analysis

The preliminary data analysis initially involved plotting the predicted noise levels against the measured noise levels to determine whether any general trends were apparent. From there, the PD values were determined and a goodness-of-fit test was applied to these to determine the form of their distribution. The prediction differences were plotted against the measured noise levels to examine whether there may be some apparent correlation between the two.

The outcome of the Chi-squared goodness-of-fit test indicated that the data could be analysed using methods that assume the data are normally distributed. Prediction differences were then plotted against the measured noise levels, as shown in Figure 1.

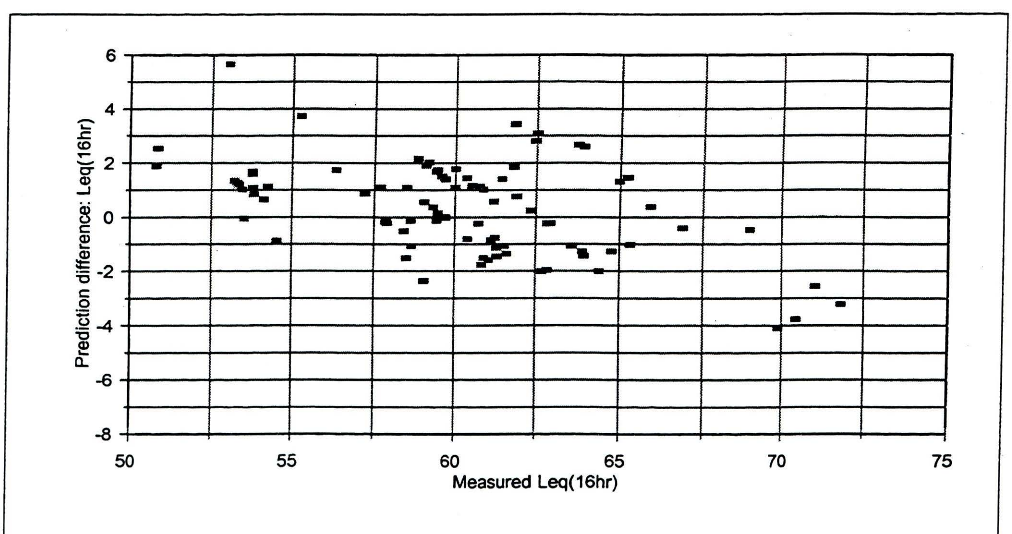

Figure 1. Prediction difference (using TNM) plotted against measured $L_{eq}(16hr)$

This process showed that there was little or no relationship between these two parameters, an observation that was subsequently supported by regression analyses (Samuels and Huybregts 1999).

The results of the preliminary analysis suggested that the prediction differences can be treated as a single population and that it is valid to quantify the mean and the associated spread of prediction differences. These conclusions were tested further in the detailed analysis.

3.4. Evaluation of CRTN

The preliminary analysis outlined above was repeated using measured and predicted values of L_{10}(18hr). Results similar to those obtained using TNM were obtained using CRTN, with the exception of the relationship between the prediction differences and the measured noise level. As shown in Figure 2, when CRTN is used to predict L_{10}(18hr), there appears to be some decrease in PD with increasing noise level. Regression analysis has indicated that this relationship is a weak one and the relationship was not investigated further.

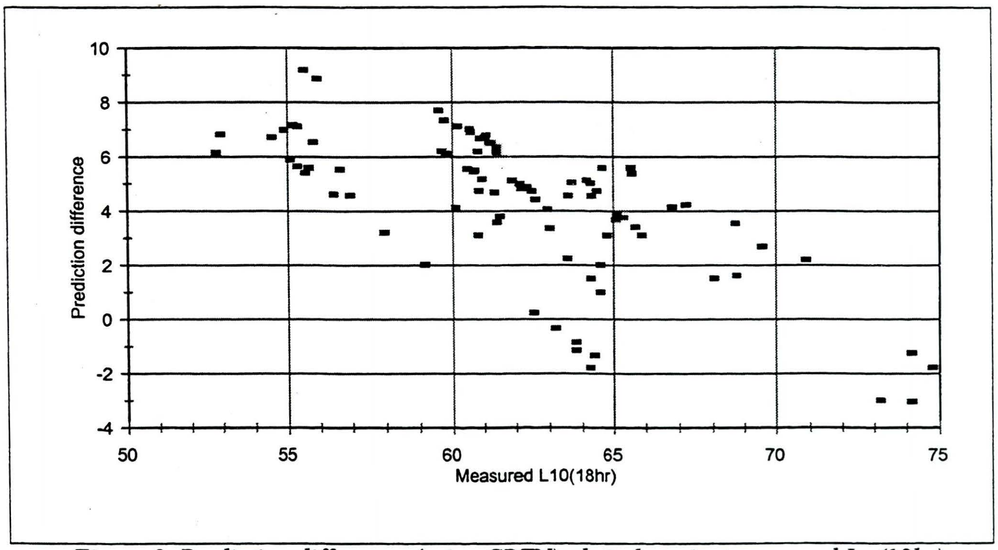

Figure 2. Prediction difference (using CRTN) plotted against measured L_{10}(18hr)

3.5. Detailed data analysis

The data were then reviewed to determine whether there were any apparent correlations with site conditions. Seven site parameters were selected for this review: traffic volume, traffic composition, mean traffic speed, road surface type, road gradient, distance to receiver and shielding by barriers. These were plotted against each other to permit an initial visual assessment of the presence of correlation between the parameters. Overall, there was very little evidence of the existence of any correlations between site parameters which suggested that interactions between site and traffic parameters would not confound any relationship between the prediction differences and site parameters.

When the prediction differences were plotted against the site parameters listed above, there was very little evidence of any correlations. This applied to both TNM and CRTN. This implied that the two sets of prediction differences could be treated as single populations and that it would not be necessary to break up either set into sub-populations. Consequently, the performance of both TNM and CRTN could conveniently be quantified in terms of the distribution of the prediction differences.

4. RESULTS.

The distribution of the prediction differences was quantified in terms of its mean and standard deviation. These parameters are presented in Table II.

Table II.
Mean and standard deviation of the prediction differences

	TNM Leq(16hr)	CRTN L10(18hr)	TNM L10(18hr)	TNM Leq(8hr)	
Mean	0.6	4.4	-1.4	-1.4	dB(A)
Standard deviation	1.9	2.7	2.2	2.5	dB(A

Note that the accuracy of TNM when used to predict L_{10}(18hr) has been evaluated. This was done by assuming that L_{10}(18hr) could be estimated by adding a fixed offset to the corresponding L_{eq}(16hr). This approach is common in the literature. In practice, this is not how TNM would be used to predict L_{10}(18hr), but it does provide an indication of the likely achievable accuracy.

The mean prediction difference can be compensated for by a fixed offset and is not a measure of the accuracy of a prediction method. The standard deviation is a more useful measure of accuracy. The results shown in Table II may be interpreted as indicating that TNM performs well in predicting noise levels of the type monitored in the present study. The practical difference in using TNM rather than CRTN was investigated using a risk analysis approach.

5. RISK ANALYSIS

The ultimate aim of this project was to estimate correction factors that may be applied to calibrate TNM for those (Melbourne) conditions covered by the present study. These correction factors are based on the means and standard deviations of the prediction differences and on the degree of risk that is deemed to be acceptable. In this discussion, "risk" refers to the probability that the measured noise level will be greater than the predicted noise level.

The current level of risk associated with noise barrier design in Victoria was estimated using the mean and standard deviation for CRTN shown in Table II. Current practice is to use CRTN uncorrected, with rounding to the nearest decibel. Because of the rounding, the risk associated with this practice is equivalent to the risk that the measured noise level will exceed the predicted noise level by more than -0.5dB(A). We estimated that current practice allows a 7% chance that the measured noise level will exceed the predicted noise level. The determination of calibration factors discussed below is based on the requirement that this level of risk be maintained.

It is important to distinguish between safety factors and calibration factors. Safety factors are added to estimated values in order to compensate for uncertainty in the estimates and are a measure of the accuracy of a calculation method. Calibration factors are adjustments used to compensate for a number of considerations, including safety factors.

The mean prediction difference does not affect the safety factor. The mean prediction difference simply locates the point at which the risk is 50%. If a risk of 50% was acceptable, the safety factor would be zero. As the safety factor increases, the risk reduces. The safety factor, then, is the "distance" between the mean prediction difference and the point at which the risk is acceptable. Table III shows the calculation of safety factors for the various combinations of prediction methods and traffic noise indices.

Table III
Calculation of safety factors

Prediction method **Traffic noise index**	**TNM** **Leq(16hr)**	**CRTN** **L10(18hr)**	**TNM** **L10(18hr)**	**TNM** **Leq(8hr)**	
Acceptable risk	7%	7%	7%	7%	
Point where the probability of exceedance = risk	2.1	-0.5	4.6	4.9	dB(A)
Mean prediction difference	-0.6	-4.4	1.4	1.4	dB(A)
Safety factor	2.8	3.9	3.2	3.6	dB(A)

Small discrepancies are due to rounding.

Note that for the same level of risk, the use of L_{10}(18hr) calculated using CRTN requires a safety factor 1.1dB(A) greater than when L_{eq}(16hr) is calculated using FHWA TNM. This is a consequence of the greater standard deviation.

To correct the predicted values so that the risk of non-compliance is acceptable, a calibration factor must be applied to the predicted noise levels. This calibration consists of an adjustment for the mean prediction difference, the addition of the safety factor and the addition of 0.5dB(A) to allow for rounding off of the predicted noise levels.

Table IV shows details of the calculation of calibration factors based on the safety factors determined above.

Table IV
Calculation of calibration factors

Prediction method **Traffic noise index**	**TNM** **Leq(16hr)**	**CRTN** **L10(18hr)**	**TNM** **L10(18hr)**	**TNM** **Leq(8hr)**	
Mean prediction difference	-0.6	-4.4	1.4	1.4	dB(A)
Safety factor	2.8	3.9	3.2	3.6	dB(A
Adjustment for rounding	0.5	0.5	0.5	0.5	dB(A)
Total calibration factor	2.7	0.0	5.1	5.4	dB(A)

Small discrepancies are due to rounding.

Note that the calibration factor for CRTN is 0.0dB(A). This is because the calculations outlined above are based on maintaining a level of risk equal to the risk associated with current practice. It does not imply that CRTN is the most accurate method - this is determined by the safety factors shown in Table III.

The outcome of the risk analysis was a set of calibration factors to be applied to the models and indices discussed in this paper for use in Victoria.

6. CONCLUSIONS AND RECOMMENDATIONS

The FHWA TNM was evaluated under Victorian conditions by comparing predicted and measured noise levels at 19 sites for a total of 87 days. Calibration factors for TNM were derived from the above outcomes by utilising a risk analysis approach. It is estimated that an acceptable level of risk will ensue if the calibration factors shown in Table V are applied to TNM or CRTN for use in Victoria under conditions such as those of the present study.

Table V
Recommended calibration factors

To calculate this traffic noise index	Use this noise prediction method	To calculate this traffic noise index	Then add this calibration factor
L_{eq}(16hr)	FHWA TNM	L_{eq}(16hr)	2.7dB(A)
L_{10}(18hr)	CRTN	L_{10}(18hr)	0.0dB(A)
L_{10}(18hr)	FHWA TNM	L_{eq}(16hr)	5.1dB(A)
L_{eq}(8hr)	FHWA TNM	L_{eq}(8hr)	5.4dB(A)

Note that the calibration factor of 0.0dB(A) for CRTN does not imply that CRTN is the most accurate method. As shown by the safety factors in Table III, FHWA TNM is the most accurate method when used to calculate L_{eq}(16hr).

7. REFERENCES

HUYBREGTS,C.P. and SAMUELS,S.E.(1998). Traffic noise model evaluation – Stage 2 evaluation report. Report 97048B to VicRoads. Marshall Day Acoustics and University of NSW.

MENGE,C.W., ROSSANO,C.F., ANDERSON,G.S. and BAJDEK,C,J.(1998). FHWA traffic noise model – Version 1.0 technical manual. Report FHWA-PD-96-010. FHWA, Washington, DC, USA.

NEILSEN,H.L., et al (1996). Road traffic noise – Nordic prediction method. TemaNord 1996:525. Nordic Council of Ministers, Copenhagen, Denmark.

SAMUELS,S.E. and HUYBREGTS,C.P. (1999). Traffic noise model evaluation – Stage 4 final report. Report 97048E to VicRoads. Marshall Day Acoustics and University of NSW.

SAUNDERS,R.E., SAMUELS,S.E., LEACH,R. and HALL,A. (1983). An evaluation of the UK DoT traffic noise prediction method. Australian Road Research Board Research Report 122. ARRB, Vermont South, Victoria.

UK DEPARTMENT of TRANSPORT (1988). The calculation of road traffic noise. HMSO, London, UK.

AUSTRALIAN ACOUSTICAL SOCIETY CONFERENCE

ACOUSTICS TODAY
Melbourne, 24 – 26 November, 1999.

IN-SITU DETERMINATION OF INSERTION LOSS OF ROADSIDE NOISE BARRIERS IN URBAN ENVIRONMENT

Edwin C.K. Chui[1], Maurice Yeung[1] and K.M.Li[2]

[1]Noise Management and Policy Group
Environmental Protection Department
The Government of the Hong Kong Special Administrative Region

[2]Department of Mechanical Engineering
The Hong Kong Polytechnic University
Kowloon, Hong Kong

ABSTRACT

The use of roadside noise barriers is a widely adopted solution to mitigate traffic noise impacts. The traffic noise levels at receivers are in general dependent on a host of factors, such as, the source and receiver geometries, the physical properties of the noise barriers and other traffic related parameters. Determination of the barrier insertion loss through in-situ measurements is one of the means to establish the performance of noise barriers. There are published procedures such as ISO 10847:1997(E) and ANSI S12.8-1987 to measure the insertion loss of noise barriers.

Hong Kong is a hyper densely populated development with more than 6.6 million people living within 1000-km^2 land of which 85% are hilly areas. It is not uncommon that residential buildings are located next to major highways. In many instances, flyovers are built on top of several at-grade roads while some new trunk road networks look like spaghetti from birds' eye view. Given this unique situation, the procedures established by ISO and ANSI therefore may not be fully applicable in some local situations. This paper presents a case study for the determination of insertion loss of noise barriers installed in a Hong Kong urban environment. The way forward of the study, while based on ISO 10847:1997(E) and ANSI S12.8-1987, have been developed through noise measurements at selected barrier locations with particular reference to specific local conditions.

1. INTRODUCTION

The use of noise barriers to screen off traffic noise is a widely adopted practice.

When a noise barrier is proposed, its performance is usually based on a theoretical or semi-empirical model for some noise-sensitive locations. Determination of the barrier insertion loss through in-situ measurements is one of the means to establish the performance of noise barriers. This will, no-doubt, help in the design and installation of noise barriers in future. For the in-situ determination of insertion loss of barriers, there are established procedures contained in e.g. ISO 10847:1997(E) [1] and ANSI S12.8-1987 [2].

Unlike the environmental settings in many overseas countries, Hong Kong is a hyper densely populated development with more than 6.6 million people living within 1000-km^2 land of which 85% are hilly areas. It is not uncommon that residential buildings are located next to major highways especially for those developments in the 70s and 80s. In many instances, noise barriers are erected at concentrated trunk road networks and flyovers built on top of several at-grade roads (Figures 1 & 2).

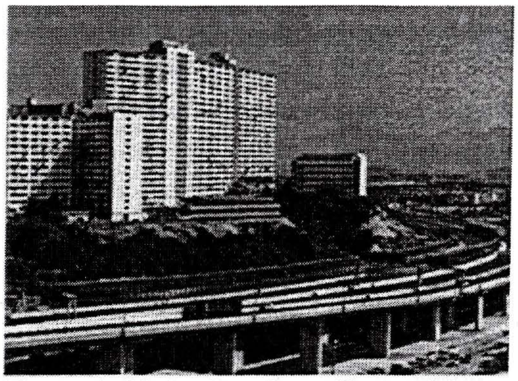
Figure 1 Noise Barrier at Route 3 in Kwai Chung


Figure 2 Noise barrier at West Kowloon Corridor

The traffic noise levels at receivers are in general dependent on a host of factors, such as, the source and receiver geometries, the physical properties of the noise barriers and other traffic related parameters. Given the unique situation of Hong Kong, direct application of the ISO and ANSI methods may not be feasible in some local situations. This paper presents a case study to evaluate the insertion loss of barriers installed in an urban environment taking into account the specific local situations.

2. STUDY APPROACH

To develop the way forward for the in-situ determination of insertion loss of roadside noise barriers suitable for local situations, two installed barriers were chosen for noise measurement [3]. The noise barriers are of plain vertical type and are located at:

(a) Police School Road, Wong Chuk Han, Hong Kong Island (Figures 3 & 4)
(b) Shatin Road near Pok Hong Estate, Sha Tin, New Territories (Figures 5 & 6)

The noise barrier at Police School Road protects Kei Hang Primary School which is a 6-storey building. For the noise barrier at Shatin Road, the protected receiver is the 5-storey Christ College.

Police School Road and Shatin Road are the only main roads in each of the selected locations. The traffic noise at the two barrier locations was used as the natural noise sources. The Due to the complicated urban environment settings, it is not possible to use the 'Indirect Predicted Method' described in ANSI S12.8-1987 as the numerical prediction of noise levels are difficult to set up in a short time-scale. The 'Indirect Measured Method' was adopted as the general study approach.

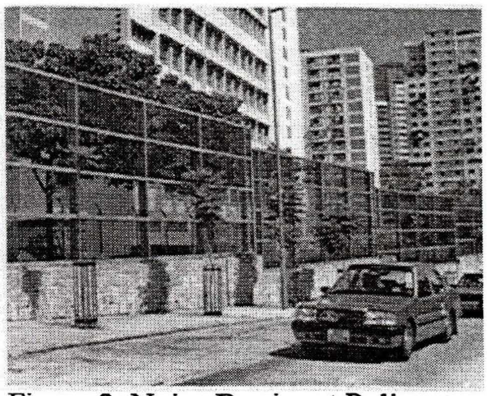

Figure 3 Noise Barrier at Police School Road

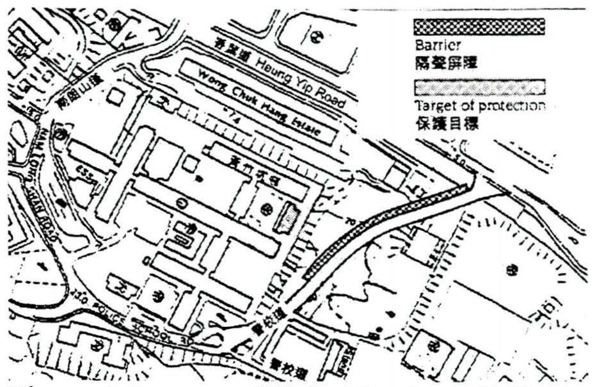

Figure 4 Layout of Noise Barrier at Police School Road

Figure 5 Noise Barrier at Shatin Road

Figure 6 Layout of Noise Barrier at Shatin Road

Noise measurements for the barriers at Police School Road and Shatin Road were essentially undertaken at Kei Hang Primary School and Christ College respectively. An equivalent site located at an estate building in the vicinity of each of the above schools was selected to enable estimation of insertion loss. In all measurements, traffic noise was the dominant noise source. L_{eq} is used to represent noise level data as a generally acceptable descriptor for the determination of insertion loss of noise barriers.

3. DETERMINATION OF INSERTION LOSS

For both locations, the main noise source is traffic noise. Since the noise levels in the measuring sites were largely dominated by the road traffic noise, it was reasonable to assume that background noise levels were negligible in all calculations. In other words, a 'lower bound' to the insertion loss was determined in accordance with ANSI S12.8-1987 Paragraph 11.2.2, instead of the actual insertion loss.

The transmission loss, TL, for noise propagating from the source side to the receiver side are defined as the difference in the adjusted L_{eq} at the source and receiver sides, i.e.

$$TL = L_s - L_r \qquad (1)$$

where L_s and L_r are the average L_{eq} at the source and receiver sides, respectively.

As a result of a geometrical spreading of the sound energy, the noise level is expected to reduce as the receiver is moved away from the source region. However, in a typical urban environment, a straightforward assumption of a 3 dB and 6 dB reduction in noise level per doubling of distance for a line source and a point source respectively may not be appropriate. The reduction in noise depends on a host of other contributing factors, the spectral characteristic of the local traffic noise and the local site environment. Nevertheless where a receiver is located at much further away from the road than that of the reference position, it is reasonable to assume that the attenuation, E(r), varies linearly with $\log_{10}(r)$ in the absence of barrier, i.e.

$$E(r) = A \log_{10}(r) \qquad (2)$$

where r is the distance measured in m and A is the proportionality constant.

To determine the proportionality constant 'A', the measurements at the equivalent site not significantly affected by the presence of barrier were obtained.

The indirect measurement method was used to establish the insertion loss, IL, i.e.

$$IL = TL - E(r) \qquad (3)$$

4. DISCUSSIONS AND RESULTS

To permit valid establishment of 'before' noise, the topographic and source characteristics of the equivalent site shall be similar to those of the barrier site. The equivalent sites were so chosen such that the noise sources are minimally affected by the installed barriers. These sites were found to have comparable sources, terrain and ground conditions to provide an equivalent conditions as the 'before' case. Hence, the site equivalence was established.

Since the noise levels measured at the two equivalent sites were not significantly affected by the presence of barriers, the measured data could be used to determine the proportionality constants 'A' as follows:

$$A = (L_s - L_r) / \log_{10}(r)$$

Table 1 indicates the derivation of 'A' based on noise levels obtained at the equivalent sites.

Table 1 Proportionality Constants 'A'

Location	$L_s - L_r$ (dB(A))	r (m)	A	
			at each measuring point	overall average
Police School Road	6.0	37.2	3.82	3.8
	5.2	25.8	3.68	
Shatin Road	9.5	118.3	4.6	4.6

Note:
There were 2 measuring points at the Police School Road equivalent site and 1 measuring point at the Shatin Road equivalent site.

As shown in Table 1, 'A' was predicted to be 3.8 for the noise barrier at Police School Road. Whilst for the noise barrier at Shatin Road, 'A' was determined as 4.6.

Making use of equations (1), (2) and (3) and the derived 'A', the insertion loss of the barriers at various locations of Kei Hang Primary School and Christ College were determined. The results of the barrier insertion loss are summarized in Tables 2 and 3 below.

Table 2 Insertion Loss of Noise Barrier at Police School Road

Kei Hang Primary School	L_{eq} Difference (After) TL, dB(A)	Predicted L_{eq} Difference (Before) E(r), dB(A)	Insertion loss IL = TL – E(r), dB(A)
Ground floor	13.4	5.1	8.3
Room 201, 2/F	13.2	5.2	8.0
Room 203, 2/F	12.7	5.2	7.5
Room 401, 4/F	9.9	5.3	4.6
Room 403, 4/F	12.4	5.4	7.0
Hall, 6/F	7.0	5.5	1.5

Table 3 Insertion Loss of Noise Barrier at Shatin Road

Christ College	L_{eq} Difference (After) TL, dB(A)	Predicted L_{eq} Difference (Before) E(r), dB(A)	Insertion loss IL = TL – E(r), dB(A)
Between 2/F & 3/F	18.4	7.0	11.4
Between 3/F & 4/F	16.9	7.0	9.9
Room 406	16.8	7.2	9.6
Room 408	15.5	7.2	8.3
Room 409	15.5	7.2	8.3
Between 4/F & 5/F	15.9	7.0	8.9
Room 509	13.5	7.3	6.2
Meeting Room, 5/F	13.8	7.2	6.6
Rooftop	10.4	7.0	3.4

The insertion loss of the roadside noise barriers was found to be dependent on the height of the receiver. At Kei Hang Primary School, the lower bounds to insertion losses of the barrier were found to be ranging from 1.5 dB (A) at the 6^{th} floor (where there is a direct line-of-sight to the road) to 8.3 dB (A) at the ground floor. The lower bounds to insertion losses measured at Christ College vary from 3.4 dB (A) at the rooftop (where there is a direct line-of-sight to the road) to 11.4 dB (A) at the staircase between 2^{nd} and 3^{rd} floor.

5. COMPARISON WITH THE PREDICTION

A noise model was set up to estimate the insertion loss of the noise barrier at Shatin Road for comparison purpose. The noise model is based on a well-established prediction scheme, Calculation of Road Traffic Noise (CRTN) developed and subsequently modified in the 80s in the United Kigndom. Details of the calculation method is described elsewhere [4]. Results of the prediction are presented in Table 4. According to the table, the predicted insertion losses fall in the range of 7.5 to 13.6

dB(A) and are dependent on the height of receiver. As the measured and predicted insertion losses differ by 0.7 to 2.9 dB(A), it would suggest that the two sets of data in general agree with each other. It should however be noted that traffic count was not conducted during the field measurement. The theoretical prediction was based on the published traffic data and this could be one of the possible reasons for the variations in the insertion losses obtained by prediction and in-situ determination.

Table 4 Measured and Predicted Insertion Loss of Noise Barrier at Shatin Road

Christ College	Insertion loss by in-situ determination dB(A)	Insertion loss by prediction dB(A)
Between 2/F & 3/F	11.4	13.6
Between 3/F & 4/F	9.9	12.8
Room 408	8.3	9.3
Room 409	8.3	7.6
Between 4/F & 5/F	8.9	11.3
Room 509	6.2	7.5

6. CONCLUSIONS

The determination of the insertion loss was generally based on the indirect measurement method. The case study has developed a way forward for determination of the 'before' noise situation using equivalent sites. The lower bounds to insertion losses of the two selected roadside barriers were measured. In sum, the insertion losses for the barrier at Policy School Road varies between 1.5 to 8.3 dB(A). For the barrier at Shatin Road, the range of insertion losses falls between 3.4 and 11.4 dB(A). As traffic noise at each selected location is dominated by a main road, further study is needed to confirm the application of the measurement procedures developed in this study for multi-roads situations.

REFERENCES

[1] International Standard ISO 10847:1997(E), Acoustics - *In-situ* determination of insertion loss of outdoor noise barriers of all types, International Organization for Standardization, 1997

[2] American National Standard, ANSI S12.8-1987 (ASA 73-1987), Methods for Determination of Insertion Loss of Outdoor Noise Barriers, American Institute of Physics for Acoustical Society of America, 1987

[3] K.M. Li, S.K. Tang and S.Y. Yam, *Consultancy Report on In-situ Determination of the Insertion Loss of Roadside Barriers* (Department of Mechanical Engineering, The Hong Kong Polytechnic University, 1999)

[4] Department of Transport, *Calculation of Road Traffic Noise* (HMSO, United Kingdom, 1988)

AUSTRALIAN ACOUSTICAL SOCIETY CONFERENCE

ACOUSTICS TODAY

Melbourne, 24 – 26 November, 1999.

TURBULENCE EFFECTS

I.D. McLeod[1] and C. G. Don

Department of Physics, Monash University
Clayton, Vic. 3056

[1]Current address: Hearing Conservation Services of Australia
139 Ormond Road, Elwood, 3184.

ABSTRACT

The effect of turbulence on impulsive sound over short distances, such as 16m, has been extensively studied by the authors over the past eight years. A large database of acoustic and meteorological data, over a variety of atmospheric conditions, has been built up during this time. Over the last two years a standard model involving turbulent eddies, or turbules, which are assumed to have a Gaussian variation in refractive index across their diameter, has been used to successfully explain most of the observed changes in pulse shape. However, delayed energy observed in a significant number of the measurements suggest this model has a limited validity. Recent efforts to determine the necessary turbule parameters directly from the raw wind speed data obtained during the flight time of the pulse have met with reasonable success. A comparison with sonic boom pulses measured over long distances and the average behaviour of our measured pulses has highlighted the differences between the two types of measurements and the implications which the turbule model has for environmental noise measurements.

1. INTRODUCTION

Fluctuations in the atmospheric conditions modify the passage of sound [1]. There are three main, but quite different, statistical models for turbulence, which generally show good correlation between statistical meteorological and the variations in continuous wave acoustic signals over a period of time [2, 3]. This suggests that these acoustic signals are not dependent on the detail atmospheric conditions but on gross or averaged properties. Therefore studies using impulsive sound were expected to correlate with the meteorological changes occurring during propagation or some average determined around that time.

Several thousand-pulse waveforms and the corresponding wind speed data have been obtained over a number of years. While the propagation time of a pulse [4] can be correlated to the wind speed data until recently, changes to the pulse waveform have proved more difficult to relate with the wind speed conditions. In summary, the earlier studies have shown that after propagating through a turbulent atmosphere:

- pulse waveforms show a huge diversity of shapes.
- the greatest effect occurs at the peak, however, a significant number of pulses contain delayed energy in the tail.
- no correlation was found between parameters derived from the detailed meteorological information and any acoustic property such as pulse height or width.
- enhanced pulses are narrower than the turbulent free pulse while reduced pulses are wider.
- changes to the peak height are independent of the wind direction.
- the averaged outdoor pulse waveform is the same as the turbulent free pulse shape obtained indoors. Thus the indoor waveshape can be used as a reference when investigating changes caused by turbulence.

It became evident that to explain the multitude of changes to the pulse waveforms, attention must be focused on the detailed behaviour of turbulence, usually described in terms of turbules. Although the effects of turbules have been examined in other papers [5] it is their statistical properties, such as the number per unit volume and distribution of size that were important. What is reported here is the result of considering the scattered components from a single turbule. In the experiments the propagation distance was kept relatively short, at 16m, to ensure that only one or at most two turbules were involved in the scattering process. Thus in this work the turbule position, size and strength is more crucial than their statistical properties.

2. THE MODEL

We consider a single turbule, which can be positioned at various distances, y, from the direct path between source and receiver. Changing y alters the delay of the scattered component, which then must be added to the directly propagated pulse, that is:

$$P_{resultant} = P_{direct} + P_{scat} \tag{1}$$

where P represents the pulse waveform, and P_{scat} has been appropriately delayed.

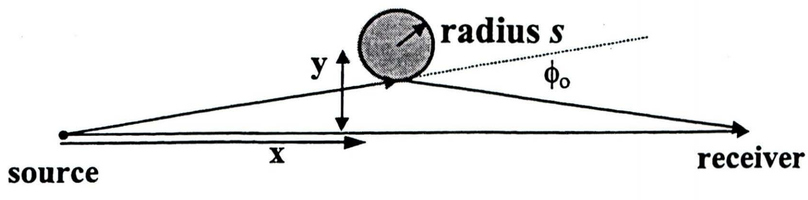

Fig.1: Scattering from a single turbule displaced a distance y from the direct path. The case shown represents Rayleigh scattering (from the hard surface of the turbule).

In the Rayleigh scattering model, the turbule has a "hard" surface, however, this model did not result in behaviour which agreed with the our experimental pulse waveforms as it produces a relatively narrow scattered component which does not change shape or intensity as the delay time is changed. Furthermore, it cannot produce an inverted component, as are frequently observed in the tails of a measured waveform.

An alternative is to assume the turbule has a "soft" outer region, allowing sound to penetrate prior to scattering. We characterise each turbule by a Gaussian refractive index profile,

$$\mu(r) = q \exp[-(\boldsymbol{r} - \boldsymbol{r}_s)^2/s^2], \tag{2}$$

where $\boldsymbol{r}_s$ is the position vector from source to centre of the turbule, $\boldsymbol{r}$ the position vector to the scattering point and s denotes the effective size of the turbule. When $q > 0$, the wave speed decreases as the centre is approached while $q < 0$ corresponds to an increasing wave speed.

Assuming the above Gaussian profile for $\mu(r)$, the scattered pressure component P_{scat} is

$$P_{scat}(r) = -A\frac{\sqrt{\pi}}{2}qk^2\frac{e^{ik(r_s+r_t)}}{r_s r_t}s_x s_y s_z\, e^{-\left(K_x^2 s_x^2/4 + K_y^2 s_y^2/4 + K_z^2 s_z^2/4\right)}, \tag{3}$$

where r_t is the distances between the turbule and the receiver. K_x, K_y, K_z, s_x, s_y and s_z involve s and the scattering angle ϕ_o. The parameter A in Eqn. (3) corresponds to the amplitude of the un-scattered waveform P_{direct}, and k is it's wavenumber. The details for these parameters are not discussed here but can be found in Ref. 6. The radius s can be related to the correlation length (L) by $s = L/\sqrt{2}$, while the magnitude of q depends on the standard deviation ($\langle\mu^2\rangle$) and the density of the turbule pattern (No/Vol) by [5, 6]

$$|q| = \sqrt{\left(\frac{8}{\pi\sqrt{\pi}}\frac{\langle\mu^2\rangle}{N_o/_{Vol}\, L^3}\right)} \tag{4}$$

In particular, this parameter introduces the statistical nature of the turbules. Note that only the magnitude of q can be determined from the wind speed parameters, its sign will have to be inferred from the observed changes to the pulse shape.

Determination of Correlation Length, *L*

The correlation length can be deduced from the auto correlation function of the wind speed time trace using a procedure suggested by Daigle [7]:

- calculate the auto-correlation function from the wind speed time trace.
- approximate the shape of the auto-correlation function with a Gaussian, exp $-(t/T_o)^2$, where T_o is estimated by doubling the time when this function reaches exp $-1/4$.
- assume the turbule pattern moves along with its associated atmosphere at an average wind speed V_{ave} determined from the complete time trace, then $L = V_{ave}\, T_o$.

During our investigations a 20s time trace, centered about the creation of the pulse, was obtained at both the source and the receiver so two estimates for the correlation length could be made. Figure 2 contains an example of a wind speed time trace and the corresponding auto-correlation function, which is far from a Gaussian shape. In 25% of the 200 cases considered, the two estimates of the correlation length did not agree in some cases one would be three times that of the other. This emphasises the need for care when analysing turbulence effects from correlation lengths. The literature suggests the correlation length is between 1m and 4m [1, 3 and 4]. Therefore a 20s time trace should result in a reliable estimate for the correlation length, as occurs in 75% of cases. Assuming an average wind speed of at least 2 ms^{-1}, such a time trace contains wind speed data over a region at least 40m long. So, correlation values calculated this way may be influenced by changes occurring well outside the propagation path, changes which could not influence the pulse waveform. Typically, the measured correlation lengths varied from 1m to about 5m, with an average of 2.2m. For 135 of the 200 cases investigated there was up to 25% uncertainty in the correlation lengths.

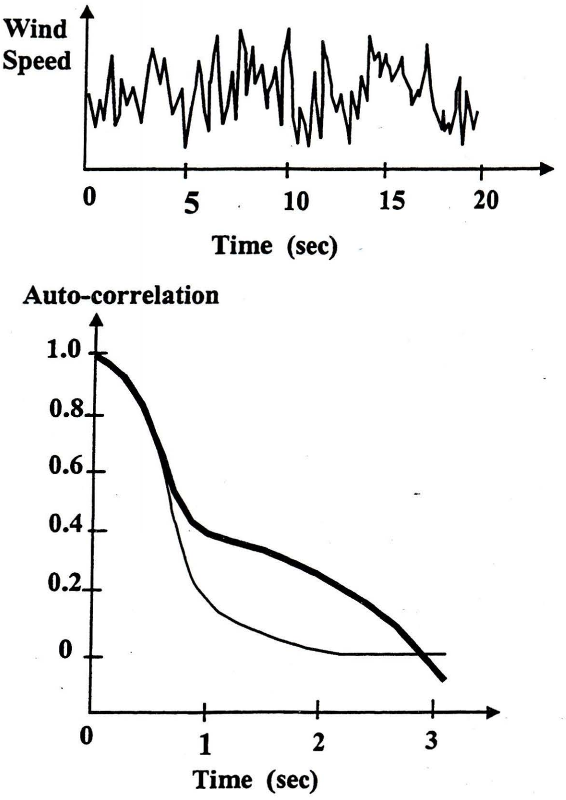

Fig.2: Typical wind speed time trace and an auto-correlation curve (dark line) and a Gaussian fit (thin line).

3. RESULTS

To determine the effect of scattering by a soft turbule, Eqn. (3) was applied to each frequency component of the source pulse and then the resulting pulse shape reconstituted. For these calculations the turbule was positioned along the perpendicular bisector between the source and receiver which are 16m apart, and the offset distance (y in Fig.1) varied between 0.1m and 0.5m. The turbule parameters s and q were determined using the mean correlation length (L=2.2m) and the variance ($<\mu^2> = 5\times10^{-6}$) deduced from the 200 wind speed measurements. A turbule density of 1 turbule per 16m^3 was assumed, in agreement with Ref. 5 and 6.

The following summarises the results of calculating the scattered waveform and then comparing the resultant pulse with the indoor pulse.

When $q < 0$, the scattered component has the same sense as the pulse, and the effects are that

- when the offset y < 0.3m, the peak height is enhanced by up to 30%,
- around y ≈ 0.4m, the peak height is relatively unaffected but it is broadened, with a small secondary peak occurring in the tail as y increases.

When q > 0, the scattered component is inverted and has a reduced intensity as the offset increases because the pulse is smeared out over a longer time. The effect on the resultant pulse is that:

- when the offset $y < 0.3$m, the peak has a reduced height and is broadened,
- when $y \approx 0.4$m, a decrease of 30% occurs in the peak width,
- beyond $y \approx 0.6$m, the peak is relatively unchanged although an "inverted" region appears in the tail, moving progressively further from the peak as y increases.

In general, the possible pulse shapes span the range observed experimentally in the data collected at 16m. Further, using the correlation length determined from the wind speed time traces taken around the propagation time allowed 50% of the pulse waveforms to be reproduced, although it was necessary to use the observed shape to decide whether to take q as positive or negative. Some examples are given in Figure 3.

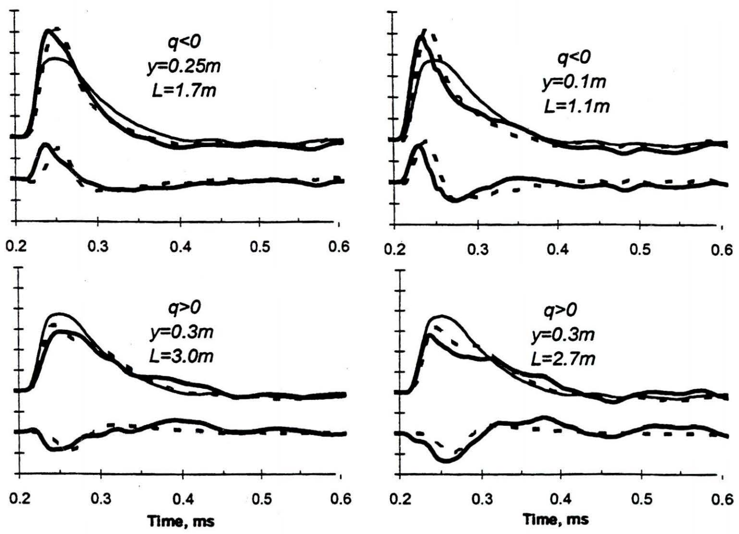

Fig.3: Four comparisons between measured (thick), calculated (dotted) and indoor (thin) waveforms at top with calculated scattered component and experimental difference below. L deduced from corresponding wind speed measurements. Turbule at x = 8m in each case.

The effect of placing the turbule away from the mid-position of the propagation path was investigated by locating the turbule at x and y co-ordinates which gave the same effective delay as the initial condition. The result was essentially unchanged between 2 and 14m, although the scattered magnitude reduced rapidly when the turbule was positioned closer than 2m to the source or receiver. Decreasing the size of the turbule caused the magnitude of the scattered component to increase. It was observed that using a radius other than that deduced from the appropriate correlation length generally produced either a much too large or too small a scattered pulse to fit with the experimental data.

In some cases it was apparent that using two or more turbules would produce a better fit. However, assuming just one is influencing the shape it is generally possible to deduce an effective size and bisector position for the turbule to fit a measured waveform.

The above approach has several short comings:

- the actual position of the turbule can not be specified from the wind speed data.
- regions well outside the propagation path may influence the value of L and therefore s.

* the sign of q can not be determined without inspecting the waveform.

So the next challenge is to relate the turbule parameters directly to the wind speed time trace, rather than its statistical properties. This can be achieved by realising the wind speed at each position along the propagation path, or wind speed profile, is the sum of the mean wind speed plus a component given by the Gaussian expression of Eqn.(2). By adjusting the strength, size and position of the turbule along the propagation path, a reasonable match of the wind speed profile can be determined, as indicated in Fig.4, where the measured and matched profiles are given by the solid and dotted lines respectively. Included on this figure are the turbule parameters q, s and x co-ordinate required to match the profile. However, the wind speed profile is not sensitive to the turbule offset, y, although the arrival time and size of the scattered component vary significantly with the offset value.

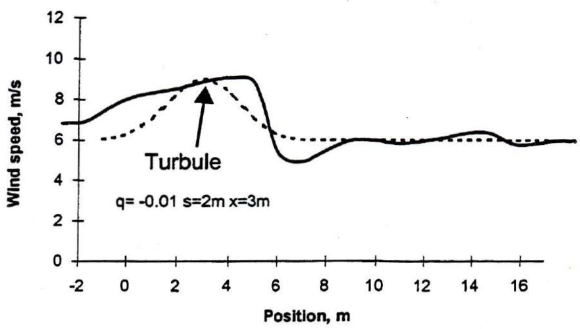

Fig.4: Matching the wind speed profile with a turbule positioned between the source and receiver.

To investigate this aspect, an experiment was performed where the pulse waveforms and wind speeds were measured at 5m intervals over 15m. Examples of the wind speed profiles deduced for the source and receiver positions and pulse waveforms recorded at 5m, 10m and 15m positions are given in Fig. 5.

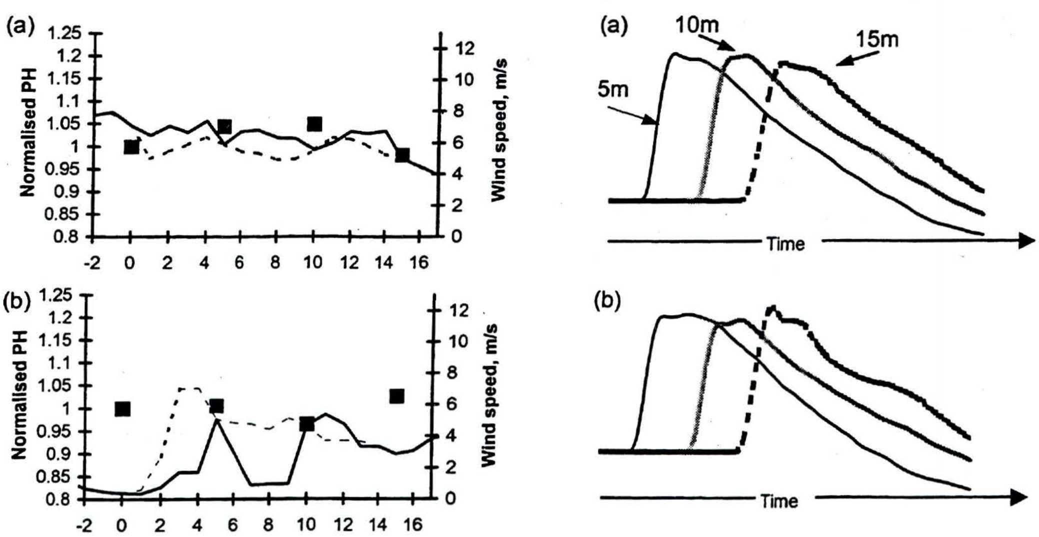

Fig.5: Two examples of wind speed profiles and pulse waveforms obtained from measurements at 5m intervals.

Assuming that only one turbule is present, its parameters can be determined from the wind speed profile and one of the pulse waveforms, by:

- Placing the turbule on the propagation path at a position where the wind speed profile suggests a turbule is located. Adjust values of q and s to obtain the best match to the profile.
- Adjust the offset y between 0.1 and 0.5m to give the correct arrival time for the scattered component for one of the three waveforms.
- Using this offset and the values of q and s already deduced, calculate the resultant pulse shape for the other microphone positions and compare with the actual measured waveforms.

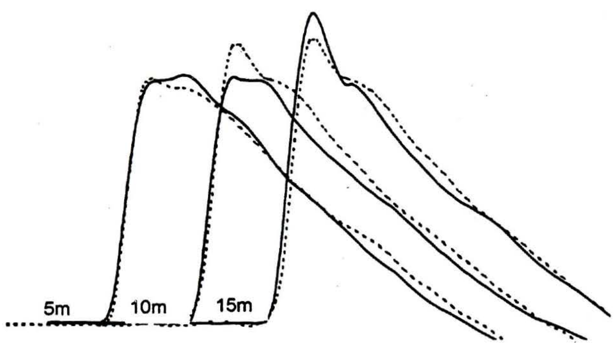

Fig.6: An example of matching the pulse waveform from the turbule parameters derived from turbule parameters form Fig. 4

An example of using the above procedure in calculating the waveforms is shown Fig.6, where the predicted and measured waveforms are displayed as dotted and solid lines respectively.

This analysis was applied to a series of 19 sets of pulses. Of the 57 pulses generated, 85% were matched once the turbule parameters were determined. In some sets it appeared that two turbules were present, so in these cases two of the pulse waveforms were required, in addition to the wind speed profile, to determine all the turbule parameters.

CONCLUSION

Consider two similar turbules, one on the direct path and the other with a 0.5m offset. Because they are physically larger than 0.5m, both would produce almost identical changes to the wind speed profile, however, the turbule with the smaller offset would produce a far greater change to the received pulse due to its smaller scattering angle. Therefore changes to the wind speed profile do not necessarily indicate changes to the scattering component and the pulse waveform. This explains the lack of correlation found at the start of this investigation.

At longer distances, many turbules will be present along the propagation path and some of them will produce significant scattering to the receiver. Another set of turbules may influence the anemometer(s). Statistically, the average scattering from one set of turbules will relate to the averaged variation of the wind speed due to the other set. Therefore there will be a reasonably high correlation between wind and acoustic properties at a statistical level – as is observed in many of the continuous wave studies.

The fact that the average indoor and outdoor pulses have the same waveform has implications in the interpretation of long distance studies. Such measurements may involve scattering by hundreds of individual turbules, so they contain a spatial average and many of the turbulent effects met over 16m will be averaged out. Thus, it is not unreasonable to expect that the statistical relations that apply at long distances will fail at 16m. By contrast, short-range propagation involves perhaps one or two turbules and so should allow a more detailed investigation into the fundamental behaviour of a turbule.

Sonic booms provide another form of impulse propagation through the atmosphere, although on a rather grander scale. Typically, they are a much lower frequency content, with a rise time that is several orders of magnitude greater than our pulses. As propagation distances are generally over 1000's of metres, they will experience a much greater degree of spatial averaging of the turbulent effects discussed above. There is scant evidence in the literature to suggest that the average shock wave pulse has the same waveform as one travelling the same distance through still air. Indeed, it is likely that the effect of multiple turbule scattering will result in a loss of energy for a sonic boom.

REFERENCES

[1] C G Don and I D McLeod, "Predicting low level acoustic pulse amplitudes in an atmosphere supporting wind and temperature gradients", *Proceedings of Internoise 96*, 1996, Liverpool, UK, pp 627 - 632.

[2] V I Tatarskii., *The effects of the turbulent atmosphere on wave porpagation* (Keter Press Binding, Jerusalem, 1971).

[3] G A Daigle, J E Piercy and T F W Embleton, "Line of sight propagation through atmospheric turbulence near the ground", J. Acoust. Soc. Am., **74**, 1983, pp 1505-1513.

[4] I D McLeod, G G Swenson and C G Don, "Single and double pulse propagation in a turbulent atmosphere", Proceedings of Australian Acoustical Society Annual Conference, Glenelg SA, Nov. 1993.

[5] W McBride, H E Bass, R Raspet and K E Gilbert, "Scattering of sound by atmospheric turbulence: A numerical simulation above a complex impedance boundary", J. Acoust. Soc. Am., 90, 1991, pp3314-3325.

[6] I D McLeod. Doctoral thesis, Monash University, May 1999.

[7] G A Daigle, J E Piercy and T F W Embleton, "Effects of atmospheric turbulence on the interference of sound waves near a hard boundary", J. Acoust. Soc. Am., **64**, 1978, pp 622-630.

AUSTRALIAN ACOUSTICAL SOCIETY CONFERENCE

ACOUSTICS TODAY

Melbourne, 24 – 26 November, 1999.

CONCERT HALL ACOUSTIC DESIGN: VARIATIONS ON A THEME OF BERANEK

Fergus Fricke

Department of Architectural and Design Science
University of Sydney, NSW 2006

ABSTRACT

A neural network analysis was undertaken to relate the acoustic quality of concert halls to Beranek's six acoustical parameters: IACC, G_{mid}, EDT, BR, SDI, and T_I. The results of the analysis are difficult to generalise but it seems that the ability to predict the acoustic quality of halls leaves something to be desired. The limitations of the data and the methodology are explained and the results of the analysis are applied to the Concertgebouw, in Amsterdam, to see how changes in the acoustic parameters might change the acoustic quality of the hall. It is also shown that several different combinations of parameters can give good predictions of acoustic quality. Finally, it is shown that there is a better way of predicting the acoustic quality of halls which uses some of Beranek's acoustical parameters and the number of seats in the hall.

INTRODUCTION

Over the last century many measures of the acoustics of concert halls have been proposed and used from Reverberation Time to Inter-aural Cross-correlation (IACC). None of these measures is now considered sufficient, in itself, for the successful design or evaluation of a hall. Unfortunately there does not seem to be a consensus on what combination of acoustic factors creates good acoustics in a concert hall. Beranek [1] opts for six orthogonal factors: IACC, early decay time (EDT), time to the first reflection (T_I), bass ratio (BR), surface diffusivity index (SDI) and G_{mid} (a measure of the average intensity of the sound at mid-frequencies). He shows how each contributes to the overall acoustic quality of a hall and gives the preferred values of each as shown in Table 1. Although Beranek does not give the evidence to support his conclusions. Beranek states that his method is based on Ando's work [2] though Ando used only four orthogonal parameters (EDT, T_I, IACC and G_{mid}). Beranek adds the two extra parameters, BR and SDI, without justification other than his method produces good predictions of acoustic quality. Beranek's method assumes a linear relationship between AQI and each of the six parameters, which are given weightings, to obtain the AQI. The basis for the assertion of orthogonality of the parameters, that the relationship between them and AQI is linear and that the weightings used are optimal is not given. One of the objects of the present work therefore is to attempt to give a more rigorous basis for Beranek's approach.

Table 1. Beranek's parameters, approximate preferred values and weightings

	IACC	G_{mid}	T_I	EDT	BR	SDI
Preferred Value	0.3	5 dB	< 20ms	2.2 s	1.2	1.0
Weighting	25%	15%	10%	25%	10%	15%

Besides the lack of detail there are some difficulties, for designers, with Beranek's approach. Some of the requirements for each of the six quantities are contradictory. A low IACC (one of Beranek's requirements), for instance, requires a narrow long hall but such a hall would be likely to have a low average G_{mid} (Table 2 shows that (1-IACC) and G_{mid} are significantly correlated.). This is catered for in Beranek's assessment method as there are a number of ways of achieving a high acoustic quality score (but not the maximum) without the need for both a low IACC and a high G_{mid}. Beranek's method is not easy to use, for designers, and any proposed change in a design may require considerable effort to evaluate and even then those changes have to be translated into changes in the size, shape and surface finishes of the hall.

What would be much more attractive to designers is a method of determining directly what the effect of changing the hall dimensions etc. is. To see whether such a method was feasible Fricke and Han [3] undertook a neural network analysis (NNA). The analysis which used ten "geometrical" inputs (hall volume, maximum length, width and height, surface area, number of seats, mean rake angle of the seating, surface diffusivity index of the walls and ceiling, stage height and stage enclosure) is shown diagrammatically in Fig.1. One limitation of the Beranek and Fricke and Han approaches is that a subjective visual assessment of the sound diffusing properties of the hall surfaces has to be made. Such assessments can vary widely [4].

In the present work the approach of Fricke and Han was applied to Beranek's acoustical parameters and data on concert halls to see whether Beranek's assumption that the problem was a linear one was reasonable. Also, a modified version of Beranek's analysis, which used a combination of Beranek's input parameters with geometrical parameters, was used to see if a mix of acoustic and geometrical inputs might be useful.

NEURAL NETWORK ANALYSIS

Neural network analysis is roughly the equivalent of multiple regression analysis. NNA can be used to handle non-linear problems, such as pattern recognition, that are not well suited to classical methods of analysis. The concept of neural network analysis has been discussed for nearly fifty years, but it is only in the last twenty that applications software has been developed to handle practical problems. The history and theory of "neural nets", and some indications for their future utility, can be found in publications such as Lawrence [5], Simpson [6] and Bishop [7] and websites such as http://www.statsoftinc.com.

People may be adept at recognising visual and aural patterns but find it more difficult to recognise patterns in numerical data. Neural networks can work with numerical or analogue data that would be difficult to deal with by other means because of the form of the data or because there are so many variables. Neural network analysis can be conceived of as a "grey box" solution to recognising patterns as though it requires some knowledge and skills to use it does not require any mathematical knowledge. Even though a neural network does not give us an equation relating the outputs to the inputs, the analysis is repeatable and can be done automatically. Thus neural networks can be used to identify an object, a person's voice or patterns in the price of shares, provided an existing data set, software and computer time are available. Neural network analysis involves non-linear mapping. It can be considered as an interpolation process in a multi-dimensional hyper-space. It is therefore desirable that the training data used contains information spread evenly throughout the entire envelope of the system but this is rarely possible. It is this pattern-recognition ability of neural networks which is of value in the present work.

The number of input and output parameters and the number of cases influence the geometry of the network. The network consists of an "input" layer of neurons (one neuron to each input) a "hidden" layer or layers of neurons (one layer is usually considered sufficient) and an output layer of one neuron for each output. The number of neurons in the hidden layer is approximately the average of the inputs and outputs though it does depend on the number of training cases too. Too many hidden layer neurons can result in "overtraining" (a lack of generalisation) and lead to large "verification" errors. Too few neurons can result in large training and verification errors. Starting from and initially randomised weighted network system, input data is propagated through the network to provide an estimate of the output value. The error between the actual output and the predicted value is used to adjust the network weightings to minimise the error in the predicted outputs. In this iterative procedure the new weights are accepted if the resulting error is smaller than that recorded using the previous set of weights. There are several different genetic algorithms that are commonly used to achieve the minimum error in the shortest time.

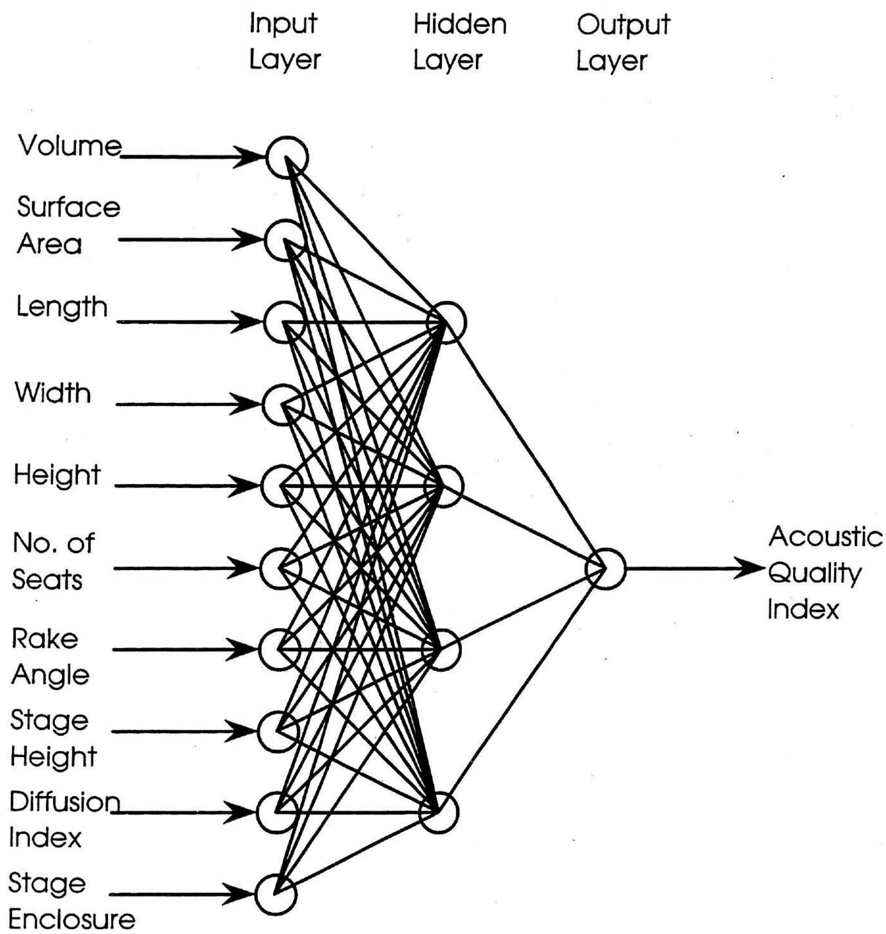

Fig. 1 Diagrammatic representation of the neural network used by Fricke and Han [2] for their concert hall study.

RESULTS

The results of neural network analyses are presented in two sections:

1 Beranek's acoustical parameter results.
2 Combined acoustical and geometrical approach.

Reworking Beranek's model

As was mentioned previously some of the analysis that Beranek undertook appears to lack justification. For instance, he has assumed orthogonality between the six input parameters and a linear relationship between these and the acoustic quality of halls. Beranek seems to have somewhat arbitrarily assigned weightings (see Table 1) to each of these orthogonal inputs to predict the acoustic quality of halls and has also indicated the preferred value of each quantity. For instance, for IACC his preferred value is 0.3 even though no hall he uses for his analysis has a value less than 0.29 and the range of values in that data is 0.29 to 0.59. Only 26 of Beranek's 37 cases could be used in the present analysis because AQI values were not available for the other 11 cases.

Using Beranek's data on 26 concert halls the orthogonality of the inputs was checked and neural networks were trained using Statistica Neural Network software [7]. The inputs are approximately orthogonal, as shown by the correlations between the parameters in Table 2, with G_{mid} and (1-IACC) being most correlated.

Table 2. Correlation matrix for Beranek's parameters

	1-IACC	T_I	G_{mid}	EDT	BR	SDI	AQI
1-IACC	1.00	-0.29	**0.53**	0.08	0.34	0.29	0.47
T_I	-0.29	1.00	-0.08	-0.19	-0.28	-0.33	-0.19
G_{mid}	**0.53**	-0.08	1.00	0.03	0.18	0.16	0.48
EDT	0.08	-0.19	0.03	1.00	-0.16	0.20	0.01
BR	0.34	-0.28	0.18	-0.16	1.00	0.06	-0.10
SDI	0.29	-0.33	0.16	0.20	0.06	1.00	0.67
AQI	0.47	-0.19	0.48	0.01	-0.10	0.67	1.00

Several combinations of Beranek's input parameters were tried from a minimum of Ando's four ((1-IACC), T_I, EDT and G_{mid}) to Beranek's six. Three hidden layer neurons and one output neuron (AQI) were used. The same twentyone cases were used for training and five for verification in each of the networks (No test data was used because of the minimal number of cases available.). The verification data were chosen to give a large range of AQIs.

The results are shown in Table 3 as standard deviation ratios (SDRs) and in Figs. 2 to 6 as AQI response surfaces, for the best trained network using Beranek's six parameters, for the particular case of the Concertgebouw, Amsterdam. The results of the analyses are presented in this way because the SDRs show the degree to which the data has been fitted (A standard deviation ratio of 0.1 is considered an excellent fit while a ratio of 1 means that the predictions are no better than using the mean value.). The rms error was approximately 10% for both the training and the verification data using Beranek's six parameters. What is shown in Table 3 is that Beranek's six input parameter model, gives an SDR of 0.40. A five parameter model using (1-IACC), T_I, EDT, G_{mid} and SDI, with an SD Ratio of 0.42, is almost as good while a four parameter model, using (1-IACC), EDT, G_{mid}, and SDI is even better with an SDR of 0.37. Ando's four parameter model has an SDR of 0.87.

However the SDRs do not show the relationship between the variables. To show all the trends predicted by the analysis would require a large number figures but a few are sufficient to check the validity of linearity and of Beranek's preferred values of the acoustic inputs. Fig. 2 shows AQI as a function of T_I and (1-IACC) for the Concertgebouw. It shows clearly that the preferred value of T_I of <20ms is fine for high values of (1-IACC) but not for low values where 12ms would be preferable though the result does not support the notion of linearity. The same figure supports Beranek's view that an IACC of 0.3 is preferable.

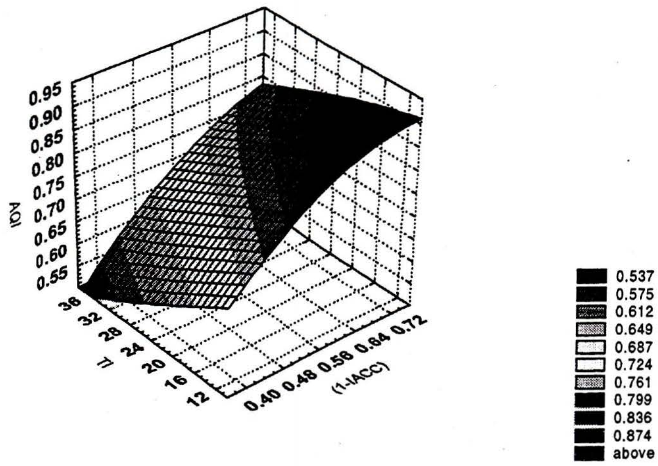

Fig.2 AQI response surface as a function of TI and (1-IACC) for the Concertgebouw

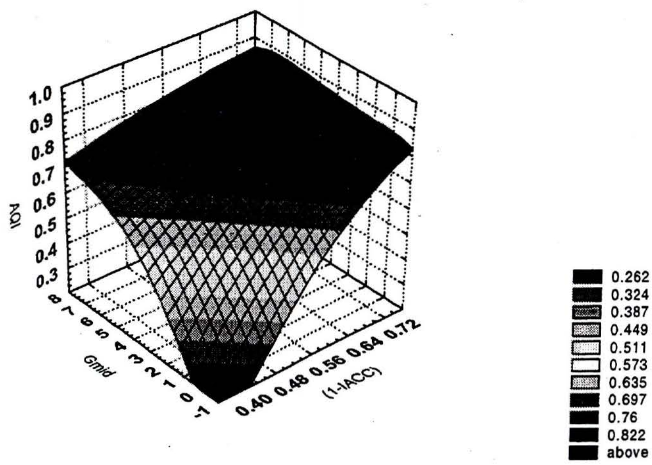

Fig.3 AQI response surface as a function of Gmid and (1-IACC) for the Concertgebouw.

Fig.3 shows AQI as a function of G_{mid} and (1-IACC). Again the concept of a minimum IACC is supported though a G_{mid} of 6 or 7 would seem to be better than Beranek's preferred value of 4 to 5.5.

Fig.4 shows AQI as a function of EDT and (1-IACC). An optimum EDT value would appear to be less than 1 s rather than Beranek's 2 to 2.3 s. Likewise in Fig.5 the preferred value of BR would seem to be less than 0.9 rather than Beranek's 1.1.

Table 3. Standard Deviation Ratios (SDR) for different combinations of Beranek's parameters for calculating the AQI of concert halls.

NN	IACC	T_I	EDT	G_{mid}	BR	SDI	SDR
1	*	*	*	*	*	*	0.40
2	*	*	*	*			0.87
3	*		*	*		*	0.77
4	*	*	*	*		*	0.42
5		*	*	*	*	*	0.86
6	*		*	*		*	0.37
7	*		*	*	*	*	0.45

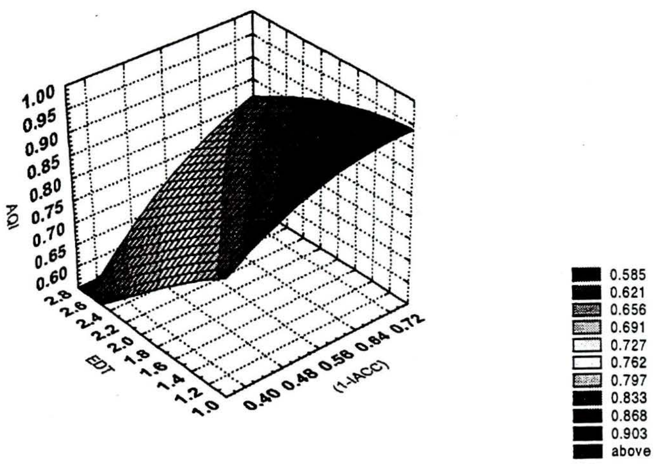

Fig.4 AQI response surface as a function of EDT and (1-IACC) for the Concertgebouw.

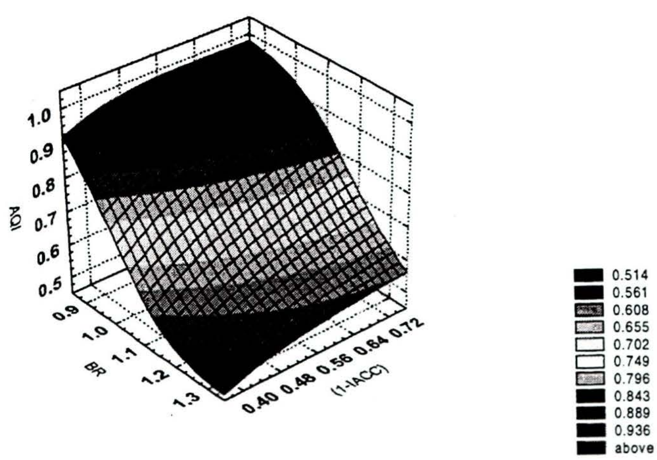

Fig.5 AQI response surface as a function of BR and (1-IACC) for the Concertgebouw.

Finally, in Fig.6, AQI is shown as a function of SDI and (1-IACC). The preferred value of SDI is obviously unity, as Beranek has suggested, though again it is shown that the situation cannot be considered linear.

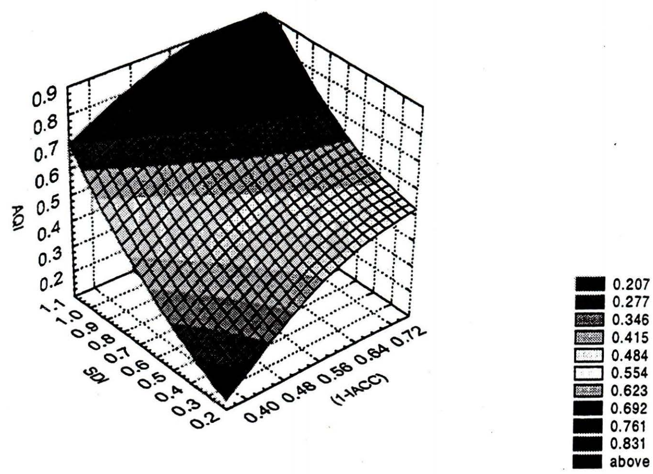

Fig.6 AQI response surface as a function of SDI and (1-IACC) for the Concertgebouw.

It should be remembered that the above results were obtained using the Concertgebouw data. The changes noted in the previous figures with factors such as (1-IACC) and EDT apply only to the specific values used of the four other input parameters; in this case the values of those parameters in the Concertgebouw.

Combined acoustical and geometrical approach

There are obviously different combinations of Beranek's acoustical parameters that are capable of producing "good" acoustics. Given Beranek's approach, (and the approach used in this paper) which is based on the evaluation of existing halls, there can only be a limited combination of parameters which give "excellent" acoustics. That combination is what approximately reproduces the acoustics of the three halls (Musikvereinsaal (Vienna), Concertgebouw (Amsterdam) and Boston Symphony Hall (Boston)) which have AQIs of 1.

It was decided, as a trial, to use a combination of some of Beranek's parameters together with the number of seats and the volume of the auditoria, in the hope of producing better predictions of AQI with a combination of inputs more useful to designers and less prescriptive than the six acoustical parameters. The answer is that there are alternative combinations that could be used (see Table 4). With six inputs the best combination is (1-IACC), T_I, EDT, G_{mid}, SDI and N which gave an SDR of the test data of 0.25. This is better than Beranek's six parameter model, which resulted in an SDR of 0.40. Other combinations of parameters are also promising eg 8 and 9.

Table 4. Standard Deviation Ratios (SDR) for different combinations of Beranek's parameters, together with N and V, for calculating AQI of concert halls.

NN	IACC	T_I	EDT	G_{mid}	BR	SDI	N	V	SDR
1	*	*	*	*		*	*		0.25
2	*	*	*	*		*		*	0.51
3	*	*	*	*			*		0.58
4	*	*	*			*	*		0.57
5	*	*	*				*		0.64
6	*	*	*			*	*	*	0.51
7	*		*	*		*	*		0.47
8	*		*	*	*	*	*		0.33
9	*			*		*	*		0.42

Samples of the AQI response surfaces resulting from this approach (NN1 in Table 4) are shown in Figs 7 to 10 for the Concertgebouw, Amsterdam. Fig.7 shows AQI as a function of (1-IACC) and G_{mid}. It shows that although (1-IACC) is important the preferred value is very dependent on G_{mid}. Fig.8 shows very little dependence on EDT while Fig.9 indicates that a minimum (1-IACC) gives the highest AQI but the relationship with the number of seats is non-linear. SDI is relatively unimportant at high values of (1-IACC) (see Fig.10) and this figure again shows the non-linearity of the situation and that high (1-IACC) or high SDI values lead to good acoustics.

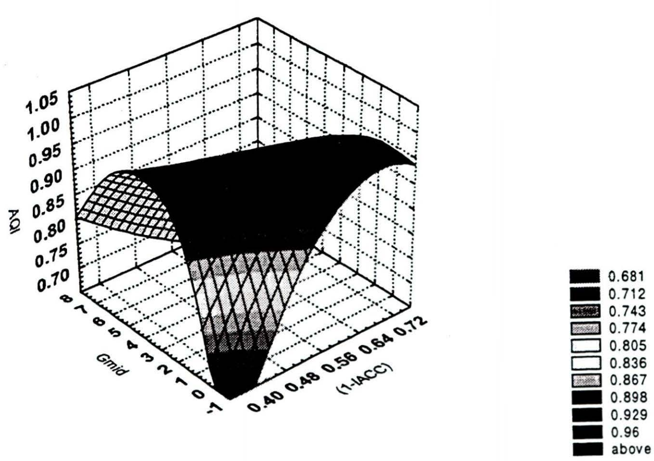

Fig.7 AQI response surface as a function of Gmid and (1-IACC) for the Concertgebouw.

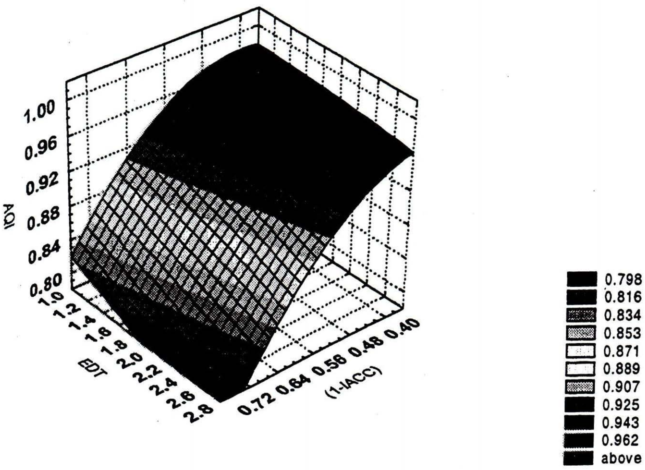

Fig.8 AQI response surface as a function of EDT and (1-IACC) for the Concertgebouw.

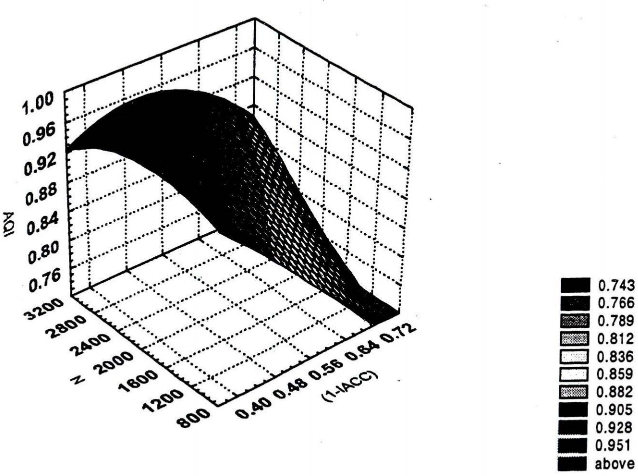

Fig.9 AQI response surface as a function of N and (1-IACC) for the Concertgebouw.

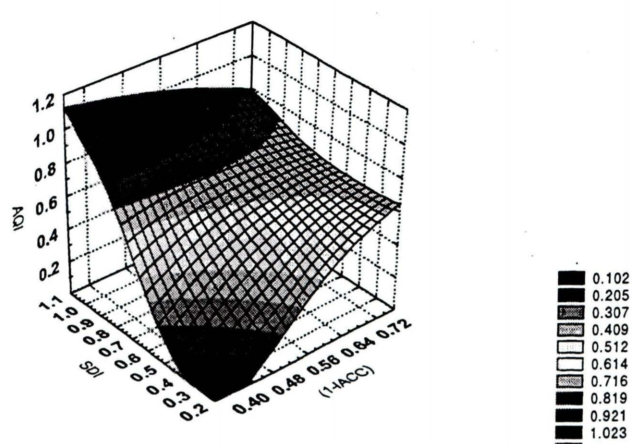

Fig.10 AQI response surface as a function of SDI and (1-IACC) for the Concertgebouw.

CONCLUSIONS & DISCUSSION

There are several limitations of the work reported on in this paper. The first is that the veracity of the data leaves something to be desired. Halls are modified and it is difficult to get data and subjective assessments on a particular version of the hall and impossible to know the seats, orchestras, scores etc on which the subjective judgements have been made. Some of the data that Beranek gives is the average of measurements made by two or more experimenters. This does not pose a problem where the differences are small but in some cases they are significantly different. This is of particular importance in the case of IACC, EDT and BR where the range of values within the data set is quite small. Also, some values of a parameter, for a given hall, have been quoted differently in different texts. For example in Beranek [1], in the table on page 517 the value of T_I for the Festspielhaus, Salzburg is quoted as 27ms whereas on page 535 it is quoted as 23ms. Where discrepancies like this have occurred an average has been taken as a matter of expediency. One cannot therefore expect to get a high degree of accuracy in predictions based on this data for these reasons, and also because of the subjectivity in assessing SDI values and the level of uncertainty in AQI assessments.

A further issue is the lack of cases to train and verify the neural networks. The number of cases is, to say the least, minimal. NNA by its very nature can give a result that is not optimal. The fit to the data will depend on the data used for training and verification for instance. This data should have a normal distribution of values of all variables and the training and verification data should have similar statistical distributions. Where there are very few cases, as in the present work, these conditions are not met and so the training and verification errors will depend on which data are selected for each of these data sets.

As mentioned above, another limitation of the present analysis is one inherent in NNA. There are many possible combinations of inputs that result in minimising errors but most of these minima are "local" whereas there is only one "global" minimum. The number of hidden layer neurons influences the results even when the number of connections used does not exceed the number of cases. The algorithms used to reach the minimum error usually result in getting stuck at a local minima. There are ways to retrain to get to other minima but there is no way of knowing whether the global minimum has been reached.

Because of these limitations it is difficult to compare the relative merits of Beranek's approach using his six acoustic parameters with the approach of Fricke and Han [3]. It is possible to compare different combinations of Beranek's parameters with Beranek's analysis with a higher degree of certainty. It is also possible to compare Beranek's analysis with one based on a combination of Beranek's parameters and other parameters such as the number of seats or the volume of the halls.

Given all the limitations outlined above the following conclusions can stated on the basis of the neural network analyses carried out and their application to the Concertgebouw, Amsterdam:

1 Beranek is justified in using his six parameters to predict AQI as the parameters are approximately orthogonal.
2 Ando's four parameter model (IACC, T_I, G_{mid}, and EDT) is not as good as Beranek's model.
3 A five parameter model using IACC, T_I, G_{mid}, EDT and SDI appears to be only marginally worse than the six parameter model. A four parameter model using IACC, EDT, G_{mid} and SDI is, surprisingly, marginally better for predicting AQI. These findings may be a result of the limited number of cases available for training and verifying the neural networks.
4 There does not appear to be a linear relationship between AQI and some of Beranek's parameters. The non-linear models, however, need to be trained and tested on more data before they can be used with confidence.
5 The most important influence on AQI is SDI (see Table 2). This is rather unfortunate as it is the only input parameter that cannot be measured objectively. A better basis for its assessment would be useful.
6 The finding in this work that a Bass Ratio of less than 1.0 is preferred is contrary to accepted wisdom. It may be that the preferred Bass Ratio is dependent on other factors besides reverberation time, as indicated by Beranek (Beranek's view that the preferred value of BR is dependent on RT is an acknowledgment that the situation is non-linear incidentally.).
7 It is possible to obtain better predictions of the acoustic performance of concert halls using IACC, T_I, EDT, G_{mid}, SDI and N (the number of seats) or IACC, EDT, G_{mid}, BR, SDI and N than it is using any combination of Beranek's parameters.

REFERENCES

1 Beranek, L.L., *Concert Halls and Opera Houses: How They Sound,* American Institute of Physics, Woodbury, 1996.
2 Ando, Y., *Concert Hall Acoustics*, Springer-Verlag, Berlin, 1985.
3 Fricke F.R. & Han Y.G. (1999), *A Neural Network Analysis of Concert Hall Acoustics*, Acustica, 85, 113-120.
4 Fricke, F.R., *Visual Assessments of the Surface Diffusion Properties of Concert Halls,* Applied Acoustics, (accepted, subject to revision, 24 May 1999)
5 Lawrence, J., *Introduction to Neural Networks,* California Scientific Software Press, Nevada City, 1994.
6 Simpson, P.K., *Artificial Neural Systems,* Pergamon Press, London, 1990.
7 Bishop, C., Neural Networks for Pattern Recognition, OUP, Oxford, 1995
8 STATISTICA Neural Networks, StatSoft Inc, Tulsa, OK. 1999

ACKNOWLEDGMENT

Lest any reader think that this paper is crifical of Leo Beranek's work may I disabuse him or her. Leo Beranek is the master chef who has almost single-handedly developed the recipe for concert hall acoustic cakes and not only selected the ingredients but sometimes even grown and supplied them and baked the cake. Without Leo Beranek's superb effort the little decoration above would have no use or relevance.

AUSTRALIAN ACOUSTICAL SOCIETY CONFERENCE

ACOUSTICS TODAY

Melbourne, 24 – 26 November, 1999.

VIBRATO FREQUENCY AND PHASE LOCK IN OPERATIC DUET QUALITY

Melanie Duncan[1], Carol Williams[2], Gordon Troup[3]

[1]Music Department, [2]School of Historical and Gender Studies, [3]Physics Department
Monash University, Clayton, Victoria.

Abstract

For a 'bel canto' trained singer, 'vibrato' is defined as a periodic variation of the fundamental frequency of the sung note, with an intensity variation of the same period. 'Tremolo' is a variation in the intensity only. The locking of vibrato frequencies in unison soprano choirs has been reported and studied.[1] A 1982 review article on the physics of the singing voice states: "It may well be that the pleasing or less pleasing quality of harmony in a vocal duet, for example, depends on whether or not the vibratos of the singers synchronise. This does not appear to have been investigated."[2] We report work agreeing with this surmise. Recordings of Dame Joan Sutherland singing the 'Flower Duet' from the opera *Lakme* by Delibes with each of 3 different singers were studied. The powerful 'SpectraPro' software was used for analysis. Our results show one singer locking in phase with Dame Joan, another locking in antiphase and another exhibiting phase wander. It is quite remarkable that such a complicatedly coupled system should behave so like a classically coupled oscillator system, for which in phase, and out of phase locking is possible, as is also phase wander. Presumably psychophysical, as well as physical, coupling occurs.

[1] G.G. Sacerdote. 'Researches on the singing voice', Acustica 7, 1957, pp 61-68.
[2] G.J. Troup. 'The physics of the singing voice', Physics, Reports 74, 1981, pp 379-401.

1. INTRODUCTION

Aim

The aim of the acoustic analysis was to demonstrate firstly, that in operatic duet singing, the vibratos of the two singers can synchronise and secondly, to determine whether or not there was vibrato synchronization in any of the chosen excerpts of the "Flower duet" from *Lakme* by Delibes. This aim developed out of expressed interest in this phenomenon by several voice researchers, namely, Troup [1] and Sacerdote [2].

Previous studies

The vibrato patterns of the solo singer have been studied by many people in great detail. Seashore [3] defined vibrato and tabled average rates and extents for famous singers. Choirs and larger ensembles have been examined with Sacerdote [2] reporting on the locking of vibrato frequencies in unison soprano choirs. It came to our attention that the locking of vibrato frequencies in duet singing had not been investigated. In a review on the physics of the singing voice published in 1981 by Troup [1], the following surmise occurs: "It may well be that the pleasing or less pleasing quality of harmony in a vocal duet for example, depends on whether or not the vibratos of the singers synchronise."

Why the interest in this topic?

One of the researchers is a singer and it was her experiencing first-hand this locking of vibratos that has interested us in this particular topic. She has performed the duet for mezzo and soprano from *Lakme*, by Delibes several times with at least four different mezzo partners. However, it has only been with one of the partners that there was an audible buzzing each time they sang together in certain passages of the duet. They were not singing the same pitch but we believed that their vibratos were synchronized and that this was creating the audible buzz. This type of vibrato locking in duet singing does not seem to occur a great deal but we feel that it is perhaps the key to a successful rendition of a duet with someone. It is the type of connection between two singers that composers probably visualize as they write their music but is seldom heard in reality.

Relevance of the study

The relevance of the results found so far in this study is quite considerable, for singers, teachers, directors, conductors and perhaps even composers. The results of the project may lead us to question some of the structures and traditions of vocal pedagogy as we know it. A structure which in focusing entirely on the solo voice, neglects to develop sensitivity to the different requirements of ensemble singing.

This project prompts the following questions. In duet singing we wonder how many singers consider how their vibrato contrasts or matches that of their partner. Do they alter their vibrato rate and extent at all, and if they do is this a conscious or a subconscious event? Do both singers alter their vibratos in order to attempt synchronization, or only one of the singers? Is it accepted that either the higher or the lower voice makes the changes or does each singer remain constant? The study provides statistics proving that vibrato synchronization or locking does indeed occur in duet singing.

It is also our belief that the synchronization of the vibratos in a duet results in a fusion of the voices that is preferred by listeners. Further research is being conducted in order to examine the relationship between this synchronization and preference rating of voice specialists. These results will not be discussed in this paper but we can say that results so far indicate that this is indeed the case. The implications will be most exciting for the opera world in the following ways:

- performers will have reason to consider their duet partner's vibrato rate and extent and will collaborate more often with their partner on phrasing and phasing of their vibrato
- vocal pedagogues may consider training their students more often with differing partners and assessing aurally and also perhaps measuring acoustically how their students synchronize when singing duets.
- directors will have to consider where they place the performers on the stage so that they can have the best possible chance of synchronizing
- conductors will have good reason to argue with directors over the staging if it interferes with balance and synchronization of the vibratos of the two singers in the duet.

2.METHODOLOGY

The procedure was to acoustically analyze the three duets and to obtain the exact rate and extent of the frequency vibrato of each singer. The software used for this analysis was the SpectraPro 3.32A, a PC-based system with high-resolution FFT signal analysis, editing and playback of the sounds of speech and singing. The results were obtained using the Spectrograph display window with settings as follows: Sampling rate: 22050 Hz; FFT size: 1024; Window: Hamming; Averaging: 2. The material analyzed consisted of three commercially available CD recordings of Delibe's "Flower Duet" from *Lakme*. The singers are all internationally renowned. Joan Sutherland is the soprano for each and the three mezzo-sopranos are (A) Hugette Tourangeau (B) Marilyn Horne and (C.) Jane Berbie. The score of the "Flower Duet" was examined and notes of crotchet duration or more were chosen for analysis.

No	Pitch - Soprano	Pitch - Mezzo	Note Value	Vowel
1.	D#5	B4	dotted crotchet	[ɘ]
2.	F#5	F#5	crotchet	[ã]
3.	G#5	E5	dotted crotchet -tied to a semiquaver	[õ]
4.	B5	G#5	crotchet	[ã]
5.	G#5	E5	crotchet	[ã]
6.	E5	G4	dotted crotchet tied to a semiquaver	[Y]
7.	G5	E5	crotchet	[ã]
8.	B4	G#4	quaver with rall.	[ã]
9.	F#5	D#5	dotted crotchet with rall.	[ã]
10	F#5	D#5	crotchet	[ɘ]

Table 1.
Duet notes selected for analysis and their characteristics

The duet notes that were selected for analysis were the sustained notes of constant frequency, and in some instances the passage from one note to another (portamento), in which the singers are singing simultaneously. Rates were determined for each singer by selecting a high, clear partial from the spectrographic display of the note and plotting the peak and trough of each cycle in a graph format in seconds. The measurements were graphed using Microsoft Excel graph spreadsheets. This provided both the frequency vibrato rate and extent for each singer on these selected notes. For this paper we will concentrate on only one of the selected pairs of duet notes, namely, pair number 9. For the soprano the note is a dotted crotchet on F#5 using the French nasalized vowel [ã]. The note for the mezzo-soprano is a dotted crotchet on D#5, using the same nasalized vowel [ã]. The reason we have chosen this pair of notes is because by showing these three examples we can demonstrate the in-phase lock, antiphase lock and wandering that occurs between the vibratos of the two singers in duet. This pair of notes also provided the longest time period to observe the vibrato of the singers.

The second part of the acoustic analysis, was the analysis of the singers in a solo capacity. At the beginning of the duet both singers sing by themselves. We have analyzed the longer notes of these solo passages and will be able to compare what the singer is doing in duet and solo on the same pitch and in some cases also the same vowel. This has proved very useful in determining whether the changes in the vibrato rates that occur in the duet singing also happen during solo singing or whether the changes are only affiliated with duet singing. We will discuss two of the selected solo notes, namely numbers 1 and 14. The notes are the same pitches that the singers sing in pair 9 and it is for this reason that we will discuss the analysis of them. Because of length limitations we are only able to discuss the solo singing of one of the excerpts, namely the Sutherland - Berbie excerpt. The same procedure was applied to selecting the solo notes of each singer for analysis.

No.	Singer	Pitch	Duration	Vowel
1	soprano	F#5	crotchet ties to a semi-quaver	[a]
2.	soprano	C#5	crotchet	[ə]
3.	soprano	E5	crotchet	[õ]
4.	soprano	B4	crotchet	[e]
5	soprano	A4	crotchet	[õ]
6.	soprano	C5	crotchet	[ə]
7.	soprano	E5	crotchet tied to a semi-quaver	[ə]
8.	mezzo-soprano	C5	crotchet	[e]
9.	mezzo-soprano	B4	dotted crotchet	[ɜ]
10.	mezzo-soprano	B4	dotted crotchet	[i]
11.	mezzo-soprano	C#5	dotted crotchet	[i]
12.	mezzo-soprano	B#4	crotchet	[u]
13.	mezzo-soprano	C#5	dotted crotchet	[e]
14.	mezzo-soprano	D#5	crotchet	[ə]
15.	mezzo-soprano	E5	crotchet	[e]

Table 2.

Solo notes selected for analysis and their characteristics.

Whilst the research has measured both the frequency and extent of the singers' vibratos, in this paper we will only be discussing the vibrato rates of the singers. The vibrato extents shown on the graphs are only approximate. We can say that the frequency vibrato extents are still under assessment and will be a major part of the study.

3. RESULTS

Listen to excerpt 1.

Leo Delibes, "The Flower Duet," ***An Evening at the Opera, Volume 1,*** **Classic Options CO 3532.**

Figure 1 depicts the pair of notes number 9, as sung by Joan Sutherland and Hugette Tourangeau.

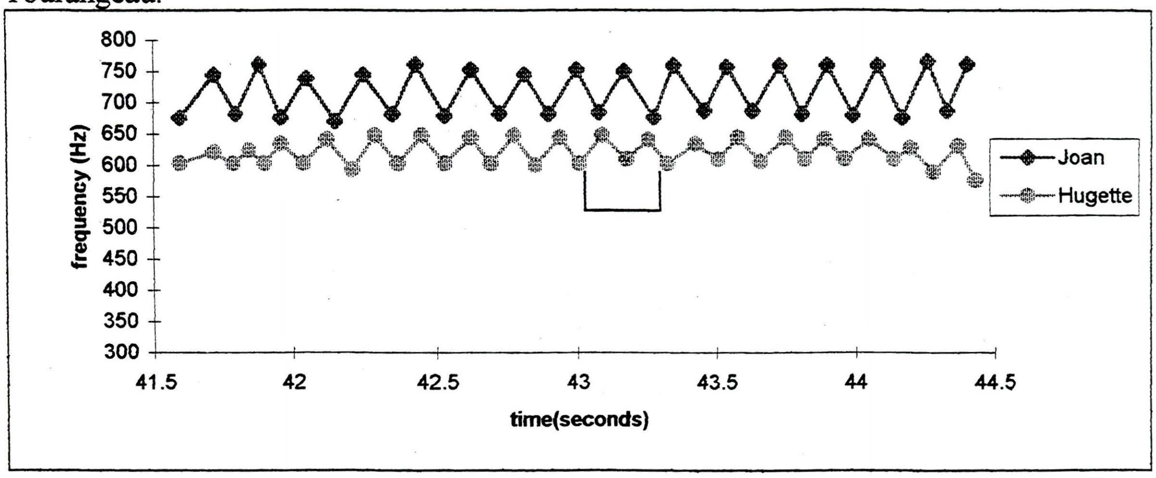

Figure 1

Pair 9 as sung by Joan Sutherland and Hugette Tourangeau.

Figure 1 demonstrates clearly the wandering pattern. The exact time period for the sung notes is 2.81 seconds for Sutherland and for Tourangeau it is 2.84 seconds. Essentially Sutherland is maintaining a vibrato rate between 5.26 and 5.88 cycles per second. Tourangeau is more erratic and her vibrato rate changes from 5.26 to 8.33 cycles per second. At the onset of the note Tourangeau begins at an averaged 7.87 cycles per second she then dramatically drops this rate to 6.10 cycles per second. At this point we see the two singers are in an anti-phase motion. The bracket shows this brief moment of anti-phase lock. The singers then move through a series of motions throughout the rest of the note, almost in-phase, out of phase and then wandering and never coming back into any phasing at all.

Listen to excerpt 2.

Leo Delibes, "The Flower Duet," ***A Gala Concert,*** **Virgin VVD 780.**

Figure 2 depicts Joan Sutherland and Marilyn Horne singing notes number 9. Figure 2 shows a clear example of anti-phase lock occurring. The duration of the notes in this example are 2.74 seconds for Sutherland and 2.94 seconds for Horne. It takes almost 2 seconds for the pattern of anti-phase lock to emerge, but once it does the singers remain locked in this anti-phase mode until the end of the note. Although the singers' vibrato rates are obviously identical when they are in anti-phase lock the cycles are out of phase and this will still cause dissonance between the voices. The exact moment that anti-phase lock occurs is 1.99 seconds after Sutherland has begun to sing and 2 seconds after

Horne has begun to sing. This point is at the time 25.65 seconds and is indicated by the arrow. We can see in this case that both singers change their vibrato rates significantly. If we break each of the notes into approximately 3 sections of almost 1 second each, we can see that this is the case. For the first second section the soprano is at 4.54 c/s, and for the second she is at 4.5 c/s. For the third second she is at an increase to 5.33 c/s. For the mezzo-soprano the first second section is at 5.43 c/s, the second section drops to 5.05 c/s and the third section increases again to match very closely with the sopranos third section at 5.31 c/s.

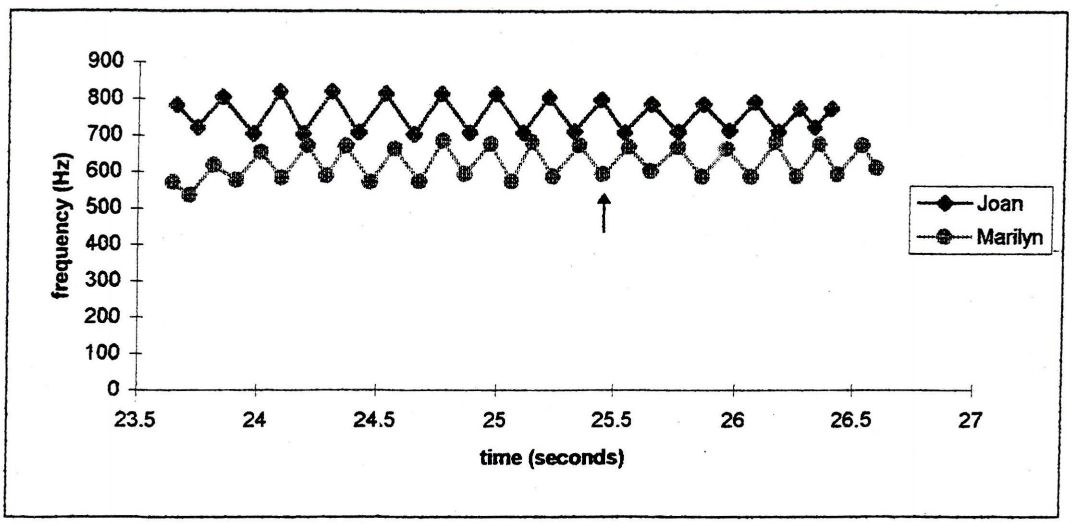

Figure 2
Pair 9 as sung by Joan Sutherland and Marilyn Horne.

Listen to excerpt 3.
Leo Delibes, "The Flower Duet," *Lakme Highlights*, Decca 436305-2.
Figure 3 is perhaps the most significant in that it depicts clearly what we recognize as vibrato synchronization resulting in an in-phase lock. The two singers are Joan Sutherland and Jane Berbie.

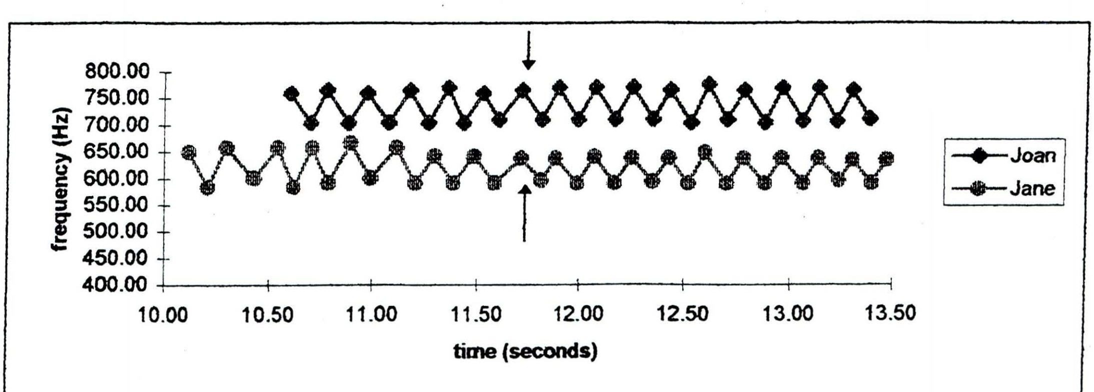

Figure 3
Pair 9 as sung by Joan Sutherland and Jane Berbie.

The duration of the notes in this excerpt are for the soprano 2.79 seconds and for the mezzo-soprano we captured 3.35 seconds. The perfect lock occurs on this time scale at the point 11.71 seconds which is 1.11 seconds after the soprano has begun her note and 1.59seconds after the mezzo has begun her note. This point is indicated by the two arrows on figure 3. The singers remain in a perfect lock for the rest of the duration of the note with only four exceptions. The four diversions from the perfect lock are only a difference of .01 of a second. We feel it is worth tabulating these data so that it is clear.

Sutherland	**Berbie**
11.71	11.71
11.81	11.81
11.89	11.88
11.99	11.99
12.07	12.07
12.17	12.17
12.25	12.25
12.35	12.35
12.43	12.43
12.53	12.52
12.61	12.60
12.70	12.70
12.78	12.78
12.88	12.88
12.96	12.96
13.06	13.06
13.14	13.14
13.23	13.24
13.31	13.31
13.39	13.40

Table 3.

The exact time values of the vibrato rates of Sutherland and Berbie demonstrating vibrato rate lock. * shaded area represents perfect vibrato lock

In order to see how this compares to when the singers are singing solo we will discuss the notes 1 and 14 of the Sutherland - Berbie recording. These notes are the same pitch that the singers are singing in the duet notes we have already discussed. Figure 4 depicts the note 1 as sung by Joan Sutherland.

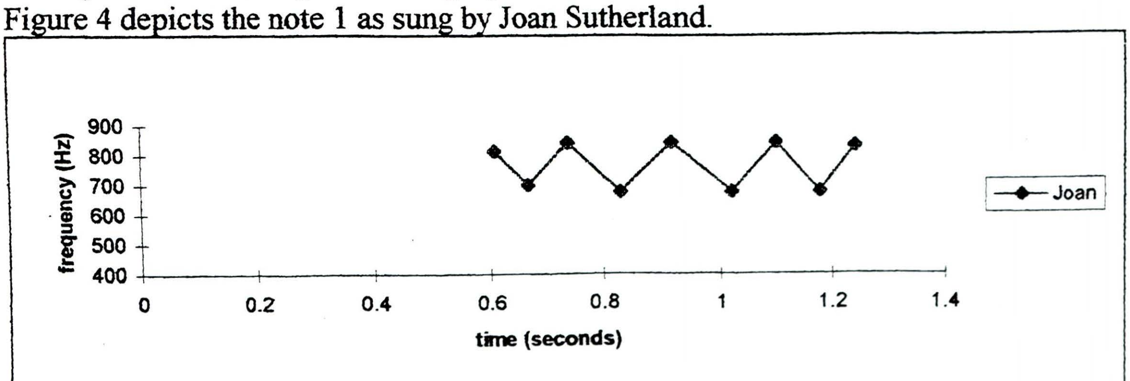

Figure 4.
Note number 1 as sung by Joan Sutherland.

In Figure 4 we see that in this example of solo singing Sutherland is singing at a rate of 6.24 cycles per second and at the same pitch in duet her singing was an average of 5.53 cycles per second. This demonstrates the theory that singers alter their vibrato rates in operatic duet singing in order to synchronize. Sutherland uses a slower vibrato rate when she is singing in duet. The same pattern is evident for Berbie. Figure 5 demonstrates this.

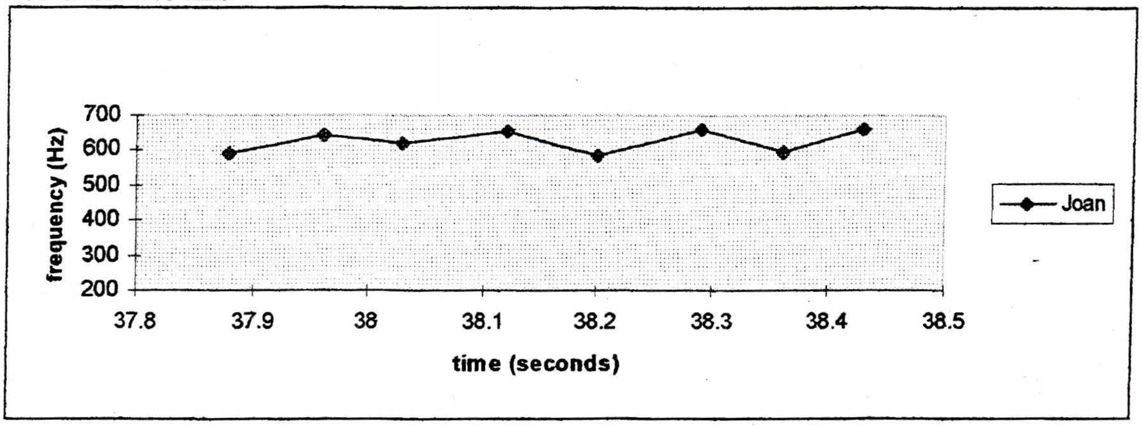

Figure 5.
Note 14 as sung by Jane Berbie.

When Berbie sings at this pitch in solo her vibrato rate is an average of 6.54 cycles per second compared to an average of 5.35 cycles per second when she is singing at the same pitch in duet. The results of the full research indicate that this pattern is the same for the other singers.

4. CONCLUSIONS

The conclusions that we can draw from these results at this point are as follows.
The aim of the paper was to demonstrate that locking of vibrato frequencies in duet singing can occur and to determine whether or not there was vibrato synchronization in the chosen excerpts of the "Flower duet" from *Lakme.* This has been done. We have shown that the vibrato patterns of duet singers behave quite remarkably like a classically coupled oscillator system, for which in-phase, out of phase and also phase wander are possible. We can conclude that in one of the excerpts we have shown today that there is in-phase vibrato synchronization. Results of the full acoustic analysis indicate that this exact synchronization is a rare event and more common is phase wander and to a lesser extent out of phase locking. However the results not yet published do reveal that this one case is not isolated and particularly in the Sutherland and Berbie recording there are several more cases of vibrato in-phase locking which prove that this was not a one off event.

A few of the questions raised in the relevance of the study can be answered. It is possible to say that in duet, singers do alter their vibrato rates. With only three examples it is impossible to conclude whether it is the lower or higher voice in the duet that more commonly makes the changes, but examining all ten pairs of notes for each singer will provide a clearer picture. The results of the three examples described here show that a pattern has emerged. In the first example it was the mezzo-soprano who altered her vibrato rate significantly. In the second example both of the singers had fluctuating vibrato rates and in the last example it is again the mezzo-soprano who alters her vibrato rate, this time with good result as the singers find perfect vibrato synchronization.

The three examples show that in order for singers to demonstrate vibrato in-phase lock two things must happen:

- the rates of vibrato in cycles per second of the two singers need to be the same; and
- the phases of the cycles of the two singers needs to be synchronized.

This raises the question of whether singers in a duet can hear if they are out of phase with their partner and if so whether they can alter the cycles per second in order to synchronize the cycle phase. Research published by Coleman [4] has concluded that when singing a sustained note in unison, two singers singing a duet adjusted their frequency modulation extent to <50% of that used in solo singing, presumably to "blend" into one tone. It is this conclusion that lead us to believe that singers would certainly do the same with their vibrato frequency rate in order "blend" or synchronize their cycles. The results indicate agreement with this hypothesis. When singing in duet, as opposed to solo singing, the singers used in this research reduced their vibrato rate cycles per second. We believe that this was in order to synchronize with their singing partner.

REFERENCES

[1] G Troup, 'The physics of the singing voice', Journal of Research in Singing, Dec., 8/1, 1982, pp 1-26.

[2] G.G Sacerdote, 'Researches on the singing voice, Acustica 7, 1957, pp 61-68.

[3] C Seashore, *Psychology of music* (Dover Publications Inc. New York. 1938.)

[4] R Coleman, 'Acoustic and Physiological Factors in Duet Singing: A Pilot Study', Journal of Voice, 8/3, 1994, pp 202-206.

AUSTRALIAN ACOUSTICAL SOCIETY CONFERENCE

ACOUSTICS TODAY

Melbourne, 24 – 26 November, 1999.

ACTIVE CONTROL OF LARGE ELECTRICAL TRANSFORMER NOISE USING NEAR-FIELD ERROR SENSING

Xun Li, Xiaojun Qiu, Rongrong Gu, Robert Koehler and Colin H Hansen

Department of Mechanical Engineering, The University of Adelaide
Adelaide SA 5005, Australia

ABSTRACT

This paper presents a theoretical study of near field control strategies for the active control of noise radiated by a large electrical transformer. Two control strategies in the near field are considered. These are the minimization of the sum of the squared pressures at a specific number of error sensors and the minimization of the sound intensities averaged over a specific number of sensors. The cost functions for both control strategies are expressed in terms of the transfer functions from the control inputs to the error sensor outputs and the primary sound field. Thus, expressions given here can be used to solve any complex problem where the control source to error sensor transfer functions and primary sound fields are given. This has practical advantages in applications where the structures are too complex to model theoretically. To evaluate the results using both control strategies, a large flat panel was modeled. A harmonic point force was applied to excite the panel and several point forces were applied as control sources. The control strategies were then applied to minimize the sound radiated by a large electrical transformer (160 MVA).

1. INTRODUCTION

Traditional means of controlling sound radiated by large electrical power transformers involve the construction of large, expensive barriers or full enclosures which compromise the maintainability of the transformers. One promising alternative is to use active noise cancellation to reduce the noise [1-9]. Hesselmann [2] and Angevine [3, 6-8] reported that global control could be achieved for a transformer in an anechoic room provided that the transformer was completely surrounded with loudspeakers. Angevine concluded also that the attenuation was dependent on the number of control sources and that this dependence was stronger at lower frequencies. McLoughlin et al [9] demonstrated that the minimization of noise radiated by a small transformer (7.5 MVA) was achieved with an average reduction of the 120 Hz and 240 Hz tones of 10-15 dB by means of near-field error sensing of sound pressure. However, no theoretical analysis was given in this paper.

In this paper, a theoretical analysis of active control of the sound radiated from the structure using the near-field control strategies is reported. These control strategies are the minimization of the sum of the squared sound pressures at a specific number of error sensors and the minimization of the sum of the sound intensities averaged over a specific number of sensors. For both control strategies, the cost functions are expressed in terms of the transfer functions from the control inputs to the error sensor outputs and the primary sound field. To evaluate the control performances achieved with both control strategies, a flat panel was modeled with a harmonic point force excitation and several point force control sources. The control strategies were then applied to minimize the sound radiated by a large electrical transformer (160 MVA). In this application the transfer functions from the control inputs to the sound pressures at error sensing points and the transformer sound radiation were measured on site.

2. NEAR-FIELD CONTROL STRATEGIES

In this section, two control strategies in the near-field, which have been developed by previous researchers, are summarized since they are important parts of evaluating the results in this paper. The control strategies are: minimizing the sum of the sound intensity [10] and minimizing the sum of the squared sound pressures [11,12] at a set of discrete sensing points.

In general, the error criterion J_p, which is the sum of the squared sound pressures at a set of discrete error sensing locations, can be expressed in quadratic form with respect to the control source strengths [11,12], i.e.,

$$J_p = \boldsymbol{Q}_c^H \boldsymbol{A} \boldsymbol{Q}_c + \boldsymbol{Q}_c^H \boldsymbol{b} + \boldsymbol{b}^H \boldsymbol{Q}_c + c, \tag{1}$$

where

$$\boldsymbol{A} = \boldsymbol{Z}_{QP}^H \boldsymbol{Z}_{QP}$$
$$\boldsymbol{b} = \boldsymbol{Z}_{QP}^H \boldsymbol{P}_p \tag{2a,b,c}$$
$$c = \boldsymbol{P}_p^H \boldsymbol{P}_p,$$

where $\boldsymbol{Q}_c$ is the $(N_c \times 1)$ vector of control source strengths; $\boldsymbol{Z}_{QP}$ is the $(N_e \times N_c)$ matrix of transfer functions between the control source strengths and the sound pressures; $\boldsymbol{P}_p(\mathbf{r})$ is the $(N_e \times 1)$ vector of complex sound pressures radiated by the primary sources at the N_e error sensing locations; H is the Hermitian of the matrix.

The optimum values of the control source strengths corresponding to equation (1) can be written as,

$$\boldsymbol{Q}_{c,opt} = -\boldsymbol{A}^{-1}\boldsymbol{b}. \tag{3}$$

The minimum sound field can be obtained by substituting equation (3) into (1).

The error criterion J_I, which defines the sum of the sound intensities at a set of discrete error sensing locations, can be expressed as,

$$J_I = \mathbf{Im}\left\{\boldsymbol{Q}_c^H \boldsymbol{a} \boldsymbol{Q}_c + \boldsymbol{b}_1 \boldsymbol{Q}_c + \boldsymbol{Q}_c^H \boldsymbol{b}_2 + c\right\} \tag{4}$$

where

$$\boldsymbol{a} = \frac{-1}{2\rho\omega d_{12}} \boldsymbol{Z}_{QP1}^H \boldsymbol{Z}_{QP2}$$
$$\boldsymbol{b}_1 = \frac{-1}{2\rho\omega d_{12}} \boldsymbol{P}_{p1}^H \boldsymbol{Z}_{QP2} \tag{5a,b,c,d}$$
$$\boldsymbol{b}_2 = \frac{-1}{2\rho\omega d_{12}} \boldsymbol{Z}_{QP1}^H \boldsymbol{P}_{p2}$$
$$c = \frac{-1}{2\rho\omega d_{12}} \boldsymbol{P}_{p1}^H \boldsymbol{P}_{p2}$$

where ρ is the density of the surrounding fluid medium; d_{12} is the distance between the two microphones on the sound intensity probe; subscripts 1 and 2 refer to the microphone indices on the sound intensity probe.

The optimum control source strength values can be obtained from equation (3) using

$$A = a - a^H$$
$$b = \left(b_{2R} - b_{1R}^T\right) + j(b_{2I} + b_{1I}^T) \quad (6a,b)$$

where the subscripts **R** and **I** indicate the real and imaginary parts of a complex quantity, respectively. The minimum sum of the sound intensities at the error sensing points can be obtained by substituting equations (3) and (6) into equation (4).

It should be noted that, for measuring the sound intensity, the two microphone technique was employed.

3. OPTIMAL CONTROL IN THE NEAR-FIELD

In general, when predicting the minimized sound field using equations (1-6), the transfer function $\boldsymbol{Z}_{QP}$ and the primary sound field $\boldsymbol{P}_p$ can be measured directly on site or be modeled theoretically or numerically for simple systems. In this paper, a simply supported panel mounted in an infinite rigid baffle was modeled first using previously developed procedures, e.g., [12] to evaluate the near-field sensing strategies. Then, data measured from a large transformer were used to minimize noise radiated from the transformer using the near-field sensing strategy.

Evaluation of the near-field sensing strategies

In this section, two near-field sensing strategies, i.e., minimizing the sum of the sound intensities and minimizing the sum of the squared sound pressures in the near-field, are evaluated. As a source, a simply supported steel flat panel of dimensions 1500×1000×6 mm mounted in an infinite rigid baffle surrounded with air was modeled with harmonic point force excitation as shown in Figure 1. Young's modulus of the panel was E=209 MPa; Poisson's ratio ν =0.29 and density ρ =7870 kg/m^3. Sound speed in air is c_0=343 m/s and the air density is ρ_0=1.21 kg/m^3. The panel oscillated at 73 Hz corresponding to the 3,1 mode resonance and the radiated sound field was calculated at 441 error sensing points (21×21 grid) at 200 mm intervals on a plane in front of the panel in the near-field, and the control results were evaluated using 1297 sensors distributed over a test hemisphere in the far-field (10 m from the panel) for each test case. The distance of the error sensor plane from the panel was normalized as $\gamma = 2r/L_x$, where r is the distance of the error sensing plane from the vibrating panel. Coordinates of the forces applied on the panel are given in Table 1.

Table 1 Coordinates of forces on the panel

Disturbance	$\bar{l}_d$ (L_x/4, 0)
Control forces	$\bar{l}_1$(L_x/4, L_y/4); $\bar{l}_2$(L_x/4, -L_y/4); $\bar{l}_3$(-L_x/4, L_y/4); $\bar{l}_4$(-L_x/4, -L_y/4).

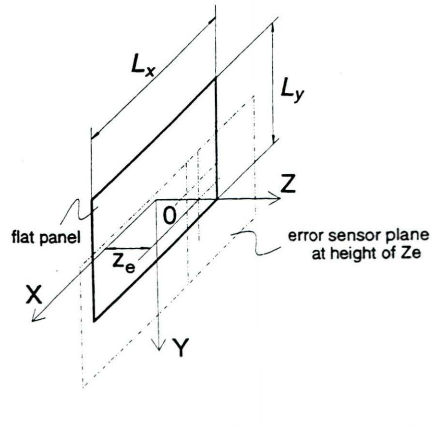

Figure 1 A simply supported plate in an infinite rigid baffle

The calculated sound intensity distribution characterizing the primary sound field is shown in Figures 2. Since the panel was excited at 73 Hz corresponding to the 3,1 mode resonance, the sound radiation pattern in Figure 2 is representative of the 3,1 mode radiation pattern. It should be noted that negative intensities in the scale in Figure 2 indicate negative intensity flow, i.e. energy flowing into the panel, not negative intensity level.

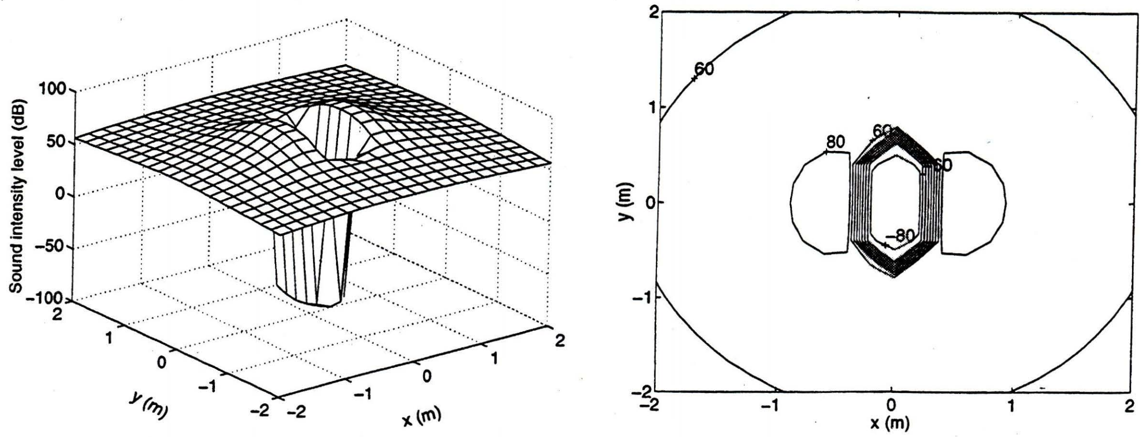

Figure 2 Distribution of sound intensity level without control; error sensors at 441 points at 200 intervals on a plane z =0.2 in front of the panel

Figure 3 shows the distributions of sound intensity levels after control. Figures 3(a) and (b) show the results from minimizing the sum of the sound intensities and the sum of the squared sound pressures, respectively. In Figure 3(a) one can see that sound intensity levels at all sensing points decrease in the near-field and the total sound power reduction is around 66 dB in the far-field. In the situation of Figure 3(b), the total sound power was reduced by about 59 dB in the far-field, which is 7 dB less than that achieved using sound intensity minimization.

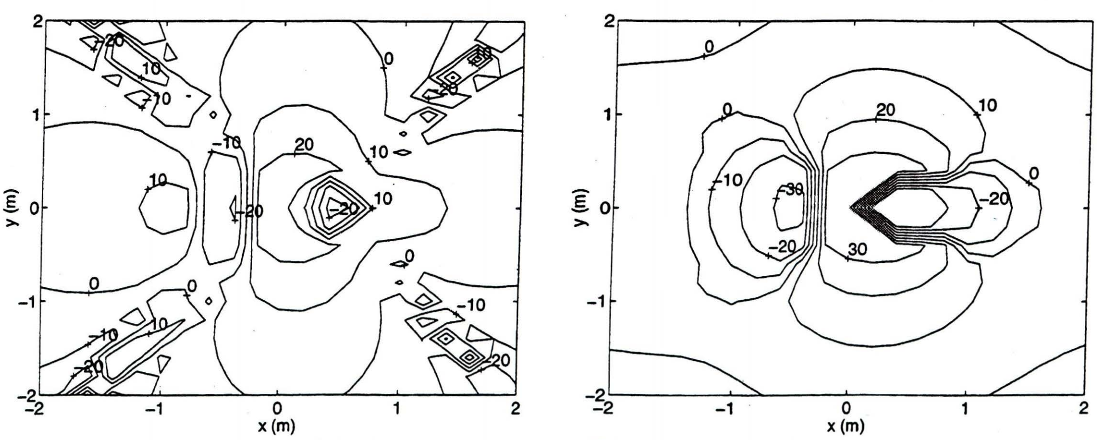

(a) sound intensity minimization (b) squared sound pressure minimization

Figure 3 Distribution of sound intensity levels after point force control (4 control sources); error sensors at 441 points at 200 mm intervals on a plane z =0.2 in front of the panel; (a) sound intensity minimization, (b) squared sound pressure minimization

The control results shown in the Figure 3 can be explained by comparing the controlled near-field sound intensity level distribution patterns shown in Figures 3(a) and (b). One can see that the complexity of the sound radiation pattern in Figure 3(a) is increased in comparison to the field shown in Figure 3(b). This more complicated sound field is less able to propagate sound energy to the far-field because areas of opposite phase are small and close together allowing fluid to move back and forth without propagating energy.

Figure 4 shows the variation of the sound power reduction in the far-field as a function of the normalized distance ($\gamma = 2r/L_x$) of the error sensor plane from the surface of the primary source. The result agrees with what was concluded in [10]. The sound power reduction achieved by minimizing the sum of the squared sound pressures increased as the separation distance between the error sensor plane and the vibrating panel increased, until the maximum sound power reduction was achieved. For this case, the corresponding γ value was 0.8. This is because within the region known as the hydrodynamic near-field, which is the region immediately adjacent to the vibrating structure, measurements of the sound pressure amplitude give no reliable indication of the sound energy radiated by the source to the far-field.

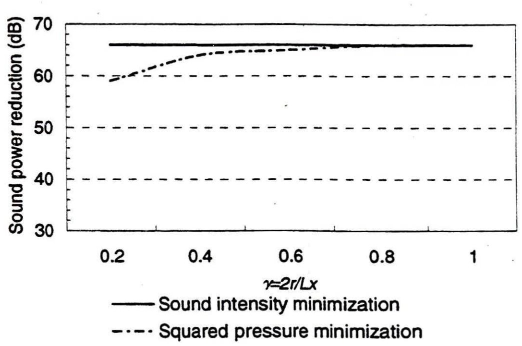

Figure 4 Variation of the sound power reduction as a function of the distance between the error sensors and the panel for 441 error sensors

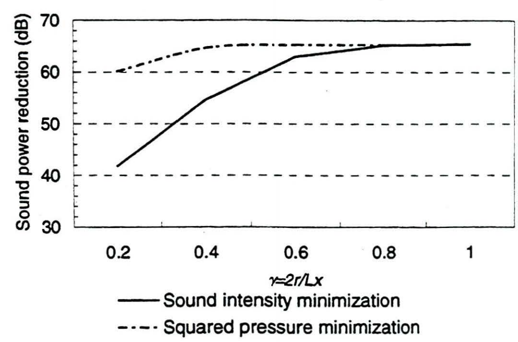

Figure 5 Variation of the sound power reduction as a function of the distance between the error sensors and the panel for 36 error sensors

Due to the complexity of the distribution of the sound energy in the near-field, the number of error sensors required to achieve control performance by the near-field sensing strategies may be quite large [10,13,14]. Figure 5 shows the control performance achieved by two sensing strategies associated with 36 error sensors (6×6 grid) at 800 mm intervals. One can see that, within the region of γ =0.8, the results from the minimization of the sum of the sound intensities corresponding to a less than optimum number of error sensors is worse than those achieved for the minimization of the sum of the squared sound pressures. This is because the cost function associated with minimizing the sum of the sound intensities is more sensitive to accurate measurement of the sound field because the sound intensity varies much more with location than does the sound pressure.

Minimization of noise radiated by a large electrical transformer

To predict the reduction of the sound radiated from a transformer, a large zone substation transformer (160 MVA) was selected for the tests as shown in Figure 6. The dimensions of the transformer are 4.6×4.0×4.0 m (not including the insulating rod). The maximum operating load of the transformer is 160 MVA and the usual operating load is 44 MVA (160A, 275KV).

Experimental set-up. The transformer was surrounded with a water pipe frame for holding sound intensity probes including the top. The distance of the frame from the transformer tank is 1 meter. 96 intensity probes (dual microphone type) at 1.5 m intervals were placed on the frame for sensing the sound field. Each sound intensity probe consisted of two electret microphones that were calibrated for each tonal frequency, i.e., 100 Hz, 200 Hz and 300 Hz, with the microphone pre-amplifier. The distance between two microphones on each intensity probe was 0.07 m.

For measuring the sound field, sound intensity probes were connected through microphone pre-amplifiers and a multiplexer to a B&K type 2816 multi data acquisition unit with four B&K type 3022 4-channel input modules. Data were transferred into a PC in which B&K PULSE LabShop V. 4.1 was installed. A photograph of the experimental set-up is shown in Figure 7.

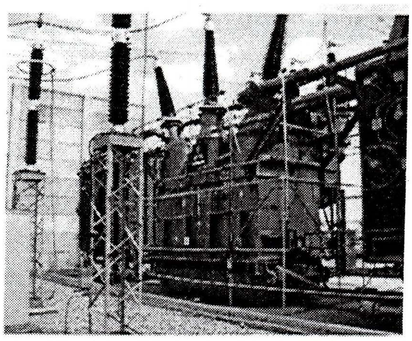

Figure 6 The test transformer located at Cherry Gardens, South Australia

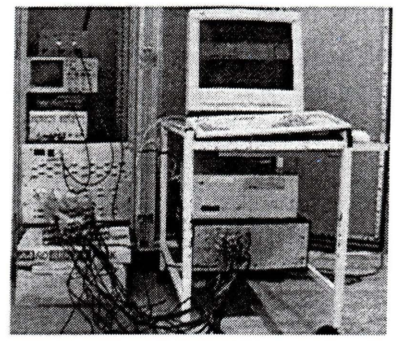

Figure 7 Photograph of the experimental set-up

For measuring transfer functions from force inputs to intensity probe outputs, a swing hammer was used to impact the transformer tank at potential positions of force control sources, while the transformer was switched off. For collecting impact data, a B&K type 4394 accelerometer was fixed to the back of the hammer. Impact signals were measured using the accelerometer connected through a B&K type 2635 charge amplifier to the B&K type 2816 multi data acquisition unit.

To measure transfer functions from acoustic sources to intensity probe outputs, a sound field was generated by a loudspeaker which was located at potential positions of acoustic control sources. The loudspeaker was driven by a signal generator which generated sine waves at frequencies of interest, 100 Hz, 200 Hz and 300 Hz through a power amplifier.

Predicted results. Figure 8 shows the distribution of sound pressure level at 100 Hz. The lighter patches in the plot indicate a higher level of sound radiation.

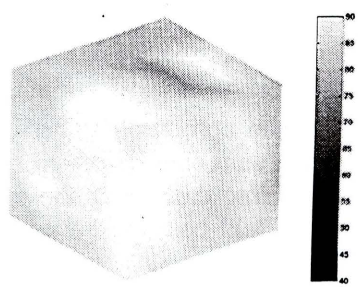

Figure 8 Distribution of sound pressure level at 100 Hz without control, at a distance of 1 meter from the transformer

Figures 9-10 show predicted distributions of sound pressure levels at 100 Hz using 80 vibration control sources and 80 acoustic control sources, respectively. The cost function that was minimized was the sum of the squared sound pressures in the near-field. A genetic algorithm, which is an evolutionary optimization technique [15], was employed as a search procedure to optimize the control source locations. From Figures 9 and 10 it can be seen that noise was significantly attenuated at most sensing locations for both types of control source even though noise was increased at a few sensing locations (2 locations for the vibration control source and 5 locations for the acoustic control source). The largest overall sound pressure reduction was around 44 dB the for vibration control source and around 41 dB for the acoustic control source.

The largest overall increase of sound pressure level was 6 dB for the vibration control source and 7 dB for the acoustic control source.

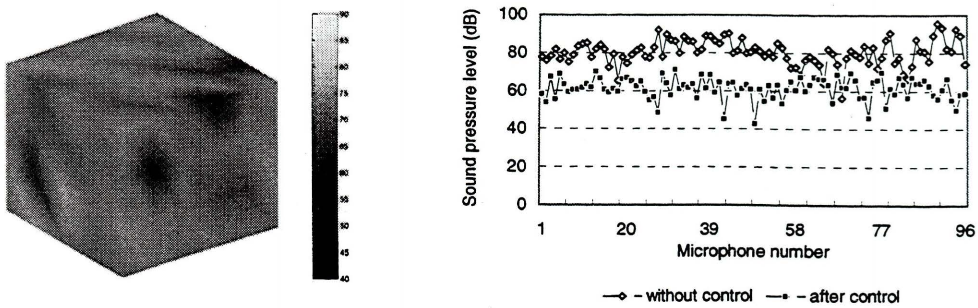

Figure 9 Predicted distribution of sound pressure level at 100 Hz after vibration-source control (80 control sources), at a distance of 1 meter from the transformer

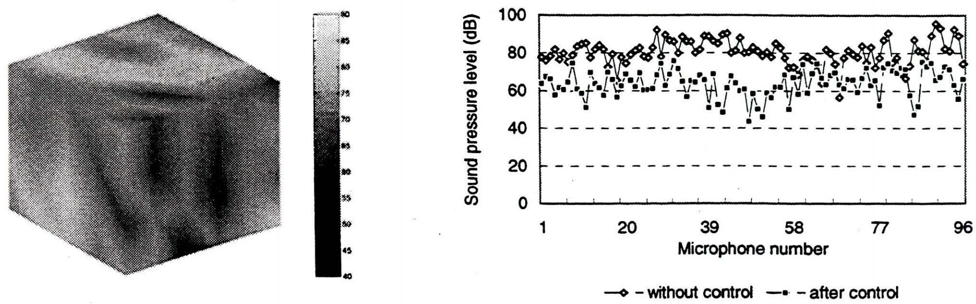

Figure 10 Predicted distribution of sound pressure level at 100 Hz after acoustic-source control (80 control sources), at a distance of 1 meter from the transformer.

The total squared sound pressure reduction levels at a distance of 1 meter from the transformer are shown in Figure 11. As was expected, the sound reduction increased as the number of the control sources increased. When comparing the sound reduction levels shown in Figures 11(a) and (b), one can see that poorer control performances are obtained using acoustic control sources than using vibration control sources. This is because, in general, the sound reduction levels achieved with each acoustic control source may be less than those achieved with each vibration control source, especially if the structural dimensions are approximately equal to (or larger than) the acoustic wavelength at the frequency of interest.

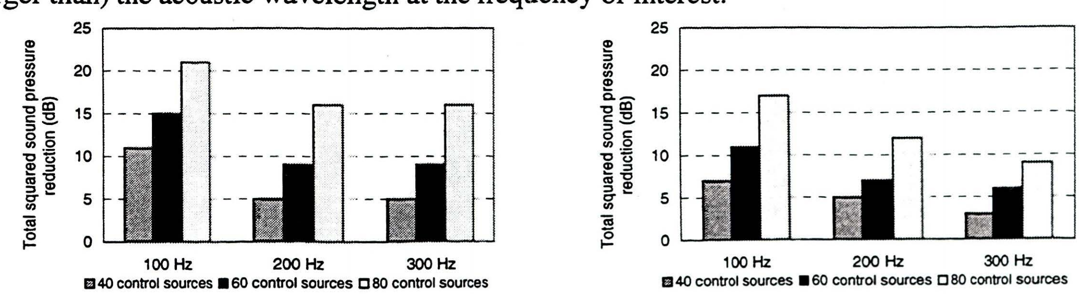

(a) vibration control sources (b)acoustic control sources

Figure 11 Variation of the squared sound pressure reduction levels with the number of the control sources in the near-field; (a) force control, (b) acoustic control

4. CONCLUSIONS

This paper has reported a theoretical analysis of near-field sensing strategies for the active control of noise radiated from structures in free field. Two sensing strategies; minimizing the sum of the sound intensities and minimizing the sum of the squared sound pressures, were considered. As an example, a simple steel panel was modeled using vibration source control. The results demonstrated that control performance can be improved by minimizing the sum of the sound intensities in the hydrodynamic near-field provided a very large number of error sensors are used. If insufficient error sensors are used better results are achieved using near-field pressure squared sensing than intensity sensing.

The method was tested on a large 160 MVA transformer using data measured on site. The results demonstrated that, in the near-field using 80 control sources and 96 error sensors, tonal noise radiated by the large transformer at 100 Hz, 200 Hz and 300 Hz could be reduced respectively by 21 dB, 16 dB and 16 dB for vibration control sources, and 17 dB, 12 dB and 9 dB for acoustic control sources. It should be noted that no evaluation of the prediction of the sum of the squared sound pressures in the far-field was given due to insufficient data.

ACKNOWLEDGEMENTS

The authors gratefully acknowledge financial support from The Electricity Trust of South Australia, The Australian Research Council and The Electricity Supply Association of Australia Ltd.

REFERENCES

[1] B. Conover, 'Fighting noise with noise', Noise Control, 2, 1956, pp 78-82.

[2] Hesselmann, 'Investigation of noise reduction on a 100 kVA transformer tank by means of active methods', Applied Acoustics 11, 1978, pp 27-34.

[3] L. Angevine, 'Active acoustics attenuation of electric transformers', Proceedings of Internois'81, 1981, pp 303-306.

[4] Berge, O. Kr. ϕ Pettersen and S. Sϕrsdal, 'Active noise cancellation of transformer noise', Proceedings of Internois'87, 1987, pp 537-540.

[5] Berge, O. Kr. ϕ Pettersen and S. Sϕrsdal, 'Active cancellation of transformer noise: field measurements', Applied Acoustics, 1988, pp 309-320.

[6] L. Angevine, 'Active cancellation of the hum of large electric transformers', Proceedings of Internois'92, 1992, pp 313-316.

[7] L. Angevine, 'Active control of hum from large power transformers-the real world', Proceedings of the Second Conference on Recent Advances in Active Control of Sound and Vibration, Virginia Tech., Blacksburg, VA, US. pp 279-290.

[8] L. Angevine, 'Active systems for attenuation of noise', International Journal of Active Control, 1, pp 65-78..

[9] M. McLoughlin, S. Hildebrand and Z. Hu, 'A novel active transformer quieting system', Proceedings of Internoise '94, 1994, pp 1323-1326..

[10] X Li, X Qiu and C H Hansen, 'Active control of sound radiated from structures using near-field error sensing', accepted by ACTIVE 99, 1999 Dec 2-4, Florida, USA

[11] P. A. Nelson and S. J. Elliott, *Active control of sound* (Academic Press, 1992)

[12] C. H. Hansen and S. D. Snyder, *Active control of noise and vibration* (E & FN SPON, 1997)

[13] A. Berry, X. Qiu and C. H. Hansen, 'Near-field sensing strategies for the active control of the sound radiated from a plate', accepted as publication by Journal of the Acoustical Society of America,1998

[14] D. A. Bies and C. H. Hansen, *Engineering Noise Control* (second edition, E & FN SPON, 1996).

[15] D. E. Goldberg, *Genetic Algorithms in Search, Optimization & machine Learning* (Addison-Wesley, 1989).

AUSTRALIAN ACOUSTICAL SOCIETY CONFERENCE

ACOUSTICS TODAY
Melbourne, 24 – 26 November, 1999.

NOISE CONTROL AT GAS-FIRED COMPRESSOR STATIONS

Tim Marks

Marshall Day Acoustics Pty Ltd, Collingwood, VIC

ABSTRACT
Three new gas compressor stations needed noise assessments as part of the planning approval process. ENM and SoundPLAN proprietary noise models were used to predict noise levels at distances up to 1600m. The validity of noise source data and the contribution of acoustical lagging were significant issues. The results from commissioning noise surveys have been used to compare the excess attenuation under calm conditions with that predicted by the two noise models. Experience at site has indicated that vibration isolation of gas piping is desirable for maximum performance and that venting noise is significant.

1. INTRODUCTION
Following the disastrous explosion at Esso Longford near Sale in Victoria in 1998, gas supplies to Melbourne for the 1999 Winter were seriously threatened.

In order to provide security of gas supply from other sources, the Victorian Government authorized the simultaneous construction of the Moomba-Melbourne Augmentation Project (MMAP) and the South West Pipeline Project (SWPP).

This paper is concerned with the noise control issues at the three compressor stations that formed part of the MMAP. These stations were located at Bulla Park and Young in New South Wales and at Springhurst, near Wangaratta in Victoria.

2. NOISE MODELLING
As part of the development approval process, noise assessment was required for all three compressor stations. Whilst Springhurst was a greenfield site, both Bulla Park and Young were existing compressor station sites. The gas turbines were Solar Turbines models and duties as follows.

Table 1
Compressor operating duties

	Bulla Park	Young	Springhurst
Turbine Model	Solar Mars 100	Solar Centaur 50	Solar Centaur 50
Power, MW	11.2	4.3	4.3
Inlet pressure, MPa	4.2	4.4	3.2

Discharge pressure, MPa	6.3	8.6	7.5
Discharge pipe dia, m	0.76	0.3	0.45
Flow ksm^3/hr	519	120	90

Following conventional practice, the individual noise sources at each station were entered into the modelling package, along with ground contour details, source directivities, and receiver locations.

The noise modelling packages used were ENM and SoundPLAN. Typically there were only 15-20 noise sources per site, making the noise modelling fairly straight forward. This was fortuitous, as the timescale for the project was extremely short. The entire project time line was only 7-8 months from ordering to start-up of the turbines.

The noise sources and the overall sound power levels for the Springhurst site are given in Table 2.

Table 2
Source sound power summary

Item	Lw dB(A)	Notes
Exhaust	110	Standard silencer type 17A1
Air inlet	85	With filters and inlet silencer
Compressor	110	Solar Turbines
Acoustic enclosure	112	85dB(A) and close fitting
Process gas cooler	85	Jord
Air compressor	76	
Generator	102	Cat diesel engine
Inlet piping	116-124	Lagged – see text
Discharge piping (before cooler)	118-124	Lagged – see text
Discharge piping (after cooler)	113-119	Lagged – see text
Blowdown vent	86	Vent silencer fitted
Bypass valve	87	No Whisper Trim

3. NOISE SOURCE DATA

Exhaust noise

To our surprise, Solar's noise data had changed from that used on a previous project [1]. A review of this data indicated that the unsilenced exhaust noise had apparently decreased from Lw 135dB(A) to Lw 125dB(A). There was no corresponding change in the silenced enclosure breakout noise data or the turbine air inlet noise data, both of which would be expected to change if the power rating (and hence noise) of the turbine had changed significantly. The new test data (Solar Ref SPNP/898/M4) had been tested to ISO 10494 but we could not draw any explanation from Solar as to the reasons for the variation [2].

Interestingly what had changed were the exhaust silencer insertion losses, typically reduced by 5-10dB. This resulted in similar overall silenced exhaust levels for versions of the same turbine. The old Solar data had been used on previous Marshall Day Acoustics projects with confidence and Solar could certainly test unsilenced turbines. Perhaps the real reasons reflected Solar's recognition of the true performance of their exhaust silencers, which had caused headaches in the past for silencer vendors in trying to meet their onerous IL performance requirements.

The old and new unsilenced exhaust sound power data for the Solar Centaur 50 turbine is presented in Figure 1.

Figure 1
Solar Centaur 50 Turbine Exhaust Lw

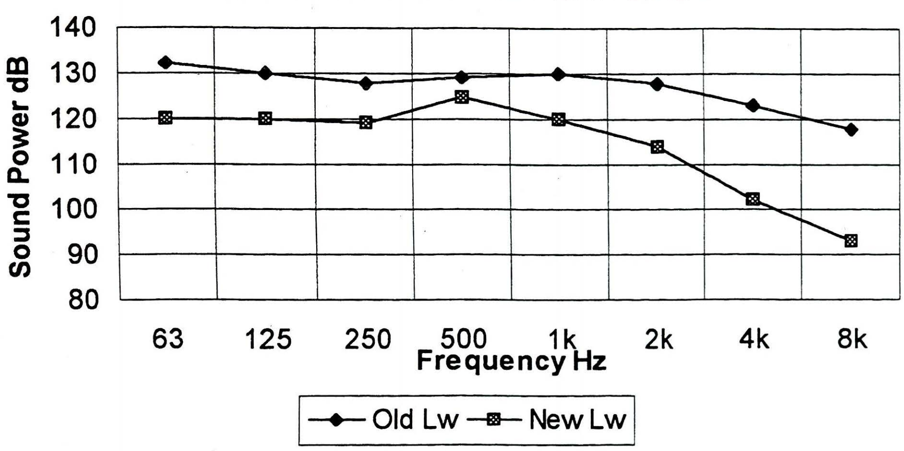

Pipe noise

As the total length of above ground piping at a compressor station can often exceed several hundred metres, the radiated pipe noise is a significant contributor to overall noise levels, particularly when stringent noise criteria are involved.

Consequently, the study of pipe noise took considerable effort. It is usually very difficult to obtain good measurement of pipe noise alone, due to the influence of other noise sources, notably valves, compressors and the turbine itself (especially the inlet which has a significant high frequency component).

In this instance, we were unable to conduct measurements at an existing compressor station operating at the same duty, so data from Marshall Day Acoustics' files were reviewed. The following reliable information was available:

Table 3
Pipe noise data Lp at 1m, dB(A)

Site	Compressor	Inlet	Discharge	Notes
Bulla Park, NSW	Dresser Rand	97	102	Unlagged
Gooding, Vic	Solar Centaur	N/a	76	Lagged
Enneabba, WA	Solar Mars	89	90	Unlagged

Using the method described in Bies and Hansen [3], the measured versus predicted noise levels were compared for the case of the Dresser Rand DR990 units at Bulla Park.

This was an outstanding measurement condition as the influence from external sources was minimal. The turbine and compressor were both located inside a building and owing to the remote site, the pipe was unlagged allowing precise pipe noise measurements. The method in Bies and Hansen appeared to predict absolute noise levels rather poorly, but was considered useful for adjusting the site measurements under alternative operating conditions. This enabled the pipe noise Lw to be determined for each station.

Unsurprisingly, pipe lagging was required at all three sites. Information from HGC in Canada [4] provided excellent information on pipe lagging acoustic performance.

Figure 2
Acoustic Lagging Insertion Loss

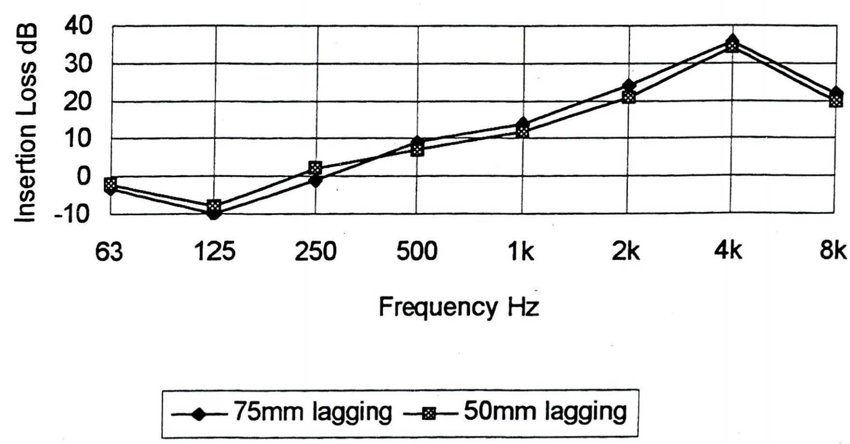

Two alternative lagging options were developed, one nominally 50m thick and $5kg/m^2$ with a wrap and the other nominally 75mm thick with a $6kg/m^2$ wrap. The densities of the 50mm Rockwool insulation were $65kg/m^3$ and the 75mm Rockwool lining was $80kg/m^3$. The insertion loss of these lagging alternatives are given in Figure 2.

4. MODELLING RESULTS

Each compressor station scenario differed in certain ways and similar noise levels could not be expected at the same distance from each. At Springhurst, the client required the EPA criterion (of 36dB(A)) to be met at 550m; this allowed for an easement boundary, where cattle could graze but no future residential development could take place. Typically the nearest residence was a distance of 800-1500m from each compressor.

The results of the modelling for the case of neutral weather conditions are given in Table 4.

Table 4
Noise modelling results

Site	Criterion	L_1 predicted level			L_2 predicted level		
		ENM	SoundPLAN	Dist.	ENM	SoundPLAN	Dist.
Springhurst	L_{eq} 36dB(A)	47	35	550m	26	27	1520m
Young	L_{10} 35dB(A)	36	32	700m	17	19	1590m
Bulla Park	L_{10} 33dB(A)	n/a	~~33~~ N/A	1000m	29	~~27~~ 24	1320m

Generally, there was good agreement at distances over 1km, but in the 500-800m range the results from both prediction models varied .

It was apparent from the program printouts that the differences were due to excess attenuation, ie that due to air absorption and ground effects. SoundPLAN uses the CONCAWE [5] algorithm whilst the ENM algorithm is described by Tonin [6]. The differences that arose are discussed in Section 5 of this paper.

This project gave a good opportunity to study excess attenuation, as EPA compliance required the background noise levels before operation of the turbine compressors to be measured, as well as the noise levels following commissioning. At Bulla Park for instance, the daytime noise level during calm conditions was 19dB(A).

5. MODELLING COMPARISON

At Springhurst (and probably at Young) where commissioning noise tests have been conducted, noise levels exceeded the design criteria by 3-4dB(A). This was due to a number of factors:

- exhaust noise exceeding design by 2-3dB(A)
- enclosure breakout exceeding guarantee by 5dB(A)
- pipe noise radiating from support structures.

The commissioning measurements at Bulla Park, showed that whilst the EPA criterion was met, the predicted noise level of less than 24B(A) under calm conditions equallled the derived value.

As at Springhurst, the turbine enclosure breakout noise exceeded the design value in this case by 17dB(A). Rework to the enclosures at Young and Springhurst was not complex and primarily consisted of:

- grouting the gap between the turbine skid and concrete slab
- correct sealing between the enclosure wall panels and the skid
- replacing damaged door gaskets
- correctly sealing compressor inlet and discharge pipe penetrations
- sealing other penetrations eg cables, bolts.

Table 5
Noise measurement results

Site	Distance	Measured noise levels	Prediction SoundPLAN	Condition
Springhurst	550m	40dB(A)	35dB(A)	Calm

Springhurst	1520m	<30dB(A)	27dB(A)	Calm
Young	700m	40 dB(A)	32 dB(A)	Tail wind
Bulla Park	1320m	25*dB(A)	24dB(A)	Occ N/E wind

* This is an estimate derived from measurements at 660m where the turbine/compressor was audible.

6. EXCESS ATTENUATION

The major differences between the results obtained from the ENM and SoundPLAN models was in the value of the excess attenuation, being primarily air and ground attenuation losses.

As both Springhurst and Bulla Park were low ambient noise level environments and the turbines could be run in the absence of other noise sources, data from these two sites was studied in detail.

A noise measurement at 60m from each site allow the plant sound power to be determined. This can be used to determine the excess attenuation by comparison with the measured noise level at a given distance, when corrected for background noise effects.

The excess attenuation is given in Table 6 in dB(A) and is plotted in octave bands in Figure 3.

Table 6
Excess attenuation dB – calm conditions

Distance	ENM	SoundPLAN	Measured
550m	5	10	10
700m	9	11	7*
1320m	10	14	12

- Probably influenced by background

Reference to Figure 3 shows that the results vary according to frequency. In rural situations MDA tends to use a grass cover of 50% to account for the Australian grasses in rural situations, rather than a value of 90-100% which would normally be assumed for "European" grass between the source and nearest receiver.

Further work is required to validate the results, as over large distances, and with lower source noise levels, estimates of the excess attenuation at mid frequencys become increasingly difficult and more widely variable.

7.FURTHER CONSIDERATIONS

One of the problems in being engaged for noise assessment purposes only is that practical noise control at the site is often inadvertantly overlooked by the client. In this project these were:

Pipe noise leakage

The inlet and discharge piping to the compressor was treated in accordance with the recommendations but an oversight derated its effectiveness. In all cases, the pipe was laid directly on the pipe supports and then lagged. With heavy pipe, including valves and flanges, pipe supports were frequent, often at spacings of 2-3m, especially when both inlet and discharge were supported by a single frame. The pipes were not well isolated from the supports and the pipe vibration was transmitted to the frame via the uninsulated section of pipe. This resulted in significant vibration sufficient to radiate noise.

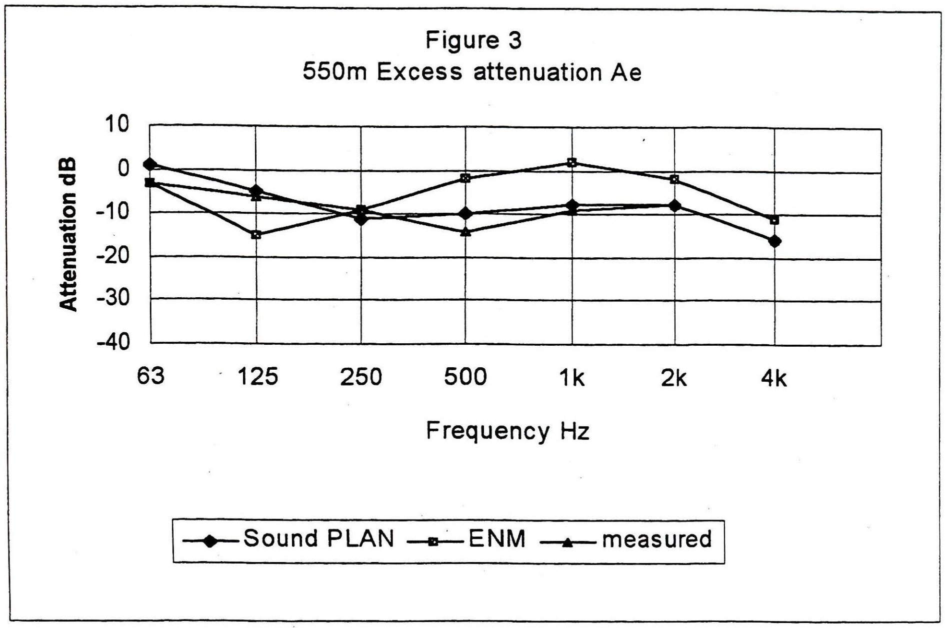

The installation of an isolation pad between the pipe and frame would have eliminated this problem but practical difficulties prevented them being installed. As the pipe contacts the frame at a line, the point loads are significant. In order to provide adequate isolation, the required pad loading (estimated by Embleton's at 100kPa) necessitated a pad of size 400 x 100mm. Hence each pipe would have required a saddle and load plate to ensure the load was uniformly distributed at each connection point, and proper isolation was achieved. Trials at site indicated that even the most rudimentary isolation system gave reductions of 5-10dB. As most vibration energy was centred around 2-3kHz, at which frequency steel structures radiate sound very efficiently, the benefit of isolation would have been significant.

This form of pipe isolation has been suggested for another compressor project currently under construction for Esso at Longford, Victoria. The cost is estimated at $60 each per pipe support.

Vibration measurements on the surface of the lagged pipe confirmed that the sound radiation from the pipes was negligible and that the acoustic lagging had performed satisfactorily, although the overall result was limited by flanking at the pipe support.

Vent noise

One noise source that had not been considered in the initial modelling was the emergency blowdown system. Consisting of 80m of unlagged 350dia pipe discharging into an attenuated blowdown vessel. However, its use is infrequent.

Assessed on a sleep disturbance basis, the noise level from the vent only needed to be 105dB(A) but was guaranteed by the silencer vendor to be 75dB(A) at 1m. Our concerns were raised when the local farmer commented that during one blowdown he could hear the venting when operating his tractor and wearing earmuffs. The venting was audible above the tractor diesel engine at a distance of 300-400m.

Subsequent measurements indicated that the noise level at 30m from the blowdown vessel was as high as 1224dB(A). This was not due solely to the vent outlet but the breakout from the 80m of unlagged vent pipe. Vibration measurements on the discharge of this pipe indicated unprecedented vibration levels on the case of a process pipe. The vibration spectrum was broadband. Maximum vibration levels are presented in Figure 3 below. At 3m from the pipe the noise was measured at L_{max} 108dB(A.

Figure 4
Pipe Vibration during Venting Lmax

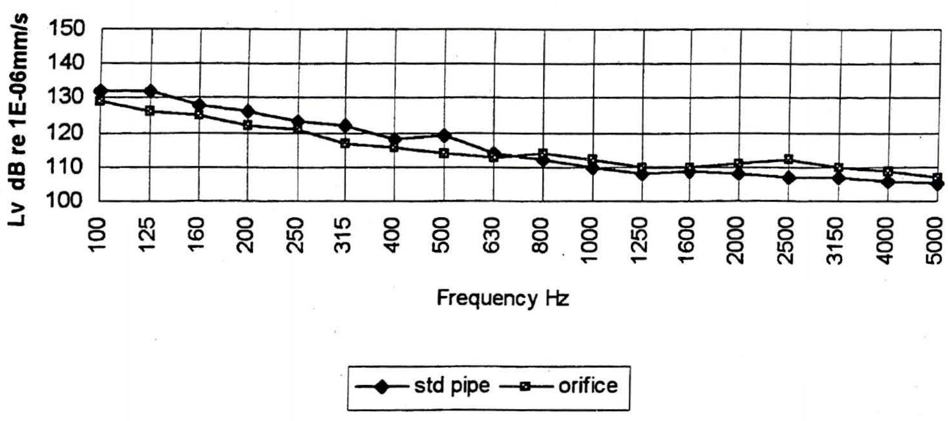

9.ACKNOWLEDGEMENTS

This technical information was supplied with kind permission of Transmission Pipelines Authority now GPU GasNet, Worley Australia and Solar Turbines Australia.

8. REFERENCES

1. Solar Turbines Incorporated, Noise Prediction Guidelines for Industrial Gas Turbines, Doc Ref SPNP/898/4M, dated August 1998.
2. Solar Turbines Incorporated, Noise Prediction Guidelines for Industrial GasTurbines, Doc Ref T10S/795, dated July 1995.
3. D. A. Bies and C. H. Hansen, Engineering Noise Control, 2nd Ed, E & F N Spon 1988.
4. HGC Canada, Acoustical Pipe Lagging Systems Design and Performance – Report PR-264-9725, 1997.
5. CONCAWE The Propogation of Noise from Petrochemical Complexes to Neighbouring Communities Report 4/81 Den Haag, 1981.
6. Renzo Tonin, Estimating Noise Levels from Petrochemical Plants, Mines and Industrial Complexes, Acoustics Australia Vol 13 Issue 2.

AUSTRALIAN ACOUSTICAL SOCIETY CONFERENCE

ACOUSTICS TODAY

Melbourne, 24 – 26 November, 1999.

SAMPLING THE REVERBERANT SOUND PRESSURE FIELD FOR SOUND POWER AND TRANSMISSION LOSS MEASUREMENTS IN THE LABORATORY

E.A. Lindqvist, P. Carrozza, J.L. Watson and P.E. Dale

RMIT, Acoustics Group in the Department of Applied Physics

ABSTRACT

Different measurement standards give different instructions regarding the number of microphone positions and their positions relative to one another to be used in obtaining an estimate of the average sound pressure level in the reverberant field. Most standards specify a random selection of microphone positions under certain restrictions. In a narrow band, diffuse sound field, the cross-correlation coefficient between two microphone signals is expected to be a $\sin(kr)/kr$ function, k being wavenumber and r the separation distance of the microphones, which indicates that positions half a wavelength apart are statistically independent. Measurements were taken at 0.2 metre interval along three separate lines, each 3.4 m long, in the reverberation chamber at RMIT. The spatial autocorrelation coefficient of time averaged microphone signals in each position was calculated for the third octave bands between 50 and 315 Hz. It was found that the $\sin(kr)/kr$ function was not closely approximated. We suggest an alternative approach to spatial sampling.

1. INTRODUCTION

Round Robin tests have clearly shown the necessity for improving the reproducibility for sound transmission loss measurements made in accordance with ISO 140 part 2 in different laboratories, see Goydke 1998. Goydke specifically mentions different niche geometries and methods of mounting the partition as sources of variability in the results obtained. Another factor is the sampling of the sound pressure level in the reverberant field, which is the topic of this paper. Current standards require the field to be sampled at a limited number of microphone positions, with certain constraints placed on the choice of positions. Our intention here has been to investigate whether another sampling method could reduce the measurement errors.

There are different instructions in different standards regarding the relative positions of the microphones for measuring the average sound pressure level in the reverberant field. Is 0.7 m[1] or $\lambda/2$[2] at the centre frequency of the lowest frequency band of interest for the measurements, more appropriate as a limit to how close microphone positions can be? For a measurement in the 100 Hz third octave band, $\lambda/2$ is 1.7 m. This more stringent criterion severely limits the number of microphone positions that are physically possible to find in the room. Initially the question was: "How close can microphone positions be allowed to be to give a good estimate of the average sound pressure level?" The question actually changed during the project as will become clear below.

The main concern is spatial averaging at low frequencies. The modal density is low in these bands and therefore larger variations in sound pressure with position are expected than at higher frequencies.

Today in Australia, sound transmission loss measurements are not normally made below 125 Hz. However, due to an increasing awareness of disturbance due to low sound transmission loss at lower frequencies, there is a push internationally to make measurements down to 50 Hz.

2. MEASUREMENTS

Microphone measurements were made at 0.20 m spacings along three separate straight lines in the reverberation chamber at RMIT. The positions of the lines were chosen so as to allow a length of up to 3.4 m to be sampled without contravening rules in the standards regarding proximity to room surfaces or diffusers. Each of the lines was at an angle of at least 10° relative to any of the room surfaces.

The field was excited with pink noise through a single 12-inch loudspeaker. The microphone signals were fed through third octave filters. The microphone signal data collected was limited to the third octave bands between 50 and 315 Hz.

For each microphone position a sequence of 60 samples of the voltage signal corresponding to acoustic pressure, averaged over 1 second intervals, was recorded using a Bruel and Kjaer Real Time Analyser type 2133. Two Bruel and Kjaer, half inch microphones of the same type were used simultaneously, one in the reference position at one end of the line and the other at an integer multiple, j, of 0.20 m increments along each line. The signals through the two channels were carefully checked to ensure that they had the same amplitude and phase calibration.

3. RESULTS AND PROCESSED DATA

Computations were done using the virtual instrument package 'LabView" and some plots have been made using Excel.

---

[1] See AS 1191 - 1985

[2] See ISO 140 Part 3, 1995

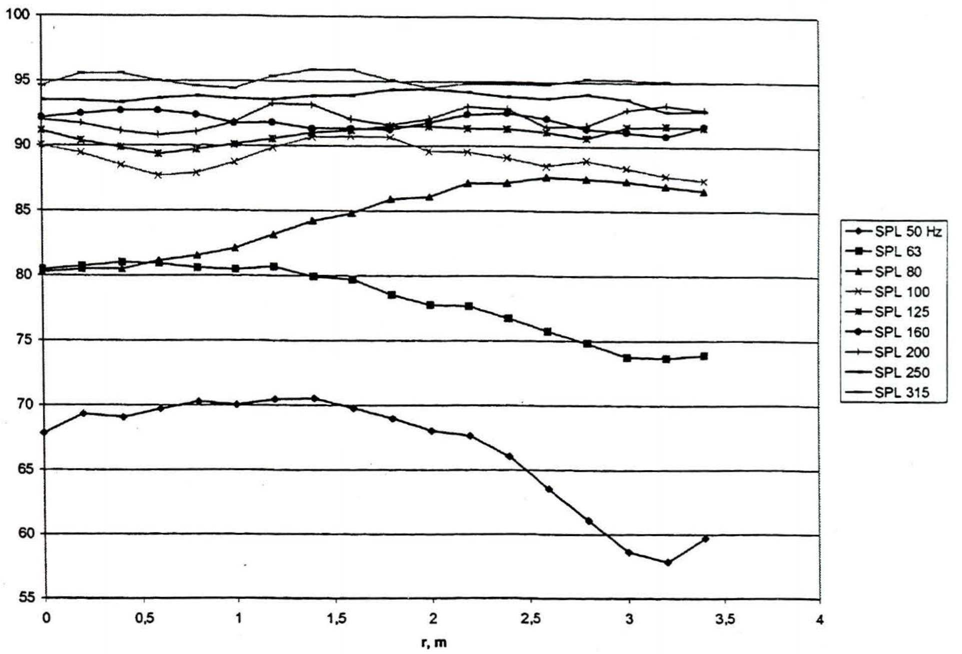

Figure 1. Sound pressure level in different 1/3-octave bands as a function of distance along line A.

The voltage signals could be converted into sound pressure levels and plotted as functions of distance along each measurement line. The results for the first line are shown in figure 1. These results, which are typical of the three lines, show at least three things quite clearly. First the overall range of sound pressure level values decreases with increasing frequency. Secondly, at the lowest frequencies, the variations from maximum level to minimum level are slow. The variations occur more rapidly with increasing frequency. This already indicates that the spatial auto-correlation function will vary more slowly with distance at lower frequencies.

Finally the graphs in figure 1 show that the energy in the field for the loudspeaker system used is relatively low at low frequencies and increases with frequency, rapidly at first and then more slowly. This was rather accidental but is convenient for showing the variations in sound pressure level at different frequencies.

The variations in sound pressure level at 100 Hz, for each of the three lines are shown in figure 2. The range of sound pressure level values is in the worst case 4.2 dB and the standard deviation for each line of results is 1.07, 0.63 and 1.81 dB respectively. Unfortunately although the average levels were constant to within approximately 2 dB, no special effort was made to ensure that the power output of the source was the same for each line of microphone positions, so the average sound pressure levels cannot be compared.

In earlier work cross-correlations, in particular, have been used to ascertain whether data points are correlated or not. The assumption is that only uncorrelated values of any quantity describing the sound field give statistically independent samples.

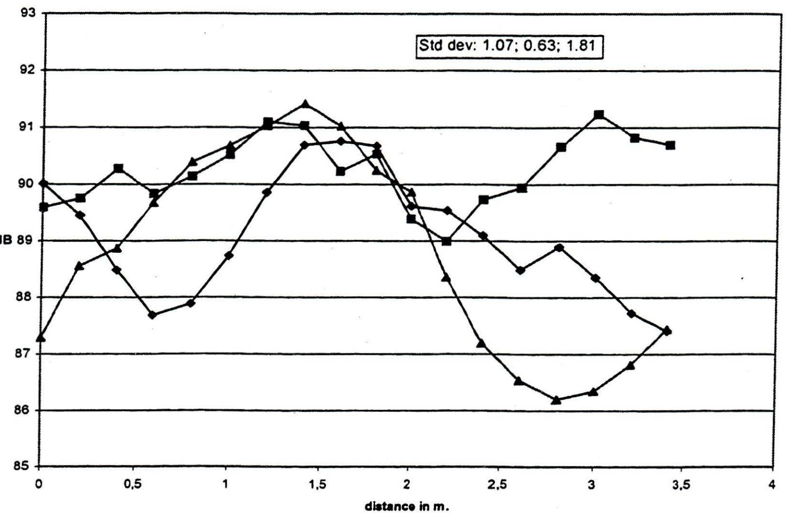

Figure 2. SPL as function of r along lines A, B and C at 100 Hz.

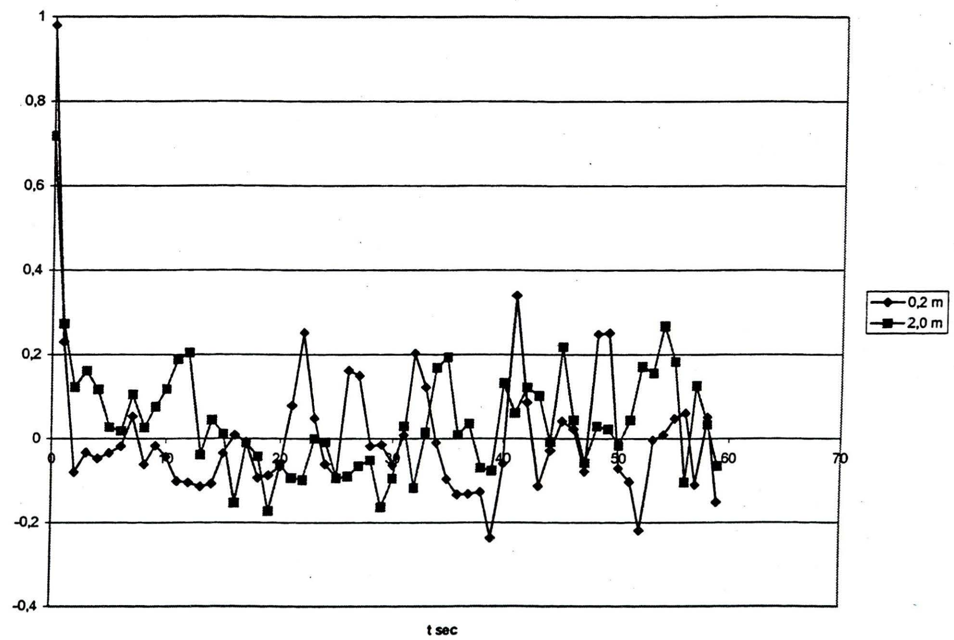

Figure 3. Example of temporal cross-correlation function, two microphone positions 0.2 and 2.0 m apart, 100 Hz band.

Examples of temporal cross-correlation coefficient between the two simultaneous microphone signals are shown in figure 3 for 100 Hz with the microphones 0.2 and 2.0 m apart. Apart from the initial value, the values seem to be less than 0.2 with a few exceptions and random.

The 120 samples in each microphone position were averaged to obtain the time average pressure in each position. These time averaged pressure values were then treated as a single signal varying with distance along the line, *p(r)*. Computing the spatial auto-correlation coefficient for these signals revealed the results examples of which are shown in figure 4, where the spatial 'delay' value has an upper limit of 2.8 m, which means that at least five products are averaged in computing the coefficient. The $\sin(kr)/kr$ function is shown for comparison, where r is the microphone separation distance and k is wavenumber at the centre frequency of the third octave band.

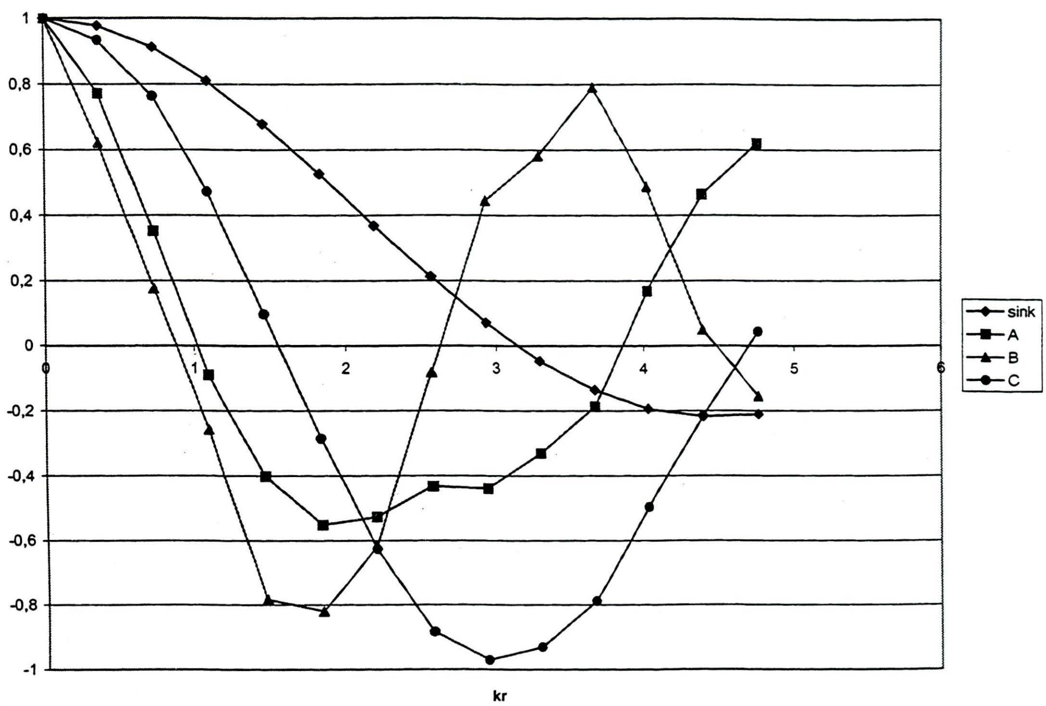

Figure 4. Spatial autocorrelation along lines A, B and C at 100 Hz. Sink function also shown.

4. DISCUSSION

The space that we are sampling is the three dimensional reverberant field. There are two problems we need to address. The first is how best to sample the field, the second is how to ascertain the statistical uncertainty in the measurements. The 'best' method of sampling would be the method that gives the highest precision with a 'reasonable' effort or number of sampling points and a valid means of ascertaining the measurement uncertainty.

In none of the third octave bands investigated was the measured correlation coefficient closely approximated by the $\sin(kr)/kr$ function. Two differences stand out. Firstly the zero crossing point is in most cases (for 25 out of 27 graphs) at values of kr less than $\pi/2$ and typically between $\pi/6$ and $\pi/4$. Secondly although the coefficient does fluctuate in a roughly sinusoidal fashion, the decrease in amplitude of the maxima and minima does not seem to decrease as $1/kr$.

The measurements show that the positions corresponding to zero correlation are less than $\lambda/2$ apart but somewhat variable. Moreover, whatever the actual autocorrelation function is, only relative positions which give zero autocorrelation are independent. Positions up to the first zero crossing are not uncorrelated with positions between the first and second crossing point. If we were to insist on only sampling at uncorrelated points, it would mean finding the relative positions, in each frequency band, which are uncorrelated and setting up a grid of measurement points to satisfy this condition. The alternative is to abandon this approach altogether and find a more viable solution.

Using the same plane wave model of the field as used to derive the $\sin(kr)/kr$ function for the correlation coefficient but averaging over the wavenumber bandwidth, k_1 to k_2, gives[3]

$$\rho(r) = \frac{3}{r^3(k_2^3 - k_1^3)} \left|\sin(kr) - kr\cos(kr)\right|_{k1}^{k2}.$$

This function does have first zero crossing at values of kr less than $\pi/2$ and the amplitude decreases at a rate less than $1/kr$. However the underlying model is still that of a diffuse field.

If a few microphone positions are chosen randomly, there is always a probability that the measured average will be significantly biased. The graphs of sound pressure levels measured as a function of distance along a line show that the values tend to change relatively slowly over one wavelength. To illustrate the probability of bias and adopting, for the sake of argument, the $\sin(kr)/kr$ auto-correlation function for acoustic pressure, then a cell of volume $(\lambda/2)^3$ about a local maximum will have a higher than average pressure squared value. Alternate cells will have 'higher than average' and 'lower than average' values.

This simplistic model gives a binomial distribution for the selection of higher than average or lower than average values of the pressure. For a random choice of five microphone positions, the probability that each position has a higher than average value of sound pressure is 3% but the probability of at least 4 randomly chosen positions having higher than average values is 18.7%. The probability of choosing at least four higher than average or four lower than average values is thus about 40%.

Imagine sampling a traffic noise signal. While a heavy truck is passing, we can expect elevated noise levels but we sample at regular intervals, which are normally closer that the time taken for the bypass of a single vehicle. "Sampling for digital data is usually performed at equally spaced intervals"...... The problem then is to determine an appropriate sampling interval .... sampling at points, which are too close together, will yield correlated and highly redundant data"[4]. The normal way of sampling such a signal is to take close, correlated samples.

It is perhaps inappropriate to think of sampling the sound field as a number of independent trials like pulling cards out of a pack. It is more appropriate to think of the noise excited field as a stationary 'space' signal in analogy to a stationary time

---

[3] Lindqvist, 1973
[4] Bendat and Piersol, § 7.3.1

signal. The sound pressure is a continuous function of space and of time. The method, which would give us the most accurate result would be to use closely spaced microphone positions throughout the three dimensional reverberant field. Since this is impracticable, what spatial sampling procedure gives the best estimate of the average pressure?

There are at least three spatial sampling options, ignoring for the time being the possibility of using a continuous microphone trace. These are 1) a random selection of positions, 2) a regular grid or grids of positions or 3) regular spatial sampling along a straight line. If we do measure along straight lines, it would seem to be appropriate to choose lines, which are at significant angles to all surfaces of the laboratory chamber.

Options for sampling at regular intervals along the line: are 1) a diameter including the corners, 2) an arbitrary line one wavelength long at the lowest frequency, and 3) an arbitrary line across the room from one surface to another, avoiding or not, positions close to the surface. The first choice has the disadvantage that it is probably difficult to implement in most laboratories because of the presence of fixed diffusers. The main disadvantage of the second proposal is that measurement over one or more whole wavelengths cannot be satisfied in all third octave bands simultaneously. The third alternative has no apparent major drawbacks and therefore seems to be the best option.

One advantage of using a line, of length L, between two surfaces relates to Fourier Analysis, which assumes that the signal segment measured is regularly repeated. The room is effectively mirrored in each surface and the signal is thus effectively repeated with a repetition interval of L m. Sound pressure measured along a line L thus represents a repetitive signal in space.

There is also the question of whether positions close to the surfaces of the room should be included in the sample. The levels are expected, and found, to be higher close to surfaces than farther away, because of standing waves being excited due to wave interference with pressure maxima close to a reflecting surface. The total energy in the field does include the energy in the field close to the surfaces but whether this should be included in measuring the average pressure squared is another matter. Suppose we take the depth of what might be called the 'surface proximity field' to be $\lambda/2$, or 1.7 m at 100 Hz, out from the surfaces. Then for a room of volume 200 m^3, the surface field occupies of the order of 90% of the volume of the room, depending on the actual shape of the room.

The next question relates to the 'sampling rate' in space. It is to be anticipated that there should be 'several' positions per wavelength, at least at the lower frequencies. As a starting point let us choose 3 positions per wavelength at 250 Hz, which corresponds to about 0.5 m separation between positions.

Our proposal is to adopt the following procedure. Choose a line of length $L > 3.5$ m between opposite walls, which is skewed by a minimum of 10° relative to all room surfaces. The 3.5 m minimum length is approximately equal to one wavelength at 100 Hz. Divide the line up into a number of increments, N, of length $\Delta s = L/N$, such that Δs is close to 0.5 m. Measure the sound pressure level at each of the N positions along the line starting at $1/2(L/N)$ m away from the first wall. The measurement procedure can of course be repeated along other lines, to which certain restrictions relative to the first line can be imposed. The average sound pressure level and standard deviation are calculated in the standard way.

More measurements to confirm how repeatable the average sound pressure level and standard deviation is using the sampling method proposed will be made before the conference.

REFERENCES

Andres H.G., Über ein Getetz der Räumlichen ZufallsSchwankung von Rauschpegeln in Räumen und seine Anwendung auf Schalleistungsmessungen. Acustica vol 16, p. 279 – 294, 1965-66.

Bendat J.S. and Piersol A.G. Random Data: Analysis and Measurement Procedures. Wiley-Interscience, New York 1971.

Bodlund K. A new quantity for comparison measurements concerning the diffusion of stationary sound fields. J. Sound and Vib., vol 44 no. 2, p. 191 – 207, 1976

Cook R.K., Waterhouse R.V., et al. Measurements of Correlation Coefficients in Reverberant Sound Fields. J. Ac. Soc. Am., vol 27, no. 6, 1955

Goydke H., Investigations on the precision of laboratory measurements of sound insulation of building elements according to the revised standard ISO 140. INTERNOISE 98, Christchurch, New Zealand.

Lindqvist E.A., A comparison between continuous averaging and discrete averaging of sound pressure level in a reverberant room. C.T.H.(Sweden), Dept of Building Acoustics, Report 73-15, 1973.

AUSTRALIAN ACOUSTICAL SOCIETY CONFERENCE

ACOUSTICS TODAY

Melbourne, 24 – 26 November, 1999.

FLOW RESISTIVITY AS A MEASURE OF SOUND ABSORPTION WITH APPLICATIONS

J P Parkinson[1], M D Latimer[2] and J R Pearse[1]

[1]Department of Mechanical Engineering, University of Canterbury, Christchurch, New Zealand

[2]D G Latimer and Associates Ltd, P O Box 12 032, Christchurch, New Zealand

ABSTRACT

Flow resistance measuring equipment was developed to help specify the properties of various sound insulating and sound absorbing materials. The equipment was used to measure the flow resistance of common polyurethane foams, fibrous boards and fabrics and the results related to a microscope examination of the materials. The inhomogeneity of a foam sheet was determined by studying the variation of flow resistance in five samples taken from the sheet. Examples are given to show the importance of flow resistance in computer modelling of sound absorbers.

1. INTRODUCTION

Porous materials, such as glass wools, foams and fabrics are commonly used to absorb sound. They typically consist of a network of interlocking pores that convert incident sound energy into heat.

An acoustic material can be described by many parameters based on the physical properties of the material such as the density and thickness of the material, the porosity, flow resistance and stiffness. Of these, the flow resistance is considered the most characteristic of a porous material's acoustic absorption, Bies et al [1] and Ingard [2]. The porosity of a material is also essential for theoretical modelling of porous materials.

2. THEORY

The steady flow resistance of a porous layer is defined as the ratio of static pressure drop across the layer to mean velocity of flow through the layer. It is usually implied that the velocity is low enough so that the pressure drop is proportional to the velocity.

Flow resistance is usually quoted in mks rayls (or Ns/m^3) while flow resistivity is quoted in mks rayls per metre (or Ns/m^4). Porous materials typically have a flow resistivity of about 20,000 mks rayls/m.

At a microscopic scale, the flow resistance is determined by the equivalent width between fibres or pores and the number of these per unit area. In oscillatory flow, as is the case for sound waves, the pressure drop contains a component proportional to the velocity and also a component proportional to the acceleration. This second component becomes apparent in flow resistance measurements at higher velocities.

Flow resistive fabrics and bulk materials tend to obey the Forchheimer equation [3]

$$\Delta p = aV + bV^2 \qquad (1)$$

where a and b are constants, Δp is the steady flow pressure drop and V is the flow speed. If $\Delta p/V$ is plotted against V, the constant a is found from a regression line through the data. a is equal to the "viscous" flow resistance or the product of the flow resistivity and material thickness at very low flow speeds.

3. EQUIPMENT

The flow resistance apparatus was built in the Department of Mechanical Engineering, University of Canterbury and is shown in figure 1.

APPARATUS FOR MEASUREMENT OF FLOW RESISTANCE

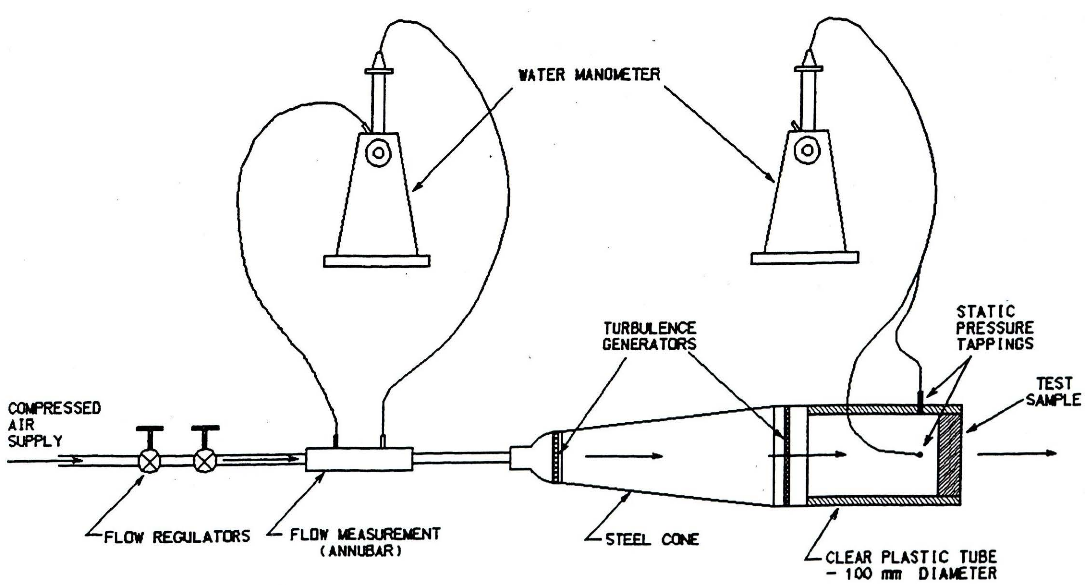

Figure 1 Flow resistance apparatus.

4. PROCEDURES

Annubar calibration

A ½" BSP annubar was calibrated using water as the working fluid. The results were then converted to air.

General procedures

Australian standard, AS 2284.14-1979 [4] and ASTM C522-1987 [5] were referred to with regard to the air flow resistance tests carried out.

Fabrics were mounted at the end of the pipe and secured with a steel pipe clip. Bulk porous materials were punched with a diameter of 102 mm to ensure a good fit inside the 100 mm diameter pipe. The edge of the bulk material in contact with the pipe was sealed with a gel. Typically, six flow rates and the corresponding static pressures were measured for each sample.

Repeatability

Repeatability tests were carried out on two foam samples. Five samples were taken from a 1.2 x 2.4m foam sheet and tested to ascertain the amount of inhomogeneity in a sheet. Six tests were carried out on one of the fabrics to measure its inhomogeneity.

Crushed foam

Foam was crushed by running it through rollers with a very small gap.

5. RESULTS

Table 1 Flow resistance results

Material	Description	Flow resistivity (mks rayls/m)
Bulk materials		
46 mm foam	Combustion modified foam	18360
46 mm foam (c)	Crushed, combustion modified foam	13700
23 mm foam	Combustion modified foam	9800
23 mm foam (c)	Crushed, combustion modified foam	8800
25 mm Polyester	Fibrous board - 80 kg/m^3, 25 mm	11700
25 mm Fibreglass	Fibrous board - 90 kg/m^3, 25 mm	47000
Homogeneity Test		
24 mm foam NC1	Non-crushed combustion modified foam 1.	10110
24 mm foam NC2	Non-crushed combustion modified foam 2.	8580
24 mm foam NC3	Non-crushed combustion modified foam 3.	9000

24 mm foam NC4	Non-crushed combustion modified foam 4.	12780
24 mm foam NC5	Non-crushed combustion modified foam 5.	10570
Repeatability Test		
24 mm foam NC4	Non-crushed combustion modified foam 4.	12780
24 mm foam NC4r	Retest on above foam 4.	12760

Bulk materials

Crushing the foam had a large effect on its flow resistivity. Crushed foam had a flow resistivity 25% less than the non-crushed 24 mm thick foam. Crushing the partially reticulated foam reduced the number of closed cells. This gave less resistance to air flow and hence a lower flow resistivity. The difference was not as large for the 23 mm thick foam samples but was still apparent (10% reduction in flow resistivity).

The 25 mm polyester board (80 kg/m^3) had a flow resistivity of 11700 mks rayls/m while corresponding figure for the 25 mm fibreglass board (90 kg/m^3) was 47000 mks rayls/m when the materials had similar densities. The polyester fibres had a density of approximately 1380 kg/m^3 while the fibreglass fibres were almost twice as dense at 2600 kg/m^3. The difference in flow resistivity implies that the fibreglass was packed significantly tighter than the polyester. This was observed in microscopic pictures of the materials.

Repeatability tests carried out on two foam samples and gave an experimental repeatability of 2.5%. Five samples of foam from one sheet showed a 32% variation in flow resistivity. This variation was attributed to the manufacturing process.

Models - sensitivity analysis

An analysis was carried out on the sensitivity of an absorber model to the various material parameters. The model of Allard et al [6,7] was used for the analysis. It is based on the work of Biot [8] which allows three types of sound wave to propagate in an elastic framed porous material. The tortuosity, porosity and flow resistivity were examined across common parameter ranges. Each parameter was held at an average value while one parameter was varied from the minimum to maximum of the range of interest, table 2. This was carried out on each parameter for a 24mm thick layer of foam.

Table 2 Material parameters

	Tortuosity ks	**Frame Density** pl (kg/m^3)	**Flow Resistivity** r (mks rayls/m) (or Ns/m^4)	**Porosity** Por	**Complex Shear Modulus** N (N/cm^2)	**Poissons Ratio** v	**Form Factor** c
MAX	7.8	33	174000	0.99	80+21i	0.4	3.37
MIN	1.0	16	2500	0.90	0.8+0.08i	0.0	1.00
AVG	2.2	27	40533	0.97	13.4+2.4i	0.3	1.67

Parameter definitions

Porosity *por* is the amount of air in a porous material that can participate in sound propagation. For open cell reticulated foams, the porosity can be determined if the density ρ of the frame material is known:

$$por = 1 - \frac{m}{V\rho} \tag{2}$$

where V is the volume and m the total mass of the sample. Open cell foams typically have porosity greater than 0.90.

Shear modulus N is a measure of foam stiffness. It is a complex quantity with a typical value of around 10(1+0.1i) N/cm^2.

Tortuosity k_s of a foam is a measure of the "straightness" of the foam pores. Air in the pores is filled with a conducting fluid, and the electrical resistivity r of the material is measured. The tortuosity is then given by:

$$k_s = h\frac{r}{r_f} \tag{3}$$

where r_f is the electrical resistivity of the conducting fluid. Reticulated foams typically have a tortuosity close to 1, while partially-reticulated foams (some closed cells) can have values as high as 7.

Form factor c is a measure of the frequency dependence of density ρ. Typical values are 1.0 for circular cross-section shapes, 1.07 for square shapes and 0.78 for rectangular slits.

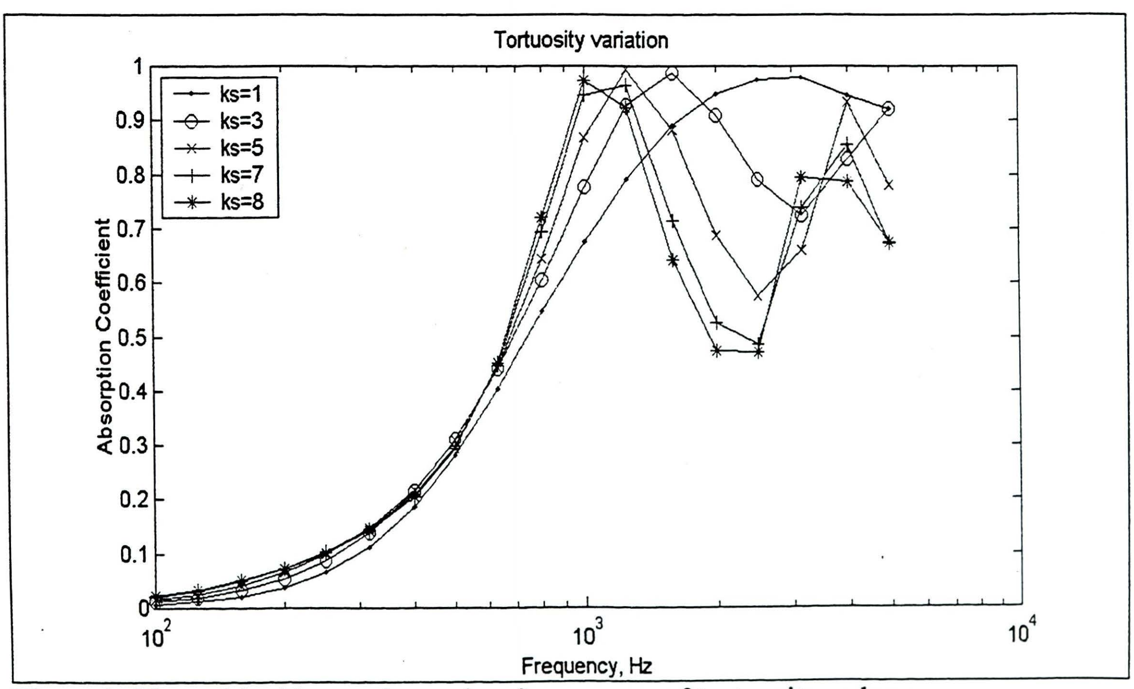

Figure 2 Normal incidence absorption for a range of tortuosity values.

Results

Figure 2 shows the absorption trends for the layer of foam with various tortuosity values. It is apparent that as the tortuosity increases the absorption peak moves to lower frequencies while the absorption at medium to high frequencies is reduced. Clearly, the absorber model is quite sensitive to the tortuosity parameter.

The variation in absorption of the foam layer with porosity is shown in figure 3. The model shows only a slight variation in absorption for the range of porosity chosen.

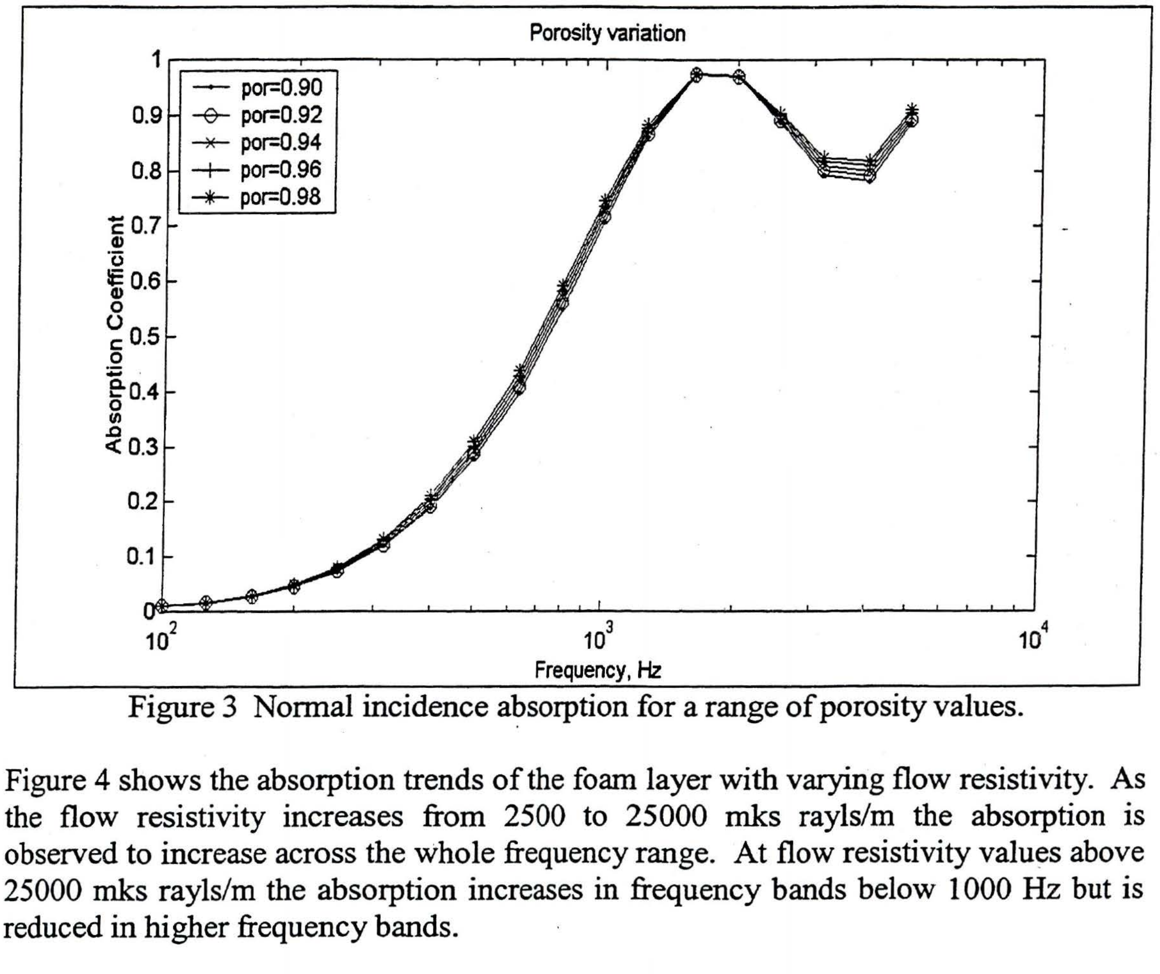

Figure 3 Normal incidence absorption for a range of porosity values.

Figure 4 shows the absorption trends of the foam layer with varying flow resistivity. As the flow resistivity increases from 2500 to 25000 mks rayls/m the absorption is observed to increase across the whole frequency range. At flow resistivity values above 25000 mks rayls/m the absorption increases in frequency bands below 1000 Hz but is reduced in higher frequency bands.

The use of flow resistance in an absorber model is illustrated in figure 5. The measured data was determined via the reverberation room method and with respect to ISO 354:1988 [9]. The "1D" model referred to in figure 5 is the same as that used in figures 1 to 4 but with the absorption coefficients statistically averaged over all angles of incidence. The "1D + edge effect" model is the previous model with a correction for edge effects according to Thomasson [10]. The parameters used in the models are shown in table 3.

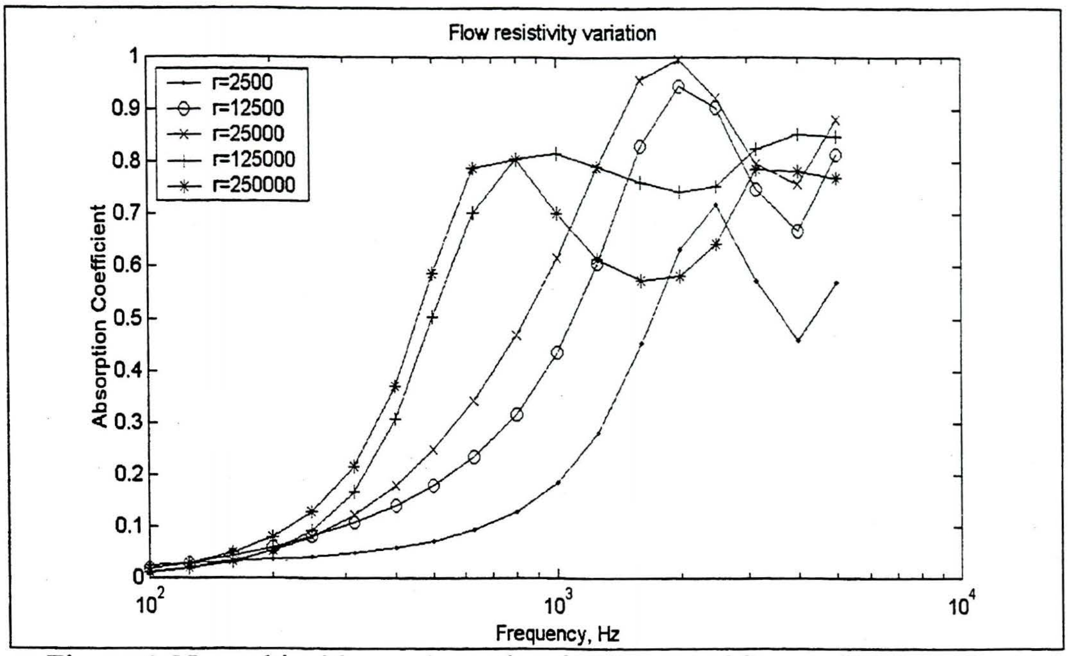

Figure 4 Normal incidence absorption for a range of flow resistivity values.

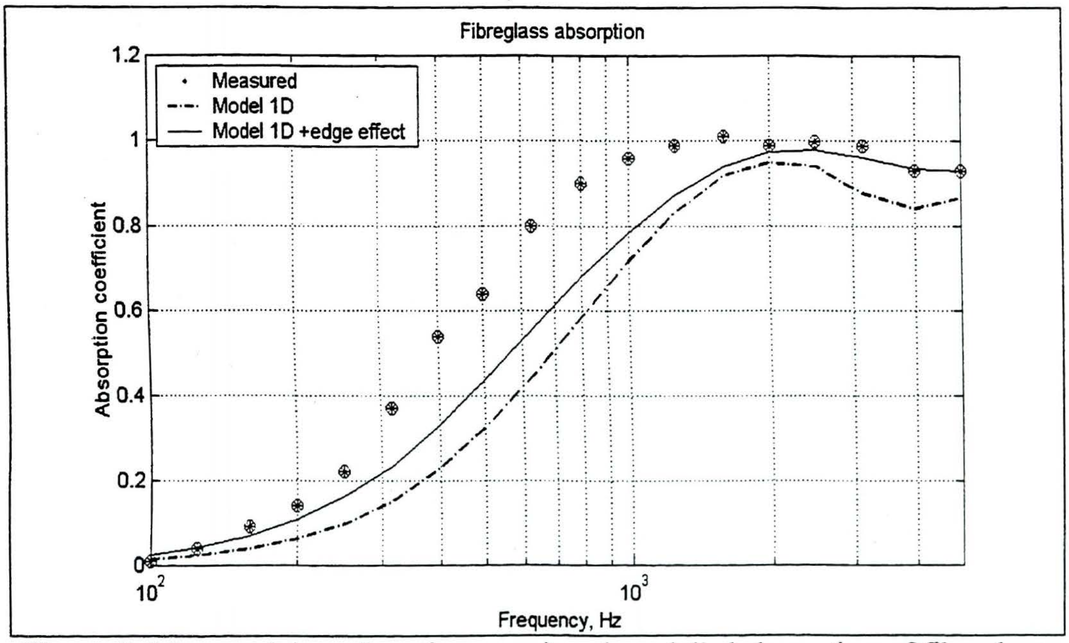

Figure 5 Measured (reverberation room) and modelled absorption of fibreglass.

Table 3 Parameters used for the model results in Figure 5.

Thickness t (mm)	**Tortuosity** ks	**Frame Density** pl (kg/m^3)	**Flow Resistivity** r (mks rayls/m) (or Ns/m^4)	**Porosity** Por	**Complex Shear Modulus** N (N/cm^2)	**Poissons Ratio** v	**Form Factor** c
24	2	90	47000	0.94	10+1i	0.3	1.4

6. CONCLUSIONS

Apparatus has been developed to accurately measure the flow resistance of porous materials. The equipment and procedures used give repeatable results within 2 to 3%. However, the materials tested showed large variations in flow resistance: 17% variation in a fabric sample and 32% variation in a foam sheet. Crushing the foam samples was observed to reduce flow resistivity between 10 and 25%.

The sensitivity analysis of an absorber model showed that absorption was very dependant on the material's tortuosity and flow resistivity and less dependant on its porosity. The absorber model was shown to approximately predict the absorption of a fibreglass absorber.

REFERENCES

[1] D Bies, C Hansen, 'Flow resistance information for acoustical design', Applied Acoustics, 13, 1980, pp 357-391.

[2] U Ingard, 'Notes on sound absorption technology', Noise Control Foundation, 1994.

[3] P Forchheimer, 'Wasserbewegung durch Boden', Zeitschrift des Vereines deutscher Ingenieure, 50, 1901.

[4] Australian Standard AS 2261.14-1979, Porosity air flow test for flexible cellular polyurethane, Standards Association of Australia, 1979.

[5] ASTM C 522-1987, Standard test method for airflow resistance of acoustical materials, American Society for Testing and Materials, 1993.

[6] J Allard, B Brouard, D Larfarge, 'A general method of modelling sound propagation in layered media', Journal of Sound and Vibration, v183, no. 1, pp 129-142, 1995.

[7] J Allard, C Depollier, P Rebillard, A Cops, W Lauriks, 'Inhomogeneous Biot waves in layered media', Journal of Applied Physics, v66, no. 6, pp 2278-2284, 1989.

[8] M Biot, 'Theory of propagation of elastic waves in a fluid-saturated porous solid', Journal of the Acoustical Society of America, v28, no. 2, pp 168-191, 1956.

[9] International Standard ISO 354:1988, Acoustics - Measurement of sound absorption in a reverberation room, International Organisation for Standardisation, Switzerland, 1988.

[10] S Thomasson, 'Theory and experiments on the sound absorption as function of the area', Trita-TAK; 8201, Royal Institute of Technology, Stockholm, 1982.

AUSTRALIAN ACOUSTICAL SOCIETY CONFERENCE

ACOUSTICS TODAY

Melbourne, 24 – 26 November, 1999.

ACCELEROMETER CALIBRATION WITH IMPERFECT EXCITERS (SHAKERS)

L. P. Dickinson and N. H. Clark

CSIRO National Measurement Laboratory (NML)

ABSTRACT

In the calibration of accelerometers, errors may be introduced due to deficiencies of the vibration exciter, the motion of which may deviate considerably from rectilinear simple harmonic motion at some frequencies. Such frequencies can be identified by fitting a theoretical curve to frequency response data from the accelerometer calibration. The errors can be reduced by application of some simple techniques, which are described in this paper and illustrated by experimental results.

1. INTRODUCTION - the transverse motion problem

An ideal accelerometer produces an output only when it is subjected to acceleration in the direction of its sensitive axis. Unfortunately, any real accelerometer produces output from other kinds of excitation [1], e.g. from thermal transients, radiation etc, and in particular, from accelerations in directions other than along its sensitive axis. This latter phenomenon is called transverse sensitivity,

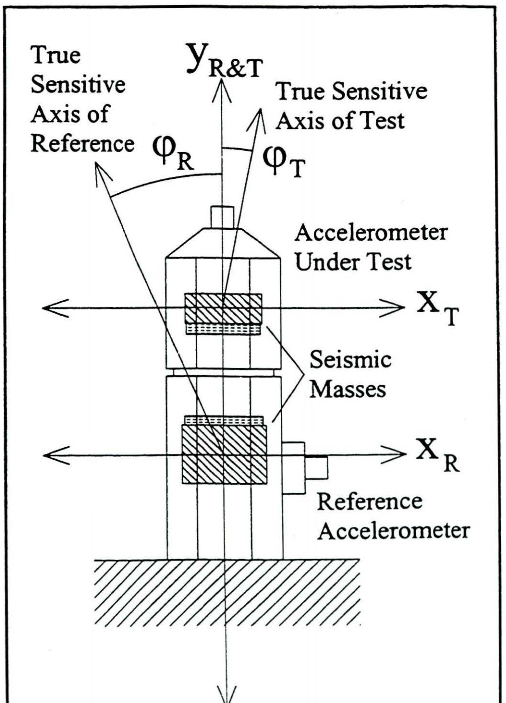

Figure 1 – The most sensitive axis of any real accelerometer is offset by an angle φ from its concentric axis.

and it can be particularly troublesome when it is desired to measure vibration in a particular direction, in the presence of large transverse vibrations. The "transverse sensitivity ratio" (TSR) of an accelerometer is defined [1] as the ratio of the output of the accelerometer, when oriented with its axis of sensitivity transverse to the direction of the input, to the output when the axis of sensitivity is aligned in the direction of the same input. TSR values are commonly about 0.01 to 0.05. It is generally assumed that transverse sensitivity is attributable to, or equivalent to, misalignment between the true sensitive axis of the accelerometer and the geometric axis, as shown in Figure 1. Clearly, this varies as a function of direction in the transverse plane.

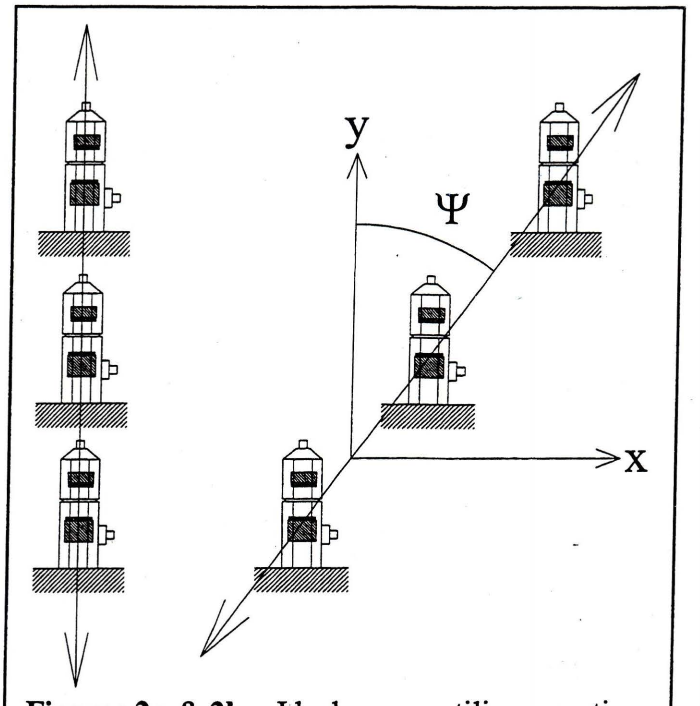

Figures 2a & 2b – Ideal pure rectilinear motion and motion with a transverse element at an angle of Ψ to the concentric axis

The problem also arises when calibrating accelerometers. For calibration, the output of an accelerometer is measured whilst it is subjected to nominally rectilinear vibration of "known" amplitude, and this is repeated at several frequencies in order to determine the frequency response. Unfortunately, real vibration exciters (shakers) are also not ideal, and there is always some deviation from rectilinearity. These deviations, which vary with frequency and with mass loading, often introduce unacceptably large error and uncertainty into a calibration. The "transverse motion ratio" (TMR) of a calibration exciter is defined as the ratio between the amplitude of exciter motion in a direction transverse to its nominal direction of motion, and the amplitude in the nominal direction. Ideally, TMR should be zero, but values of about 0.3 are not uncommon at certain frequencies.

Figure 1 and Figure 2 illustrate the manner in which non-ideal motion can introduce error when an accelerometer is being

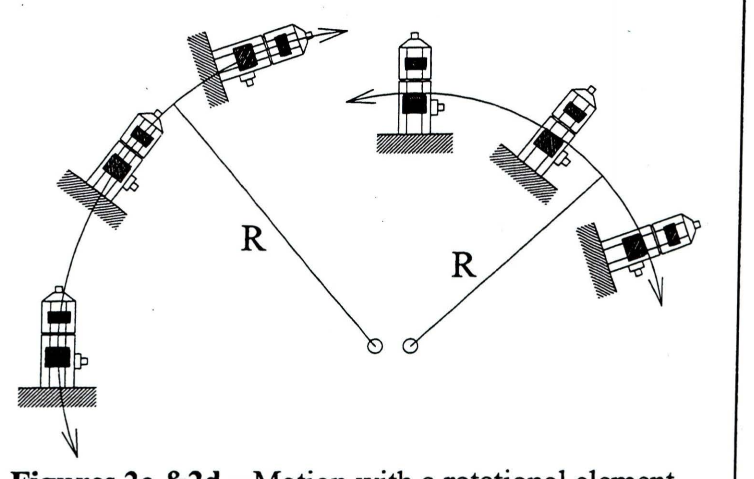

Figures 2c &2d – Motion with a rotational element

Puruswatc

V., T., L

calibrated by comparison with a reference standard accelerometer. Figure 2(a) shows the ideal case, in which both accelerometers are subjected to identical rectilinear motion along their coincident sensitive axes. The sensitivity of the test accelerometer is found simply from the ratio between the two measured outputs, multiplied by the sensitivity of the reference accelerometer. In Figure 2(b), the motion is still rectilinear, but it has a component transverse to the accelerometer axes, identical for the two accelerometers. As the two accelerometers will have transverse sensitivities which in general are neither identical in magnitude nor direction, such motion can introduce an error in the comparison calibration up to the value of the TMR times the sum of the two TSRs.

In Figures 2(c) and 2(d), the motion is further complicated by a rocking component about a center, distant R from the accelerometers. In both cases, the motion to which each accelerometer is subjected can be resolved into an axial linear component, a transverse linear component, and a component of rotation about the accelerometer's effective center of mass. Most piezoelectric accelerometers do not respond to the rotational component, but, as a result of the rocking, the transverse components are no longer identical for the two accelerometers.

2. METHODS OF DEALING WITH TSR AND TMR.

John Field [2] encountered this problem when attempting to calibrate a triaxial accelerometer array for a machine tool dynamometer. For the calibration, he took three sets of readings of accelerometer outputs, with the accelerometer array oriented in each of three orthogonal directions, and then solved the nine (complex) simultaneous equations. The excitation was assumed to remain constant for the three sets of readings.

J D Ramboz [3] developed a method for separating the TSR of an accelerometer from the TMR of the shaker. In Ramboz's method, the accelerometer is oriented with its sensitive axis perpendicular to the nominal direction of excitation. Four sets of readings are taken and between each set the accelerometer is rotated through 90 degrees about its own sensitive axis. A simple algorithm is then applied to solve for TSR and TMR. It is assumed that the main axis of sensitivity of the accelerometer is known.

Two recent papers by X Boutillon and C-A Faure [4] deal exhaustively with the problem of TSR and TMR determination. Their approach is similar to that of Ramboz, but much more rigorous, and more attention is paid to uncertainty and to geometric tolerances. However, again it is assumed that the main axis sensitivity is known.

3. ACCELEROMETER CALIBRATION AT NML

At the National Measurement Laboratory, concern is not principally with the actual magnitudes of TSR and TMR. The main requirement is to minimise or correct for errors, which they may introduce in calibration of the main axis sensitivity of an accelerometer.

When an accelerometer is calibrated at NML, a technique is routinely used to compensate for the combined effect of TSR and TMR. For this technique, it is assumed that transverse sensitivity is attributable to, or equivalent to, misalignment between the true sensitive axis of the accelerometer and the geometric axis, and also that the accelerometer geometric axis coincides with the shaker axis.

For both comparison calibrations and "absolute" (first level) calibrations, three sets of readings are taken with the accelerometer main sensitive axis always oriented to coincide with the main axis of the exciter. Between each set, the accelerometer is rotated through 120 degrees around this (assumed common) axis, and the results are averaged over the three sets. A precise rotation is attained by mounting the accelerometer on each in turn of three precision spacer washers, the thickness of which differ by one third of the pitch of the mounting stud thread.

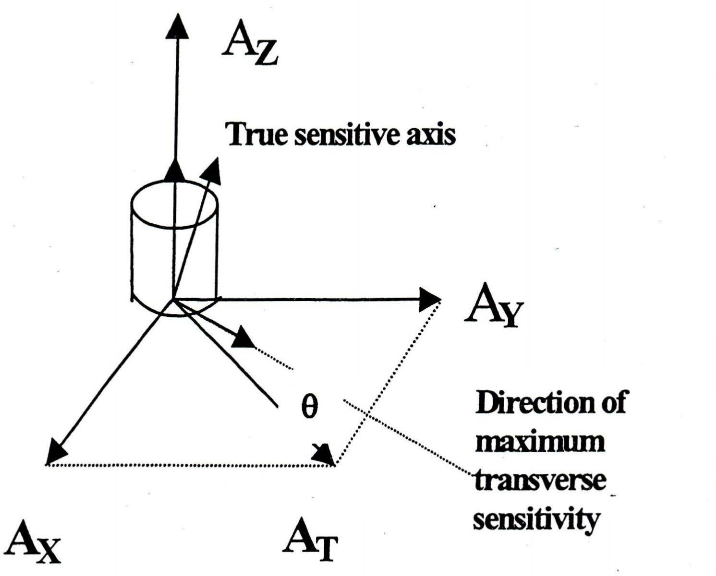

Figure 3 – Transverse sensitivity varies with direction.

If the transverse component of motion has the direction of A_T (Figure 3), and the direction of maximum transverse sensitivity of the accelerometer is at an angle θ to this, then for an acceleration axial input of $A_Z \cos(\omega t)$ with transverse component $A_T \cos(\omega t + \phi)$, the accelerometer output can be written as

$$e_1(\omega t) = A_Z\ S_Z \cos(\omega t) + A_T\ S_T \cos(\omega t + \phi) \cos\theta \qquad (1)$$

where S_Z and S_T are the accelerometer main axis sensitivity and the maximum transverse sensitivity. If the accelerometer is now rotated about an angle of $2\pi/3$ and subjected to the same acceleration, the output is

$$e_2(\omega t) = A_Z\ S_Z \cos(\omega t) + A_T\ S_T \cos(\omega t + \phi) \cos(\theta + 2\pi/3). \qquad (2)$$

and if the accelerometer is rotated through a further $2\pi/3$ and the above repeated, the output is then

$$e_3(\omega t) = A_Z\ S_Z \cos(\omega t) + A_T\ S_T \cos(\omega t + \phi) \cos(\theta - 2\pi/3). \qquad (3)$$

Adding equations 1, 2 and 3, and dividing by three, we get simply

$$e(\omega t) = A_Z\ S_Z \cos(\omega t). \qquad (4)$$

Application of this technique has been found to reduce uncertainty from measurement scatter from several percent at some frequencies, down to tenths of a percent.

When a primary reference accelerometer is calibrated using interferometry (so-called "absolute" or "first-level" calibration), the displacement of the surface on which the accelerometer is mounted is measured with a laser beam normally incident at a point adjacent to the accelerometer. Any rocking component in the motion can cause the measured displacement to differ from the displacement experienced by the accelerometer, as shown in Figure 4.

With absolute calibration of quartz reference accelerometers, there is the additional problem of rotational motion about axes normal to the main axis. This can be compensated for by measuring the displacement at several points or targets ($I_{1\text{-}6}$ in Figure 4) equi-spaced around a circle concentric with the accelerometer axis and determining the apparent sensitivity of the accelerometer at each measurement, with nominally the same input. By averaging over this set of apparent sensitivities, the sensitivity is determined with reference to acceleration at the mid-point, and it is not necessary to assume that the input remains strictly constant for all the measurements. Figure 5 shows the results for six targets; the sinusoidal variation is clear evidence of a rocking component in the motion. This whole procedure is then repeated three times with re-orientation of the accelerometer, as described in the previous paragraph, to compensate for purely transverse components of motion.

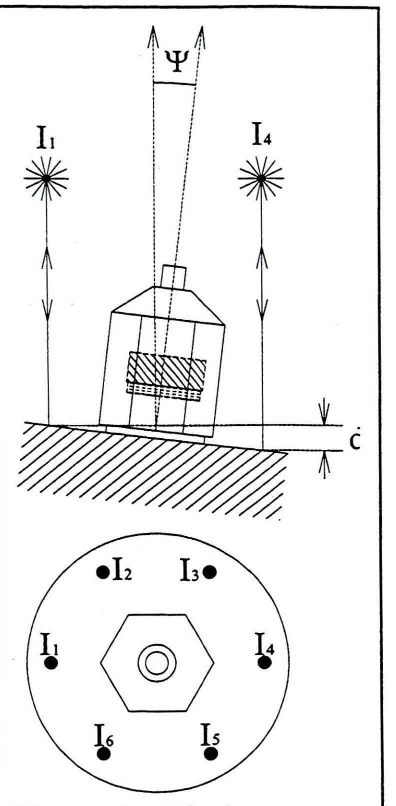

Figure 4 – Displacement error when calibrating by laser interferometry

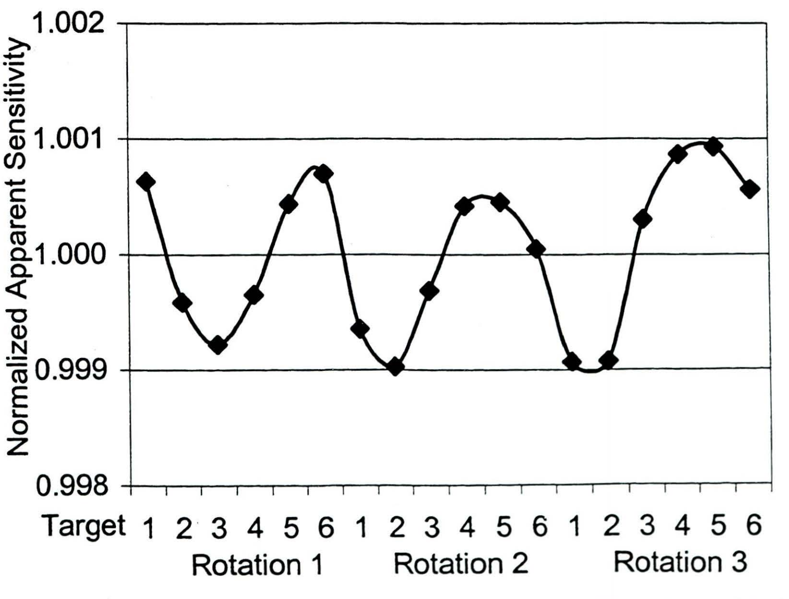

Figure 5 – Experimental data for an absolute calibration with 18 sampled targets.

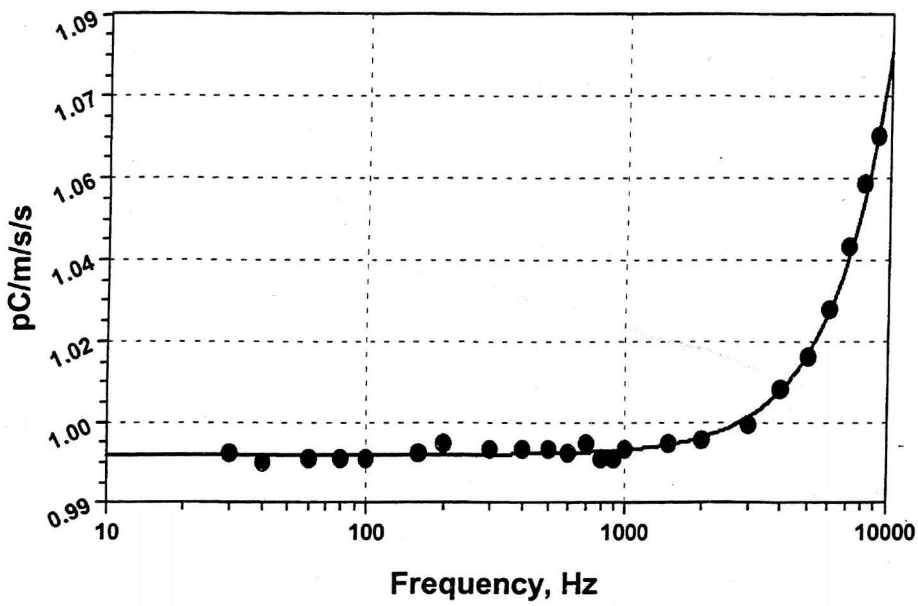

Figure 6 – Experimental data for an absolute calibration of an accelerometer with a theoretical curve fitted to the data

4. FREQUENCY RESPONSE.

The response, at frequency f, of an unloaded ideal accelerometer with resonance frequency f_0 and damping p, can be represented [5] *by*

$$Sensitivity\ S = S_0 / \{[1-(f/f_0)^2]^2 + 4p^2 (f/f_0)^2\}^{0.5} \tag{5}$$

where S_0 is the nominal sensitivity at zero hertz. (This equation does not include the influence of any signal conditioning circuit.)

Figure 6 shows some calibration results fitted to Equation 5 using CurveExpert software [8]. The nominal resonance frequency was used as an initial estimate, and the damping was initially estimated to be close to zero. It was found that regions where the calibration results differed from the fitted theoretical curve corresponded to frequencies where the TMR was high.

A quartz reference accelerometer is a simple structure, and there is no obvious reason why the charge sensitivity should deviate from the above simple function, if the excitation is truly rectilinear simple harmonic motion. When absolute calibrations have been done without compensating for transverse motion and rocking, apparent systematic deviations from a simple fitted curve have been observed. However, when such compensation has been applied, the frequency response has been observed to approximate more closely the character of Equation 5. In a separate study, data from several laboratories in an international comparison [6] was also fitted to Equation 1, and the results [7] strongly suggested that deviation from the curve were functions of the calibration process, and not characteristic of the test accelerometer.

5. CONCLUSION

The technique of fitting a theoretical curve to a set of calibration results seems to be a useful method of finding frequency regions where the vibration shaker motion has strong non-rectilinear components. Taking additional repeat readings using many targets and rotational orientations of the accelerometer can minimize the effects of the non-rectilinear components on the transverse sensitivity of the accelerometer.

6. REFERENCES

1. ISO 16063-1 Methods for the calibration of vibration and shock transducers – Part 1: Basic concepts. (1999)
2. John Field, "Investigation of the frequency response of cutting force dynamometers by transient loading" Int. J. Prod. Res. 20 1982. No 1 p 57-64
3. Ramboz, J D "A proposed method for the Measurement of Vibration Transducer Transverse Sensitivity" *Instrument Society of America Transactions,* Vol 7, 1968 pp231-236]
4. Boutillon, X, and Faure, C-A "The mean-projection method for the calibration of accelerometers" *ACUSTICA –acta acustica* Vol 84 (1998) pp 348-358 and 359-371]
5. IEC 184 "Methods for specifying the characteristics of Electro-mechanical transducers for shock and vibration measurements", Fig A-1, page 33 (1965)
6. Shing Chen, "APMP Intercomparison of Standard Accelerometers, Final Report", APMP-IC-4-95, 1998
7. Clark, N H , "Accelerometer first-level calibrations" Metrologia 36(4), 1999
8. Hyams, Daniel "*Curve Expert 3.1*" software (1995,1997)

AUSTRALIAN ACOUSTICAL SOCIETY CONFERENCE

ACOUSTICS TODAY
Melbourne, 24 – 26 November, 1999.

ON ACOUSTIC LAGGING OF PIPES

S Kanapathipillai and K P Byrne

School of Mechanical and Manufacturing Engineering
The University of New South Wales
Sydney, Australia

ABSTRACT

Pipe laggings are used as a means of inhibiting the transmission of sound radiated from pipes. They are usually formed of porous jackets such as fibreglass or rockwool blankets and impervious jackets such as metal cladding sheets. Sometimes air spaces are used to separate these jackets from the pipe and each other. Papers in the readily available literature relating to the acoustic performance of pipe laggings are generally concerned with presenting experimental results such as frequency dependent insertion losses. The authors have developed a model to calculate the insertion losses produced by such laggings when the lagged pipes are vibrating in their low order structural modes. The results of the model indicate that negative insertion losses are not unexpected with conventional pipe laggings, particularly at low frequencies.

1. INTRODUCTION

Excessive noise radiated by pipes is a common problem in many practical situations. For instance, the noise radiated by piping systems has been found to be a major contributor to the overall environmental noise in process and power generation plants. Although mechanical equipment or control valves are generally responsible for the generation of the acoustic energy, the piping system serves as a passive element that distributes and radiates noise throughout the plant. With continuous improvements in silencers and enclosures, pipe radiated noise has become one of the dominant remaining source of noise in many installations.

Control of pipe radiated noise is usually achieved by lagging the pipe. Pipe laggings constructed of combinations of jackets made of a porous material such as fibreglass and jackets made of an impervious material such as a metal cladding sheet are often applied to pipes with the intention of inhibiting the transmission of the sound radiated from the external pipe surfaces. Papers related to pipe laggings which have appeared in the readily available literature have presented, in essence, experimental results such as frequency dependent insertion losses produced by laggings [1- 6].

The authors have developed a theoretical model to evaluate the frequency dependent insertion losses produced by a particular lagging when the pipe is supporting individual low order mode propagating structural waves such as breathing mode type wave in which the pipe cross-section expands and contracts, the bending mode type wave in which the pipe cross-section translates and the ovalling mode type wave in which the pipe cross-section becomes oval. Often the bending mode type is of particular importance as unlike other structural waves in pipes the bending mode type wave does not exhibit a cut-off frequency. Further, the bending mode type wave is usually relatively effective in radiating sound.

2. MODELLING

The model of the lagged pipe is shown in Figure 1. The complex representation of the radial velocity v_r of the outer surface of the infinitely long pipe is defined by $\mathbf{v}_r = \mathbf{V}_r \cos n\phi \exp[j(\omega t - k_z z)]$. The value of n, which is an integer, describes the motion of the pipe cross-section. When n=0 the pipe is supporting the breathing mode type wave which is travelling in the positive z direction with a wave number of k_z. When n=1 the pipe is supporting a bending mode type wave and when n=2 the pipe is supporting an ovalling mode type wave.

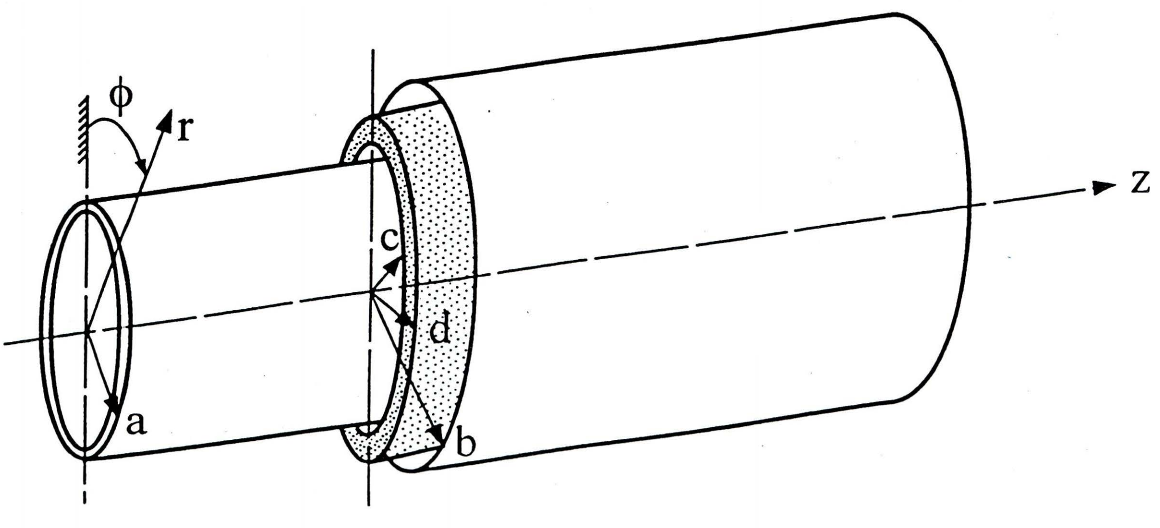

Figure 1: Lagged pipe showing air gaps, porous jacket and impervious jacket

Sound energy can be radiated from such a vibrating pipe so long as k_z, the axial wave number which describes the wave motion of the pipe surface, is less than k, the acoustic wave number of the fluid which surrounds the pipe. Generally there is a non-linear relation between ω and k_z for the pipe; for example when n=1, $k_z^2 \propto \omega$. However, there is a linear relationship between k and ω, that is $k \propto \omega$. Thus a particular pipe cannot radiate energy in particular mode until some critical frequency is reached. When k_z= 0 the wave propagation direction is normal to the pipe axis. As k_z increases the wave propagation direction becomes inclined to the pipe axis and "conical" waves are radiated by the pipe. When k_z= k the wave propagation direction is parallel to the pipe axis and no sound power is radiated by the pipe.

As shown in Figure 1 the lagging is usually be constructed of a number of types of jackets. These jackets are the air space(s), porous jacket(s) and impervious jacket(s). When the pipe is vibrating the waves in all of these jackets have the same values of ω and k_z. The acoustic pressure and radial acoustic particle velocity just outside the outer surface of the lagging are assumed to vary with ϕ according to $\cos n\phi$ whether the jacket is present or not. Thus the radial intensities vary with $\cos^2 n\phi$ with and without jacket and so the ratio of sound powers radiated from unit lengths of the bare and the lagged pipe can be found from the ratio of the radial intensities at a convenient point just outside the outer surface of the porous jacket whether or not it is present. The point just on the outer surface of the lagging , that is, at r = b and ϕ = 0 is convenient. The radial intensities can be obtained from the pressures and radial particle velocities. The radial particle velocities can be obtained from the pressures and the radial impedances. Thus the basic strategy is to determine the radial impedance at the point r = b, ϕ = 0 and the pressures at this point with and without the porous jacket. The radial impedance at this point, being dependent only on the medium beyond this point, is of course unchanged by the presence or absence of the lagging.

Appendix A presents the development of an expression which enables the radial intensity at the point r = b, ϕ = 0 to be determined in terms of the acoustic pressure and the radial impedance at this point. Appendix B presents the development of expressions which give the radial impedance at this point and the pressure produced at this point by the unlagged vibrating pipe. Appendices C and D present formulae which allow the radial impedances on the inner surface of the different jackets to be found in terms of the fundamental physical quantities which describe the jackets and the radial impedances on the outer surface of the jackets. These appendices also include formulae which enable the acoustic pressures at ϕ = 0 on the outer surfaces of the jackets to be found when the acoustic pressures at ϕ = 0 on the inner surfaces are known as are the radial impedances on the inner and outer surfaces.

Consider first, with reference to Figure 1, the situation when the lagging is not present. The radial intensity at the point of interest (that is, at r = b, ϕ = 0) can be found from the pressure and impedance formulae given in Appendix B. The radial intensity can then be found as described in Appendix A.

A similar procedure is followed when the lagging is present. The radial impedance on the outer surface of the lagging, that is, at $r = b$, $\phi = 0$ is found first as before. The radial impedance formulae in Appendices C and D are then successively used to find the radial impedance at the pipe surface. The pressure at $\phi = 0$ on the pipe surface can be found as the pipe radial velocity and the radial impedance at this point is known. The pressure formulae in Appendices C and D are then successively applied to give the pressure on the outer surface of the lagging at $\phi = 0$. The pressure, along with the original radial impedance at this point, gives the radial intensity at $\phi = 0$ on the outer surface of the lagging. The insertion loss can be obtained from this intensity and that found at the same point without the lagging.

3. TESTING OF THE MODEL

Figure 2 shows comparisons of the predicted and measured one third octave band insertion losses produced by two different porous jackets. These jackets were used to lag a 6 m long ammonia pipe having an outside diameter of 48.3 mm and a wall thickness of 7.5 mm. An electrodynamic shaker was used apply a fluctuating force to one end of the pipe so that the pipe was forced to vibrate and radiate sound. The pipe was selected so that over a wide frequency range the only modes which could be effectively excited and so radiate sound were the bending modes. This enabled the predicted insertion loss of the lagging associated with pipe vibration in the bending mode to be compared with the measured insertion loss for that mode. An analysis of the dispersion characteristics of the pipe shows that the breathing mode cutoff frequency is approximately at 50 kHz and the ovalling mode cutoff frequency is approximately at 27 kHz whereas the bending mode starts to propagate at zero frequency. The critical frequency for the bending mode, that is, the frequency above which sound will be radiated, is 230 Hz. The porous jackets were aligned with the pipe such that there was an air gap of 6 mm between the surface of the pipe and the inner surface of the porous jacket.

The sound power radiated from a length of bare and lagged pipe was determined by measuring the sound intensity at 60 points on a 1.5 m-long imaginary cylindrical surface surrounding the pipe. A Bruel & Kjaer (B & K) Real Time Analyzer Type 2133 and a B & K Sound Intensity Probe Type 2519 were used to measure the sound intensity.

Figure 2(a) contains the results for a 25mm thick jacket made of a high density rockwool, whose flow resitivity was 121,000 rayls/m. Figure 2(b) contains the results for a jacket made of low density fibreglass which was also 25 mm thick but whose flow resitivity was only 15,300 rayls/m. Although over a frequency range of 500 to 2500 Hz the agreement between the predicted and measured results is satisfactory the agreement is not as good outside this range. Difficulties encountered with the intensity measurements could account for the discrepancies, as could the semi-empirical expressions for and k and Z_o given by Delaney and Bazley [7] which were used here.

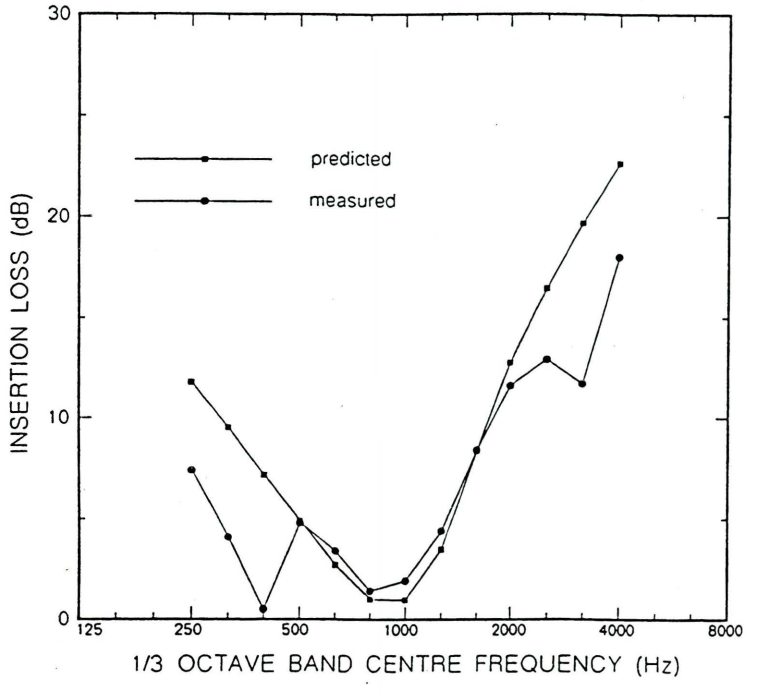

Figure 2 (a): Predicted and measured insertion losses for a porous jacket. Flow resitivity = 121,000 rayls/m, thickness = 25 mm and air gap = 6mm

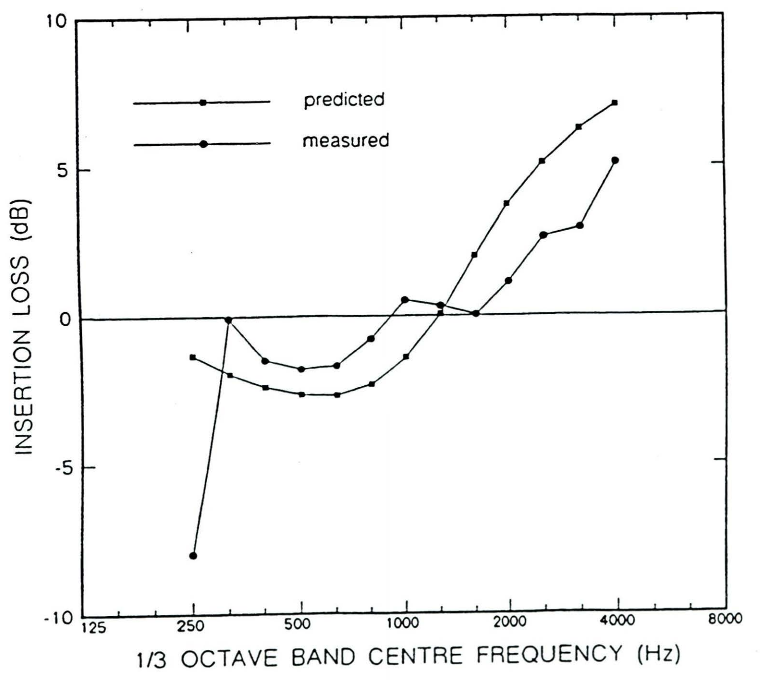

Figure 2 (b): Predicted and measured insertion losses for a porous jacket. Flow resitivity =15,300 rayls/m, thickness = 25 mm and air gap = 6mm

4. EFFECT OF AIR GAP

The results given in the previous section give some confidence in the model and it is instructive to use the model for a parametric study. The first parametric study relates to the effect of the air gap. Figure 3 shows the predicted insertion losses associated with the bending mode for the ammonia pipe referred to previously. The curves in this figure give an indication of the effect of air gap on insertion loss for a 40 mm thick porous jacket with flow resitivity of 80,000 rayls/m. It can be seen that in the low frequency region, which is of particular interest, the propensity for negative insertion losses to occur is reduced by increasing the air gap between the jacket and the pipe.

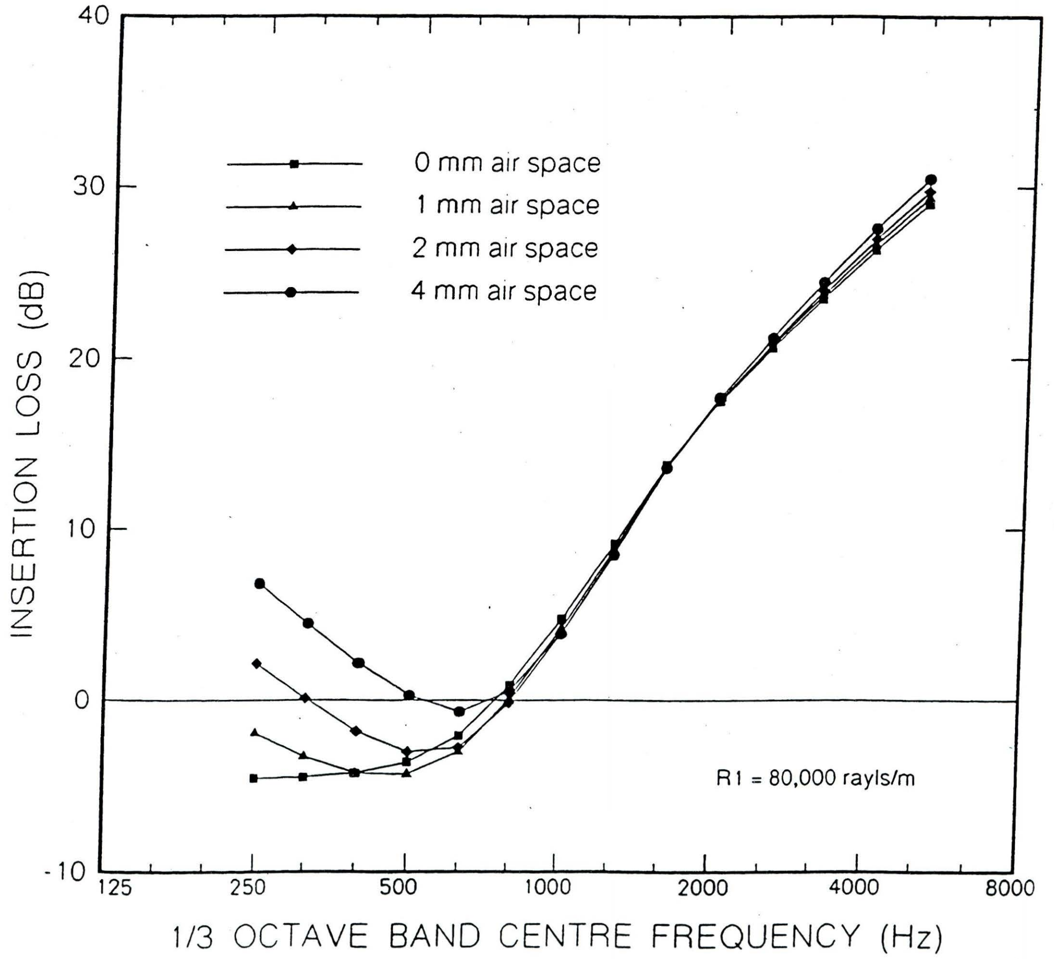

Figure 3: Predicted insertion losses for a 40 mm thick porous jacket

5. EFFECT OF IMPERVIOUS JACKET

The two key elements of an acoustic pipe lagging are the porous jacket and the impervious jacket. Figure 4 presents predicted results which show the effect of a thin aluminium outer impervious jacket on the lagging. Aluminium is assumed to have a density of 2700 kg/m^3, a Young's modulus of 71 GPa, a Poisson's ratio of 0.33 and a loss factor of 0.01. The "without impervious jacket" curves in these figures correspond to those given in Figure 2. It can be seen that the application of the impervious jacket to a simple porous jacket lagging produces an unexpected effect in the insertion loss curve in Figure 4(b) in that there is a peak and followed by a 'dip'. This unexpected 'dip' occurs as the wave impedance of the impervious jacket becomes very small at the dip frequency as shown in Figure 5.

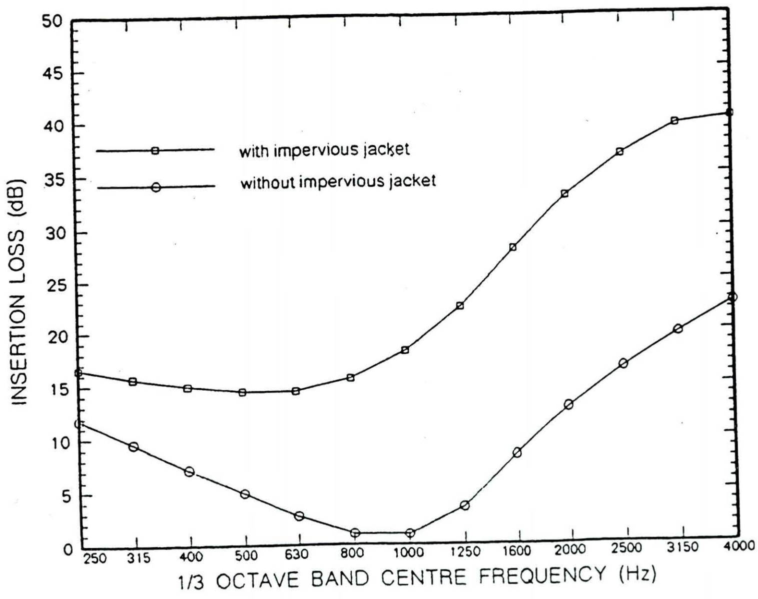

Figure 4(a): Predicted insertion losses for porous and impervious jacket lagging.
Air gap 6 mm, Porous jacket thickness 25 mm and flow resitivity 121,000 rayls/m.
Impervious jacket 0.1 mm aluminium.

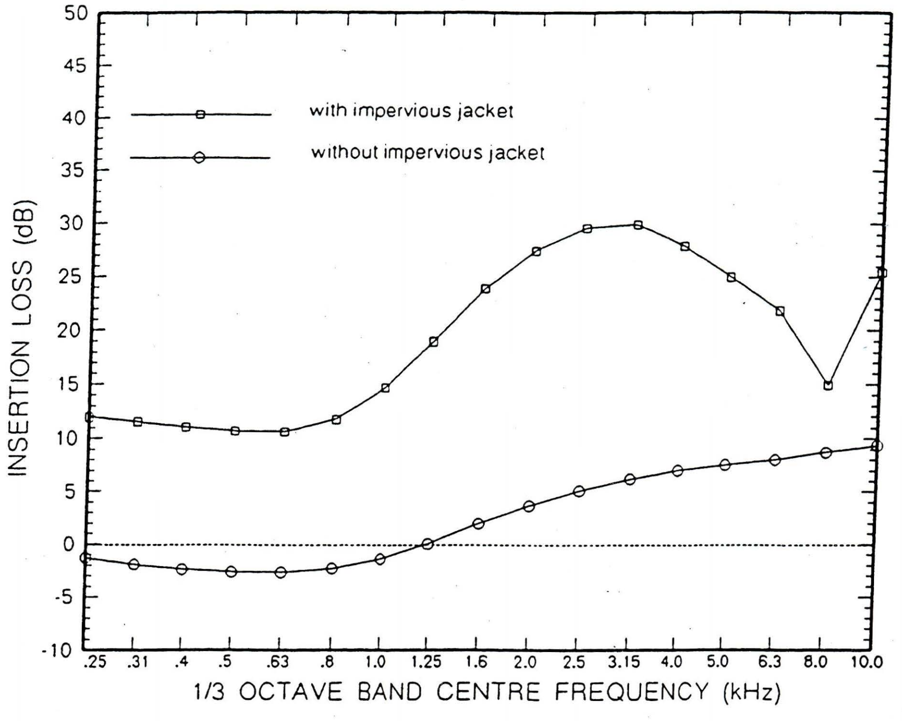

Figure 4(b): Predicted insertion losses for porous and impervious jacket lagging. Air gap 6 mm, Porous jacket thickness 25 mm and flow resitivity 15,300 rayls/m. Impervious jacket 0.1 mm aluminium.

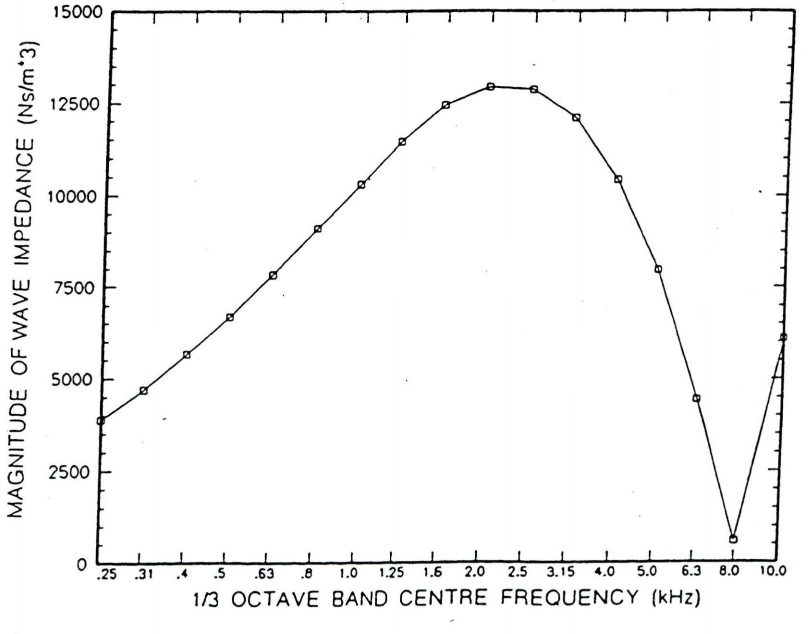

Figure 5: Magnitude of the wave impedance at the inner surface of 0.1 mm thick aluminium impervious jacket

6. CONCLUSIONS

The results obtained by use of the model show that negative insertion losses can occur for at low frequencies when the pipe is vibrating in the bending mode unless there is a significant air gap between the pipe and the porous jacket. The agreement between the predicted and measured results, although not perfect, is sufficiently good to indicate that the model is useful for parametric studies For example, the model predicts that the insertion loss at high frequencies can be considerably reduced at frequencies where the wave impedance of the impervious jacket becomes small.

7. REFERENCES

[1] W Loney, 'Insertion Loss Tests for Fibreglass Pipe Insulation', J. Acoust. Soc. Am, **76**(1), pp 150-157, 1984.

[2] M E Hale and B A Kugler, 'The Acoustic Performance of Pipe Lagging Systems', Petroleum Division, ASME Winter Annual Meeting, Houston, Texas, 1975.

[3] G L Brown and D C Rennison, 'Sound Radiation from Pipes Excited by Plane Acoustic Waves', Proceedings of the Noise, Shock and Vibration Conference, Monash University, Melbourne, pp 416-425, 1974.

[4] G F Kuhn and C L Morfey, 'Transmission of Low-frequency Internal Sound through Pipe walls', Journal of Sound and Vibration, **47**, pp 147-161, 1976.

[5] K P Byrne, 'The Acoustic Performance of Plastic Foam and Fibrous Preformed Thermal Pipe Insulation for Small Diameter Pipes', 4th Western Pacific Regional Acoustics Conference, Brisbane, pp 112-119, 1991.

[6] R D Stevens, 'A Survey of Analytical Prediction Models for the Acoustic Performance of Pipe Lagging Systems', Proceedings of the Spring Environmental Noise Conference – 'Innovations in Noise Control for the Energy Industry', Banff, Alberta, Canada, April 19 – 22 , 1998.

[7] M E Delaney and E N Bazley, 'Acoustical Properties of Fibrous Absorbent Materials', Applied Acoustics, **3**, pp 105-116, 1970

[8] von F P Mechel, Ausweitung der Absorberformel von Delaney and Bazely zu tiefen Frequenzen, Acustica, **35**, pp 210-213, 1976.

[9] A W Leissa, 'Vibration of Shells', NASA SP-288, Office of Technology Utilization, National Aeronautics and Space Administration, Washington DC, 1973.

[10] S Kanapathipillai and K P Byrne, 'Effects of a Porous Jacket on Sound Radiated from a Pipe', J. Acoust. Soc. Am, **100**(2), pp 882-888, 1996.

APPENDIX A

EXPRESSION FOR RADIAL INTENSITY IN AIR SURROUNDING PIPE

The computational procedure described in the body of the paper is based on the use of pressure and radial impedance and so it is convenient to derive the expression for the radial intensity terms of these quantities. At a point defined by r, ϕ and z in the air surrounding the lagged pipe the complex representations of the acoustic pressure, $p = P\cos(\omega t + \phi_p)$ and the radial particle velocity, $u_r = U_r \cos(\omega t + \phi_u)$ are $\mathbf{p} = \mathbf{P}\exp[j\omega t]$ and $\mathbf{u}_r = \mathbf{U}_r \exp[j\omega t]$ where $\mathbf{P} = P\exp[j\phi_p]$ and $\mathbf{U}_r = U_r \exp[j\phi_u]$. The radial impedance, $\mathbf{z}_r$, is given by $\mathbf{z}_r = \mathbf{P}/\mathbf{U}_r = |\mathbf{P}/\mathbf{U}_r| \angle \phi_P - \phi_u = P/U_r \angle \phi_P - \phi_u$. The instantaneous radial intensity, I_r is given by pu_r and the average radial intensity, $\overline{I}_r$, obtained by averaging I_r over one cycle, is given by $\overline{I}_r = 0.5\,PU_r\cos(\phi_p - \phi_u)$. This expression for $\overline{I}_r$ can be rewritten as equation (A.1) by use of the results $P = U_r|\mathbf{z}_r|$ and $\mathrm{Re}\{\mathbf{z}_r\} = |\mathbf{z}_r|\cos(\phi_p - \phi_u)$.

$$\overline{I}_r = 0.5|\mathbf{P}/\mathbf{z}_r|^2\,\mathrm{Re}\{\mathbf{z}_r\} \qquad (A.1)$$

APPENDIX B

EXPRESSIONS FOR PRESSURE AND RADIAL IMPEDANCE IN SURROUNDING AIR

Suppose that the outer surface of the infinitely long pipe of radius a whose axis is aligned with the z axis has a radial velocity v_r whose complex representation is $\mathbf{v}_r = \mathbf{V}_r \cos n\phi \exp[j(\omega t - k_z z)]$. The acoustic pressure, whose complex representation is $\mathbf{p}$, produced by this pipe motion at a point defined by r and ϕ can be found by expressing the wave equation $\nabla^2\mathbf{p} + k^2\mathbf{p} = 0$ in cylindrical coordinates, assuming a separable solution $\mathbf{p} = \mathbf{P}\,R(r)\,\Phi(\phi)\exp[j(\omega t - k_z z)]$ and solving the resulting differential equations B.1 for R(r) and $\Phi(\phi)$ to give the solutions defined by equation B.2.

$$\frac{d^2R}{dr^2} + \frac{1}{r}\frac{dR}{dr} + (k^2 - k_z{}^2 - \frac{n^2}{r^2})R = 0, \quad (a) \qquad \frac{d^2\Phi}{d\phi^2} + n^2\Phi = 0 \quad (b) \qquad (B.1)$$

$$R(r) = A\,J_n(k_r r) + B\,N_n(k_r r), \quad (a) \qquad \Phi(\phi) = C\cos n\phi \quad (b) \qquad (B.2)$$

A, B and C are constants and J_n and N_n are the n^{th} order Bessel & Neumann functions in which $k_r{}^2 = k^2 - k_z{}^2$. The radial particle velocity, u_r, can be found from the linearized Euler equation $\partial p/\partial r = -\rho\partial u_r/\partial t$. This radial particle velocity can be made equal to the radial velocity, v_r of the pipe surface. The radiation condition provides a further boundary condition and so the constants AC and BC can be determined. The pressure at the point r=b, ϕ=0 then can be found as can the radial impedance. They are as follows:

$$\mathbf{p} = -j\mathbf{V}_r\,\rho c\,\frac{k}{k_r}\,\frac{J_n(k_r b) - jN_n(k_r b)}{J_n'(k_r a) - jN_n'(k_r a)}\exp[j(\omega t - k_z z)] \qquad (a)$$

$$\frac{\mathbf{z}_r}{\rho c} = -j\,\frac{k}{k_r}\left[\frac{J_n(k_r b) - jN_n(k_r b)}{J_n'(k_r b) - jN_n'(k_r b)}\right] \qquad (b) \qquad (B.3)$$

APPENDIX C

EXPRESSIONS RELATING THE RADIAL IMPEDANCES AND PRESSURES AT THE INNER AND OUTER SURFACES OF A RIGID POROUS JACKET

A rigid porous jacket whose inner and outer radii are a and b respectively is made of a homogeneous and isotropic material with a flow resitivity of R_1 and porosity of Ω. The arrangement is shown in Figure C.1. The propagation of sound waves in this material is governed by the wave equation. $\nabla^2 \mathbf{p} + \mathbf{k}^2 \mathbf{p} = 0$. The term $\mathbf{k}$ is the complex wave number. The acoustic pressure and radial particle velocity in this jacket are assumed to vary with ϕ according to $\cos n\phi$.

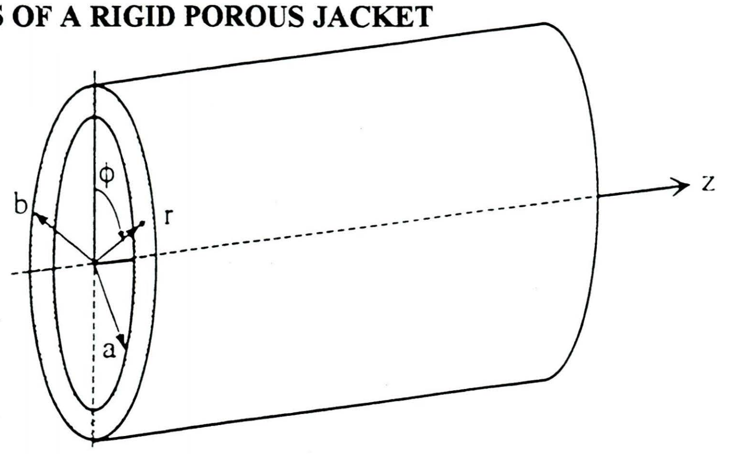

Figure C.1 Porous Jacket Model

The wave equation can be expressed in cylindrical coordinates and solved to derive expressions for the acoustic pressure and the radial particle velocity. It is then possible to derive an expression which allows the impedance in the radial direction on the inner surface of the porous jacket, ie at r = a, to be found when that on the outer surface, ie at r = b, is known. This expression is given by equation C.1(a). It is also possible to derive an expression which enables the pressure on the outer surface, ie at r = b, to be found when that on the inner surface, ie at r = a, is known as are the radial impedances on these surfaces. This expression is given by equation C.1(b)

$$\frac{z_{ra}}{Z_o} = -j\frac{\mathbf{k}J_n(\mathbf{k}_r a) + \alpha N_n(\mathbf{k}_r a)}{\mathbf{k}_r J_n'(\mathbf{k}_r a) + \alpha N_n'(\mathbf{k}_r a)} \quad \text{(a)} \quad \text{and} \quad P_b = P_a \frac{J_n(\mathbf{k}_r b) + \alpha N_n(\mathbf{k}_r b)}{J_n(\mathbf{k}_r a) + \alpha N_n(\mathbf{k}_r a)} \quad \text{(b) (C.1)}$$

$$\text{where } \alpha = -\frac{[z_{rb}/Z_o\,\mathbf{k}_r/\mathbf{k}\,J'_n(\mathbf{k}_r b) + jJ_n(\mathbf{k}_r b)]}{[z_{rb}/Z_o\,\mathbf{k}_r/\mathbf{k}\,N'_n(\mathbf{k}_r b) + jN_n(\mathbf{k}_r b)]}, \quad \text{(C.2)}$$

The quantity $\mathbf{k}_r$ which appears in these equations is given by $\mathbf{k}_r^2 = \mathbf{k}^2 - \mathbf{k}_z^2$. Various models can be used to determine $\mathbf{k}$ and $\mathbf{Z}_0$ which are needed in the evaluation of equations (C.1) and (C.2). The semi-empirical formulae of Delany and Bazely [7] and Mechel [8] are convenient. These formulae are given below in forms compatible with the notation used in this paper. They are expressed in terms of the dimensionless quantity $C=R_1/\rho f$ where R_1 is the flow resitivity of the porous material, ρ is the density of the gas involved and f is the frequency. Equations (C.3) apply when $C \geq 60$ and equations (C.4) apply when $C<60$.

$$\mathbf{k} = -jk[-1.466 + j0.212C]^{1/2} \qquad \frac{\mathbf{Z}_0}{\rho c} = [(C/2\pi + j1.403)/(-1.466 + j0.212C)^{1/2}] \quad \text{(C.3)}$$

$$\mathbf{k} = -jk[0.189C^{0.618} + j(1+0.0978C^{0.693})] \qquad \frac{\mathbf{Z}_0}{\rho c} = [1+0.0489C^{0.754} - j0.087C^{0.731}] \quad \text{(C.4)}$$

Equations C.1 and C.2 can be used also when the jacket is an air space rather than a porous layer. In this case **k** is replaced by ω/c and $\mathbf{Z_0}$ is replaced by ρc.

APPENDIX D

EXPRESSIONS RELATING THE RADIAL IMPEDANCES AND PRESSURES AT THE INNER AND OUTER SURFACES OF A CYLINDRICAL IMPERVIOUS JACKET

A thin walled cylindrical shell of nominal radius a and wall thickness h is made of a material with a Young's Modulus of E, Poisson's Ratio ν, density ρ and loss factor of η. The arrangement is shown in Figure D.1. Donnell's formulation of the equations of motion for such a shell is expressed in terms of w, v and u, the displacements of the mid-surface of the shell in the r, ϕ and z directions as shown in Figure D.1. His equations are given in [9].

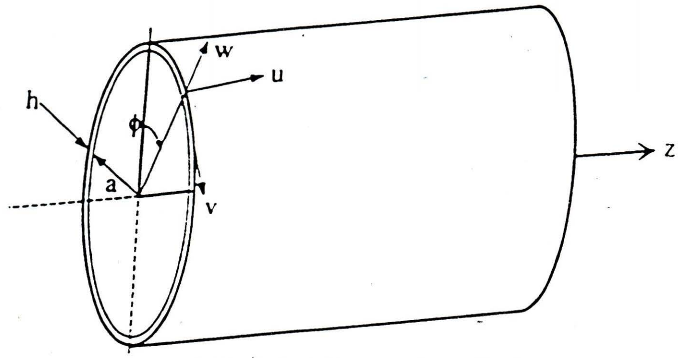

Figure D.1 Cylindrical Impervious Jacket Model

$$\frac{\partial^2 u}{\partial z^2}+\frac{1-\nu}{2a^2}\frac{\partial^2 u}{\partial \phi^2}+\frac{1+\nu}{2a}\frac{\partial^2 v}{\partial z\partial\phi}+\frac{\nu}{a}\frac{\partial w}{\partial z}-\frac{\ddot{u}}{c_p^2}=0 \qquad \text{(D.1a)}$$

$$\frac{1+\nu}{2a}\frac{\partial^2 u}{\partial z\partial\phi}+\frac{1-\nu}{2}\frac{\partial^2 v}{\partial z^2}+\frac{1}{a^2}\frac{\partial^2 v}{\partial \phi^2}+\frac{1}{a^2}\frac{\partial w}{\partial \phi}-\frac{\ddot{v}}{c_p^2}=0 \qquad \text{(D.1b)}$$

$$\frac{\nu}{a}\frac{\partial u}{\partial z}+\frac{1}{a^2}\frac{\partial v}{\partial \phi}+\frac{w}{a^2}+\beta_o^2\left(a^2\frac{\partial^4 w}{\partial z^4}+2\frac{\partial^4 w}{\partial z^2\partial\phi^2}+\frac{1}{a^2}\frac{\partial^4 w}{\partial\phi^4}\right)+\frac{\ddot{w}}{c_p^2}=\frac{p_a(1-\nu^2)}{Eh} \qquad \text{(D.1c)}$$

The terms β_o^2 and c_p^2 are given by $\beta_o^2 = h^2/12a^2$ and $c_p^2 = E/\rho(1-\nu^2)$.

The term p_a which appears in equation (D.1c) is a function of time, ϕ and z. It is the net pressure which is applied to the cylindrical shell and it is assumed here that it has the complex representation given by equation (D.2) in which the subscripts i and o relate to the pressures inside and outside the cylindrical shell.

$$\mathbf{p}_a = (\mathbf{P}_i - \mathbf{P}_o)\cos n\phi \exp[j(\omega t - k_z z)] \qquad \text{(D.2)}$$

In view of the assumed form of loading on the cylindrical shell, that is, equation D.2, the complex representations of the u, v and w displacements are given by equations D.3.

$$\mathbf{u} = \mathbf{U}\cos n\phi\exp[j(\omega t - k_z z)],\ \mathbf{v} = \mathbf{V}\sin n\phi\exp[j(\omega t - k_z z)],\ \mathbf{w} = \mathbf{W}\cos n\phi\exp[j(\omega t - k_z z)] \qquad \text{(D.3)}$$

Substitution of equations D.3 into equations D.1 leads to the radial impedance and pressure equations D.4 and D.5.

$$z_i = z_o + j\gamma/\omega \tag{D.4}$$

$$P_o = P_i - j\gamma U/\omega \tag{D.5}$$

γ is given by equation (D.6). $\mathbf{P_o}$, $\mathbf{P_i}$ and $\mathbf{U}$ are the complex representations of the pressures and radial particle velocities at ϕ=0.

$$\gamma = \frac{\mathbf{E}h}{(1-\nu^2)}\left[\frac{L(QC-BR)C + M(AR-PC)C}{A(QC-BR)+B(AR-PC)} - N\right] \tag{D.6}$$

E in this equation is the complex Young's Modulus. It is given by **E** = E(1+jη). E is the conventional Young's Modulus and η is the loss factor for the material of the cylindrical shell. The terms **A**, **B**, **C**, **P**, **Q**, **R**, **L**, **M** and **N** are given by the equations:

$$A = (\omega/c_p)^2 - k_z^2 - n^2(1-\nu)/2a^2; \quad B = -jnk_z(1+\nu)/2a; \quad C = -jk_z\nu/a;$$
$$P = jnk_z(1+\nu)/2a; \quad Q = (\omega/c_p)^2 - (1-\nu)k_z^2/2 - (n/a)^2; \quad R = -n/a^2; \tag{D.7}$$
$$L = -jk_z\nu/a; \quad M = n/a^2 \text{ and } N = 1/a^2 + \beta_o^2(a^2k_z^4 + 2n^2k_z^2 + n^4/a^2) - \omega^2/c_p^2 .$$

APPENDIX E

DERIVATION OF THE DISPERSION RELATIONSHIPS FOR A THIN WALLED CYLINDRICAL SHELL

The dispersion relationships which relate the axial wavenumber, k_z and the frequency, ω for the various modes of vibration, that is, n = 0, 1, 2 can be obtained by substituting the solutions given by equations (D.3) into the homogeneous forms of equations (D.1). The resulting three equations involving **U**, **V** and **W** have non-trivial solutions for **U**, **V** and **W** only if the determinant of the coefficients of U, **V** and **W** is equal to zero. Thus, in terms of **A**, **B**, **C** etc as defined by equations (D.7), it is necessary that:

$$\det\begin{vmatrix} A, & B, & C \\ P, & Q, & R \\ L, & M, & N \end{vmatrix} = 0 \tag{E.1}$$

Since **A**, **B**, **C** etc. are expressed terms of k_z and ω, equation (E.1) defines the dispersion relationship which must exist between k_z and ω for a given thin walled cylindrical shell (as defined by a, c_p and ν) and a given mode (as defined by n).

AUSTRALIAN ACOUSTICAL SOCIETY CONFERENCE

ACOUSTICS TODAY

Melbourne, 24 – 26 November, 1999.

ATTENUATING NOISE IN PIPES

J P Parkinson[1], M D Latimer[2] and J R Pearse[1]

[1]Department of Mechanical Engineering, University of Canterbury, Christchurch, New Zealand

[2]D G Latimer and Associates Ltd, P O Box 12 032, Christchurch, New Zealand

ABSTRACT

Attenuating Noise in Pipes - The noise reduction properties of acoustic pipe lagging were investigated in a typical plumbing system. A bath was installed above a reverberation room, the associated waste water system was constructed to run through the room. The effect of different lagging thickness, barrier weights and materials on the discharge piping system was investigated in the reverberation room. Lagging coverage variation around the pipe was also investigated. Lagging the entire pipe system gave a significant loss in radiated noise, a less significant noise reduction was achieved by lagging one metre either side of and including the pipe's "P" trap bend. Transient discharge noise was reduced by the lagging but not to the same extent as with “steady state” water noise.

1. SUMMARY

The noise reduction properties of a flexible pipe lagging material (Acoustop Barrierwrap) developed and manufactured in Christchurch, New Zealand was investigated in a typical plumbing system. A bath and associated waste water system was constructed.

The effects of different lagging thickness, barrier weights and materials on the discharge piping system were investigated in a reverberation room. Lagging coverage variation around the pipe was also investigated. The Acoustop Barrierwrap gave a nominal 10 dBA insertion loss. A reduction of around 6 dBA was achieved by lagging one metre either side and including the pipe's “P” trap and bend. Transient discharge noise was reduced by the lagging but not by the same amount as with steady pipe noise.

2. INTRODUCTION

Waste water noise is produced by the intermittent use of showers, baths, toilets and basins as well as storm water pipes. This intermittent noise is of particular concern in multi-storey apartments and hotel rooms. The flow of water in the pipe creates pressure fluctuations, which result in noise being radiated from the walls of the pipe (1) and (2).

This noise can be significantly reduced by the use of pipe lagging, which commonly consists of a dense material (to absorb the noise) and a foam which acts as a decoupling agent, breaking down the vibration path.

This paper describes the results of tests of a proprietary lagging material, Acoustop Barrierwrap. This product was developed and is being manufactured in Christchurch by D G Latimer & Associates Ltd and has been widely used in Australasia since 1978. Barrierwrap uses a natural rubber mass loaded barrier which enables easy installation due to the products highly limp, flexible nature. This is of great advantage over more traditional rigid vinyl barriers (PVC - Polyvinyl Chloride) products, which are more difficult to fit around complicated bends e.g. “P” Traps.

3. PROCEDURES

A bath was installed immediately above a reverberant room. The discharge and overflow pipe from the bath was routed through the concrete ceiling and far wall of the reverberant room. The 40mm PVC discharge pipework and overflow pipework complied with the New Zealand Building Code (1992) and was fitted with a 'P' trap and vent.

Each type of lagging was installed according to the manufacturer's instructions. Background noise spectra, discharge noise profiles and the baths steady noise spectra were measured using a Bruel and Kjaer precision sound level meter. Lagging coverage variation was achieved by removing sections of the lagging and re-measuring the noise produced. Pipe support vibration isolation was achieved by using oversized pipe clips attached on the outside of the lagged pipe.

Lagging sound power insertion loss was calculated using (3):

$$L_{wi} = L_{po} - L_{pi}$$

where L_{wi} = insertion loss of lagging in decibels

L_{po} = mean band pressure level of the unlagged noise source

L_{pi} = mean band pressure level of the lagged noise source.

4. RESULTS

Lagging: Lagging the entire pipe gave a nominal 10 dB(A) insertion loss, as shown in figure 1. The lagging with the heaviest barrier gave the greatest insertion loss [11 dB(A)]; the better performance of this barrier at the lower frequencies was due to its heavier mass 8kg/m^2.

Support isolation: Isolation of the pipe from the metal hangers did not affect the amount of noise transmitted. This was attributed to the pipe supports being bolted directly to the concrete ceiling; any vibrations travelling through these supports would be absorbed by the large mass of the concrete ceiling.

Lagging coverage variation: Most of the waste water noise was generated at the bends of the pipe which were located at 0, 0.5m and 5.0m from the 'P' trap. Typically a 6 dB(A) insertion loss was obtained by lagging the 'P' trap and 1m from it. The noise increased slightly over the next 4m. Lagging the second bend gave an insertion loss of 3-4 dB(A).

Bath discharge noise profiles: The start and finish discharge noises were significantly reduced by the pipe laggings, as shown in figure 3. However the amount of noise reduction in these regions appear to be considerably less than in the steady region.

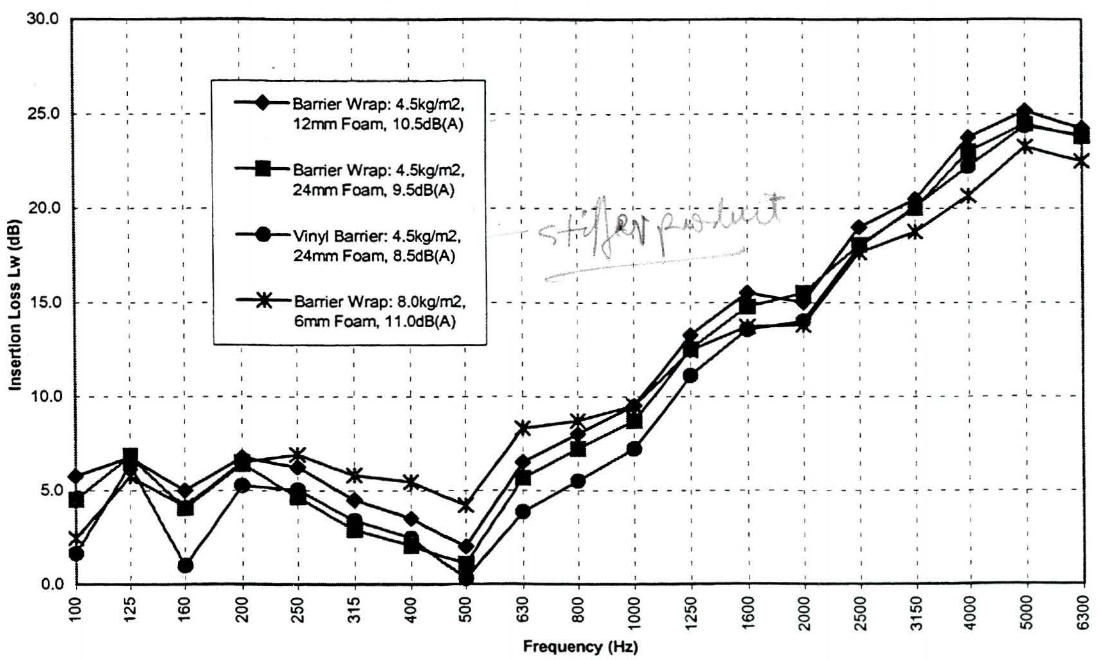

Figure 1 Insertion loss of various laggings

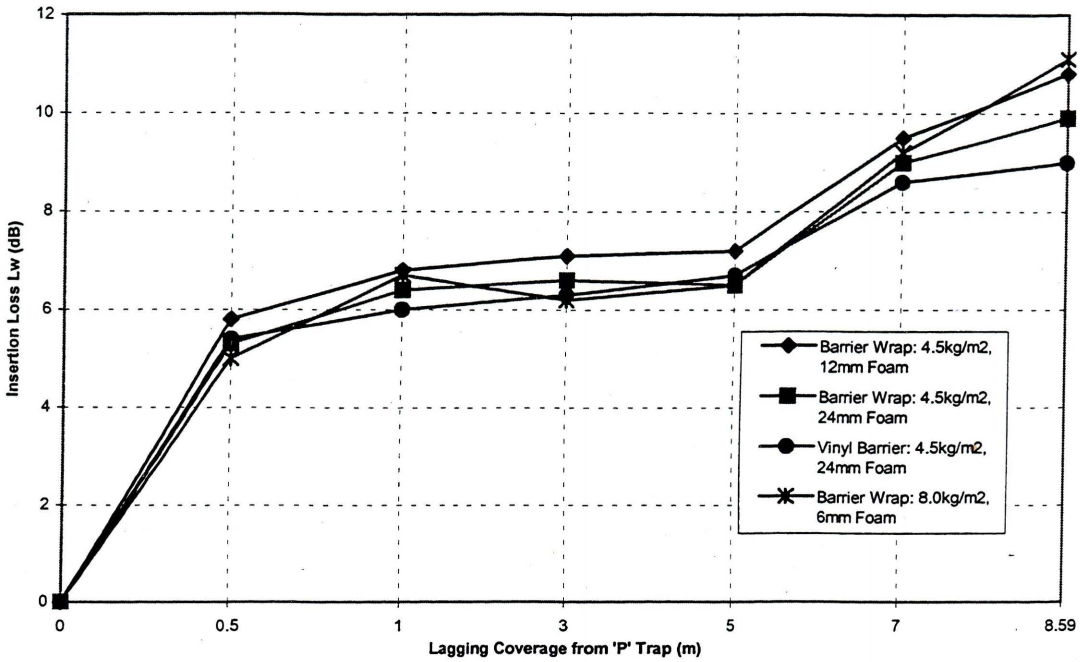

Figure 2 Insertion loss variation with lagging coverage

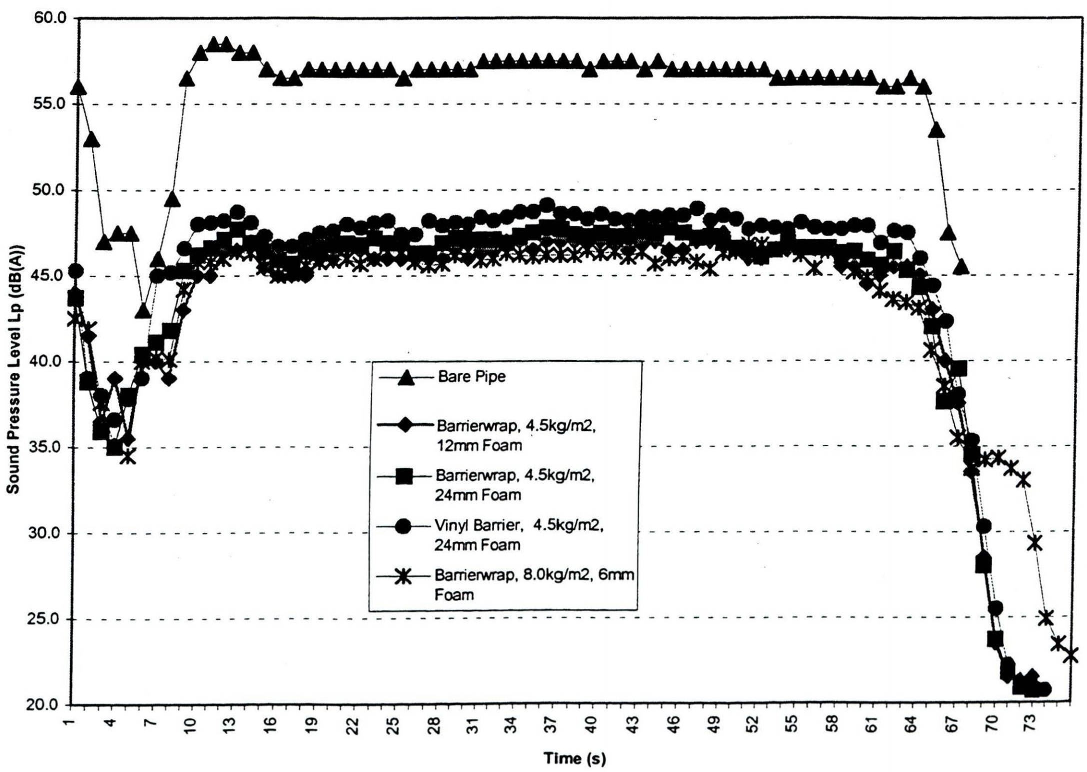

Figure 3 Bath discharge noise profile

5. CONCLUSIONS

The greatest insertion loss [11 dB(A)] was obtained from the heaviest barrier (Acoustop 8.0 kg/m^2) on 6mm foam. The transient noise was not reduced as much as the steady state noise. A 6 dB(A) insertion loss was achieved by lagging the 'P' trap bend and 1 metre beyond it.

Figure 1 shows that the vinyl barrier having an equal mass of 4.5 kg/m^2 provided less performance overall compared to the same weight per m^2 of the rubber based barrier products. The reduced performance is possibly due to a number of factors a) difficulty of installation, b) product resonance. All products recorded a reduced acoustic performance at 500hz, this phenomenon is to be investigated further and is the subject of ongoing research.

6. REFERENCES

1. Fuchs, H V (1992a) Generation and control of noise in water supply installations. Part 2: Sound source mechanisms, Applied Acoustics, v38, 1993:50-85.

2. Fuchs, H V (1992b) Generation and control of noise in water supply installations. Part 3: Rating and abating procedures, Applied Acoustics, v39, 1993:165-190.

3. AS 1217.2-1985, Acoustics-Determination of sound power levels of noise sources. Part 2: Precision methods for broad-band sources in reverberation rooms. AS, Standards Association of Australia, 1985.

AUSTRALIAN ACOUSTICAL
SOCIETY CONFERENCE